



INTERDISCIPLINARY TOPICS IN MINING, GEOLOGY AND GEOMATICS



INTERDISCIPLINARY TOPICS IN MINING, GEOLOGY AND GEOMATICS

Scientific editor
Justyna Woźniak



WUST Publishing House
Wrocław 2025

Reviewers

Lucia BEDNÁROVÁ, Jakub CIAŻELA, Isabel FERNANDES,
Lidia FIJAŁKOWSKA-LICHWA, Justyna GÓRNIAK-ZIMROZ,
Urszula KAŻMIERCZAK, Artur KRAWCZYK, Bogumiła PAŁAC-WALKO,
Monika PODWÓRNA, Krzysztof SKRZYPKOWSKI, Danuta SZYSZKA,
Magdalena WORSZA-KOZAK, Paweł ZAGOŹDŻON

Technical editors

Stanisław GANCARZ
Mateusz SZCZĘŚNIEWICZ

Cover illustration, Patrons and Sponsors page design

Paulina KUJAWA

Cover design

Janusz M. SZAFRAN

All rights are reserved. No part of this publication may be reproduced, stored in a retrieval system or transmitted in any form or by any means, electronic, mechanical, including photocopying, recording or any information retrieval system, without permission in writing form the publisher.

© Copyright by Wrocław University of Science and Technology Publishing House, Wrocław 2025

WROCLAW UNIVERSITY OF SCIENCE AND TECHNOLOGY PUBLISHING HOUSE

Wybrzeże Wyspiańskiego 27, 50-370 Wrocław

<http://www.oficyna.pwr.edu.pl>;

e-mail: oficwyd@pwr.edu.pl

zamawianie.ksiazek@pwr.edu.pl

ISBN 978-83-8134-007-6

https://doi.org/10.37190/Interdisciplinary_topics

Print and binding: beta-druk, www.betadruk.pl

HONORARY PATRONAGE AND SPONSORS



**DOLNY
ŚLĄSK**

PATRONAT HONOROWY MARSZAŁKA WOJEWÓDZTWA
DOLNOŚLĄSKIEGO PAWŁA GANCARZA



Wrocław University
of Science and Technology
Rector's Honorary Patronage

Polish
Association
of Doctoral
Candidates



ASSOCIATION OF
TECHNICAL UNIVERSITIES
DOCTORAL STUDENTS



STATE MINING AUTHORITY
(WYŻSZY URZĄD GÓRNICZY)



polteqor – instytut



POLSKA AKADEMIA NAUK
KOMISJA NAUK GÓRNICZYCH

**Oddział
we Wrocławiu**



Ministry of Science and Higher Education
Republic of Poland

The project is financed by funds from the state budget granted by the Minister of Science and Higher Education within the framework of the "Excellent Science II".

CONTENTS

1. Inducing alteration in volcanic rocks in a fumarolic field: a case study in S. Miguel Island (<i>Maria Luísa Pereira, Lucia Pappalardo, Gianmarco Buono, Alessia Falasconi, Isabel Fernandes, Vittorio Zanon, Fátima Viveiros, António Cordeiro</i>)	7
2. Factors affecting water retention in post-mining reservoirs (<i>Kamil Gromnicki</i>)	17
3. Potential sources of lithium in Poland (<i>Mateusz Szczęśniewicz, Dominika Ciapka, Konrad Blutstein</i>)	29
4. Assessment of bearing capacity in bilayer rock masses: The case of Oporto granite (<i>Ana Alencar, Rubén Galindo Aires, Mauro Muñiz-Menéndez, António Viana Da Fonseca</i>)	49
5. Tensile strength variation in transversely isotropic rocks (<i>Ana Alencar, Rubén Galindo Aires, Mauro Muñiz-Menéndez, Miguel Ángel Millán</i>)	59
6. The stability graph method: state-of-the-art (<i>César Torrero, Luis Jordá, Salvador Senent</i>)	71
7. Implementation of object detection algorithms in the inventory of technical infrastructure, case study insulators detection (<i>Mateusz Czyrznia, Jacek Rapiński</i>)	87
8. A comparative study of deterministic and stochastic methods for groundwater flow modelling (<i>Amr Moharram, Balázs Kovács</i>)	101
9. Mineral property appraisal with reference to local spatial development plan limitations (<i>Michał Dudek, Anna Nowel-Śmigaj</i>)	119
10. Analysis of the reconstruction of an accident from a curt case to improve occupational safety (<i>Kinga Martuszevska, Dawid Szurgacz</i>)	127
11. Assessment framework for artisanal and small-scale mining: case study of Podmoký, Czech Republic (<i>David Stejskal</i>)	137
12. Green hydrogen: a key driver of sustainable energy systems in Europe (<i>Maroš Begáni</i>)	151
13. Legal analysis of Polish court case law on the phenomenon of a reactive depressive on the example of mining employee (<i>Kinga Martuszevska</i>)	159

1. INDUCING ALTERATION IN VOLCANIC ROCKS IN A FUMAROLIC FIELD: A CASE STUDY IN S. MIGUEL ISLAND

MARIA LUÍSA PEREIRA^{1,2,3}, LUCIA PAPPALARDO⁴, GIANMARCO BUONO⁴,
ALESSIA FALASCONI⁴, ISABEL FERNANDES³, VITTORIO ZANON¹,
FÁTIMA VIVEIROS^{1,2}, ANTÓNIO CORDEIRO²

¹ Instituto de Investigação em Vulcanologia e Avaliação de Riscos (IVAR),
Universidade dos Açores, Rua Mãe de Deus, Ponta Delgada 9500-123, Portugal.

² Faculdade de Ciências e Tecnologia, Universidade dos Açores, Rua Mãe de Deus,
Ponta Delgada 9500-123, Portugal.

³ Instituto Dom Luiz (IDL), Faculdade de Ciências, Universidade de Lisboa,
Campo Grande, 1749-016 Lisboa, Portugal.

⁴ Istituto Nazionale di Geofisica e Vulcanologia, Osservatorio Vesuviano,
Via Diocleziano, 328, 80124 Naples, Italy.

Hydrothermal alteration is widespread in volcano-hydrothermal systems, affecting the physical and mechanical properties of volcanic rocks. In the S. Miguel Island (Azores, Portugal), however, only drill cuttings are available from Ribeira Grande geothermal field, which are unsuitable for mechanical testing due to their limited size and shape. Given the importance of their characterisation and the limited information on alteration timescales, fresh volcanic rocks of different compositions and textures, previously characterised in detail, were exposed to natural alteration in the field. Samples were buried near the soil surface within a hydrothermal fumarolic area on the northern flank of Fogo Volcano for approximately four months. After retrieval, they were examined through macroscopic inspection, scanning electron microscopy, and X-ray microtomography to assess microstructural changes, complemented by whole-rock chemical analyses. Results show limited alteration: porosity values remained similar, mineral microstructures were preserved, and only minor surface coatings of secondary minerals were observed. Chemical indicators (loss in ignition, Chemical Index of Alteration, Chemical Weathering Index) suggest larger variations in trachytes, which, nevertheless, remained largely unaffected. Overall, alteration was limited to the rock surfaces, regardless of texture, indicating that controlled laboratory experiments may be required to induce accelerated alteration in these rocks.

Keywords: volcanic rocks, diffuse degassing area, microstructure

1.1. INTRODUCTION

In geothermal fields, altered materials prevail over fresh rocks, controlling the sub-surface dynamics of fracturing, ductility, and porosity evolution over time and space.

Hydrothermal alteration leads to unpredictable physical and mechanical behaviour of the host rocks, affecting geothermal exploitation, conditioning wellbore failure, and induced seismicity [1]. However, the influence of alteration and the required timescales for its development are not yet understood [2].

The study of altered materials is challenging in obtaining a specimen of suitable size for mechanical testing, as many of the collected samples are drill cuttings, as it occurs in Ribeira Grande geothermal field, located in the northern flank of Fogo Volcano (S. Miguel Island – Azores, Portugal).

Such difficulty has prompted alteration of lavas in the laboratory, where cylinders of andesites were either immersed in a batch reactor filled with an acid solution at ambient temperature up to four months [3] or autoclaved using a heated and pressured brine (temperature up to 280°C; 20 MPa of pressure) for one month [1]. During the process, several physical and mechanical properties of the rocks were measured periodically, complemented by a microstructural investigation. To the authors' knowledge, no previous studies have attempted to induce alteration of volcanic rocks directly within a fumarolic field, making this a novel exploratory approach.

This research intends to explore a different venue by inserting irregular fresh volcanic rocks, previously assessed for their physical and mechanical properties by [4], in a hydrothermal fumarolic ground located at the Caldeiras da Ribeira Grande (north flank of Fogo Volcano), which contains soil diffuse degassing areas [5, 6], for four months. Subsequently, the rocks are investigated through macroscopic inspection, scanning electron microscopy (SEM), and X-ray microtomography (μ CT) to assess microstructural changes. Whole-rock chemical analyses allowed to calculate and plot several chemical metrics known to indicate hydrothermal alteration in volcanic rocks, such as loss in ignition (LOI), Chemical Index of Alteration (CIA), Chemical Weathering Index (CIW), sulfur (S) content, and a combination of oxides descriptive of felsic ($\text{CaO} + \text{K}_2\text{O} + \text{Na}_2\text{O}$) and mafic ($\text{Fe}_2\text{O}_3^{\text{T}} + \text{MnO} + \text{MgO}$) minerals [7–9].

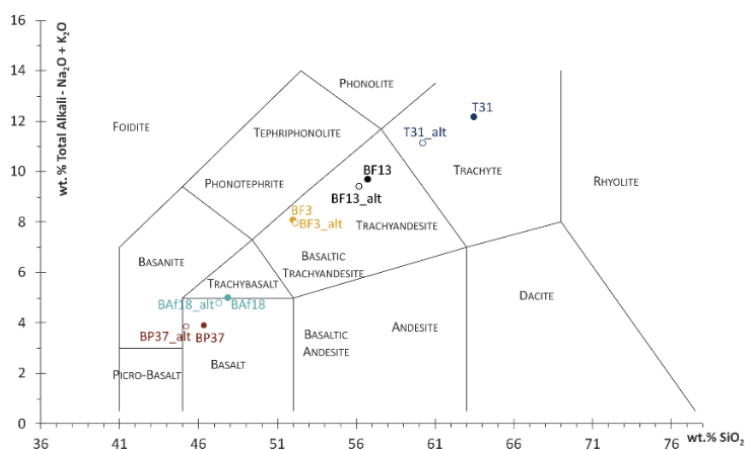
The primary objective of this research is to determine whether the field-induced alteration strategy is suitable for application in 45 mm diameter cylinders required for mechanical tests.

1.2. MATERIALS AND METHODS

1.2.1. MATERIALS

Unaltered specimens obtained from the same blocks assessed by [4] were buried ~50 cm below the soil surface, at 98.6°C, in Caldeiras da Ribeira Grande from July 30 to December 6, 2024, intercepting the rainy and relatively dry seasons in the Azores [10]. Although local soil properties were not measured, data from a permanent soil CO_2 flux station at Caldeiras da Ribeira Grande [11] indicate soil water content between

The samples subjected to induced alteration in the field have the following references: BP37_ult, BAF18_ult, BF3_ult, BF13_ult, and T31_ult. BP and BAF basalts are basalts to trachybasalts (Fig. 1) collected in Mosteiros and Sto António parishes, respectively, in lava flows produced by Sete Cidades Volcano (S. Miguel, Azores, Portugal). These basalts are compact and dense, with a porphyritic texture, containing olivine, clinopyroxene and plagioclase phenocrysts. The content in plagioclase increases for the intermediate basalts BF, chemically classified as basaltic trachyandesites to trachyandesites (Fig. 1), collected in a lava flow produced by Fogo Volcano and located in Ribeirinha Parish (S. Miguel). Within these samples, BF3 has a compact texture, whereas BF13 and BF15 are vesicular in appearance, containing millimetric and centimetric pores. Trachytes (T), characterised by a compact and trachytic texture, are mostly composed of alkali-feldspar [4] and were collected in Vale das Lombadas (Fogo Volcano, S. Miguel).



1.2.2. METHODS

After being collected from the field, the samples were cut into prisms measuring 9–11 × 16–19 mm. SEM analysis, performed on the Hitachi® T4000 Plus from Insti-

tuto de Investigação e Avaliação de Riscos (Universidade dos Açores, Portugal), was conducted to obtain surface morphology images, which were acquired in secondary electron and mix modes with varying optical magnification. μ CT imaging was obtained in the ZEISS® Xradia Versa-410 μ CT scanner at the Istituto Nazionale di Geo-fisica e Vulcanologia – Osservatorio Vesuviano (INGV-OV, Italy). The analysis was performed in the absorption mode, acquiring 4001 2D radiographs (projections) over a 360° rotation, with the selected conditions (air, 100–120 kV, 83–100 μ A, 0.4 \times) resulting in a nominal voxel size of 14.68 μ m, as [4] used for fresh homologous material. Image analysis on 3D μ CT reconstructed images (ZEISS® XRM Reconstructor) enabled the quantification of the volume fraction of the void space (total porosity – n_T and effective/open porosity – n_{eff}), opaque minerals (Op), tortuosity (T), and absolute permeability (k) using PerGeos®.

Whole-rock chemical analyses were conducted at Actlabs®, Ltd. (Canada), where major elements were analysed via lithium metaborate/tetraborate fusion, with the molten bead digested in a 5% nitric acid solution containing an internal standard. The solution was analysed by inductively coupled plasma optical emission spectrometry and mass spectrometry, with calibration performed using 14 prepared US Geological Survey and Canada Centre for Mineral and Energy Technology certified reference materials. The LOI was determined by the gravimetric method, whereas the sulfur content was determined via total digestion using four acids and analysed with ICP. Major oxides were used for the total alkali silica (TAS) classification of the samples (Fig. 1) and to calculate the CIA [17] and CIW [18] indices, using both Microsoft® Excel and the GCDkit of R®.

1.3. RESULTS

1.3.1. MACROSCOPIC OBSERVATION AND MICROSTRUCTURAL ANALYSIS

Macroscopic observations reveal that the alteration is superficial, with reddish to brownish colour modifications due to the possible formation of clays and oxides. Most oxidation develops as a thin coating in the pores of the vesicular BF13_alt sample and in T31_alt, while the BP and BAf remain similar to their fresh counterparts.

As depicted in Fig. 2, SEM photographs confirm an induced alteration limited to the rock surface, and μ CT images show that the morphology of the void space and minerals remains similar to the fresh counterparts [4, 19].

BP37_alt basalt (Fig. 2a) has a groundmass and phenocrysts not covered by secondary products, and the isolated, intragranular, and coalescent pores in the rock's interior, in agreement with the void space of fresh samples [4]. n_T of BP37_alt (4.04%) is 2% higher than that of fresh BP37 (2.07%), whereas opaque minerals, primary, have similar amounts (0.58% for BP37 and 0.36% for BP37_alt).

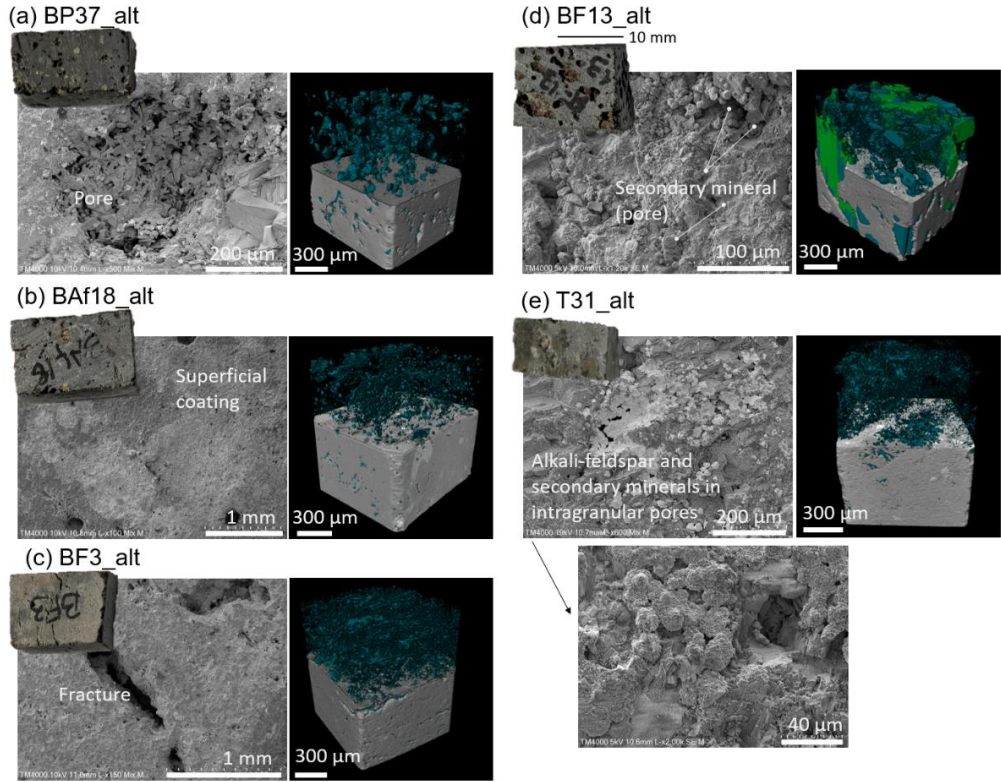


Fig. 2. Macroscopic appearance, scanning electron imaging (SE or mix mode) of the surfaces, and void space segmentation of physical properties of the specimens: (a) BP37_alt, (b) BAf18_alt, (c) BF3_alt, (d) BF13_alt, (e) T31_alt

BAf18_alt (Fig. 2b) has scarce clay minerals inside surficial pores and coatings in dispersed spots of the groundmass. Internally, the number of opaques and pores is reduced from BAf18 ($n_T = 2.20\%$, $Op = 0.20\%$) to BAf18_alt ($n_T = 1.19\%$, $Op = 0.80\%$), because the fresh prism contained transgranular microcracks. On the contrary, the pores in B18_alt, rounded and isolated, are larger.

BF3_alt (Fig. 2c) maintains an unaltered surface, without coatings and fracture infillings. The internal rock ($n_T = 2.88\%$, $Op = 0.52\%$) is composed of a network of irregular, open, and empty microcracks, typically limiting the phenocrysts, as verified for BF3 ($n_T = 2.44\%$, $Op = 0.19\%$). The minerals (opaque minerals, plagioclase) are similar in BF3 and BF3_alt.

Besides the surficial coatings, BF13_alt comprises secondary minerals with a spheroidal and/or veneer morphology inside the pores (Fig. 2d) because of the vesicular nature. However, alteration does not extend to the internal part of rocks, as several features are maintained from BF13 ($n_T = 19.21\%$, $n_{eff} = 12.85\%$, $Op = 0.34\%$, $T = 2.59$,

$k = 256$ mD) to BF13_alt ($n_T = 19.52\%$; $n_{eff} = 12.81\%$, $Op = 0.45\%$, $T = 1.63$, $k = 143$ mD). Porosity values are similar, and both samples display a prevalence of coalescent empty pores, whose elongation varies from BF13 (x -axis) to BF13_alt (z -axis). This preferred orientation explains the differences in k , which were simulated along the z -axis of the digital prisms.

T31_alt has a more pervasive surface alteration than other samples, with dispersed or concentrated surface coatings in the groundmass or secondary products along intra-granular pores of phenocrysts (Fig. 2e). However, internally, modifications are minor between T31 ($n_T = 1.29\%$, $Op = 0.35\%$) and T31_alt ($n_T = 1.10\%$, $Op = 0.39\%$), with similar mineral morphology and a slight difference in porosity given the fact that the prisms, despite being from the same block, are distinct.

1.3.2. CHEMICAL DATA ANALYSIS

Figure 3 depicts several chemical metrics for field-altered and fresh samples to verify if differences were produced in the samples due to exposure to degassing.

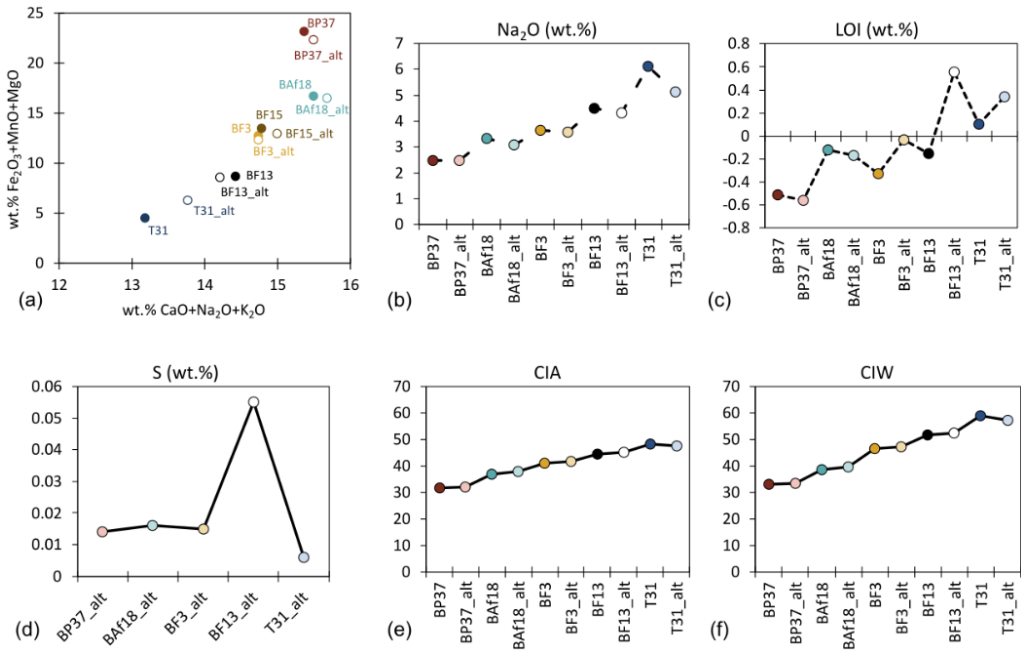


Fig. 3. Chemical characterisation of fresh (BP38, BAF18, BF3, BF13, T31) and field-altered samples (BP38_alt, BAF18_alt, BF3_alt, BF13_alt, T31_alt) using the binary diagram of felsic ($CaO + K_2O + Na_2O$) against mafic ($Fe_2O_3^T + MnO + MgO$) oxides, Na_2O content, loss in ignition (LOI), S content, Chemical Index of Alteration (CIA), and Chemical Weathering Index (CIW)

The binary diagram (Fig.3a) shows proximity between the samples “_alt” and fresh samples. T31_alt is more distant from T31 because the sample experiences an increment in CaO despite the Na depletion (Fig.3b), similar to BF13_alt. T31_alt also shows an increase in $\text{Fe}_2\text{O}_3^{\text{T}} + \text{MnO} + \text{MgO}$, which is not verified in the remaining samples that are richer in oxides composing mafic minerals. The LOI (Fig.3c) increases for most samples, particularly for BF13_alt (0.71 wt.%), except for BAF18 and BP37. S (Fig.3d) was only determined in “_alt” samples, presenting higher values for BF13_alt (0.055 wt.%) and lower levels T31 (0.006 wt.%). Variations between fresh and altered samples in CIA (Fig.3e) and CIW (Fig.3f) are minor (0.2 to 1), with T31_alt even reducing the value of these indices relative to T31, whereas the other rocks have values close to those of their fresh counterparts.

1.4. DISCUSSION

Results indicate that modifications in macroscopic appearance, rock surface, microstructure, and chemical composition were minor, regardless of rock type (basalt or trachyte) or texture (compact or vesicular). Noticeable surface changes were observed only in samples T31_alt and BF13_alt, where the formation of clay minerals or oxides was likely, based on morphology [20]. However, no evidence of enhanced void-space connectivity or secondary mineral formation was identified internally.

Variations in physical properties, particularly n_{T} and k , as well as in opaque mineral content, are attributed to the intrinsic heterogeneity of these lavas, which can lead to variations even within a single block. Such heterogeneity has been previously reported for volcanic rocks [2]. Although opaque minerals were quantified because surface rocks in the Ribeira Grande geothermal field are known to form secondary oxides in weakly altered and smectite zones [13, 21], their morphology and mode of occurrence here suggest a primary, rather than secondary, origin.

Chemical indicators also support that alteration was minimal. The rock type appears to exert a stronger control, as T31 samples seem more susceptible to degassing exposure, although variations relative to the fresh counterparts remain limited. Na_2O depletion, commonly observed in hydrothermally altered volcanic rocks [9], was below 1.5 wt. %, indicating negligible change. The LOI, which reflects the H_2O^+ content in a sample heated at $> 105^\circ\text{C}$ [22], is reported to increase because of the hydration of rocks (e.g., clay formation, oxidation of Fe^{2+}) due to alteration [23]. Similarly to Na, the LOI remained below 4 wt. %, the threshold typically used to classify volcanic rocks as altered [9]. Nevertheless, slightly higher LOI values were observed in the sample with higher n_{T} , suggesting that porosity and microstructure influence this metric. A similar trend was noted for S content, with higher values in vesicular specimens; however, the measured concentrations are near the detection limit (0.001 wt.%) and indicate that sulfur mineral formation or acidic alteration [24] did not occur.

Both the CIA and the CIW are expected to increase with progressive alteration in volcanic rocks [7–9]. A threshold value of 60 is generally used to distinguish between fresh and altered materials [17, 18, 23]. All analysed lavas fall below this limit, confirming that induced alteration was ineffective.

Overall, the findings demonstrate that short-term field exposure in fumarolic environments did not induce significant alteration in the samples, even in those with a vesicular texture containing millimetric to centimetric pores. This outcome suggests that longer exposure periods may be required to achieve measurable alteration, particularly for less porous materials. However, the field method would benefit from improved characterisation of the local soil characteristics, including moisture and chemistry, to better constrain and reproduce the experimental conditions, which are also valuable for future laboratory approaches. In addition, comparing these results with naturally altered samples, such as drill cuttings from the Ribeira Grande geothermal field, could clarify whether the lack of alteration is primarily due to insufficient exposure time or the combined influence of lava structure and system conditions (temperature, pressure, and fluids).

1.5. CONCLUSION

This study aimed to produce hydrothermally altered samples suitable for standardised mechanical and physical testing, contributing to a better understanding of alteration effects on volcanic rocks. However, the limited availability of drillhole cores from geothermal fields for such tests necessitated inducing alteration artificially. To this end, a field-based approach was adopted, taking advantage of the hydrothermal fumarolic field on S. Miguel Island, where samples were buried within a diffuse soil degassing zone to promote natural alteration.

After approximately four months, results revealed minimal microstructural and chemical modification, likely due to the compact nature of the lavas, even in vesicular specimens. Changes were restricted to superficial coatings, with no significant mineralogical transformations or variations in void space. Chemically, slight increases in Na and LOI and minor shifts in the CIA and CIW indices remained below thresholds typically associated with altered volcanic rocks.

Although significant induced alteration was not achieved, the findings indicate that short-term natural exposure in fumarolic environments is insufficient to promote considerable changes in compact volcanic rocks. Future work should instead focus on controlled laboratory alteration experiments, allowing for accelerated processes, supported by a more comprehensive characterization of the field environment. Moreover, comparing these materials with naturally altered cuttings of the Ribeira Grande geothermal field (S. Miguel, Azores, Portugal) with similar composition and structure could help determine whether the lack of alteration is a matter of timescale or the absence of specific conditions (pressure, temperature, and circulating fluids).

REFERENCES

- [1] NICOLAS A., LÉVY L., SISSMANN O., LI Z., FORTIN J., GIBERT B., SIGMUNDSSON F., *Influence of hydrothermal alteration on the elastic behaviour and failure of heat-treated andesite from Guadeloupe*, *Geophysical Journal International*, 2020, Vol. 223, No. 3, 2038–2053, <https://doi.org/10.1093/gji/ggaa437>
- [2] HEAP M.J., VIOLAY M.E., *The mechanical behaviour and failure modes of volcanic rocks: a review*, *Bulletin of Volcanology*, 2021, Vol. 83, article 33, <https://doi.org/10.1007/s00445-021-01447-2>
- [3] FARQUHARSON J.I., WILD B., KUSHNIR A.R.L., HEAP M.J., BAUD P., KENNEDY B., *Acid-induced dissolution of andesite: Evolution of permeability and strength*, *Journal of Geophysical Research: Solid Earth*, 2019, Vol. 124, 257–273, <https://doi.org/10.1029/2018JB016130>
- [4] PEREIRA M.L., PAPPALARDO L., BUONO G., CUETO N., VÁZQUEZ-CALVO C., FORT R., COSTA E SILVA M., FERNANDES I., ZANON V., AMARAL P., *A multi-method approach in the physical and mechanical assessment of lava rocks with distinct microstructure*, *Engineering Geology*, 2025, Vol. 346, 107907, <https://doi.org/10.1016/j.enggeo.2025.107907>
- [5] VIVEIROS F., GASPAS J.L., FERREIRA T., SILVA C., MARCOS M., HIPÓLITO A., *Mapping of soil CO₂ diffuse degassing at São Miguel Island and its public health implications*, *Geological Society, London, Memoirs*, 2015, Vol. 44, 185–195, <https://doi.org/10.1144/M44.14>
- [6] VIVEIROS F., BALDONI E., MASSARO S., STOCCHI M., COSTA A., CALIRO S., CHIODINI G., ANDRADE C., *Quantification of CO₂ degassing and atmospheric dispersion at Caldeiras da Ribeira Grande (São Miguel Island, Azores)*, *Journal of Volcanology and Geothermal Research*, 2023, Vol. 438, 107807, <https://doi.org/10.1016/j.jvolgeores.2023.107807>
- [7] WEYDT L.M., LUCCI F., LACINSKA A., SCHEUVENS D., CARRASCO-NÚÑEZ G., GIORDANO G., ROCHELLE C.A., SCHMIDT S., BÄR K., SASS I., *The impact of hydrothermal alteration on the physicochemical characteristics of reservoir rocks: The case of the Los Hornos geothermal field (Mexico)*, *Geothermal Energy*, 2022, Vol. 10, 20, <https://doi.org/10.1186/s40517-022-00231-5>
- [8] PANDARINATH K., RIVAS-HERNÁNDEZ J.L., ARRIAGA-FUENTES J.A., YÁÑEZ-DÁVILA D., GONZÁLEZ-PARTIDA E., SANTOYO E., *Hydrothermal alteration of surficial rocks at Los Hornos geothermal field, Mexico: a magnetic susceptibility approach*, *Arabian Journal of Geosciences*, 2023, Vol. 16, article 259, <https://doi.org/10.1007/s12517-023-11306-3>
- [9] PANDARINATH K., MUNDO A.C., VERMA S.K., GONZALEZ-PARTIDA E., MISHRA S., YÁÑEZ-DÁVILA D., SANTOYO E., TORRES-HERNÁNDEZ J.R., *Geochemical signature of hydrothermal alteration in surface rocks of Cerritos Colorados geothermal field of Mexico*, *Geochemistry*, 2024, Vol. 84, article 126200, <https://doi.org/10.1016/j.chemer.2024.126200>
- [10] MARQUES R., ZÊZERE J.L., TRIGO R.M., GASPAS J.L., TRIGO I.F., *Rainfall patterns and critical values associated with landslides in Povoação County (São Miguel Island, Azores): relationships with the North Atlantic Oscillation*, *Hydrological Processes*, 2008, Vol. 22, 478–494, <https://doi.org/10.1002/hyp.6879>
- [11] OLIVEIRA S. VIVEIROS F., SILVA C., PACHECO J.E., *Automatic filtering of soil CO₂ flux data; different statistical approaches applied to long time series*, *Frontiers in Earth Science*, 2018, Vol. 6, article 208, 1–14.
- [12] CALIRO S., VIVEIROS F., CHIODINI G., FERREIRA T., *Gas geochemistry of hydrothermal fluids of the S. Miguel and Terceira Islands, Azores*, *Geochimica et Cosmochimica Acta*, 2015, Vol. 168, pp. 43–57, <https://doi.org/10.1016/j.gca.2015.07.009>
- [13] PEREIRA M.L., MATIAS D., VIVEIROS F., MORENO L., SILVA C., ZANON V., UCHÔA J., *The contribution of hydrothermal mineral alteration analysis and gas geothermometry for understanding high-temperature geothermal fields – the case of Ribeira Grande geothermal field, Azores*, *Geothermics*, 2022, Vol. 105, article 102519, <https://doi.org/10.1016/j.geothermics.2022.102519>
- [14] MATIAS D., ANTLAUF M., VIVEIROS F., MORENO L., SILVA C., OLIVEIRA S., *Monitoring hydrothermal fumaroles in the Azores archipelago – Applications and sources of analytical un-*

- certainties*, Journal of Volcanology and Geothermal Research, 2024, Vol. 450, article 108076, <https://doi.org/10.1016/j.jvolgeores.2024.108076>
- [15] AIUPPA A., VIVEIROS F., CORDEIRO A., *Fumarolic CO₂ emissions from weakly degassing, hydrothermal volcanoes: a case from Fogo volcano, São Miguel, Azores*, Applied Geochemistry, 2025, Vol. 191, article 106516, <https://doi.org/10.1016/j.apgeochem.2025.106516>
- [16] LE BAS M., LE MAITRE R.W., STRECKEISEN A., ZANETTIN B., IUGS SUBCOMMISSION ON THE SYSTEMATICS OF IGNEOUS ROCKS, *A chemical classification of volcanic rocks based on the total alkali silica diagram*, Journal of Petrology, 1986, Vol. 27, No. 3, 745–750, <https://doi.org/10.1093/petrology/27.3.745>
- [17] NESBITT H.W., YOUNG G.M., *Early Proterozoic climates and plate motions inferred from major element chemistry of lutites*, Nature, 1982, Vol. 299, 715–717, <https://doi.org/10.1038/299715a0>
- [18] HARNOIS L., *The CIW index: a new chemical index of weathering*, Sedimentary Geology, 1988, Vol. 55, 319–322, [https://doi.org/10.1016/0037-0738\(88\)90137-6](https://doi.org/10.1016/0037-0738(88)90137-6)
- [19] PEREIRA M.L., PAPPALARDO L., BUONO G., ZANON V., FERNANDES I., *Microstructural, textural, and physical characteristics of volcanic rocks from Fogo volcano – S. Miguel Island (Azores), Portugal*, MedGU 2023 Conference Proceedings, Istanbul, 26–30 November 2023, 5 pp.
- [20] WELTON J.E., *SEM Petrology Atlas*, Vol. 4, Tulsa, Oklahoma, American Association of Petroleum Geologists, 1984, <https://doi.org/10.1306/Mth4442>
- [21] FRANCO A., *Subsurface geology and hydrothermal alteration of Cachaços-Lombadas sector, Ribeira Grande geothermal field*, Geothermal Training in Iceland 2015, Report 10, UNU-GTP, Iceland, 2016, 113–160.
- [22] JOHNSON W.M., MAXWELL J.A., *Rock and Mineral Analysis*, 2nd ed., Wiley-Interscience, New York 1981, 489 pp.
- [23] PANDARINATH K., *Application potential of chemical weathering indices in the identification of hydrothermally altered surface volcanic rocks from geothermal fields*, Geosciences Journal, 2022, Vol. 26, 415–442, <https://doi.org/10.1007/s12303-021-0042-2>
- [24] BÓLOS X., CIFUENTES G., MACÍAS J.L., SOSA-CEBALLOS G., GARCIA-TENORIO F., ALBOR M., *Geophysical imaging of fluid circulation and its relation with the structural system of Cerritos Colorados geothermal field, La Primavera caldera (Mexico)*, Journal of Volcanology and Geothermal Research, 2019, Vol. 369, 238–249, <https://doi.org/10.1016/j.jvolgeores.2018.11.015>

WYWOŁYWANIE PRZEOBRAŻEŃ W SKAŁACH LAWOWYCH W POLU FUMAROLI: STUDIUM PRZYPADKU NA WYSPIE S. MIGUEL

Przeobrażenia hydrotermalne są powszechne w systemach wulkaniczno-hydrotermalnych i modyfikują właściwości skał lawowych. Na wyspie S. Miguel (Azory, Portugalia) dostępne są jedynie zwierciny z pola geotermalnego Ribeira Grande, które nie nadają się do testów mechanicznych. Dlatego świeże skały lawowe o zróżnicowanym składzie i teksturze poddano naturalnemu procesowi przeobrażenia. Próbkę zakopano tuż pod powierzchnią gruntu w obszarze fumaroli na północnym stoku wulkanu Fogo na około cztery miesiące. Po wydobyciu przebadano je makroskopowo, za pomocą skaningowego mikroskopu elektronowego oraz mikrotomografii rentgenowskiej, uzupełnionych analizami chemicznymi. Porowatość i mikrostruktury minerałów pozostały w dużej mierze niezmienione, a jedynie na powierzchni pojawiły się niewielkie powłoki minerałów wtórnych. Wskaźniki chemiczne wykazały większe zróżnicowanie w trachitach, choć próbki pozostały w większości niezmienione. Przeobrażenie ograniczało się do powierzchni skał, niezależnie od ich tekstury. Dlatego do przyspieszenia tego procesu mogą być potrzebne kontrolowane eksperymenty laboratoryjne.

2. FACTORS AFFECTING WATER RETENTION IN POST-MINING RESERVOIRS

KAMIL GROMNICKI

Wrocław University of Science and Technology, Faculty of Geoengineering, Mining and Geology,
Wybrzeże S. Wyspiańskiego 27, 50-370 Wrocław, Poland.

Water retention in post-mining reservoirs is a key aspect of water resource management in areas affected by mining activities. The capacity of these reservoirs to store water depends on multiple factors, including geological structure, watershed hydrology, land reclamation measures, climate change, and anthropogenic pressure. Geological properties, such as soil permeability and the presence of aquifers, directly influence infiltration rates and water storage capacity. Watershed characteristics, including slope, vegetation cover, and surface runoff, affect the volume of water reaching the reservoirs. Mining operations and subsequent land reclamation can significantly modify the landscape and hydrological balance, either enhancing or reducing retention potential. Additionally, climate variability, including changes in precipitation and drought frequency, impacts water availability in these reservoirs. Human activities surrounding the reservoirs, such as urbanization, agriculture, and industrial operations, can further alter water quality and retention. This study reviews the main factors influencing water retention in post-mining reservoirs and highlights the importance of integrated monitoring and management strategies to optimize their ecological, recreational, and hydrological functions.

Keywords: water retention, post-mining reservoirs, land reclamation, climate change, water resources management

2.1. INTRODUCTION

Water retention in post-mining reservoirs is an important issue from the point of view of water management, environmental protection, and spatial planning. These reservoirs are created as a result of mining activities and constitute potential water reservoirs that can be used for ecological, recreational, or economic purposes [1]. Identifying the factors that influence water retention in such reservoirs allows for better management of water resources in post-mining regions. Knowledge of which elements of the environment and human activity influence the ability of reservoirs to store water enables the planning of reclamation activities and the assessment of the effects of potential climate and anthropogenic changes [2]. Scientific literature has noted that post-mining reservoirs not only serve as water storage facilities, but also have a significant impact

on local ecosystems, microclimates, and biodiversity. Analysis of the factors determining their retention allows for the assessment of the effectiveness of various reclamation strategies and the design of new water facilities [3]. Knowledge of these factors is also essential to minimize the negative effects of mining activities, such as land degradation, changes in the region's water balance, and deterioration of water quality. Through systematic research and monitoring, it is possible to identify priority areas for reclamation and optimize the use of reservoirs [4]. Research to date shows that an interdisciplinary approach-combining hydrology, geology, ecology, and spatial planning-allows for a comprehensive understanding of the factors affecting water retention and their impact on the environment and local communities. The identification of these factors therefore forms the basis for both science and the practical management of post-mining reservoirs [5]. Research work aims to provide a comprehensive overview of the factors influencing water retention in post-mining reservoirs and to assess their significance for water management and environmental protection.

2.2. FACTORS AFFECTING WATER RETENTION IN POST-MINING RESERVOIRS

2.2.1. GEOLOGY AND SUBSOIL STRUCTURE

The geological composition and substrate structure play a fundamental role in determining the water retention capacity of post-mining reservoirs. The mineralogical properties of the parent material, including waste rock and mine tailings, directly influence the soil texture and its capacity to store and release water [6]. The pore system of the substrate-comprising macropores, mesopores, and micropores-controls the amount and distribution of water stored in the material [7]. Fine-textured materials, such as clays or fine-grained tailings, tend to retain more capillary water, while coarse substrates enhance infiltration and reduce water storage capacity [8]. Field studies in post-mining landscapes demonstrated that reclaimed areas with finer fractions show improved soil water regimes compared to unreclaimed spoil heaps [9].

Bulk density is another critical parameter; higher dry density reduces effective porosity and therefore decreases water retention capacity [10]. In uncompacted mine spoils, the loose structure often leads to rapid water percolation and low storage efficiency. Laboratory experiments with hard-rock tailings showed that compacted samples exhibited different retention curves compared to loose samples, with higher water retention under specific matric suctions. The shrinkage and cracking of tailings upon drying are closely related to pore geometry and may disrupt water retention continuity [11]. Substrates with dual-porosity structures behave differently, as micropores act as storage zones while macropores act as conduits, complicating water balance modelling [12]. The presence of coarse rock fragments significantly alters the effective water retention char-

acteristics. Studies have shown that soils and substrates with high gravel content exhibit lower available water capacity, as coarse fragments replace fine fractions that normally store water [13]. In post-mining environments, waste rock layers often consist of heterogeneous mixtures, producing strong spatial variability in infiltration and retention. Stratified deposits, where coarse materials overlay fine-textured layers, can cause preferential flow and rapid water loss from reservoirs. Mineralogical composition also plays a significant role: clay minerals and fine aluminosilicates exhibit high sorption and capillary storage potential, which increases water retention [14].

Reclamation practices often involve covering mine spoils with topsoil or organic-mineral amendments, which act as a buffer layer and improve water holding capacity. Empirical evidence shows that the addition of fine fractions and organic matter enhances pore connectivity and storage potential [8]. Field comparisons confirmed that reclaimed post-mining sites with finer soil layers maintain higher soil moisture content than bare spoil heaps [9]. In column experiments with tailings, particle size distribution and compaction intensity were shown to alter water content profiles and drying rates significantly [15].

Geophysical surveys of former mining sites revealed that subsurface heterogeneity, including variable permeability and porosity, strongly influences long-term reservoir storage potential [16]. The spatial variability of substrate properties means that generalized parameters often fail to predict actual water retention behavior at the site scale. Small changes in porosity or bulk density can result in disproportionately large changes in retention curves, highlighting the non-linear nature of soil-water interactions [7].

In summary, geological structure and substrate composition determine whether post-mining reservoirs function as effective water retention systems or lose water rapidly through infiltration and drainage. Incorporating detailed geological and soil-physical parameters into hydrological models is therefore essential for accurate assessment and for designing reclamation strategies that enhance retention potential.

2.2.2. HYDROLOGY OF THE CATCHMENT AREA

Catchment hydrology, i.e., the way water moves into, through, and out of a watershed, is a critical determinant of how much water can be retained by a post-mining reservoir.

The total area of the catchment influences the volume of precipitation that can potentially contribute to inflow, as larger catchments collect more runoff and can buffer extreme events. Analysis of two adjacent mountain catchments in the Polish Carpathians (Czarna Woda and Biała Woda) revealed that catchments with more forest cover and less agricultural land use had greater retention capacity and slower runoff response [17]. Vegetation cover in catchments plays a dual role: it intercepts rainfall, reducing direct surface runoff, and enhances infiltration through root systems and litter layer, increasing soil water storage [18].

Slope and topographic features of the catchment, such as steepness and aspect, strongly affect hydrological response—the steeper a slope, the faster the runoff, limiting time for infiltration and reducing retention [19].

Soil type within the catchment is also essential: permeable soils enable quicker infiltration and potentially greater baseflow, while impermeable or compacted soils lead to quicker surface runoff and more flash floods [20]. Long-term monitoring in Carpathian catchments shows that catchments dominated by forest cover maintain higher minimum flows during dry periods than more disturbed catchments, implying better water retention even beyond immediate storm events [17].

Catchment hydrology also interacts with precipitation patterns: catchments receiving more uniform or frequent rainfall tend to have smoother hydrological responses and more consistent storage, while those with intense but sporadic rainfall have more extreme runoff and less stable retention [21, 22].

Human alterations of catchment land use – such as deforestation, conversion to agriculture, or construction – can reduce infiltration capacity, alter evapotranspiration, and thereby impair retention potential [21].

Drainage network density within a catchment (number of tributaries, channels) affects how quickly runoff is routed to the reservoir; higher stream density can reduce retention by conveying water more rapidly downstream [19]. The presence and design of small retention structures or reservoirs within the catchment can significantly modulate the hydrological response, by retaining water upstream, reducing peak flows, and thus improving overall retention capacity [23].

Catchment slope aspect (which direction slopes face) influences soil moisture and evaporation rates; north-facing slopes (in northern hemisphere) often retain moisture better, which supports greater baseflow and steady source of water into reservoirs [21].

Groundwater recharge potential of a catchment is another key parameter: catchments with favorable subsurface geology allowing infiltration to groundwater support sustained baseflow into reservoirs, prolonging retention. Disturbance of the shallow subsurface (e.g., by mining) can impede recharge and reduce storage. In studies of paired catchments in Australian mining regions, open-cut mining in some cases increased baseflow, whereas underground mining tended to reduce it [24].

Evapotranspiration, i.e., vegetation transpiration plus soil and surface evaporation, acts as a loss term in the water balance of a catchment; in forested or vegetated catchments. Evapotranspiration may be high but the vegetation also improves infiltration and soil structure, so net effect on retention can be positive [8, 21]. Seasonality and snowmelt in catchments with cold climates further influence temporal distribution of inflows to reservoirs; snowmelt may provide gradual input improving retention, but sudden melts combined with rain can overwhelm retention capacity. For example Seen in mountain catchment studies in Poland [17, 22]. Catchment management practices like retention of vegetation buffer strips, reforestation, or maintaining riparian zones

help slow down runoff, enhance infiltration, and reduce erosion, which in turn protects reservoir capacity from sedimentation [10, 25].

The shape of the catchment (its geometry) matters: elongated vs. compact catchments differ in how fast water reaches the outlet; compact catchments often generate higher peak flows for given rainfall event, reducing retention time. Though specific studies for mining reservoirs are fewer, hydrology theory and general catchment flood studies support this [25]. Soil moisture antecedent conditions (how wet or dry the catchment is before a rainfall event) strongly influence retention: a wet antecedent soil reduces infiltration capacity, increasing runoff; dry antecedent soil increases initial storage but may reduce infiltration if the soil surface is crusted. Many catchment models include this as key input [21, 22].

Land cover heterogeneity (mix of forest, pasture, agriculture) within the catchment causes spatial variability in infiltration, evaporation, and runoff; catchments with more continuous forest cover tend to retain more water [17, 10]. Sediment transport from catchment influences reservoir retention by filling storage volumes; thus, catchment hydrology that accelerates erosion (steeper slopes, lack of vegetation) indirectly reduces retention over time [13, 25]. Atmospheric inputs such as frequency, intensity, and distribution of rainfall are primary drivers; in catchments with high rainfall intensity, overland flow dominates and reduces retention, unless countered by good infiltration and retention structures [21, 22].

Retention of baseflow – the sustained component of streamflow during dry periods – is improved in catchments with permeable soils, lower human disturbance, and good vegetation cover; such baseflow extends the period during which water is available in reservoirs. Catchment response to extreme rain events is heavily influenced by catchment hydrology: rapid runoff, channel network connectivity, and lack of storage depressions lead to higher peaks and lower retention [19, 23].

2.2.3. MINING ACTIVITIES AND LAND RECLAMATION

Mining activity has always been associated with significant environmental disturbance, including the transformation of landforms, alteration of hydrological regimes, and changes in soil and water chemistry. Mineral extraction leads to the creation of large open pits, spoil heaps, and degraded areas that require specialized reclamation measures to restore their environmental and social functions. One of the most important impacts of mining is the destruction of the natural soil cover, which directly reduces water retention capacity and accelerates surface runoff [8].

In many regions of the world, mining activity results in the formation of post-mining reservoirs, which can serve as retention structures, although their effectiveness strongly depends on geological, hydrological, and post-exploitation management conditions [9].

Landscape degradation also includes modifications of catchment structures – such as vegetation removal, slope reshaping, or stream redirection – which significantly alter water

circulation and retention processes [19]. Land reclamation of post-mining areas is a crucial process for restoring hydrological balance and enhancing water retention capacity. Depending on the type of mining activity, reclamation strategies may include soil restoration, vegetation planting, and the construction of water bodies functioning as buffers within the landscape [23]. Studies demonstrate that the introduction of suitable soil layers and organic materials significantly improves substrate structure and increases water-holding capacity [14]. In practice, reclamation must address not only vegetation recovery but also sustainable management of surface and groundwater. Literature highlights that appropriate reshaping of post-mining landscapes can improve the overall water balance while reducing erosion and sedimentation of reservoirs [25]. An equally important element is the selection of plant species with high water accumulation capacity and soil-improving functions, which help stabilize ecosystems and increase retention potential [18].

There are many examples in Poland and worldwide of successful post-mining land reclamation projects, where degraded sites have been transformed into valuable aquatic and forest ecosystems. Reclaimed open pits demonstrate that well-designed measures can restore not only hydrological functions but also create new habitats and improve local microclimates [22]. In this context, mining activity, although commonly perceived as destructive, can – if followed by appropriate reclamation – become an opportunity for developing new forms of water retention and water resource protection.

2.2.4. CLIMATE CHANGE AND ITS IMPACT ON THE WATER BALANCE

Climate change is increasingly recognized as a major factor affecting the hydrological cycle and water balance in both natural and post-mining landscapes. Rising global temperatures influence precipitation patterns, evapotranspiration rates, and snowmelt dynamics, all of which directly impact water retention in reservoirs and soils [26].

Changes in rainfall intensity and distribution result in more frequent extreme events, including both floods and droughts, which alter surface runoff and groundwater recharge [27]. Increased air temperatures accelerate evapotranspiration from soil and vegetation, reducing available water for retention in reservoirs and natural catchments. Seasonal shifts in precipitation, including altered snow accumulation and melt timing, affect the timing and quantity of inflows to post-mining water bodies, potentially reducing their capacity to buffer water extremes. Longer periods of drought reduce soil moisture, lower groundwater tables, and increase the risk of reservoir desiccation [28, 29].

Climate change also exacerbates the urban heat island effect in cities and settlements near post-mining areas, increasing water demand and evaporation from reservoirs and catchments. Shifts in precipitation seasonality lead to increased peak flows during heavy rainfall events, which can overwhelm retention structures and increase erosion and sediment transport into reservoirs. Conversely, decreased winter precipitation in some regions may reduce snowpack formation, leading to lower spring and early summer in-

flows [30]. Changes in extreme weather frequency also influence post-mining ecosystems ability to retain water. For example, heavy storms can saturate soils rapidly, increase surface runoff, and reduce the proportion of water infiltrating into the substrate. In contrast, prolonged dry periods reduce the soil's water content, limiting baseflow contributions to reservoirs. The combination of these factors leads to higher variability in water balance and challenges for long-term management of post-mining water bodies.

Scientific studies emphasize that climate change interacts with local land use, geology, and hydrology, modifying the effectiveness of existing retention structures. Areas with degraded soils or improperly reclaimed post-mining sites are particularly vulnerable, as their reduced storage capacity cannot compensate for increased evapotranspiration or irregular precipitation patterns. Adaptive management strategies, such as adjusting reservoir operation, enhancing infiltration through soil amendments, or planting drought-tolerant vegetation, are necessary to maintain water balance under changing climatic conditions [10, 31]. Overall, climate change imposes complex, multidimensional pressures on water resources in post-mining landscapes. Its impacts on precipitation, temperature, evapotranspiration, and extreme events highlight the need for integrated water management approaches that consider both natural variability and long-term trends. By understanding these dynamics, it is possible to optimize water retention in reservoirs, reduce vulnerability to droughts and floods, and maintain ecosystem services in reclaimed mining areas.

2.2.5. ANTHROPOGENIC PRESSURE AND LAND USE

Anthropogenic pressure and land use significantly influence water retention in post-mining landscapes and other modified environments. Human activities such as urbanization, industrial development, and agriculture alter the natural hydrological cycle, often reducing infiltration and increasing surface runoff. Intensive land use in catchments surrounding reservoirs leads to soil compaction, reduction of vegetative cover, and disruption of natural drainage patterns, all of which diminish water storage capacity. Urbanization increases the extent of impervious surfaces, such as roads, buildings, and paved areas, which prevents water from infiltrating into the soil, accelerates runoff, and elevates flood risk [10, 32]. Similarly, agricultural activities can degrade soil structure through tillage, overgrazing, and removal of vegetation, reducing the ability of soils to retain water [33].

Mining operations themselves represent a major form of anthropogenic pressure, creating disturbed landscapes that often require reclamation to restore hydrological functions. Infrastructure development, including roads, drainage systems, and industrial sites, alters flow paths within catchments, potentially increasing peak flows into reservoirs and reducing retention times. Reclamation and restoration of post-mining areas often include measures to mitigate these impacts, such as re-vegetation, construction of buffer strips, and creation of retention ponds. Land use changes also influence sediment transport and water quality. Deforested or poorly managed areas increase erosion, leading to sedimentation in reservoirs, which reduces their storage capacity and alters water balance. Urban

and industrial pollutants further affect water quality and may impact vegetation and soil structure, indirectly reducing water retention potential. Population pressure and intensive exploitation of land often result in over-extraction of water for irrigation, industrial use, and domestic consumption, which further decreases the availability of water in reservoirs and catchments [10, 34].

Studies show that integrated land use planning, including maintaining green spaces, protecting riparian zones, and limiting impervious surfaces, significantly improves water retention in both urban and post-mining landscapes. In conclusion, anthropogenic pressure and land use patterns are key determinants of water balance in altered landscapes. Proper management and planning can mitigate negative impacts by enhancing infiltration, reducing runoff, preventing erosion, and maintaining reservoir capacity, ultimately supporting ecosystem services and resilience to climate change.

2.3. SUMMARY

Water retention in post-mining reservoirs is a complex process shaped by geological, hydrological, climatic, and anthropogenic factors. The interaction between substrate composition, catchment hydrology, and reclamation practices determines the long-term stability and functionality of these reservoirs. Effective management requires understanding how soil properties, vegetation cover, and land use influence infiltration, storage, and runoff dynamics. Climate change further modifies these relationships by intensifying extreme weather events and altering precipitation patterns, thereby challenging the resilience of post-mining ecosystems. Anthropogenic pressures, including urbanization, agriculture, and industrial activities, exacerbate degradation processes that reduce retention capacity and water quality. Integrated approaches that combine reclamation, sustainable land management, and adaptive water governance are essential to maintain hydrological balance and ecosystem functions. The synthesis of current research highlights that interdisciplinary strategies are necessary to enhance retention and mitigate environmental risks in transformed mining regions. Ultimately, post-mining reservoirs, when properly managed, can serve as valuable elements of sustainable water resource systems and regional landscape restoration.

REFERENCES

- [1] STACHOWSKI P., KRACZKOWSKA K., OLŚKIEWICZ-KRZYWIACKA A., LIBERACKI D., *Water Reservoirs as an Element of Shaping Water Resources of Post-Mining Areas*, Journal of Ecological Engineering, 2018, Vol. 19, No. 4, 217–225, DOI: 10.12911/22998993/89658.
- [2] SZAFARCZYK A., GAWAŁKIEWICZ R., *An inventory of opencast mining excavations recultivated in the form of water reservoirs as an example of activities increasing the retention potential of the natural environment: a case study from Poland*, Geology, Geophysics and Environment, 2023, Vol. 49, No. 4, 401–418, DOI: 10.7494/geol.2023.49.4.401.

-
- [3] BELLA G., *Water retention behavior of tailings in unsaturated conditions*, Geotechnical and Geological Engineering, 2021, Vol. 26, No. 2, DOI: 10.12989/gae.2021.26.2.117.
- [4] SINGH P.D., KLAMERUS-IWAN A., WOŚ B., PIETRZYKOWSKI M., *Influence of reclamation techniques and vegetation types on water retention in hard coal spoil heaps*, Land Degradation and Development, 2024, Vol. 35, No. 14, 4343–4351, DOI: 10.1002/ldr.5226.
- [5] JAWECKI B., DĄBEK P.B., PAWĘSKA K., WEI X., *Estimating Water Retention in Post-mining Excavations Using LiDAR ALS Data for the Strzelin Quarry in Lower Silesia*, International Journal of Mine Water, 2018, Vol. 37, No. 4, 744–753, DOI: 10.1007/s10230-018-0526-0.
- [6] HUNTLEY B.J., *Soil, Water and Nutrients, Ecology of Angola*, Springer, 2023, 127–147, DOI: 10.1007/978-3-031-18923-4_6.
- [7] RUSSELL A.R., *How water retention in fractal soils depends on particle and pore sizes, shapes, volumes and surface areas*, Geotechnique, 2014, Vol. 64, No. 5, 379–390, DOI: 10.1680/geot.13.P.165.
- [8] SINGH P.D., KLAMERUS-IWAN A., PIETRZYKOWSKI M., *Water Retention Potential in Novel Terrestrial Ecosystems Restored on Post-Mine Sites: A Review*, Forests, 2022, Vol. 14, No. 1, DOI: 10.3390/f14010018.
- [9] CEJPEK J., KURÁŽ V., VINDUŠKOVÁ O., FROUZ J., *Water regime of reclaimed and unreclaimed post-mining sites*, Ecohydrology, 2017, Vol. 11, No. 6, DOI: 10.1002/eco.1911.
- [10] SINGH P.D., KLAMERUS-IWAN A., PIETRZYKOWSKI M., *Water Retention Potential in Novel Terrestrial Ecosystems Restored on Post-Mine Sites: A Review*, Forests, 2023, Vol. 14, No. 1, DOI: 10.3390/f14010018.
- [11] SALEH-MBEMBA F., AUBERTIN M., MBONIMPA M., LI L., *Experimental Characterization of the Shrinkage and Water Retention Behaviour of Tailings from Hard Rock Mines*, Geotechnical and Geological Engineering, 2016, Vol. 34, No. 1, DOI: 10.1007/s10706-015-9942-0.
- [12] MUÑOZ-CASTELBLANCO J., DELAGE P., PEREIRA J.-M., CUI Y.J., *The water retention properties of a natural unsaturated loess from Northern France*, Geotechnique, 2012, Vol. 62, No. 2, 95–106, DOI: 10.1680/geot.9.P.084.
- [13] SEKUCIA F., DLAPA P., KOLLÁR J., CERDÀ A., *Land-use impact on porosity and water retention of soils rich in rock fragments*, Catena, 2020, Vol. 195, 104807, DOI: 10.1016/j.catena.2020.104807.
- [14] SAHLAOUI T., RAKLAMI A., HEINZE S., MARSCHNER B., OUFDUO K., *Nature-based remediation of mine tailings: Synergistic effects of narrow-leafed lupine and organo-mineral amendments on soil nutrient-acquiring enzymes and microbial activity*, Journal of Environmental Management, 2024, DOI: 10.1016/j.jenvman.2024.123035.
- [15] DAGENAIS A.-M., AUBERTIN M., BUSSIÈRE B., *Parametric study on the water content profiles and oxidation rates in nearly saturated tailings above the water table*, Reclamation Sciences, 2006, No. 2, DOI: 10.21000/JASMR06020405
- [16] DE ALMEIDA H., GOMES MARQUES M.C., SANT’OVAIA H., MOURA R., *Environmental Impact Assessment of the Subsurface in a Former W-Sn Mine: Integration of Geophysical Methodologies*, Minerals, Vol. 13, No. 1, 2022, DOI: 10.3390/min13010055.
- [17] KOWALCZYK A., JAGUŚ A., *Retencja wody w zróżnicowanych geograficznie zlewniach górskich*, Polish Journal of Materials and Environmental Engineering, 2023, Vol. 6, No. 26, 1–12, DOI: 10.53052/pjme.2023.6.01.
- [18] GASTAUER M., MASSANTE J.C., RAMOS S.J., DA SILVA R.d.S.S., BOANARES D., GUEDES R.S., CALDEIRA C.F., MEDEIROS-SARMENTO P.S., DE CASTRO A.F., PRADO I.G.d.O. et al., *Revegetation on Tropical Steep Slopes after Mining and Infrastructure Projects: Challenges and Solutions*, Sustainability, 2022, Vol. 14, No. 24, art. 17003, DOI: 10.3390/su142417003.

- [19] GAO H., CAI H., DUAN Z., *Understanding the impacts of catchment characteristics on the shape of the storage capacity curve and its influence on flood flows*, Hydrology Research, 2018, Vol. 49, No. 1, 90–106, DOI: 10.2166/nh.2017.245.
- [20] KORDANA-OBUCH S., STARZEC M., SŁYŚ D., *Evaluation of the Influence of Catchment Parameters on the Required Size of a Stormwater Infiltration Facility*, Water, 2023, Vol. 15, No. 1, art. 191, DOI: 10.3390/w15010191.
- [21] GEROY I., GRIBB M.M., MARSHALL H.P., CHANDLER D.G., BENNER S.G., MCNAMARA J.P., *Aspect influences soil water retention and storage*, Hydrological Processes, 2011, Vol. 25, No. 25, 3836–3842, DOI: 10.1002/hyp.8281.
- [22] HALECKI W., ŁYSZCZARZ S., LASOTA J., BŁOŃSKA E., CHATTOPADHYAY S., *Quantifying the Soil Water Storage Capacity of Flysh Catchments Surrounded by Mixed Forests in Outer Carpathians*, Environmental Processes, 2023, Vol. 10, art. 28, DOI: 10.1007/s40710-023-00641-y.
- [23] RABELO U. P., COSTA A. C., DIETRICH J., FALLAH-MEHDIPOUR E., VAN OEL P., LIMA NETO I. E., *Impact of Dense Networks of Reservoirs on Streamflows at Dryland Catchments*, Sustainability, 2022, Vol. 14, No. 21, art. 14117, DOI: 10.3390/su142114117.
- [24] SUN W., SONG X., ZHANG Y., CHIEW F., POST D., ZHENG H., SONG S., *Coal Mining Impacts on Baseflow Detected Using Paired Catchments*, Water Resources Research, 2020, Vol. 56, No. 2, e2019WR025770. DOI: 10.1029/2019WR025770.
- [25] ZHAO X., LI H., LI P., CHEN Y., DAI Q., SHI P., LI X., QU Y., MA J., *Impact of Mining Area Steep Slope Conditions on the Soil and Water Conservation Benefits of Ecological Restoration*, Water, Vol. 17, No. 2, 2025, art. 256, DOI: 10.3390/w17020256.
- [26] WANG X., LIU L., *The Impacts of Climate Change on the Hydrological Cycle and Water Resource Management*, Water, Vol. 15, No. 13, 2023, art. 2342, DOI: 10.3390/w15132342.
- [27] CIAMPITIELLO M., MARCHETTO A., BOGGERO A., *Water Resources Management under Climate Change: A Review*, Sustainability, 2024, Vol. 16, No. 9, art. 3590, DOI: 10.3390/su16093590.
- [28] DUQUE L.-F., O'DONNELL G., CORDERO J., JARAMILLO J., O'CONNELL E., *Analysis of the Potential Impacts of Climate Change on the Mean Annual Water Balance and Precipitation Deficits for a Catchment in Southern Ecuador*, Hydrology, 2025, Vol. 12, No. 7, art. 177, DOI: 10.3390/hydrology12070177.
- [29] EEKHOUT J.P.C., HUNINK J.E., TERINK W., DE VENTE J., *Why increased extreme precipitation under climate change negatively affects water security*, Hydrology and Earth System Sciences, Vol. 22, No. 11, 2018, s. 5935–5946. DOI: 10.5194/hess-22-5935-2018.
- [30] CHEN H., ZHANG Y., LIU Y., *Revealing the response of urban heat island effect to water evaporation and urbanization*, Journal of Hydrology, 2023, Vol. 616, art. 128574. DOI: 10.1016/j.jhydrol.2023.128574
- [31] TWOOD A., SMITH J., BROWN L., *Landscape controls on water availability limit revegetation success in post-mining ecosystems*, Nature Geoscience, 2025, Vol. 18, No. 4, 321–329, DOI: 10.1038/s43247-025-02332-y
- [32] LI C., LIU M., HU Y., SHI T., ZONG M., WALTER M.T., *Assessing the Impact of Urbanization on Direct Runoff Using Improved Composite CN Method in a Large Urban Area*, International Journal of Environmental Research and Public Health, 2018, Vol. 15, No. 4, art. 775, DOI: 10.3390/ijerph15040775.
- [33] KOZŁOWSKI M., OTREMBA K., PAJĄK M., PIETRZYKOWSKI M., *Changes in Physical and Water Retention Properties of Technosols by Agricultural Reclamation with Wheat – Rapeseed Rotation in a Post-Mining Area of Central Poland*, Sustainability, Vol. 15, No. 9, 2023, art. 7131, DOI: 10.3390/su15097131.
- [34] ANTÓN R., RUIZ-SAGASETA A., ORCARAY L., ARRICIBITA F.J., ENRIQUE A., DE SOTO I., VIRTO I., *Soil Water Retention and Soil Compaction Assessment in a Mediterranean Agricultural*

Region: Implications for Climate Change Adaptation Strategies, Agronomy, 2021, Vol. 11, No. 3, Art. 607, DOI: 10.3390/agronomy11030607.

CZYNNIKI WPLYWAJĄCE NA RETENCJĘ WODY W ZBIORNIKACH POEKSPLOATACYJNYCH

Retencja wody w zbiornikach poeksploatacyjnych stanowi kluczowy element gospodarki zasobami wodnymi na obszarach dotkniętych działalnością górnictwem. Zdolność tych zbiorników do magazynowania wody zależy od wielu czynników, w tym od budowy geologicznej, hydrologii zlewni, działań rekultywacyjnych, zmian klimatycznych oraz presji antropogenicznej. Właściwości geologiczne, takie jak przepuszczalność gruntu czy obecność warstw wodonośnych bezpośrednio wpływają na tempo infiltracji i zdolność retencyjną. Cechy zlewni, takie jak nachylenie terenu, pokrycie roślinnością oraz spływ powierzchniowy determinują ilość wody docierającej do zbiorników. Działalność górnictwa oraz następująca po niej rekultywacja terenów mogą znacząco przekształcać krajobraz i bilans hydrologiczny zarówno zwiększając, jak i zmniejszając potencjał retencyjny. Dodatkowo zmienność klimatu, obejmująca m.in. zmiany w rozkładzie opadów i częstotliwości susz, ma istotny wpływ na dostępność wody w tych zbiornikach. Czynniki antropogeniczne, takie jak urbanizacja, rolnictwo czy działalność przemysłowa w otoczeniu zbiorników mogą dodatkowo modyfikować zarówno ilość, jak i jakość retencjonowanej wody. W niniejszym opracowaniu dokonano przeglądu głównych czynników wpływających na retencję wody w zbiornikach poeksploatacyjnych oraz podkreślono znaczenie zintegrowanych strategii monitoringu i zarządzania, które mają na celu optymalizację ich funkcji ekologicznych, rekreacyjnych i hydrologicznych.

3. POTENTIAL SOURCES OF LITHIUM IN POLAND

MATEUSZ SZCZĘŚNIEWICZ¹, DOMINIKA CIAPKA¹,
KONRAD BLUTSTEIN²

¹ Wrocław University of Science and Technology, Faculty of Geoengineering, Mining and Geology,
Wybrzeże S. Wyspiańskiego 27, 50-370 Wrocław, Poland.

² Graduate of the Wrocław University of Science and Technology, Faculty of Geoengineering,
Mining and Geology, Wybrzeże S. Wyspiańskiego 27, 50-370 Wrocław, Poland.

Access to mineral resources essential for the energy transition is crucial to the implementation of the European Green Deal strategy. However, their extraction is often highly concentrated in a few countries, which poses a supply risk. Ensuring stable and long-term lithium supplies within the European Union is particularly important for Poland, which in recent years has maintained its position as the largest exporter of lithium-ion batteries in the EU. According to the Polish Economic Institute, in the first quarter of 2025, Poland retained its leading position in the EU, accounting for 20% of total lithium-ion battery exports. Currently, Poland significantly contributes to reducing the European automotive industry's dependence on lithium-ion batteries produced and supplied by China. To strengthen the potential of the Polish battery sector, joint efforts are required. Continuous exploration of raw materials necessary for the production of cell and battery components within Poland is essential. Regarding lithium, the greatest potential in Poland lies in brines extracted during copper and crude oil production. Additionally, the development of battery recycling technologies is key to establishing a closed-loop system for production, operation, and disposal, as well as to reinforcing Europe's lithium value chain. This review provides a comprehensive overview of the current state of lithium extraction, reserves, resources, and demand, with a particular focus on potential lithium sources in Poland.

Keywords: lithium, lithium deposits, critical raw materials, Poland

3.1. INTRODUCTION

Lithium is a chemical element belonging to the alkali metal group, situated in the first group of the periodic table. It is a light metal with atomic number 3 and the symbol Li. Lithium is a relatively rare element on Earth, however, it possesses numerous useful chemical properties that make it unique and significant in the field of science and technology [1].

Lithium is one of the most economically significant elements of the 21st century. This is attributed to its possession of the highest electrochemical potential among met-

als, which is utilised for energy storage [1, 2]. Lithium-ion batteries serve as the primary source of energy for portable devices such as smartphones and laptops, as well as the increasingly popular electric means of transport [3]. Lithium also finds applications in medicine, glass and ceramics production, and the production of special metal alloys. Liquid lithium is used as a coolant in nuclear reactors. Furthermore, lithium is an excellent conductor [4–6].

In 2020, the European Union included lithium, along with bauxite, titanium, and strontium, on the list of Critical Raw Materials. Lithium is also considered a critical or strategic raw material in the United States and the United Kingdom [7].

Poland, as a large country located in the heart of Europe, should have the capability to secure at least a modest supply of a wide range of raw materials in times of crisis to enhance the nation's security [8]. Lithium is assuming an increasingly crucial role in the global economy, and in the event of supply chain disruptions, Poland should ensure a source of this metal to cover, to some extent, a part of the demand in critical and strategic areas of national security. Lithium minerals were first identified as a key raw material for the Polish economy in 2016 [9]. In Poland, they hold particular significance for the defence industry and innovation technologies [7]. Poland plays a pivotal role in the battery sector's supply chain. Europe's largest lithium-ion battery factory is currently operational in Biskupice Podgórne near Wrocław, launched by LG Energy Solution [10].

Imports covered 100% of the demand for lithium (oxides, hydroxides, and lithium carbonate) in Poland [7, 11, 12]. The value of imports was in the range of USD 1-5 million in most years, but after 2020, there was a sudden increase in the value of imports, which, for example, in 2022 reached over USD 87 million [12]. This is a direct result of the absence of domestic deposits or industrial facilities producing lithium compounds.

The main objective of this paper is to provide a comprehensive overview of potential lithium sources in Poland. The article aims to identify and discuss various types of lithium occurrences, including hard-rock deposits, brines, clays, and secondary sources such as recycling, and to assess their potential significance for Poland's raw material security. Moreover, the study seeks to highlight opportunities and limitations for future lithium exploration and recovery within the country.

3.2. LITHIUM IN THE WORLD

According to information compiled and disseminated by the U.S. Geological Survey [13], there was a notable increase in global lithium production during the year 2024, hitting 240 000 tons (t) of lithium content (this data excludes U.S. production), which is over 36 000 t more than in 2023 (204 000 t).

Currently, the global lithium production market is predominantly dominated by Australia, Chile, and China, collectively accounting for more than 70% of the total output.

In 2021, global lithium production exceeded 100 000 t for the first time, and over just three years it rose rapidly to nearly 240 000 t by 2024, representing a 140% increase. This growth is driven by strong demand from the lithium-ion battery market, elevated lithium prices from 2021 to early 2023, and an expansion of global lithium production capacity. Since 2013, Australia has remained the leader in mine production of lithium, surpassing Chile in annual output. In 2024, global lithium production unfolded as follows (in tons, [13]): Australia (88 000), Chile (49 000), China (41 000), Argentina (18 000), Brazil (10 000), Zimbabwe (22 000), Canada (4300), Portugal (380), and the USA (exact data unavailable). The largest year-on-year increases in lithium production were recorded by Argentina, Chile and Zimbabwe, with output rising by 9370 t, 7600 t, and 7100 t, respectively. Portugal is the only European Union country involved in lithium mining, with a production level of 380 t [13]. Figure 1 illustrates the change in mining production from 1995 to 2024. There is a noticeable sharp increase in lithium production after 2016, undoubtedly influenced by the growing demand for lithium-ion batteries used in the increasing number of electric vehicles. By the end of 2024, the USGS estimated the global lithium reserves at 30 million tons [13].

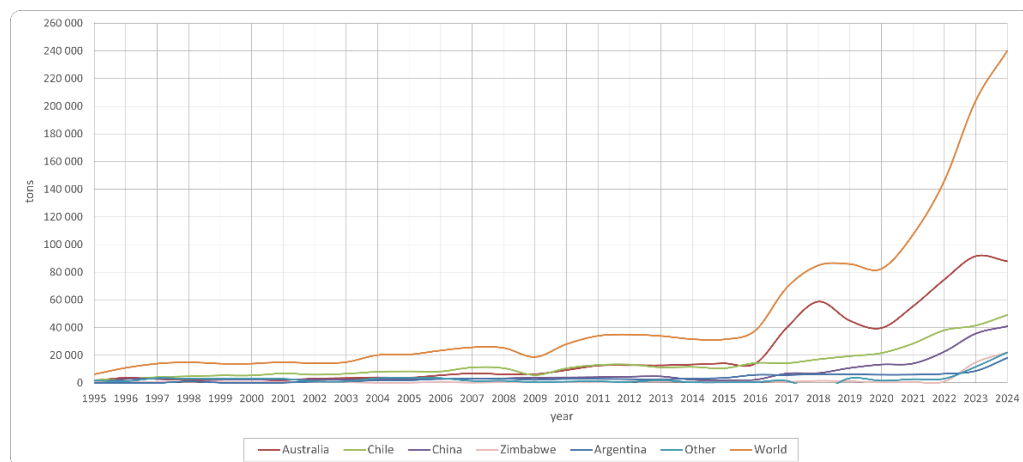


Fig. 1. Mining production of Lithium from 1995 to 2024 for Australia, Chile, China, Zimbabwe, Argentina and other countries, as well as the total global production (based on USGS data from 1996 to 2025 [13])

The largest reserves of lithium were identified in (in tons, [13]): Chile (9 300 000), Australia (7 000 000), Argentina (4 000 000), China (3 000 000), the USA (1 800 000), and Canada (120 000). Chile holds the world's largest lithium reserves and is the world's second-largest producer. In 2024, the most significant year-on-year additions to lithium reserves were recorded in Australia, with an increase of 800 000 t, followed by the United States, which added 700 000 t [13].

Figure 2 illustrates the known world's reserves from 1995 to 2024. Based on the presented data, it is evident that after 2008, the base of economically significant resources (reserves) significantly increased, and since 2018, reserves in countries other than Chile, Australia, Argentina and China, which are also major lithium producers, have been on the rise.

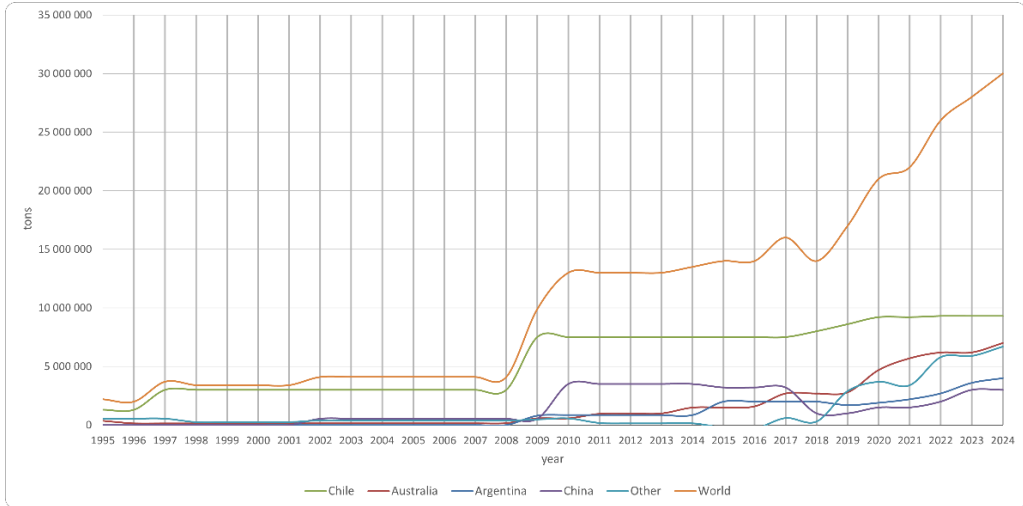


Fig. 2. Lithium reserves from 1995 to 2024 for Chile, Australia, Argentina, China, and other countries, as well as the total global reserves (based on U.S. Geological Survey data from 1996 to 2025 [13])

Drawings, According to data published by the USGS [13], global lithium resources reached 115 000 000 tons in 2024 (this data excludes U.S. production), representing a year-on-year increase of slightly over 9%. The largest potential resources were identified in (in tons, [13]): Bolivia (23 000 000), Argentina (23 000 000), the USA (19 000 000), Chile (11 000 000), Australia (8 900 000), China (6 800 000), and the European Union (7 205 000). Resources in other countries total 35 095 000 t [13]. As in 2023, the largest lithium reserves remained concentrated in Bolivia and Argentina, with both countries holding approximately 23 million tons each. The United States recorded the most substantial increase, with resources rising from 14 million to 19 million tons.

Figure 3 illustrates the known lithium resources from 1995 to 2024. Based on the presented data, it is evident that the number of identified lithium deposits significantly increased after the year 2008. New lithium resources have also been discovered within the European Union (in tons, [13]): Germany 4 800 000, Czech Republic 1 300 000, Spain 320 000, Portugal 270 000, Finland 55 000, Austria 60 000). A significant expansion in lithium resources has also been recorded in several other countries, including Canada (5 700 000 tons), Congo (3 000 000 tons), Mexico (1 700 000 tons), and Mali (1 200 000 tons) [13].

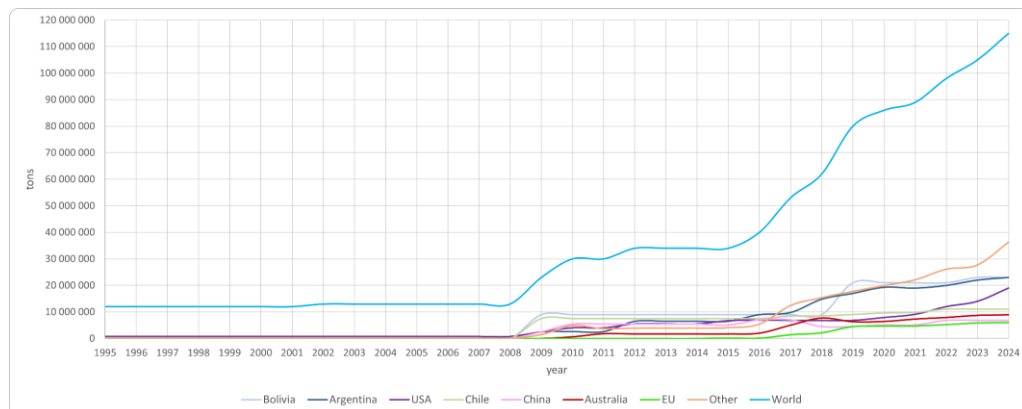


Fig. 3. Lithium resources from 1995 to 2024 for Bolivia, Argentina, USA, Chile, China, Australia, the European Union, and other countries, as well as the total global resources (based on U.S. Geological Survey data from 1996 to 2025 [13]).

Figure 4 illustrates the projection for the total demand for lithium until 2050 based on three scenarios. These scenarios assume an increase in demand for lithium by three to eight times by 2050. The production of electric vehicles will have the greatest impact on the increase in demand for lithium.

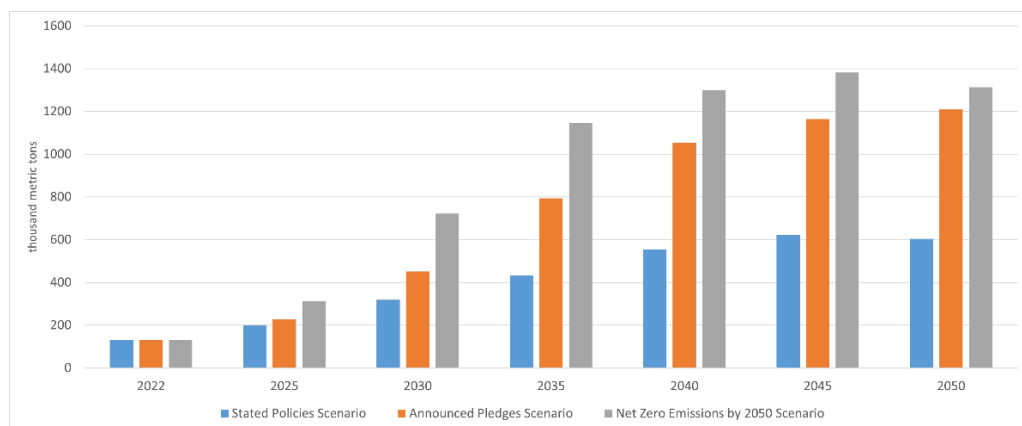


Fig. 4. Total demand projection for lithium (based on IAE data:
<https://www.iea.org/data-and-statistics/data-tools/critical-minerals-data-explorer> [14])

In Europe, lithium is present in various types of deposits ranging in age from the Precambrian to the Miocene. Approximately thirty hard-rock deposits have been identified, such as lithium-caesium-tantalum (LCT) pegmatites, rare-metal granites (RMG), and greisen [6]. European deposits, both currently exploited and prospective, are located in

the following countries: Austria (Wolfsberg), Czech Republic (Cinovec), Finland (Emmes, Hirvikallio, Kietyönmäki, Länttä, Leviäkangas, Outovesi, Rapasaari, Syväjärvi), France (Beauvoir, Chédeville, Montebbras, Tréguennec – Prat-ar-Hastel, Tréguennec – Tréluan), Germany (Altenberg, Cornelia Mine, Sadisdorf, Silbergrube, Zinnwald), Ireland (Aclare), Portugal (Alijo, Alvarrões, Argemela, Guarda-Goncalo, Mina do Barroso, Romano/Sepe-da), Serbia (Jadar), Spain (Alberta I, Fregenda-Almerenda area, Valdeflórez/San José), Ukraine (Polokhovskoe, Shevchenkovskoe, Stankovaskoe), United Kingdom (Meldon aplite quarry, St. Austell) [6]. Additionally, rocks hosting lithium-bearing minerals have also been identified in Norway, Poland, Slovakia, Sweden, and Switzerland [6, 15].

Lithium is extracted from two types of deposits: brines, for which the Li_2O content is approximately 0.1%, and hard-rock deposits, for which the Li_2O content varies between 0.6 to 1.0% [6]. Australia stands as the primary global provider, extracting lithium predominantly from hard rock mines [16]. The lithium recovery from brine deposits is approximately 97%, while from hard-rock deposits, it is around 94% [2]. Brine deposits being under exploitation are primarily found in tectonically active Quaternary basins in arid or hyper-arid climates, resulting from rapid evaporation. The source of lithium in such deposits varies depending on the brine, but it is mostly derived from the weathering of lithium-rich rocks and local hydrothermal activity [6]. Argentina, Chile, and China predominantly derive their production from salt lakes [16].

3.3. POTENTIAL SOURCES OF LITHIUM

According to Bukowski and Czapkowski [17], industrial significance may be associated with waters containing lithium in concentrations exceeding 10 mg/dm^3 , while Sun and Ma [18] suggest a threshold of 13.1 mg/dm^3 . Various cut-off grades are also known in the literature for different projects, such as 0.80% for the underground mine and 0.43% Li_2O for the open pit mine in the Whabouchi project in Canada. In the Kaliber project in Finland, the cut-off grade is 0.5% of Li_2O , while in the Sonora project in Mexico, it is 1200 ppm of Li. The Pilgangoora project in Australia has a cut-off grade of 0.43% of Li_2O . In the case of brines, the Cauchari-Olaroz project in Argentina has a cut-off grade of 354 mg/dm^3 [2]. Of course, the cut-off grade is not a universal indicator of the profitability of every project. Profitability is influenced by many factors, including the mining method, deposit conditions, and the presence of associated minerals. Nevertheless, such data provide us with a general overview of the situation.

Until recently, the primary sources of lithium in the global economy were hard-rock deposits, primarily lithium-bearing minerals such as amblygonite ($\text{LiAl(PO}_4\text{)F}$), lepidolite ($\text{KLi}_2\text{Al(Si}_4\text{O}_{10}\text{)(F,OH)}_2$), petalite ($\text{LiAl(Si}_4\text{O}_{10}\text{)}$), and spodumene ($\text{LiAlSi}_2\text{O}_6$) [6]. Currently, the main sources of lithium are brines rich in lithium carbonate and lithium chloride. Economically significant sources of lithium can also be found in highly mineralized underground waters (brines), geothermal waters, granitic pegmatites, clays, zeolites, and

saline lakes. Lithium is also present in seawater, however, its low concentration (approximately 0.2 ppm) makes this source economically unfeasible [4].

It is worth noting that there may be significant concentrations of lithium in coastal waters and sediments. In Portugal, Ria de Aveiro, the concentration of lithium in seawater is in the range 251–300 ppm, and for Baltic sea sediments, the lithium concentration is in the range 20–50 ppm [19].

3.3.1. ROCKS

In Poland, there are no known lithium deposits of significant mining importance [20]. Lithium occurrences have been reasonably well documented in the Zechstein potash-bearing deposits, but the lithium content is low, and researchers have deemed its extraction economically unviable. The highest recorded lithium content for sulphate K-Mg salts (polyhalite) ranged from 15.1 to 59.6 mg/kg (mean 26.3) [21]. It is worth mentioning that spodumene ($\text{LiAlSi}_2\text{O}_6$) has been observed in Potash-Bearing Deposits. Other potential sources of lithium from rocks in Poland include LCT pegmatites in Michałkowa in the Sowie Góry Block, associated with the Variscan orogeny [6] and pegmatites from the Piława Górna and Lutomia quarries [22]. However, the Polish Geological Institute emphasises that, as yet, there are no prospects for discovering economically significant lithium deposits in Poland. The presence of zinnwaldite ($\text{KLi}_2\text{AlSiO}_4\text{O}_{10}(\text{F},\text{OH})_2$) has also been observed in Kostrzyca [5]. Rock deposits can be enriched manually, by gravity, or by flotation [23].

3.3.2. BRINES

Groundwaters, particularly brines, can serve as sources of various raw materials, including lithium, iodine, bromine, boron, and strontium [24]. Geothermal waters, geothermal brines, and oilfield brines are considered potential sources, although current technology does not yield satisfactory results. In Europe, such deposits are likely to be found in Iceland (Reykjavik area), Italy (Cesano), and France (Alsace) [15].

The concentration of lithium in groundwater depends on the lithium content in the geological formations through which the water flows [24] reported that Mesozoic brine deposits in Poland contain an average of $2.12 \text{ mg/dm}^3 \text{ Li}^+$, with a median of 1.31 mg/dm^3 , and a range is from 0.0 to 14.6 mg/dm^3 . Furthermore, they found that Li^+ content increases with the depth of groundwater and that the richest in lithium groundwater sources are found at depths exceeding 1500 meters.

The highest lithium concentrations, exceeding 100 mg/dm^3 , were observed in Zechstein waters [17]. Elevated lithium levels have also historically been observed in mineral waters in the Outer Carpathians (up to 26.5 mg/dm^3) and along the Baltic Sea coast (up to 10 mg/dm^3) [4].

Razowska-Jaworek [25] emphasized that the lithium concentrations in the waters they studied ranged from 0.005 to 100.0 mg/dm³. However, it should be noted that 70% of the measurements were below 2.0 mg/L. The highest lithium concentrations were recorded in waters from the PGNiG (Polish Oil and Gas Company) well Bogdaj–Uciechów, other PGNiG wells in the Wielkopolska region, the salt mine in Kłodawa, and in concentrated brine from the Dębieńsko plant. In these locations, the concentrations exceeded 10 mg/dm³, which is considered a promising threshold for potential lithium recovery from water sources.

Lithium sources can include brines that are already extracted due to the necessity of dewatering coal and copper mines. In 2008, research results on mine waters from the coal mines of Kompania Węglowa S.A., Centralny Zakład Odwadniania Kopalń (CZOK), and the dewatering areas of copper ore mines were published. Samples from coal mining waters did not yield promising results. The highest measured lithium content was 5.85 mg Li/dm³ in a sample from KWK Knurów. However, the determined lithium content in the KGHM copper mines was significantly higher. The most promising waters appear to be those from ZG Polkowice-Sieroszowice 1 (23.3 mg/dm³), ZG Polkowice-Sieroszowice 2 (10.1 mg/dm³), and ZG Rudna 2 (11.0 mg/dm³) [11]. Lithium resources from dewatering ZG Polkowice-Sieroszowice were estimated at approximately 3800 tonnes Li₂O/year [11]. Even higher lithium concentrations in mining waters in the Copper Basin were published in 2017 by Chudy and Worsa-Kozak [26]. Out of 47 measurements, lithium ranged from 5.23 to 74.00 mg/dm³, with a clear increase in lithium content with the depth of the brine occurrence. The relatively high lithium concentrations in mining brines suggest the possibility of their utilization with existing technology. However, in the case of mine dewatering waters, the challenge lies in their extraction at a stable rate and chemical composition. This is due to the way in which these brines get into the mining excavations [26].

A significant European initiative focused on lithium recovery from brines was the BrineRIS project, co-financed by EIT Raw Materials and carried out between 2022 and 2024. Efforts to extract lithium from brines, including in Poland, were conducted within the framework of this project, which aimed to enhance the capacity of RIS countries to recover valuable metals, particularly lithium, from geothermal brines. The consortium identified promising sources of highly mineralised waters in Poland, Hungary, Spain, Slovakia, Belgium, Germany, and Finland, while promoting sustainable mining practices and innovative recovery technologies to strengthen Europe's raw material supply chain for battery manufacturing. During the project, researchers utilised open-access geological and environmental datasets to map potential brine resources, organised training programs for professionals and students, and tested direct lithium extraction (DLE) methods along with technologies for recovering other critical raw materials from the EU 2023 CRM list. Furthermore, BrineRIS produced a case study for the European Raw Materials Alliance (ERMA) and developed an interactive digital platform designed to attract investment to regions with identified geothermal

potential [2, 27, 28]. The results obtained during the project were used by Razowska-Jaworek [29] to compile a dataset of brines with lithium concentrations exceeding 50 mg/dm^3 . Among these, 50% of the sampling sites showed lithium contents greater than 100 mg/dm^3 , with the highest concentration recorded in the Wyrzysk IG-1 bore-hole (290 mg/dm^3).

In Polish conditions, prospective sources of lithium could also be the brines co-occurring with hydrocarbon deposits, which are extracted in conjunction with crude oil and natural gas production. Extracting lithium from these sources would enhance the efficiency of hydrocarbon exploitation and significantly bolster Poland's raw material security [4]. The presence of lithium in brines co-occurring with hydrocarbons at levels ranging from 1 to 100 ppm was demonstrated as early as 1969, based on 823 oil-field water samples [30]. Besides lithium, the occurrence of other metals, such as rubidium, caesium, manganese, strontium, barium, copper, zinc, and cadmium, has also been described [31]. As evidence of the prospects of such deposits, research on lithium and other element recovery from oil-field waters is ongoing in China and Canada [4].

Unfortunately, reservoir waters co-occurring with hydrocarbon deposits have not been subjected to detailed chemical analysis, including lithium content, or the results have not been published. However, considering the data on lithium content in waters associated with hydrocarbon deposits and the information regarding medicinal waters from their vicinity, an enrichment of lithium in these sources can be expected [4]. Nevertheless, methods for the preparation (purification) of oilfield brines for further lithium recovery using combined sorption and membrane techniques are also being developed. Research efforts are underway as part of the CompLithium project [32].

Lithium contained in brines can be enriched thermally or chemically. In the case of chemical enrichment combined with flotation, lithium chloride-rich brines with a LiCl content of 0.021% (0.32 g/dm^3) can yield a concentrate with a lithium oxide (Li_2O) content of 20–22% and a 90% efficiency [23]. There are also other potential methods for lithium extraction from brines, including precipitation, chromatography, ion-exchange, liquid-liquid extraction, liquid-liquid extraction using ionic liquid, and membrane process [33].

The recovery of lithium from waters in Poland remains at the R&D stage, including both technical and legal analyses. Currently, there is no industrial facility operating in Poland that extracts lithium from brines or geothermal waters on a commercial scale.

3.3.3. LITHIUM-BEARING CLAYS

While such deposits are not known in Poland, it is worth considering their potential. In nature, Li is associated with minerals such as lepidolite, zinnwaldite, masutomilite, swinefordite, hectorite, cookeite, and jadarite. Currently, Li-bearing clays constitute 7% of the world's lithium resources [34, 35]. According to Malhi [36], the extraction of Li from Li-bearing clay minerals may soon ensure the Li supply and expand the Li market.

The main regions in the world where lithium resources in clays are found include: The Clayton Valley area (USA), The Kings Valley area (USA), The La Ventana area (Mexico), The Sonora area (Mexico), The Jadar area (Serbia), The Ning'wu area (China), and The Wu'chuan-Zheng'an-Dao'zhen area (China). The deposits with the highest lithium content, considering the Li_2O content, are found in the Clayton Valley area ($5.126 \cdot 10^6$ t) and The Sonora area ($3.754 \cdot 10^6$ t) (Benson et al. 2017; Ellis et al. 2018; Gourcerol et al. 2019; Gu et al. 2013; Verley and Vidal 2013; Wang et al. 2020) [6, 37–41].

Lithium-bearing clays, particularly with hectorite, are a promising source of lithium due to their stable distribution and low mining cost [42]. Hectorite was discovered in the United States (California, Nevada/Oregon), Mexico, and Turkey [15]. These clays are often found in carbonate-hosted deposits, which are formed through carbonate weathering-sedimentation [43]. The performance of lithium-modified bentonite, a type of lithium-bearing clay, is superior to that of calcium-sodium bentonite in molding sands [44].

It should be noted that although the extraction of Li from Li-bearing clay minerals seems promising, the production process requires efficient technology and equipment. The most well-known methods for extracting lithium from clays are acidification, salt roasting, and alkalization, with acidification appearing to be the most suitable method due to its high extraction efficiency and low costs [35].

Unfortunately, official data on lithium content in clays in Poland are not currently available. The only available data are from the analyses presented in the publication by Motowicka-Terelak [45]. This study reported the results of lithium content analyses in soils from selected regions of Poland, mainly in the northern and central parts, at depths ranging from 0 to 1.0 m. The research indicated that soils in the Lake Districts (Pojezierza) exhibited the highest lithium content, while those in the lowlands (Niziny) showed the lowest. The lithium content varied from 1 to 39 mg/kg and increased with depth. Hence, there is a need for further research on Polish soils, especially clays, to determine their lithium content.

3.3.4. RECYCLING

Due to the relatively high lithium reserves in the form of brine deposits and hard rock deposits, the global economy has paid limited attention to the possibility of lithium extraction through recycling. In 2012, it was predicted that by 2050, recycling, primarily from lithium batteries, would account for approximately 25% of global production [46]. However, since then, large new lithium deposits have been discovered, and in 2017, it was estimated that lithium reserves would last for about 435 years [47]. This further reduces the motivation for lithium extraction through recycling.

Nevertheless, given the uncertain global situation, including armed conflicts and financial crises, it is once again time for reflection. Should raw materials be acquired

inexpensively from third countries, or should a secure source of raw material extraction be established within one's own territory or in low-risk destabilization ally countries?

The possibilities arising from the recycling of lithium-ion batteries have been the subject of numerous scientific articles. Recycling of batteries used in electric vehicles is considered a future source of valuable raw materials, including lithium and cobalt. Among the recycling methods that can be used to obtain lithium are pyrometallurgical recovery, physical materials separation, hydrometallurgical metals reclamation, direct recycling, and biological metals reclamation. The highest level of recovery is achieved with direct recycling, but it is a very costly process. Hydrometallurgical metals reclamation is intermediate, while pyrometallurgical recovery may not perform as well in terms of manganese and lithium recovery, but is effective in the recovery of cobalt, nickel, and copper [48].

In recent years, China has heavily invested in battery recycling, establishing hydrometallurgical and pyrometallurgical processes that place its operations among the most efficient and largest globally. According to the International Energy Agency [49], China leads the global battery recycling industry, representing more than 80% of worldwide capacity in both pretreatment and material recovery processes, with a total recycling capacity of approximately 2 000 000 tons per year [50].

Europe holds the second position globally in lithium-ion battery recycling, with Germany, France, and the United Kingdom serving as the principal contributors. Currently, EU member states, together with the United Kingdom, Norway, and Switzerland, recycle approximately 50 000 tons of lithium-ion batteries annually. Forecasts suggest that this figure could increase to between 200 000 and 800 000 tons by 2030, potentially reaching up to 3 300 000 tons per year by 2040 [50]. European companies are playing an increasingly significant role in the lithium-ion battery recycling market. Rapidly advancing projects, numerous announcements of new investments, and the expansion of existing facilities demonstrate that Europe not only possesses a solid technological foundation for battery recycling but is also actively fostering the growth of a strong, domestic recycling sector [51].

In Poland, Elemental Holding received a grant from the Ministry of Science and Higher Education in 2020 to establish a recycling facility dedicated to used lithium-ion batteries. The facility, located in Zawiercie in southern Poland, is operated by Elemental Strategic Metals and represents a key component of Poland's secondary lithium resource base. The plant, which has been operating since last year, has a capacity of 12 000 tons of spent batteries per year, equivalent to around 28 000 electric vehicle battery packs. The facility processes used batteries into so-called "black mass", which is then used in the production of new battery materials. In 2026, the Zawiercie plant plans to launch a commercial-scale lithium recovery installation. In the coming years, Element Group, under the EU Temporary Crisis and Transition Framework (TCTF), will implement another project in Zawiercie [52].

As part of the Polvolt project, a plant for the production of metals used in strategic industries and a battery metal refinery for lithium, nickel, and cobalt will be established. The development of such infrastructure aligns with the requirements of the EU Regulation 2023/1542, which raises the recycling efficiency targets for lithium-based batteries by 2030, making recycling in Poland a crucial part of the country's raw material security strategy and an important complement to the lack of domestic lithium deposits [15, 53–55].

3.4. DISCUSSION

The global lithium market is undergoing a dynamic transformation driven by the rapid electrification of transport and the expansion of renewable energy storage. Although Poland is not a lithium-producing country, the data presented in this paper indicate that the country's geological setting and industrial infrastructure could support the development of secondary or unconventional lithium sources. Compared to major producers such as Australia or Chile, Poland's resources are small, however, they represent an important strategic supplement to imported supplies and align with EU objectives of raw material independence.

From the perspective of resource security, it is crucial that the source of key resources, including lithium, comes from domestic mines or friendly countries with a low risk of trade disruption. Lithium batteries have broad applications, both civilian and military. Figure 5 illustrates the import and export values of lithium compounds from 1993 to 2024. A noticeable surge in lithium imports in 2022 is evident, which corresponds to a sudden increase in lithium value in the global market. In 2024, there is a lower import value due to changes in the lithium prices in the market.

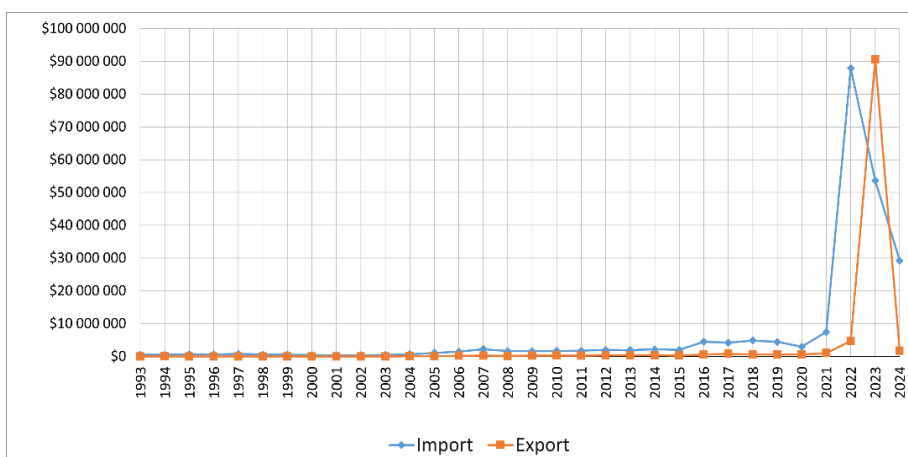


Fig. 5. The value of Polish import and export of lithium compounds (in USD) from 1993 to 2024 [12]

Figure 6 illustrates the average value of imported lithium compounds per kilogram each year from 2008 to 2024. The low stability of price (significant fluctuations) makes it challenging to assess the profitability of commencing production from less abundant sources, let alone prospecting for these sources. Nevertheless, available historical data suggest that lithium recovery from brines is feasible in Poland.

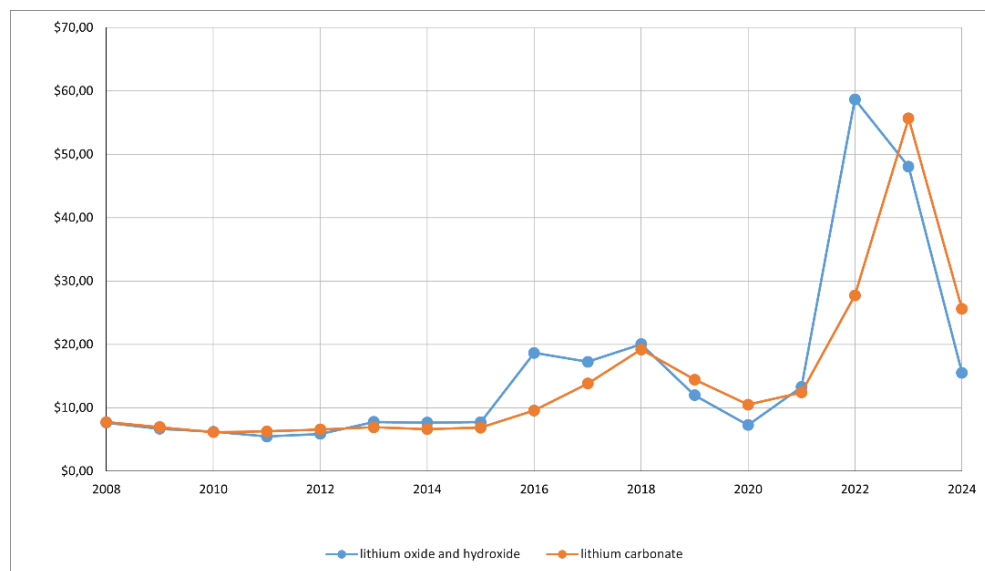


Fig. 6. Price Trends of Lithium Compounds (lithium oxide and hydroxide, and lithium carbonate) per kilogram from 2008 to 2024 (USD) [12]

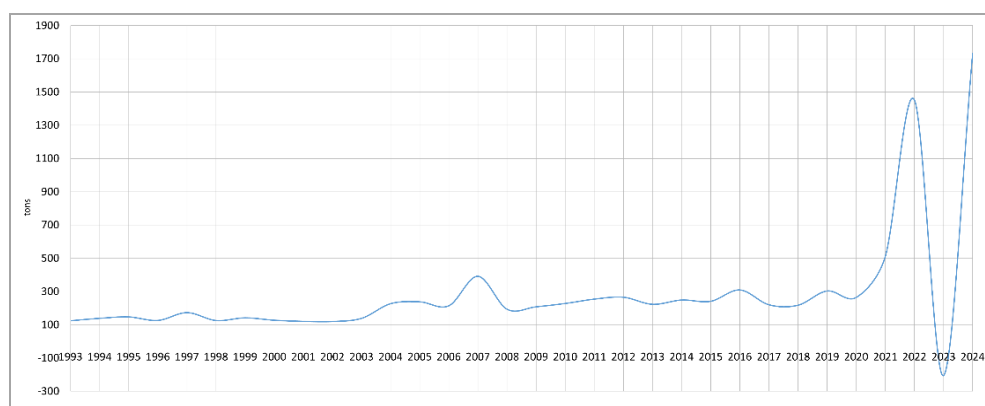


Fig. 7. Domestic Consumption of Lithium Compounds (in tons) in Poland (1993–2024): Import Minus Export [12].

Figure 7 displays the quantity of lithium compounds consumed within the country, calculated as the difference between imports and exports. This figure underscores the growing demand for lithium compounds within the country, emphasizing the need for secure and reliable sources of lithium.

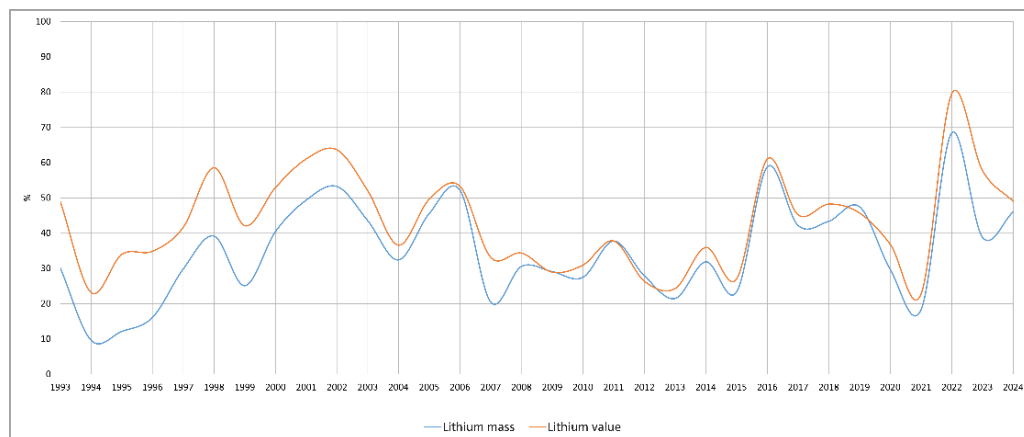


Fig. 8. Percentage Share of Imported Lithium Mass (Blue Line) and Value (Orange Line) in Friendly Countries (NATO, EU, and Full Democracy Nations), 1993–2024 [12]

Figure 8 illustrates the percentage share of the mass and value of imported lithium in friendly countries (NATO, EU, and countries recognized for their full democracies). This data is crucial for understanding the geopolitical implications of lithium sourcing. In 2022, almost 80 wt. % of lithium by mass was imported from safe, stable countries, but in 2021, it was less than 20 wt. %. This value rarely exceeded 50 wt. %.

In the context of technological feasibility, the main challenge lies in the economic recovery of lithium from low-concentration brines. Emerging methods such as direct lithium extraction (DLE) and hybrid membrane-sorption techniques offer promising efficiency but remain at the R&D stage in Poland. The adaptation of such technologies could transform the country's existing brine management systems into a new source of strategic raw materials. Furthermore, integrating lithium recovery with geothermal and hydrocarbon operations could generate additional environmental and economic benefits.

3.5. CONCLUSIONS

While no economically significant lithium source has been confirmed in Poland, a comprehensive scientific examination of available resources, ranging from brines, rocks and groundwater to recycling initiatives, uncovers a diverse spectrum of promising opportunities. These prospects highlight the need for a diversified and forward-looking

approach to ensure stable supplies of this key raw material, consistent with Poland's strategic interests in sustainable resource development and national security.

Geopolitical considerations play a crucial role in Poland's efforts to ensure the security of its lithium supplies. Prioritizing domestic sources of key raw materials like lithium is not only prudent, but also a strategic imperative. Also, by creating collaborative relationships with low-risk partners and developing solid supply chains, Poland can effectively reduce its vulnerability to potential disruptions in the global market. This is also in line with current Western expectations to reduce dependence on China and unstable countries such as Chile [51].

Striving for a diversified raw materials portfolio should be a priority for Poland. This involves continuous exploration of resource potential, including the assessment of existing brine deposits. It is worth noting that, despite an agreement among authors regarding the absence of lithium deposits in Poland, some analyzed brine sources show lithium concentrations exceeding the proposed cut-off grade values: 10 mg/dm³ [17] or 13.1 mg/dm³ [18]. These primarily include underground waters found in copper mines [11, 26]. In the case of mine water extracted because of mine dewatering or co-occurring with hydrocarbons, the initial investment cost would be much lower. These waters are being extracted but are not currently used. Additionally, the country should actively consider assessing other sources, such as hard-rock and clay deposits.

The significance of lithium recycling may gain greater importance. Although lithium recycling is not and is unlikely to be the primary source of this metal, the evolving geopolitical dynamics underscore its significance. Polish investments in lithium-ion battery recycling facilities highlight the commitment to long-term sustainable development and environmental responsibility. By implementing recycling practices, Poland not only reduces its dependence on foreign entities but also contributes to the development of a circular economy that promotes resource protection and minimizes environmental impact, aligning with broader global efforts toward sustainability.

REFERENCES

- [1] BARANOWSKI, M., CICHOWICZ E., KMIŃSKI, P., LEWANDOWSKI M., SOJKA A., ZYBERTOWICZ K., ŻELISKO W., *Baterie litowo-jonowe wciąż najważniejszym hitem eksportowym Polski*. In: I kwartał 2025 r., Tygodnik Gospodarczy PIE, Polski Instytut Ekonomiczny, Warszawa 2025, Retrieved from: <https://pie.net.pl/tygodnik-gospodarczy/>
- [2] STERBA J., KRZEMIEN A., FERNÁNDEZ P.R., GARCÍA-MIRANDA C.E., VALVERDE G.F., *Lithium mining: Accelerating the transition to sustainable energy*, Resources Policy, 2019, 62, pp. 416–426, DOI: 10.1016/J.RESOURPOL.2019.05.002.
- [3] LI M., LU J., CHEN Z., AMINE K., *30 Years of Lithium-Ion Batteries*, Advanced materials (Deerfield Beach, Fla.), 2018, DOI: 10.1002/adma.201800561.
- [4] ULIASZ-MISIAK B., *Water accompanying hydrocarbon deposits as a potential source of iodine, lithium and strontium [Wody towarzyszące złożom węglowodorów jako potencjalne źródło jodu, litu i strontu]*, Gospodarka Surowcami Mineralnymi – Mineral Resources Management, 2016, 32 (2), pp. 31–44, DOI: 10.1515/gospo-2016-0012 (in Polish).

- [5] KAVANAGH L., KEOHANE J., GARCIA CABELLOS G., LLOYD A., CLEARY J., *Global Lithium Sources – Industrial Use and Future in the Electric Vehicle Industry: A Review*, Resources, 2018, 7, DOI: 10.3390/RESOURCES7030057.
- [6] GOURCEROL B., GLOAGUEN E., MELLETON J., TUDURI J., GALIEGUE X., *Re-assessing the European lithium resource potential—A review of hard-rock resources and metallogeny*, Ore Geology Reviews, 2019, 109, 494–519.
- [7] GALOS K., LEWICKA E., BURKOWICZ A., GUZIK K., KOT-NIEWIADOMSKA A., KAMYK J., SZLUGAJ J., *Approach to identification and classification of the key, strategic and critical minerals important for the mineral security of Poland*, Resources Policy, 2021, 70, DOI: 10.1016/j.resourpol.2020.101900.
- [8] KUSTRA A., LORENC S., PODOBIŃSKA-STANIEC M., WIKTOR-SULKOWSKA A., *Value chains in the high-tech raw materials industry- the example of the lithium value chain*, Mineral Resources Management, 2023, 39 (4), pp. 5–22, DOI: 10.24425/gsm.2024.149302.
- [9] KULCZYCKA J., *Key Raw Materials for the Polish Economy*, IGSMiE PAN, Kraków 2016.
- [10] PSPA 2023 – *Europe runs on Polish lithium-ion batteries. The potential of the battery sector in Poland and the CEE Region*, Report. [Online], https://pspa.com.pl/wp-content/uploads/2023/05/PSPA_Polskie_akumulatory_litowo-jonowe_napedzaja_Europe_PL.pdf [Accessed: May 23, 2024].
- [11] FIJAŁKOWSKA A., KUROWSKI R., CZAPLICKA M., *The Polish raw material base of lithium in the context of global trends in the production of lithium carbonate from brines and lithium-bearing thermal waters [Polska baza surowcowa litu w kontekście światowych tendencji produkcji węglanu litu z solanek i litonośnych wód termalnych]*, Rudy i Metale Nieżelazne, 2008, 53 (9), pp. 548–554 (in Polish).
- [12] MIDAS – *System Gospodarki i Ochrony Bogactw Mineralnych Polski MIDAS PIG-PIB 2023 – moduł Gospodarka Surowcami Mineralnymi – dane dotyczące eksportu i importu za: tabulogramy Centrum Analitycznego Izby Administracji Skarbowej w Warszawie*.
- [13] USGS 2024 – *U.S. Geological Survey, Mineral commodity summaries 1996–2024: Lithium*, [Online], <https://www.usgs.gov/centers/national-minerals-information-center/mineral-commodity-summaries> [Accessed: March 28, 2024].
- [14] IEA 2024 – *Critical Minerals Data Explorer*, [Online], <https://www.iea.org/data-and-statistics/data-tools/critical-minerals-data-explorer> [Accessed: March 28, 2024].
- [15] SZLUGAJ J., RADWANIEK-BAK B., *Lithium sources and their current use*, Gospodarka Surowcami Mineralnymi – Mineral Resources Management, 2022, 38, pp. 61–88, DOI: 10.24425/gsm.2022.140613.
- [16] MAXWELL P., *Analysing the lithium industry: Demand, supply, and emerging developments*, Mineral Economics, 2014, 26, pp. 97–106, <https://doi.org/10.1007/s13563-013-0041-5>.
- [17] BUKOWSKI K., CZAPOWSKI G., *Wody mineralne jako źródło surowców chemicznych*. [In:] *Surowce chemiczne na tle geologicznej historii Polski*, 2024, [Online], Available at: http://surowce-chemiczne.pgi.gov.pl/wody_min.htm [Accessed: January 1, 2024] (in Polish).
- [18] SUN Mg., MA Lc., *Potassium-rich brine deposit in Lop Nor basin, Xinjiang, China*, Scientific Reports, 2018, 8, 7676, DOI: 10.1038/s41598-018-25993-6.
- [19] BARBOSA H., SOARES A.M.V.M., PEREIRA E., FREITAS R., *Lithium: A review on concentrations and impacts in marine and coastal systems*, The Science of the total environment, 2023, 857 (Pt. 2), DOI: 10.1016/j.scitotenv.2022.159374.
- [20] WITKOWSKA-KITA B., BIEL K., BLASCHKE W., ORLICKA A., *Analiza możliwości pozyskiwania deficytowych surowców mineralnych w Polsce*, Annual Set The Environment Protection – Rocznik Ochrona Środowiska, 2017, 19, pp. 777–794 (in Polish).
- [21] CZAPOWSKI G., TOMASSI-MORAWIEC H., HANDKE B., WACHOWIAK J., PERYT T.M., *Trace Elements and Mineralogy of Upper Permian (Zechstein) Potash Deposits in Poland*, Applied Sciences, 2022, 12 (14), DOI: 10.3390/app12147183.

- [22] ZGLINICKI K., *Lit. Metale zielonej rewolucji*, Państwowy Instytut Geologiczny, 2025 – PIG, Available at: <https://www.pgi.gov.pl/aktualnosci/display/13364-lit-metale-zielonej-rewolucji.html>
- [23] BLASCHKE Z., *Przeróbka kopalin litowych*, Inżynieria Mineralna, 2007, 9 (2), pp. 62–66 (in Polish).
- [24] ULIASZ-MISIAK B., WINID B., *Brines from the Mesozoic formations of northern and central Poland as a prospective source of chemical raw materials*, *Gospodarka Surowcami Mineralnymi – Mineral Resources Management*, 2018, 34 (2), pp. 5–20, DOI: 10.24425/118655.
- [25] RAZOWSKA-JAWOREK L., PATERNAK M., KARPIŃSKI M., BĘDKOWSKI Z., KACZOROWSKI Z., WYSOCKA I., DRZEWICZ P., *Wstępna ocena możliwości pozyskiwania pierwiastków wartościowych z wód kopalnianych oraz wód termalnych i leczniczych w Polsce*, *Przegląd Geologiczny*, 2022, Vol. 70, No. 6, <http://dx.doi.org/10.7306/2022.13>
- [26] CHUDY K., WORSZA-KOZAK M., *Useful elements in brine flowing into the copper ore mines of the fore-sudetic monocline [Pierwiastki użyteczne w solankach dopływających do wyrobisk kopaliń rud miedzi na monoklinie przedsudeckiej]*, *Biuletyn Państwowego Instytutu Geologicznego*, 2017, 469, pp. 93–104, DOI: 10.5604/01.3001.0010.0076.
- [27] GROMNICKI K., KOWALEWSKA I., SZOSTAK K., WORSZA-KOZAK M., *Geothermal lithium for Europe – review of existing resources and operating projects*, *Book of abstracts XXII Conference of PhD Students and Young Scientists, June 29–July 01, 2022*, Oficyna Wydawnicza Politechniki Wrocławskiej, Wrocław 2022, 37–38.
- [28] GROMNICKI K., KOWALEWSKA I., SZOSTAK K., WORSZA-KOZAK M., *Technological review of lithium recovery from brines – an introduction to the BrinerIS project. Book of abstracts XXII Conference of PhD Students and Young Scientists June 29–July 01, 2022*, Oficyna Wydawnicza Politechniki Wrocławskiej, Wrocław 2022, 39–40.
- [29] RAZOWSKA-JAWOREK L., BURLIGA S., BELZYT S., TOMASZEWSKA B., *Prospects of lithium extraction from geothermal brines and evaporite deposits in Poland*, *Przegląd Geologiczny*, 2025, Vol. 37, No. 3, <http://dx.doi.org/10.7306/2025.29>
- [30] RITTENHOUSE G., FULTON R.B., GRABOWSKI R.J., BERNARD J.L., *Minor elements in oil-field waters*, *Chemical Geology*, 1969, 4, pp. 189–209, DOI: 10.1016/0009-2541(69)90045-X.
- [31] COLLINS A.G., *Geochemistry of oilfield waters*, Elsevier Scientific Publishing Company, Amsterdam 1975.
- [32] KNAPIK E., ROTKO G., MARSZALEK M., *Recovery of Lithium from Oilfield Brines – Current Achievements and Future Perspectives: A Mini Review*, *Energies*, 2023, 16 (18), DOI: 10.3390/en16186628.
- [33] SWAIN B., *Recovery and recycling of lithium: A review*, *Separation and Purifications Technology*, 2017, 172, pp. 388–403, DOI: 10.1016/j.seppur.2016.08.031.
- [34] BULATOVIC S.M., *Beneficiation of Lithium Ores*, *Handbook of Flotation Reagents: Chemistry, Theory and Practice*, 2015, 3, pp. 41–56, DOI: 10.1016/B978-0-444-53083-7.00028-2.
- [35] ZHAO H., WANG Y., CHENG H., *Recent advances in lithium extraction from lithium-bearing clay minerals*, *Hydrometallurgy*, 2023, 217, 106025, ISSN 0304-386X, DOI: 10.1016/j.hydromet.2023.106025.
- [36] MALHI G.S., *Lithium: a global perspective*, *Pharmacopsychiatry*, 2018, 51 (5), pp. 220–221, DOI: 10.1055/a-0581-5100.
- [37] BENSON T.R., COBLE M.A., RYTUBA J.J., MAHOOD G.A., *Lithium enrichment in intracontinental rhyolite magmas leads to Li deposits in caldera basins*, *Nature Communications*, 2017, 8 (1), pp. 270–279, DOI: 10.1038/s41467-017-00234-y.
- [38] ELLIS B.S., SZYMANOWSKI D., MAGNA T., NEUKAMPF J., DOHMEN R., BACHMANN O., ULMER P., GUILLONG M., *Post-eruptive mobility of lithium in volcanic rocks*, *Nature Communications*, 2018, 9 (1), DOI: 10.1038/s41467-018-05688-2.
- [39] GU J., HUANG Z., FAN H., YE L., JIN Z., *Provenance of lateritic bauxite deposits in the Wuchuan–Zheng’an–Daozhen area, Northern Guizhou Province, China: LA-ICP-MS and SIMS U-Pb*

- dating of detrital zircons, *Journal of Asian earth sciences*, 2013, 70, pp. 265–282, DOI: 10.1016/j.jseas.2013.03.018.
- [40] VERLEY C.G., VIDAL M.F., *Preliminary Economic Assessment for the La Ventana Lithium Deposit*, Sonora, Mexico, 2018. Canada: Bacanora Minerals, Ltd.
- [41] WANG D.H., DAI H.Z., LIU S.B., WANG C.H., YU Y., DAI J.J., LIU L.J., YANG Y.Q., MA S.C., *Research and exploration progress on lithium deposits in China*, *China Geology*, 2022, 3 (1), pp. 137–152, DOI: 10.31035/cg2020018.
- [42] MEYER J.M., SWAYZE G.A., KOKALY R.F., STILLINGS L.L., BENZEL W.M., HOEFEN T.M., COX E.M., *Mapping Lithium Bearing Hectorite Clay Using Imaging Spectroscopy*. IGARSS 2023 – 2023 IEEE International Geoscience and Remote Sensing Symposium, Pasadena, CA, USA, 2023, pp. 3708–3709, DOI: 10.1109/IGARSS52108.2023.10282680.
- [43] WEN H., LUO C., DU S., YU W., GU H., LING K., CUI Y., LI Y., YANG J., *Carbonate-hosted clay-type lithium deposit and its prospecting significance*, *Chinese Science Bulletin*, 2019, 65, pp. 53–59, DOI: 10.1360/TB-2019-0179.
- [44] QI-ZHONG C., JIAQI P., YAQIN S., *Experimental Research on Lithium Bentonite Clay Sand*, *Hot Working Technology*, 2011, Issue 7, 18–21, https://caod.oriprobe.com/articles/27295347/Experimental_Research_on_Lithium_Bentonite_Clay_Sand.htm
- [45] MOTOWICKA-TERELAK T., TERELAK H., PIETRUCH Cz., *Content of lithium in soils of some regions of Poland [Zawartość litu w glebach niektórych regionów Polski]*, *Zeszyty Problemowe Postępów Nauk Rolniczych*, 1997, 448b, pp. 211–216 (in Polish).
- [46] RECK B.K., GRAEDEL T.E., *Challenges in Metal Recycling*, *Science*, 2012, 337, pp. 690–695, DOI: 10.1126/science.1217501.
- [47] MARTIN G., RENTSCH L., HÖCK M., BERTAU M., *Lithium market research – global supply, future demand and price development*, *Energy Storage Materials*, 2017, 6, pp. 171–179, DOI: 10.1016/j.ensm.2016.11.004.
- [48] HARPER G., SOMMERVILLE R., KENDRICK E., *Recycling lithium-ion batteries from electric vehicles*, *Nature*, 2019, 575, pp. 75–86, DOI: 10.1038/s41586-019-1682-5.
- [49] INTERNATIONAL ENERGY AGENCY (IEA), *Global Critical Minerals Outlook 2025*, Paris: OECD/IEA, June 2025, Available at: <https://www.iea.org/reports/global-critical-minerals-outlook-2025>
- [50] POLSKI INSTYTUT EKONOMICZNY, *Tygodnik Gospodarczy PIE*, nr 52/2024, Warszawa, 30 grudnia 2024, Available at: https://pie.net.pl/wp-content/uploads/2024/12/Tygodnik-PIE_52-2024.pdf
- [51] FRAUNHOFER INSTITUTE FOR SYSTEMS AND INNOVATION RESEARCH ISI, *Recycling capacities for lithium-ion batteries will exceed demand in Europe for the time being*, *Battery Update Blog*, 24 July 2025, Available at: <https://www.isi.fraunhofer.de/en/blog> [Accessed: 10 October 2025].
- [52] ISBNEWS 2025. Grupa Elemental otrzymała 1,038 mld zł grantu na projekt Polvolt w Zawierciu. Investing.com, <https://pl.investing.com/news/stock-market-news/grupa-elemental-otrzymala-1038-mld-zl-grantu-na-projekt-polvolt-w-zawierciu-1095948> [Accessed: 03.10.2025].
- [53] REGULATION (EU) 2023/1542 of the European Parliament and of the Council of 12 July 2023 concerning batteries and waste batteries (OJ L 191, 28.7.2023).
- [54] BRUNELLI K., LEE L.Y., MOERENHOUT T., *Lithium in the Energy Transition: Roundtable Report*. 2024, [Online], <https://www.energypolicy.columbia.edu/publications/lithium-in-the-energy-transition-roundtable-report/> [Accessed: March 17, 2024].
- [55] ELEMENTAL STRATEGIC METALS, 2025, Company website. Available at: <https://elementalsm.pl/>

POTENCJALNE ŹRÓDŁA LITU W POLSCE

Dostęp do surowców mineralnych niezbędnych dla transformacji energetycznej jest kluczowy dla realizacji strategii Europejskiego Zielonego Ładu. Jednak ich wydobycie często jest silnie skoncentrowane w kilku

krajach, co wiąże się z ryzykiem dostaw. Zapotrzebowanie na lit wzrasta na całym świecie, głównie ze względu na rosnące zapotrzebowanie na samochody elektryczne (EVs). Zapewnienie stabilnych długoterminowych dostaw litu przez Unię Europejską jest istotne dla Polski, która w ostatnich latach utrzymuje pozycję największego eksportera akumulatorów litowo-jonowych w UE. Polska obecnie znacząco przyczynia się do niezależności europejskiego przemysłu motoryzacyjnego od baterii litowo-jonowych produkowanych i dostarczanych przez Chiny. Aby wzmocnić potencjał sektora baterii w Polsce, konieczne są wspólne działania. Należy kontynuować poszukiwania surowców niezbędnych do produkcji komponentów ogniw i baterii na terenie Polski. Niniejszy przegląd przedstawia kompleksowy obraz obecnego stanu wydobycia litu, jego rezerw, zasobów i zapotrzebowania. Autorzy skupili się na potencjalnych źródłach litu na terenie Polski.

4. ASSESSMENT OF BEARING CAPACITY IN BILAYER ROCK MASSES: THE CASE OF OPORTO GRANITE

ANA ALENCAR¹, RUBÉN GALINDO AIRES^{1,2},
MAURO MUÑIZ-MENÉNDEZ³, ANTÓNIO VIANA DA FONSECA²

¹ Universidad Politécnica de Madrid, Madrid, Spain.

² CONSTRUCT-GEO, Universidade do Porto, Porto, Portugal.

³ Laboratorio de Geotecnia, CEDEX, Madrid, Spain.

Traditional approaches to estimating bearing capacity in rock mechanics generally assume a homogeneous and isotropic rock mass. However, rock masses often consist of multiple layers with varying properties or different geotechnical qualities within the same rock matrix. This behavior is clearly observed in the Oporto granite. This study simulates various stratigraphic combinations commonly found in the region and their corresponding ultimate bearing capacities, calculated using the finite difference method (FDM). A parametric analysis is carried out to derive a modified bearing capacity factor as a function of layer thickness and rock mass quality (expressed through GSI). The results are presented in the form of a chart, offering a practical tool for estimating the bearing capacity of bilayer rock masses.

Keywords: rock mass, finite difference method, bearing capacity, Oporto granite, bilayer

4.1. INTRODUCTION

In the city of Porto, northern Portugal, two facies of igneous origin can be found, differentiated according to their mineralogy: a) biotite granites with calcic plagioclase, and b) two-mica granites (Oporto granite). This rock was formed during the third phase of deformation of the Variscan orogeny (D3) [7]. The climatic characteristics associated with high humidity favor the weathering and outcrops of Oporto granite often display different degrees of weathering. The weathering profiles can reach depths of around 20 or even 30 m, being the material composed of quartz, microcline, plagioclase, muscovite and biotite [4, 8, 9].

Paper [1] proposed a correlation factor that allows to estimate the bearing capacity of a rock mass formed by two layers with distinct geological strength index (GSI). It is important to highlight that the GSI was originally developed to characterize the condition of the rock mass, with emphasis on the degree of fracturing and discontinuity surface condi-

tions. Therefore, from a strictly theoretical standpoint, a lower GSI does not necessarily imply a reduction in the uniaxial compressive strength (UCS) of the intact rock.

However, observing some geological formation like the Oporto granite – that is the base of the present study – the variation of GSI is associated to the changes of the uniaxial compressive strength of the intact rock (UCS). Once, in the case of the Oporto granite, the variation in GSI is closely linked to the degree of material weathering and decomposition, which significantly affects the UCS. As the granite weathers, not only does the structure of the rock mass change (justifying a lower GSI), but the intact rock material itself undergoes a substantial loss of strength.

Therefore, considering the different degrees of weathering observed in the Oporto area, the use of a simplified model of a rock mass composed of two layers with distinct GSI and UCS values is proposed. The geotechnical parameters employed in the numerical model were derived from typical values reported for Oporto granite.

This correlation between GSI and UCS – as well as other geotechnical parameters – in the Oporto granite has been documented and analyzed by various authors, including, [2, 3, 6] among others.

4.2. METHODOLOGY

4.2.1. GEOTECHNICAL PARAMETERS

The rock type in this study is granite, which is typically associated with a material constant $m_i = 33$. Based on the available literature [2, 5, 6], the following geotechnical parameters have been associated with different GSI of the granite (Table 4.1).

Table 4.1. Oporto granite parameters

Degree of weathering	UCS [MPa]	GSI	E [GPa]	Dry density [kg/m ³]
W4	10	20	3	2300
		30		
W3	30	20	9	2450
		30		
		50		
W2	70	30	11	2600
		50		
		75		
W1	100	50	25	2650
		75		

Based on the possible combinations listed in Table 4.1, ten different configurations cases were generated and implemented in the numerical analyses (Table 4.2).

Table 4.2. Study cases

Cases	UCS [MPa]	GSI	E [GPa]	ν	Bulk modulus [GPa]	Shear modulus [GPa]	s	mb	a	Dry density [kg/m ³]
1	10	20	3	0.24	1.92	1.21	0.000138	1.8953	0.54372	2300
2	10	30	3	0.24	1.92	1.21	0.000419	2.7088	0.52234	2300
3	30	20	9	0.24	5.77	3.63	0.000138	1.8953	0.54372	2450
4	30	30	9	0.24	5.77	3.63	0.000419	2.7088	0.52234	2450
5	30	50	9	0.24	5.77	3.63	0.003866	5.5333	0.50573	2450
6	70	30	11	0.24	7.05	4.44	0.000419	2.7088	0.52234	2600
7	70	50	11	0.24	7.05	4.44	0.003866	5.5333	0.50573	2600
8	70	75	11	0.24	7.05	4.44	0.062177	13.5130	0.50091	2600
9	100	50	25	0.24	16.03	10.08	0.003866	5.5333	0.50573	2650
10	100	75	25	0.24	16.03	10.08	0.062177	13.5130	0.50091	2650

4.2.2. NUMERICAL MODEL

The same numerical models used by [1] were employed (Fig. 4.1), but with new combinations of geotechnical parameters. In summary, numerical calculations were carried out using two-dimensional models based on the finite difference method, with the commercial software FLAC. The plane strain condition was applied to a symmetrical model, representing only half of the strip footing. The model boundaries were placed far enough to avoid any influence on the results. In all simulations, the rock mass was considered weightless, and both an associative flow rule and a rough interface at the foundation base were adopted.

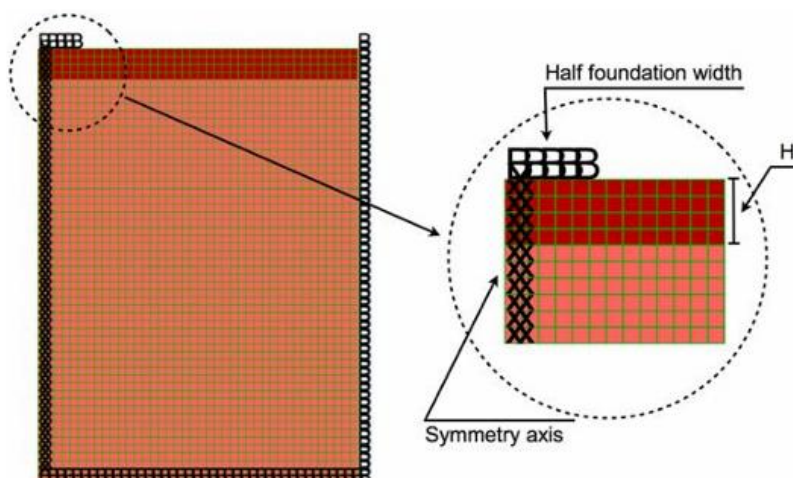


Fig. 4.1. Model used same of [1]

Numerically, it is assumed that the ultimate bearing capacity is reached when the continuous medium can no longer sustain additional load due to the formation of an internal failure mechanism. The load is applied through incremental increases in velocity, and the ultimate bearing capacity is determined from the stress–displacement relationship at a selected node – specifically, the central node of the foundation in this study.

A convergence study is also conducted, which involves analyzing the values of the ultimate bearing capacity obtained using different velocity increment sizes. As the rate of increments decreases, the results converge toward a final value that corresponds to the upper bound predicted by the theoretical method. For each configuration, defined by a distinct combination of geometrical and geotechnical parameters, a separate convergence analysis is performed using various velocity increment values.

The bilayer models were generated by combining the 10 soil layers listed in Table 4.2, resulting in a total of 45 bilayer cases and 10 homogeneous cases analyzed. Each bilayer case was evaluated considering 8 different thicknesses and layer positions (Table 4.3). Like show in Fig. 4.1, the distance from the foundation level to the top of the second layer is denoted as H , while the foundation width is represented by B .

Table 4.3. Summary of the bilayer geometric configuration

	H/B
Weak upper layer	0.33
	0.44
	0.67
	1
Weak bottom layer	0.44
	1
	1.44
	2

4.3. RESULTS

The results are presented following the approach proposed by [1], where the coefficient B_F is defined as the ratio between the bearing capacity of the bilayer rock mass (P_{hB}) and the bearing capacity of the homogeneous and isotropic model formed by the upper layer (P_{hUP}). Table 4.4 show the values obtained.

Therefore, when $B_F = 1$, the bearing capacity of the bilayer rock mass is equal to that of the homogeneous and isotropic material formed by the upper layer ($P_{hB} = P_{hUP}$). In this case, the bottom layer is located at a depth that does not influence the bearing capacity. When $B_F > 1$, it indicates that the weak layer is the upper layer, since the value of P_{hB} is higher than that of the upper layer alone (P_{hUP}). Finally, $B_F < 1$ cor-

responds to cases where P_{hB} is less than P_{hUP} , meaning that the bottom layer is the weaker stratum.

Table 4.4. Summary of result obtained

Cases		$B_F > 1$				$B_F < 1$				$\frac{P_{hUP}}{P_{hBO}}$ (*) (**)
Less resistant	More resistant	0.33	0.44	0.67	1	0.44	1	1.44	2	
1	2	1.39	1.31	1.17	1.0	0.73	0.91	0.99		1.7
1	3	–	1.61	1.20	1.0	0.49	0.75	0.98	1.00	3.0
1	4	–	1.67	1.20	1.0	0.35	0.63	0.92	1.00	5.0
1	5	–	–	–	–	–	–	–	–	
1	6	–	1.67	1.20	1.0	0.20	0.45	0.75	1.01	11.6
1	7	–	1.67	1.20	1.0	0.12	0.34	0.62	1.00	25.9
1	8	–	1.67	1.20	1.0	0.08	0.25	0.51	1.00	65.3
1	9	–	1.67	1.20	1.0	0.10	0.30	0.57	1.01	36.8
1	10	–	1.67	1.20	1.0	0.06	0.23	0.47	1.00	93.3
3	4	1.39	1.31	1.17	1.0	0.74	0.92	1.00		1.7
3	5	–	–	–	–	–	–	–		
3	6	–	1.67	1.20	1.0	0.42	0.71	0.97		3.9
3	7	–	1.67	1.20	1.0	0.25	0.53	0.83	1.00	8.6
3	8	–	–	1.20	1.0	0.15	0.37	0.66	1.00	21.8
3	9	–	–	1.20	1.0	0.20	0.46	0.76	1.00	12.3
3	10	–	1.67	1.20	1.0	0.12	0.33	0.60	1.00	31.1
2	3	1.44	1.33	1.15	1.0	0.68	0.88	1.00		1.8
2	4	1.87	1.56	1.17	1.0	0.49	0.75	0.98		3.0
2	5	–	–	–	–	–	–	–		
2	6	2.17	1.59	1.17	1.0	0.27	0.53	0.83	1.01	6.9
2	7	2.17	1.59	1.17	1.0	0.16	0.39	0.68	1.00	15.5
2	8	2.17	1.59	1.17	1.0	0.10	0.28	0.54	1.00	39.2
2	9	2.17	1.59	1.17	1.0	0.13	0.34	0.62	1.01	22.1
2	10	2.17	1.59	1.17	1.0	0.08	0.25	0.50	1.00	56.0
4	5	1.63	1.46	1.17	1.0	0.60	0.84	0.99	0.99	
4	6	1.67	1.47	1.17	1.0	0.59	0.83	1.00		2.3
4	7	–	1.59	1.17	1.0	0.34	0.62	0.91	1.00	5.2
4	8	–	1.59	1.17	1.0	0.19	0.43	1.00		13.1
4	9	–	1.59	1.17	1.0	0.27	0.54	0.84	1.01	7.4
4	10	–	1.59	1.17	1.0	0.15	0.38	0.66	1.00	18.7
6	7	1.63	1.46	1.18	1.0	0.61	0.85	1.00		2.2
6	8	–	1.60	1.18	1.0	0.34	0.62	0.90		5.7
6	9	1.93	1.59	1.18	1.0	0.48	0.76	0.99		3.2
6	10	2.19	1.60	1.18	1.0	0.26	0.53	0.83		8.1

Table 4.4 continued

5	6	—	—	—	—	0.97	1.00	1.00		
5	7	1.64	1.45	1.14	1.0	0.58	0.82	0.99		1.0
5	8	2.04	1.52	1.15	1.0	0.31	0.58	0.87	1.00	2.3
5	9	1.90	1.52	1.14	1.0	0.46	0.73	0.98	1.00	5.8
5	10	2.04	1.52	1.14	1.0	0.25	0.50	0.79	1.00	8.3
7	8	1.73	1.48	1.16	1.0	0.56	0.81	1.00		2.5
7	9	1.26	1.21	1.11	1.0	0.81	0.95	1.00		1.4
7	10	1.97	1.54	1.16	1.0	0.44	0.71	0.97		3.6
9	8	1.45	1.33	1.15	1.0	0.71	0.91	1.00		1.8
9	10	1.73	1.50	1.16	1.0	0.56	0.81	1.00		2.5
8	10	1.27	1.21	1.12	1.0	0.81	0.95	1.00		1.4

(*) Considering the up layer the more resistant.
(**) P_{hBO} equal to the bearing capacity of the bottom layer.
[—] Due to numerical instability, valid results were not achieved.

Figure 4.2 presents the new results obtained in this study, while Fig. 3 shows the chart proposed by [1].

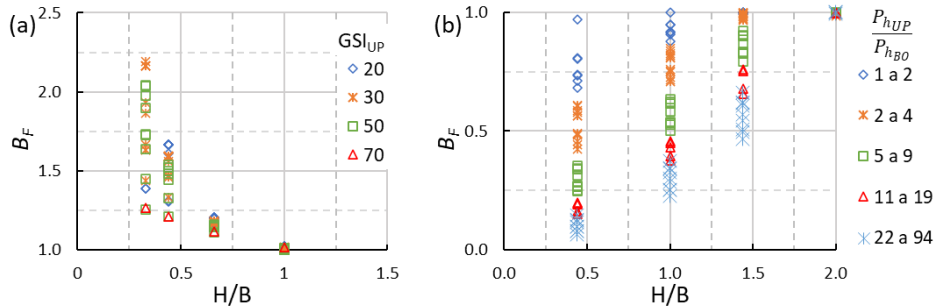


Fig. 4.2. Results of Oporto granite: (a) $B_F > 1$, (b) $B_F < 1$

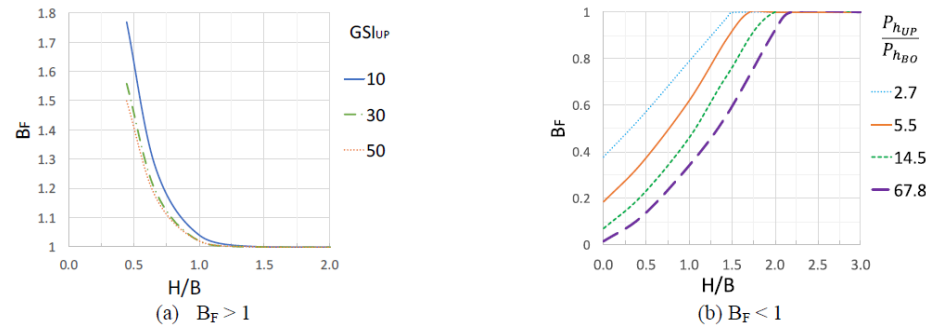


Fig. 4.3. Chart proposed by [1]

By observing Fig. 4.2b, it is evident that a wide range of $\frac{P_{h_{UP}}}{P_{h_{BO}}}$ ratios have been studied. Therefore, a new way of presenting the data for cases with $B_F < 1$ is proposed, as shown in Fig. 4.4.

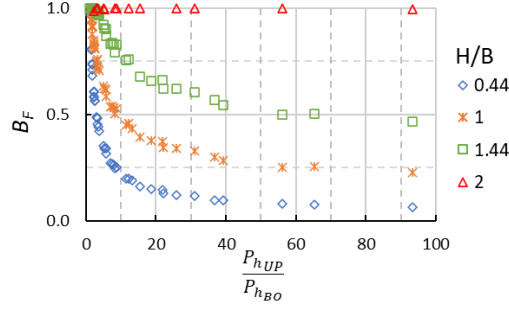


Fig. 4. Results of Oporto granite ($B_F < 1$)

4.4. ANALYSIS OF RESULTS

With the new combinations of geotechnical parameters adopted, the effect of the $\frac{P_{h_{UP}}}{P_{h_{BO}}}$ ratio on the B_F factor could be observed more clearly. In the cases where $B_F > 1$, it becomes evident that there is an upper limit to the increase in bearing capacity, which depends on the GSI. This limit is reached when $\frac{P_{h_{UP}}}{P_{h_{BO}}} \geq 3.5$. In cases where this difference is smaller, as previously noted by [1], it is not recommended to use the B_F chart.

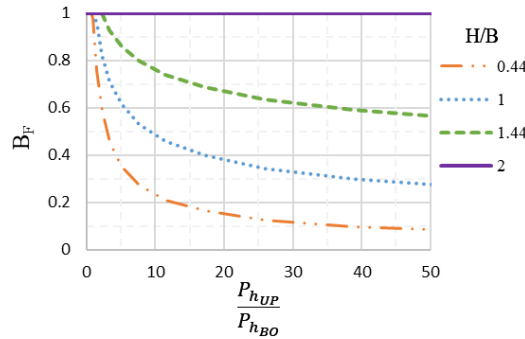


Fig. 4.5. New chart proposed for $B_F < 1$

On the other hand, in cases where $B_F < 1$, if the results are presented in the same manner as [1], the interpretation is not clear. However, a new way of presenting the results for $B_F < 1$ is proposed in Fig. 4.4, based on the ratio $\frac{P_{h_{UP}}}{P_{h_{BO}}}$, where a clear trend can be observed. Figure 5 shows the results in the form of a chart that allows for easier interpretation and practical use.

4.5. DISPLACEMENT ANALYSIS

According to the literature [1], when the bottom layer is the stronger stratum, the stress bulb tends to be reduced. This can be observed in the results, since the depth at which the B_F acts is greater when the bottom layer is the weaker stratum.

On the other hand, from a graphical perspective, it can also be seen that when the upper stratum is the weaker one, the failure wedge formed is considerably smaller than in the case with the same geotechnical parameters but with the layers inverted (Fig. 4.6).

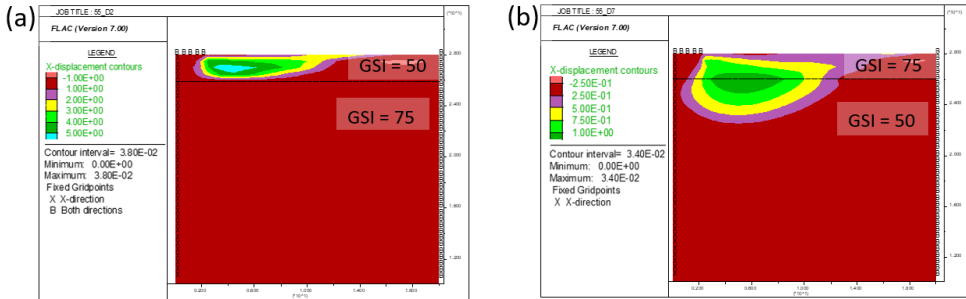


Fig. 6. The variation of horizontal displacements obtained by FDM under the foundation:
(a) the weak layer is up, (b) the weak layer is in the bottom (UCS = 100 MPa)

4.6. CONCLUSIONS

Numerical models were developed considering geotechnical parameters typically found in Porto granite, which is characterized by outcrop profiles where rock material exhibits varying strength and degrees of weathering.

In bilayer rock masses, when the upper layer is the weaker one, the presence of a stronger lower layer increases the ultimate bearing capacity. This increase mainly depends on the GSI of the upper layer and the strength contrast between the upper and

lower layers. There is an upper limit to this increase, which is a function of the GSI of the upper layer, and it is reached when $\frac{P_{h_{UP}}}{P_{h_{BO}}} \geq 3.5$.

When the lower layer is the weaker one, regardless of the variation in other geotechnical parameters, the bearing capacity of the bilayer model depends on the ratio $\frac{P_{h_{UP}}}{P_{h_{BO}}}$. The results obtained are consistent with those of [1], in which only the GSI of the layers was varied. However, with a broader dataset, it has been observed that the interpretation of the B_F value is clearer when the chart is plotted as a function of $\frac{P_{h_{UP}}}{P_{h_{BO}}}$.

ACKNOWLEDGMENT

The research described in this paper was supported by the project “Neural networks and optimization techniques for the safe design and maintenance of transportation infrastructures: geotechnics of volcanic rocks and slope stability, IA-PYROSLOPE (PID2022-139202OB-I00)” of the Ministry of Education and Science.

REFERENCES

- [1] ALENCAR A., GALINDO R., MELENTIJEVIC S., *Bearing capacity of shallow foundations on the bilayer rock*, Geomech. Eng., 2020, 21 (1), 11–21, <https://doi.org/10.12989/gae.2020.21.1.011>
- [2] ALENCAR A., GALINDO R., VIANA DA FONSECA A., MUÑIZ-MENÉNDEZ M., LAMAS R., *An experimental study of tensile deformation modulus considering different degrees of weathering* (under review).
- [3] AMBROSIO A.C., BRITO J.A.M., ROMEIRO M.J., MORUJÃO P., *Fundações da ponte Infante d. Henrique*, 9º Congresso Nacional de Geotecnia – Sigarra, 2004.
- [4] BEGONHA A., SEQUEIRA BRAGA M.A., *Weathering of the Oporto granite: geotechnical and physical properties*, Catena, 2002, 49, 57–76, [https://doi.org/10.1016/S0341-8162\(02\)00016-4](https://doi.org/10.1016/S0341-8162(02)00016-4)
- [5] LAMAS R., *Estudo da variabilidade geológico-geotécnica dos perfis de alteração do granito do Porto*, PhD Thesis, Universidade do Porto (Portugal), 2023.
- [6] RUSSO G., KALAMARAS G.S., ORIGLIA P., GRASSO P., *A probabilistic approach for characterizing the complex geological environment for the design of the new Metro do Porto*, Proceedings, Congress ITA, Milan 2001, 463–470.
- [7] TEIXEIRA R.J.S., NEIVA A.M.R., SILVA P.B., GOMES M.E.P., ANDERSON T., RAMOS J.M.F., *Combined U-Pb geochronology and Lu-Hf isotope systematics by LAM-ICPMS of zircons from granites and metasedimentary rocks of Carrazeda de Ansiães and Sabugal areas, Portugal, to constrain granite sources*, Lithos, 2011, 125, 321–334, <https://doi.org/10.1016/j.lithos.2011.02.015>
- [8] VIANA DA FONSECA A., *Geomecânica dos Solos Residuais do Granito do Porto. Critérios para o Dimensionamento de Fundações Directas*, PhD Thesis, Universidade do Porto (Portugal), 1996, <http://hdl.handle.net/10216/11101>
- [9] VIANA DA FONSECA A., *Characterizing and deriving engineering properties of a saprolitic soil from granite, in Porto*, Characterization and Engineering Properties of Natural Soils, Eds. Tan et al., 2003, 1341–1378.

OCENA NOŚNOŚCI DWUWARSTWOWYCH MASYWÓW SKALNYCH NA PRZYKŁADZIE GRANITU Z PORTO

Tradycyjne podejścia do szacowania nośności w mechanice skał zazwyczaj zakładają jednorodny i izotropowy masyw skalny. Jednak w rzeczywistości masywy skalne często składają się z wielu warstw o zróżnicowanych właściwościach lub odmiennych parametrach geotechnicznych w obrębie tej samej matrycy skalnej. Takie zachowanie jest wyraźnie obserwowane w granicie z Porto. W niniejszym badaniu zasymulowano różne kombinacje stratygraficzne powszechnie występujące w regionie oraz odpowiadające im graniczne nośności, obliczone z wykorzystaniem metody różnic skończonych (FDM). Przeprowadzono analizę parametryczną w celu wyznaczenia zmodyfikowanego współczynnika nośności w funkcji grubości warstw oraz jakości masywu skalnego (wyrażonej za pomocą wskaźnika GSI). Wyniki przedstawiono w formie wykresu, stanowiącego praktyczne narzędzie do szacowania nośności dwuwarstwowych masywów skalnych.

5. TENSILE STRENGTH VARIATION IN TRANSVERSELY ISOTROPIC ROCKS

ANA ALENCAR¹, RUBÉN GALINDO AIRES¹,
MAURO MUÑOZ-MENÉNDEZ², MIGUEL ÁNGEL MILLÁN¹

¹ Universidad Politécnica de Madrid, Madrid, Spain.

² Laboratorio de Geotecnia, CEDEX, Madrid, Spain.

Given the existence of several classifications aimed at estimating the degree of anisotropy in transversely isotropic rocks – where, for instance, parameters such as P-wave velocity are used to infer variations in uniaxial compressive strength – the present study seeks to propose a classification of anisotropy based on the variation in tensile strength. In the transversely isotropic rocks the mechanical properties vary with the angle (β) between the loading direction and the discontinuity planes. While tensile strength and P-wave velocity typically reach minimum values at $\beta = 90^\circ$, the minimum uniaxial compressive strength is observed around $\beta = 30^\circ$, indicating different anisotropic responses. The research is structured in three parts: (1) an experimental study involving direct tensile tests on sandstone samples from the same source but with varying P-wave velocities, revealing significant strength differences linked to small velocity changes; (2) transversely isotropic slate specimens have been tested by ring tests, uniaxial compressive tests, and seismic velocity measurements; (3) an analysis of the results was carried out, combined with data from the literature, enhance understanding of strength variation in anisotropic rocks.

Keywords: rock, tensile strength, anisotropic rock, laboratory test

5.1. INTRODUCTION

In rock mechanics, the uniaxial compressive strength (UCS) is a widely studied parameter, and various correlations and rock classifications are based on its value. Tensile strength is a parameter that is gaining increasing attention due to its importance in tunnel stability, anchors, etc. Nevertheless, no classification has yet been established to quantify the degree of anisotropy in relation to variations in tensile strength. In the present study, it is investigated whether, by knowing the variation of a parameter – such as UCS or P-wave velocity – it would be possible to estimate the extent of variation in tensile strength.

In anisotropic rocks with transversely isotropic behavior, UCS, as well as tensile strength and P-wave velocity, vary as a function of the angle between the discontinuity planes and a loading direction during the test (β). So β would be equal to 0° when the load is applied parallel to the discontinuity; and 90° with the load is perpendicular to the discontinuity. It should be emphasized that, in the Brazilian test (BT), the load is applied in a diametral manner, leading to a mechanical response that differs significantly from that observed in direct tension (DTT) and uniaxial compression tests (UCT). These distinctions will be discussed in detail in subsequent sections. Furthermore, the minimum tensile strength value does not coincide with the same orientation as the minimum UCS value. The minimum values obtained in the case of DTT and P-wave velocity are typically associated with 90° [13, 15], while for UCS, they are approximately 30° [6, 7].

The available anisotropy classifications, which provide an initial idea of the range in which rock strength varies, are based on seismic wave velocity, UCS, or values obtained from the point load test (PLT). Paper [23] presents several of these classifications and propose a new one based on seismic waves, using the extreme values of β (0 and 90°).

The ratio between compressive and tensile strengths does not have a defined standard correlation. Among the many published equations that correlate UCS and tensile strength values, the presence of a constant coefficient C can be observed [9, 14, 21, 28].

According to the modified Hoek and Brown's failure criterion [8], the change in tensile strength is directly proportional to the change in compressive strength; if the UCS doubles, the tensile strength undergoes the same proportional increase.

However, according to the authors, the criterion does not assess tensile strength properly [9]. Therefore, based on triaxial test data they proposed a correlation between the UCS and direct tensile strength DTS as a function of Hoek–Brown parameter m_i .

$$\frac{\sigma_{ci}}{\sigma_t} = 0.81 \cdot m_i + 7. \quad (5.1)$$

Applying Eq. (5.1), as the value of m_i depends on the type of rock and remains constant independent of the variation of UCS, the value of the tensile strength remains directly proportional to that of the compressive strength.

Paper [14] studied the variation of tensile strength and UCS in gneissosity, considering different directions and observing that their correlation is not the same and depends on orientation. Khanlari et al. [11] proposed a correlation between the indirect tensile strength (BTS) and the point load strength index ($Is(50)$) for different anisotropy angles. Considering this evidence, the available anisotropy classifications based primarily on UCS do not allow for an estimation of the range in which tensile strength will vary.

On the other hand, tensile strength has traditionally been estimated indirectly through the Brazilian test (BT) [20]. Among the studies on the variation of tensile strength in anisotropic rocks with transversely isotropic behavior, the study conducted by [16]

stands out. This study presents various BTS, analyzing how tensile strength varies depending on the type of rock but does not correlate this variation with any other geotechnical parameter [29] propose the Normalized Failure Strength (NFS), which is the ratio between the minimum and maximum tensile strength values obtained. This parameter allows for an understanding of how the variation trajectory changes depending on the type of rock.

This study focuses on analyzing the tensile strength values obtained at $\beta = 0^\circ$ and 90° , correlating them with seismic wave velocity and UCS to jointly assess the variation of these three parameters.

The study is divided into three parts: (a) an experimental study, in which several direct tensile tests (DTT) are conducted on a sandstone from the same quarry but with different P-wave velocity values, revealing significant strength variation with minor wave velocity changes; (b) additionally, ring tests (RT), uniaxial compressive tests (UCT), and seismic wave velocity tests are performed on slates with transversal isotropic behavior; (c) a compendium of information available in the literature is presented, combined with the experimental results, allowing for an analysis of tensile strength variation in transversely anisotropic rocks, correlating it with UCS and P-wave velocity.

5.2. EXPERIMENTAL STUDY

The present experiment study was divided into two parts, the first one consisted in realized DTT, UCT and measure the P-wave velocities; the studied rock was a Lower Cretaceous (Weald facies) medium grain quartzarenite from Burgos, Spain (Fig. 5.1a). This rock shows a beige tone with veining pinkish and orange stains. This sandstone was chosen for the present study because, despite being from the same quarry, its blocks show variability in wave velocities and tensile strength, three blocks were employed in the present study.

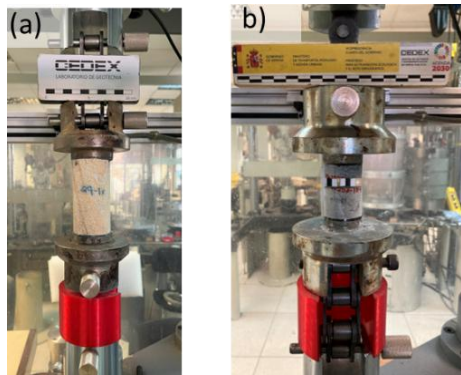


Fig. 5.1. DTT samples: (a) sandstone, (b) slate

In the second part, RT, UCT and also measure of P-wave velocities were carried out with slate from Fm. Santa María, which belongs to the Schist-Graywacke complex, located in Segovia, Spain (Fig. 5.1b). The summary of tests performed is show in Table 5.1.

Table 5.1. Summary laboratory test carried out

Rock Type	Laboratory test	$\beta [^\circ]$	Number of test
Sandstone	DTT	0	16
		90	11
	UCT	0	3
		90	7
	P-wave	0	19
		90	18
	Density	–	10
Slate	DTT	0	7
		90	7
	UCT	0	6
		90	6
	RT	0	14
		90	17
	P-wave	0	8
		90	18
	Density	–	15

It is important to note that in order to compare the results of DTT with BT or RT it is necessary to consider that the β are inverse, since in DTT the load was applied perpendicularly, and in the other test it was diametrically applied. So, the minimum BTS is achieved with $\beta = 0^\circ$ (vertical discontinuities) while in DTT with that orientation the maximum value is obtained (Fig. 5.2).

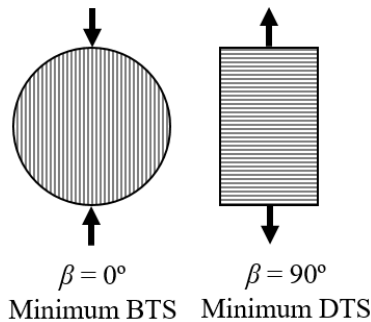


Fig. 5.2. Tensile strength value as function of β

For the first part of study the P-wave velocity were measured on the cylinders of 49 mm on diameter, and the DTT was performed with a minimum diameter-thickness ratio of 1:1, based on [18] recommendation. The BT and RT tests were carried out by applying load increments (kN/s), whereas the DTT and UCT tests were performed with stress increments (MPa/s). Failure in the tensile tests was expected to occur in approximately 5 minutes, while in the compression tests it occurred in about 10 minutes.

In the second part, no valid BT has been obtained with $\beta = 0^\circ$, once the failure does not occur under the diametrical line. For this reason, it has been decided to perform RT by applying the empirical solution proposed by [1] and [2].

The RT were carried out with flat platens according to [3], applying a continuously increasing compressive load to produce the failure in about 5 minutes. The tests were carried out on samples with 49 mm in diameter, and for the case of RT specimens, three different inner-to-outer diameter ratios (ρ) were considered (0.1, 0.3, and 0.5).

Due to the reduced thickness of the available slate blocks, it was not possible to cut cylinders with a slenderness of 2.5 to make UCTs with $\beta = 90^\circ$. Therefore, the slenderness correction coefficient proposed in the Spanish standard NLT 250/91 [4] has been applied.

5.3. RESULTS

According to the laboratory tests the sandstone had a mean dry density is 2133 kg/m^3 (min = 2080 kg/m^3 , max = 2159 kg/m^3 , SD = 28 kg/m^3). Figure 5.3 shows the DTS results as a function of P-wave velocities, from which it can be deduced that a 30% increase in wave velocity results in nearly a doubling of the tensile strength. This correlation is quite different from that expected with UCS, according to the classification presented by [23], in which a 100% increase in UCS would require a wave velocity increase of more than 50%.

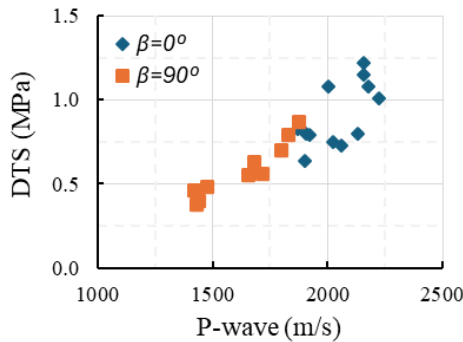


Fig. 5.3. Tensile strength obtained by DTT in function of P-wave velocities

To facilitate a more effective analysis of the results, a new parameter, Δ , is introduced, defined as the ratio between the maximum and minimum values obtained, expressed as a percentage (%) (Eq. (1)). Table 5.2 presents the results obtained for the sandstone, organized by block. As expected, the data indicate a general trend of increasing DTS with increasing P-wave velocity.

$$\Delta = \left(\frac{\text{maximum value}}{\text{minimum value}} - 1 \right) [\%]. \quad (5.2)$$

Table 5.2. A summary of the results obtained for the sandstone

Block	UCS [MPa]			P-wave [m/s]			DTS [MPa]		
	0°	90°	Δ [%]	0°	90°	Δ [%]	0°	90°	Δ [%]
1	20.3	26.2	29	2130	1835	16	1.1	0.8	41
2	20.0	22.4	12	2085	1677	24	0.8	0.6	31
3	18.4	27.2	48	1920	1446	33	0.8	0.4	79

Table 5.3 presents the results obtained with the slate in the laboratory tests. It can be observed that the variation in tensile strength obtained from DTT and RT (i.e., DTS and RTS, respectively) is significantly greater than that of the P-wave velocity or UCS.

Table 5.3. Results of the laboratory test carried out as a function of β

UCS (MPa)			P-wave (m/s)			RTS (MPa)			DTS (MPa)		
0°	90°	Δ [%]	0°	90°	Δ [%]	0°	90°	Δ [%]	0°	90°	Δ [%]
99.4	121.8	22	5103	5285	4	11	26.9	145	10.8	7.3	48

5.4. REVIEW OF AVAILABLE INFORMATION

Results from various authors who have studied the variation in tensile strength as well as P-wave velocities, PLT or UCS have been compiled. These results are presented in Table 5.4, as function of the anisotropic classification correlated. In the last column of the table, the variation in tensile strength is presented using ΔT (maximum value divided by the minimum).

Table 5.4. Available results of tensile strength variation in function of anisotropic classification

Authors	Rock type	$I_{a(50)}$ [10]	I_{vp} [23]	VA* [26]	I_{ucs} [22]	ΔT
	Sandstone I			14		1.4
	Sandstone II			21		1.3

Table 5.4 continued

	Sandstone III			28		1.8
	Slate		1.2	4		2.5
	Slate		1.2	4		1.5
[19]	Sandstone				2.0	2.6
[17]	Lyons sandstone		1.2	14		1.2
	Pyrophyllite		1.2	21		1.2
[12]	Sandstone I		1.7	53		1.4
	Sandstone II		1.1	11		1.8
	Sandstone III		1.1	12		1.4
[11]	Phyllite	5.7				2.7
	Sillimanite garnet hornfels	3.5				1.5
	Slate	3.6				3.3
	Andalusite garnet hornfels	2.2				2.5
	Staurolite andalusite schist	1.8				1.3
[27]	Postaer sandstone		1.1	7		1.0
	Modave Sandstone		1.1	8		1.4
	Leubsdorfer Gneiss		1.1	12		2.0
	Freiberger Gneiss		1.1	8		2.5
	Mosel Slate		1.2	22		4.2
	Herbeumont Slate		2.7	91		39
[24]	Mancos shale		1.1	9	1.4	1.1
[25]	Modave sandstone I		1.1	7		1.7
	Modave sandstone II		1.0	4		1.2
	Modave sandstone III		1.1	9		1.3
[5]	Asan Gneiss				2.3	2.6
	Boryeong shale				2.4	1.2
	Yeoncheon Schist				14.0	3.5

* Velocity anisotropy index (VA).

In Table 5.5 is present the anisotropic classes associated with the values presents in Table 5.4. Following the variation of strength recommended by [10], the same ratio of classification was associated to the tensile strength.

Table 5.5. Available results of tensile strength variation in function of anisotropic classification

$I_{a(50)}$ [10]	I_{vp} [23]	VA [26]	I_{UCS} [22]	ΔT	Classes of anisotropic
1	–	<2	1.0–1.1	1	Isotropic
1–2	≤1.5	2–6	1.1–2.0	1–2	Fairly
	1.5–2.0	6–20	2.0–4.0		Moderately
2–4	>2.0	20–40	4.0–6.0	2–4	Highly
>4	–	>40	>6.0	>4	Very highly

For a better combined visualization of the results in Table 5.4, Table 5.6 presents the different degrees of anisotropy represented by color-coded.

Table 5.6. Anisotropic classification represent by color-coded

Authors	Rock type	$I_{\alpha(50)}$ [10]	I_{vp} [23]	VA [26]	Iucs [22]	ΔT
	Sandstone I			Moderately		Fair. / Mod
	Sandstone II			Highly		Fair. / Mod
	Sandstone III			Highly		Fair. / Mod
	Slate		Fairly	Fairly		Highly
	Slate		Fairly	Fairly		Fair. / Mod
[19]	Sandstone				Fairly	Highly
[17]	Lyons sandstone		Fairly	Moderately		Fair. / Mod
	Pyrophyllite		Fairly	Highly		Fair. / Mod
[12]	Sandstone I		Moderately	Very highly		Fair. / Mod
	Sandstone II		Fairly	Moderately		Fair. / Mod
	Sandstone III		Fairly	Moderately		Fair. / Mod
[11]	Phyllite	Very highly				Highly
	Sillimanite garnet hornfels	Highly				Fair. / Mod
	Slate	Highly				Highly
	Andalusite garnet hornfels	Highly				Highly
	Staurolite andalusite schist	Moderately				Fair. / Mod
[27]	Postaer sandstone		Fairly	Moderately		Isotropic
	Modave Sandstone		Fairly	Moderately		Fair. / Mod
	Leubsdorfer Gneiss		Fairly	Moderately		Highly
	Freiberger Gneiss		Fairly	Moderately		Highly
	Mosel Slate		Fairly	Highly		Very highly
	Herbeumont Slate		Highly	Very highly		Very highly
[24]	Mancos shale		Fairly	Moderately	Fairly	Fair. / Mod
[25]	Modave sandstone I		Fairly	Moderately		Fair. / Mod
	Modave sandstone II		Fairly	Moderately		Fair. / Mod
	Modave sandstone III		Fairly	Moderately		Fair. / Mod

5.5. ANALYSIS OF RESULTS

Before beginning the analysis of the results, it is important to distinguish between two concepts. In transversely anisotropic rocks, whose behavior depends on β , one aspect concerns whether the increases in certain parameters are correlated – for example, whether higher P-wave velocities correspond to higher density. The other aspect considers whether the variation between the maximum and minimum values of different parameters follows clear trends, so knowing the change in one parameter can be used to estimate the variation in another.

Based on the available results, it is observed that the variation in tensile strength in anisotropic rocks with transverse isotropy follow a direct correlation with P-wave velocity (Fig. 3).

The direct correlation that could exist between the variation in tensile strength and P-wave velocity – considering that their maximum and minimum values occur at the same inclinations – is not empirically observed. As shown in Fig. 5.4, which combines the results of this study with those in Table 5.4, no direct correlation is apparent between the variations in tensile strength and P-wave velocity. This can be justified by the fact that the presence of microcracks or points of weakness scattered throughout the rock does not hinder the transmission of seismic waves but significantly reduces tensile strength.

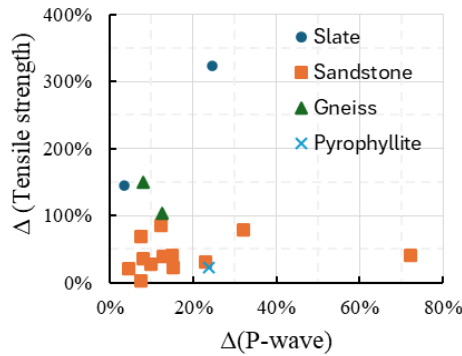


Fig. 5.4. Tensile strength variation as function of P-wave variation

Considering that anisotropy classifications do not allow for a sufficiently rigorous estimation of the expected variation in tensile strength in rocks with transverse isotropy (Table 5.5). One option for making an initial assessment of the variation in tensile strength in transversely isotropic rocks is based on rock type. Figure 5.5 shows the typical values of ΔT as a function of rock type.

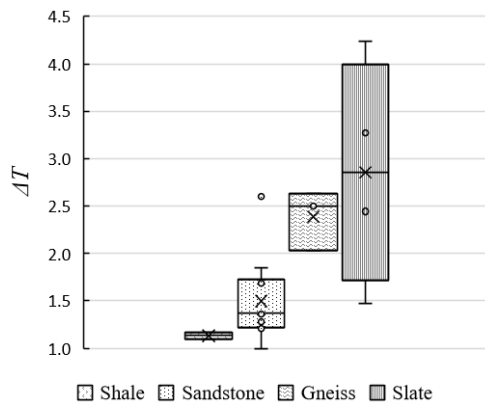


Fig. 5.5. Tensile strength variation as function of rock type

Based on Figure 5.4, it can be observed that sandstones typically do not exceed a variation of 100%, whereas slates generally show a minimum increase of 50%, which can exceed 300%.

5.6. CONCLUSIONS

Based on the analyzed results, it has been demonstrated that the use of anisotropy classifications based on P-wave velocity and UCS does not adequately predict the variation in tensile strength.

When analyzed according to rock type, it is noteworthy that metamorphic rocks typically show a variation in tensile strength greater than 100%, while sedimentary rocks tend to show variations below this value.

ACKNOWLEDGEMENT

The research described in this paper was supported by the project “Neural networks and optimization techniques for the safe design and maintenance of transportation infrastructures: geotechnics of volcanic rocks and slope stability, IA-PYROSLOPE (PID2022-139202OB-I00)” of the Ministry of Education and Science.

REFERENCES

- [1] ALENCAR A., MUÑIZ-MENÉNDEZ M., GALINDO R., *Ring test: a new interpretation to estimate tensile strength of rock*, Rock Mech. Rock Eng., 2024, <https://doi.org/10.1007/s00603-024-03894-7>
- [2] ALENCAR A., MUÑIZ-MENÉNDEZ M., GALINDO R., *Ring test: an experimental study on anisotropic rock*, Rock Mech. Rock Eng., 2025, <https://doi.org/10.1007/s00603-025-04586-6>
- [3] ASTM, *Standard test method for splitting tensile strength of intact rock core specimens with flat loading platens*, Designation: D 3967 – 23, 2023.
- [4] CENTRO DE ESTUDIOS Y EXPERIMENTACIÓN DE OBRAS PÚBLICAS – CEDEX. *NLT 250/91: Método de ensayo para la determinación del equivalente de arena*, Ministerio de Transportes, Movilidad y Agenda Urbana, Madrid, España, 1991.
- [5] CHO J.W., KIM H., JEON S.K., MIN K.B., *Deformation and strength anisotropy of Asan gneiss, Boryeong shale, and Yeoncheon schist*. Int J Rock Mech Min Sci 50, 2012, 158–169. <https://doi.org/10.1016/j.ijrmms.2011.12.004>
- [6] DUVEAU G., SHAO J.F., *A modified single plane of weakness theory for the failure of highly stratified rocks*, Int. J. Rock. Mech. Min. Sci., 1998, Vol. 35 (6), [https://doi.org/10.1016/S0148-9062\(98\)00013-8](https://doi.org/10.1016/S0148-9062(98)00013-8)
- [7] GHOLAMI R., AND RASOULI V., *Mechanical and elastic properties of transversely isotropic slate*, Rock Mech. Rock Eng., 2014, 47, 1763–1773. <https://doi.org/10.1007/s00603-013-0488-2>
- [8] HOEK E., CARRANZA-TORRES C., CORKUM B., *Hoek–Brown failure criterion – 2002 edition*. In: R. Hammah, W. Bawden, J. Curran, M. Telesnicki (Eds.), *Mining and tunnelling innovation and opportunity*. Proceedings of the 5th North American rock mechanics symposium and 17th tunnelling association of Canada conference, Toronto, Canada. University of Toronto, Toronto 2002, 267–273.
- [9] HOEK E., BROWN E.T., *The Hoek–Brown failure criterion and GSI – 2018 edition*, J. Rock Mech. Geo. Eng., 2018, 11 (3), <https://doi.org/10.1016/j.jrmge.2018.08.001>

- [10] ISRM, *Rock characterization, testing and monitoring, ISRM suggested methods*, Pergamon Press, Oxford, U.K., 1981.
- [11] KHANLARI G., HEIDARI M., SEPAHI A.A., FEREIDOONI D., *Determination of geotechnical properties of anisotropic rocks using some index tests*, *Geotechnical Testing Journal*, 2014, 37, <https://doi.org/10.1520/GTJ20130078>
- [12] KHANLARI G., RAFIEI B., ABDILOR Y., *An experimental investigation of the Brazilian tensile strength and failure patterns of laminated sandstones*, *Rock Mech. Rock Eng.*, 2015, 48, 843–852, <https://doi.org/10.1007/s00603-014-0576-y>
- [13] KIM H., CHO J.W., SONG I., MIN K.B., *Anisotropy of elastic moduli, P-wave velocities, and thermal conductivities of Asan Gneiss, Boryeong Shale, and Yeoncheon Schist in Korea*, *Engineering Geology*, 2012, 147–148, <https://doi.org/10.1016/j.enggeo.2012.07.015>
- [14] KONG F.M., HAN M., ZHAO Y.T. et al., *Influence of rock heterogeneity on the correlation between uniaxial compressive strength and Brazilian tensile strength*, *Sci. Rep.*, 2025, 15, 437, <https://doi.org/10.1038/s41598-024-84715-3>
- [15] LIU P., LIU Q., HUANG X. et al., *Direct tensile test and FDEM numerical study on anisotropic tensile strength of Kangding Slate*, *Rock Mech. Rock Eng.*, 2022, 55, 7765–7789, <https://doi.org/10.1007/s00603-022-03036-x>
- [16] MA T., PENG N., ZHU Z., ZHANG Q., YANG C., ZHAO J., *Brazilian tensile strength of anisotropic rocks: review and new insights*, *Energies*, 2018, 11 (2), 304, <https://doi.org/10.3390/en11020304>
- [17] MIGHANI S., SONDERGELD C.H., RAI C.S., *Observations of tensile fracturing of anisotropic rocks*, *SPE J.*, 2016, 21, 2015, 1–13.
- [18] MUÑIZ-MENÉNDEZ M., PÉREZ-REY I., *Influence of the specimen slenderness on the direct tensile strength of rocks*, 15th ISRM Congress, Salzburgo (Austria), October 2023.
- [19] NOORI M., KHANLARI G., SARFARAZI V. et al., *An experimental and numerical study of layered sandstone's anisotropic behaviour under compressive and tensile stress conditions*, *Rock Mech. Rock Eng.*, 2024, 57, 1451–1470. <https://doi.org/10.1007/s00603-023-03628-1>
- [20] PACKULAK T., DAY J., MCDONALD M., JACKSTEIT A., DIEDERICH S., *Measurement of true tensile strength from Brazilian tensile strength laboratory tests*, *Canadian Geotechnical Journal*, 2025, 62, 1–14, <https://doi.org/10.1139/cgj-2023-0204>
- [21] RAJABZADEH M.A., MOOSAVINASAB Z., RAKHSHANDEHROO G., *Effects of rock classes and porosity on the relation between uniaxial compressive strength and some rock properties for carbonate rocks*, *Rock Mech. Rock Eng.*, 2012, 45 (1), 113–122.
- [22] RAMAMURTHY T., *Strength and modulus responses of anisotropic rocks*, *Comprehensive Rock Engineering*, 1993, Vol. 1, 313–329.
- [23] SAROGLOU H., TSIAMBAOS G., *Classification of anisotropic rocks*. In: *Proceedings of the 11th ISRM Congress*, Lisbon, Portugal, 9–13 July 2007.
- [24] SIMPSON N.D.J., *An analysis of tensile strength, fracture initiation and propagation in anisotropic rock (Gas Shale) using Brazilian tests equipped with high speed video and acoustic emission*, Master's Thesis, Norwegian University of Science and Technology, Trondheim, Norway, 2013.
- [25] TAVALLALI A., VERVOORT A., *Behaviour of layered sandstone under Brazilian test conditions: Layer orientation and shape effects*, *J. Rock Mech. Geotech. Eng.*, 2013, 5, 366–377, <https://doi.org/10.1016/j.jrmge.2013.01.004>
- [26] TSIDZI K., *Propagation characteristics of ultrasonic waves in foliated rocks*, *Bull. Int. Association of Eng. Geology*, 1997, Vol. 56, 103–113.
- [27] VERVOORT A., MIN K.B., KONIETZKY H. et al., *Failure of transversely isotropic rock under Brazilian test conditions*, *Int. J. Rock Mech. Min. Sci.*, 2014, 70, 343–352, <http://dx.doi.org/10.1016/j.ijrmms.2014.04.006>

- [28] YESILOGLU-GULTEKIN N., GOKCEOGLU C., SEZER E.A., *Prediction of uniaxial compressive strength of granitic rocks by various nonlinear tools and comparison of their performances*. Int. J. Rock. Mech. Min. Sci., 2013, 62, 113–122.
- [29] XU G., HE C., CHEN Z. et al., *Effects of the micro-structure and micro-parameters on the mechanical behaviour of transversely isotropic rock in Brazilian tests*, Acta Geotech., 2018, 13, 887–910, <https://doi.org/10.1007/s11440-018-0636-7>

ZMIANY WYTRZYMAŁOŚCI NA ROZCIĄGANIE W SKAŁACH POPRZECZNIE IZOTROPOWYCH

Uwzględniając istnienie kilku klasyfikacji mających na celu oszacowanie stopnia anizotropii w skałach poprzecznie izotropowych, w których na przykład parametry takie jak prędkość fali podłużnej (P-fala) są wykorzystywane do wnioskowania o zmianach jednoosiowej wytrzymałości na ściskanie, niniejsze badanie ma na celu zaproponowanie klasyfikacji anizotropii opartej na zmienności wytrzymałości na rozciąganie. W skałach poprzecznie izotropowych właściwości mechaniczne zmieniają się w zależności od kąta (β) pomiędzy kierunkiem obciążenia a płaszczyznami nieciągłości. Podczas gdy wytrzymałość na rozciąganie i prędkość P-fali zwykle osiągają wartości minimalne przy $\beta = 90^\circ$, minimalna jednoosiowa wytrzymałość na ściskanie obserwowana jest w pobliżu $\beta = 30^\circ$, co wskazuje na odmienne odpowiedzi anizotropowe. Badania zostały podzielone na trzy części: (1) badania eksperymentalne obejmujące bezpośrednie próby rozciągania próbek piaskowca pochodzących z tego samego złoża, lecz o różnych prędkościach P-fal, które ujawniły istotne różnice wytrzymałości związane z niewielkimi zmianami prędkości; (2) próbki łupka poprzecznie izotropowego zostały przebadane testami pierścieniowymi, jednoosiowymi próbami ściskania oraz pomiarami prędkości sejsmicznych; (3) przeprowadzono analizę wyników, uzupełnioną danymi z literatury, w celu pogłębienia zrozumienia zmienności wytrzymałości w skałach anizotropowych.

6. THE STABILITY GRAPH METHOD: STATE-OF-THE-ART

CÉSAR TORRERO, LUIS JORDÁ, SALVADOR SENENT

UPM (Universidad Politécnica de Madrid, Spain, ETSI Caminos, Canales y Puertos,
C/ Profesor Aranguren N° 3, Madrid 28040, Spain.

Traditional approaches to estimating bearing capacity in rock mechanics generally assume a homogeneous and isotropic rock mass. However, rock masses often consist of multiple layers with varying properties or different geotechnical qualities within the same rock matrix. This behavior is clearly observed in the Oporto granite. This study simulates various stratigraphic combinations commonly found in the region and their corresponding ultimate bearing capacities, calculated using the finite difference method (FDM). A parametric analysis is carried out to derive a modified bearing capacity factor as a function of layer thickness and rock mass quality (expressed through GSI). The results are presented in the form of a chart, offering a practical tool for estimating the bearing capacity of bilayer rock masses.

Keywords: underground space, mining, rock mechanics

6.1. INTRODUCTION

Determining the maximum stable unsupported span for underground openings is a key design aspect in mining engineering.

Specifically, in underground mining, when designing access tunnels and supported underground openings, the support design charts based on rock engineering classifications (e.g., Barton, Bieniawski et al. [1–3]) are systematically applied.

In the particular case of non-entry open stope mining method, providing a suitable design for stopes is crucial in metal underground mining operations. This involves achieving allowable levels of dilution and to guarantee roof and hanging wall stability so that eventual rockfalls could be managed by mucking equipment. Open stope dimensions must be optimized to reduce costs but, as a counterpart, exceeding stable

span could lead to fatal consequences impacting production, costs and even workers safety. For this purpose, the stability graph method was introduced in 1980 by Mathews et al. [4] and it has been used up to present day in engineering design practice across different geographies [5–7]. Since the 1980's, this method has undergone several modifications, extensions and refinements, together with the application of innova-

tive techniques such as statistical analysis, numerical modelling and, recently, machine learning.

A review of the stability graph method evolution since 1980 and a publication analysis are presented in this paper. Within this analysis, worldwide geographical distribution of the publications has been studied.

6.2. THE STABILITY GRAPH METHOD

The inception of the stability graph method was a report commissioned to Golder Associates by the Department of Energy, Mines and Resources of the Canada Centre for Mineral and Energy Technology. The report was written by Mathews [4] and its subject of study was the prediction of stable spans for mining at depth bellow 1000 m in hard rock. This study was based on 26 case histories.

The method consists of a chart (in Fig. 6.1) in which the stability number N is plot against the hydraulic radius (HR = area/perimeter), defined as a shape factor of one of the slope exposed surfaces [4]. In the graph, stable, potentially unstable and caving zones are delimited.

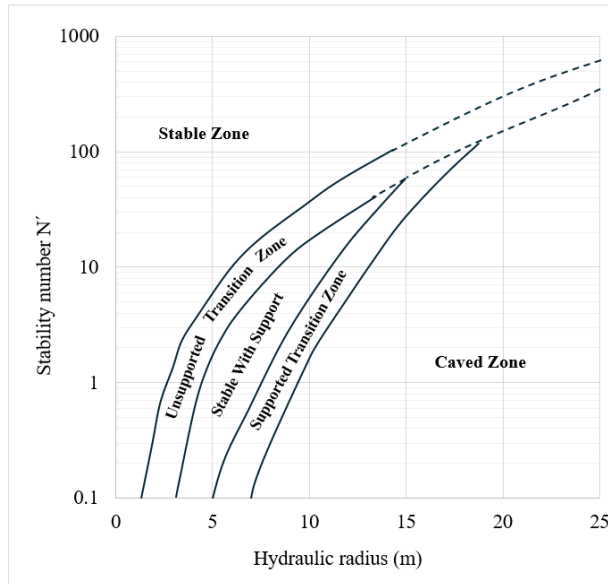


Fig. 1. Stability graph method chart, based on [8]

The stability number (Eq. (6.1)) is obtained as follows:

$$N = Q' \times A \times B \times C, \quad (1)$$

where:

- Q' is the rock mass quality index Q [1] assuming a Stress Reduction Factor $SRF = 1$ and a Joint water reduction factor $J_w = 1$.
- A , which ranges from 0.1 to 1, is the stress factor. It depends on the relation in between the induced compressive stress and the uniaxial compressive strength of the intact rock.
- B , which ranges from 0.2 to 1, is the rock defect orientation factor. It depends on both the difference in dip and the difference in strike of the critical joint and the stope surface.
- C , which ranges from 2 to 8, is the gravity or design surface orientation factor. It is defined for two failure modes:
 - gravity-induced roof fall or slabbing in sidewalls, where C depends on the stope surface dip,
 - sliding in sidewalls, where C depends on the inclination of the critical joint.

6.3. EVOLUTION AND DEVELOPMENTS

The evolution of the method and its different developments after three decades in use was reviewed in 2010 and 2012 by Suorineni [9, 10] and in 2014 by Potvin [11]. These developments have consisted in redefining the stability graph method factors, the transition zones and adding new factors related to complementary design conditions [9]. In 2012 Suorineni updated his first state-of-the-art review including the outstanding publications during the period 2010–2012 [10]. Potvin emphasizes in the origin and in aspects related to the application of the method such as gathering data, common mistakes, challenges and calibration [11].

The first and most significant method development was made by Potvin in 1988 [12]. In his PhD thesis, Potvin proposed some modifications for the factors basing on open stope 175 case histories in Canada. Most of the further developments are based on Potvin stability graph method factors.

Some developments were proposed with the aim of quantifying dilution in underground mining operations. Dilution is the waste material content in ore, and it is crucial in mining production. The concept of equivalent linear overbreak/slough (ELOS) was introduced in 1997 by Clark and Pakalnis in the stability graph method [13]. ELOS allows to quantify the dilution depth in meters along the open stope height. Three ELOS contours were introduced in the graph: 0.5, 1 and 2 m.

Related to the addition of new factors, an exposure time correction factor (Eq. (6.2)) was introduced by Tannant and Diederichs in 1997 to adjust the rock mass quality Q' based on their experience in Kidd Mine [14]. One year later Suorineni incorporated a fault factor (Eq. (6.3)) with the intention of penalizing the stability number because of the presence of a fault dipping to the stope walls [15]. Experience showed that the

presence of fault involved a significant dilution and cost increase specially when the angle between the fault and the side wall was 20–30° [8].

The modified stability number, accounting for the new factors, is calculated using the following expressions:

$$N^* = Q' \times A \times B \times C \times T, \quad (6.2)$$

$$N'_f = Q' \times A \times B \times C \times F, \quad (6.3)$$

where:

- N^* , is the modified stability number to account for time.
- T , is the time factor (Table 6.1).
- N'_f , is the modified stability number to account for nearby faults.
- F , is the fault factor which is the relation between the stability number corresponding to the ELOS caused by the fault and the stability number at the ELOS = 0.5 contour [13].

Table 6.1. Time correction factor [14]

Wall exposure time	Time factor, T	
	$Q' > 10$	$Q' < 10$
<3 months	1	0.8
3–5 months	0.8	0.5
5–12 months	0.5	0.3
>12 months	0.3	0.2

Apart from adding new factors, original factors have been also further studied, for example, applying numerical methods. In 2009 Bewick and Kaiser validated the B factor by means of finite element method (FEM) models [16]. The software Phase2 was used to conduct these models, implanting the rock mass as an isotropic model and plastic behaviour adopting a Mohr–Coulomb plasticity criterion with a tension cut-off. Joint elements were explicitly simulating by implementing its strength and stiffness parameters.

6.4. LATEST INNOVATIONS

In this section the innovations introduced since the Suorineni and Potvin historical overviews [10, 11] are reviewed. These latest innovations of the method mainly consist of the application of the artificial intelligence with the aim of optimizing the stability graph.

Machine learning techniques have been used to improve stability graph method in 2024 [17, 18]. For that purpose, a robust database of 980 records of unsupported stopes

stability data was compiled, sourced from various publications on mines located in countries such as Canada, Australia, South Africa and China [18]. This database was used to delimit updated stable and transition limits.

Suorineni and Madenova also reviewed recent developments in 2022 [19], highlighting the ones focused on statistics [20, 21] and artificial networks [22]. They conclude that the statistical treatment of databases to redefine zones or the consideration of average and standard deviations of the parameters of the stability graph method are far from the principles upon which the method was conceived and have no relevance in mining engineering practice. These authors state that the parameters N , Q' , HR , A , B and C are specific for each slope surface and do not make engineering sense to consider dispersions of their values in databases.

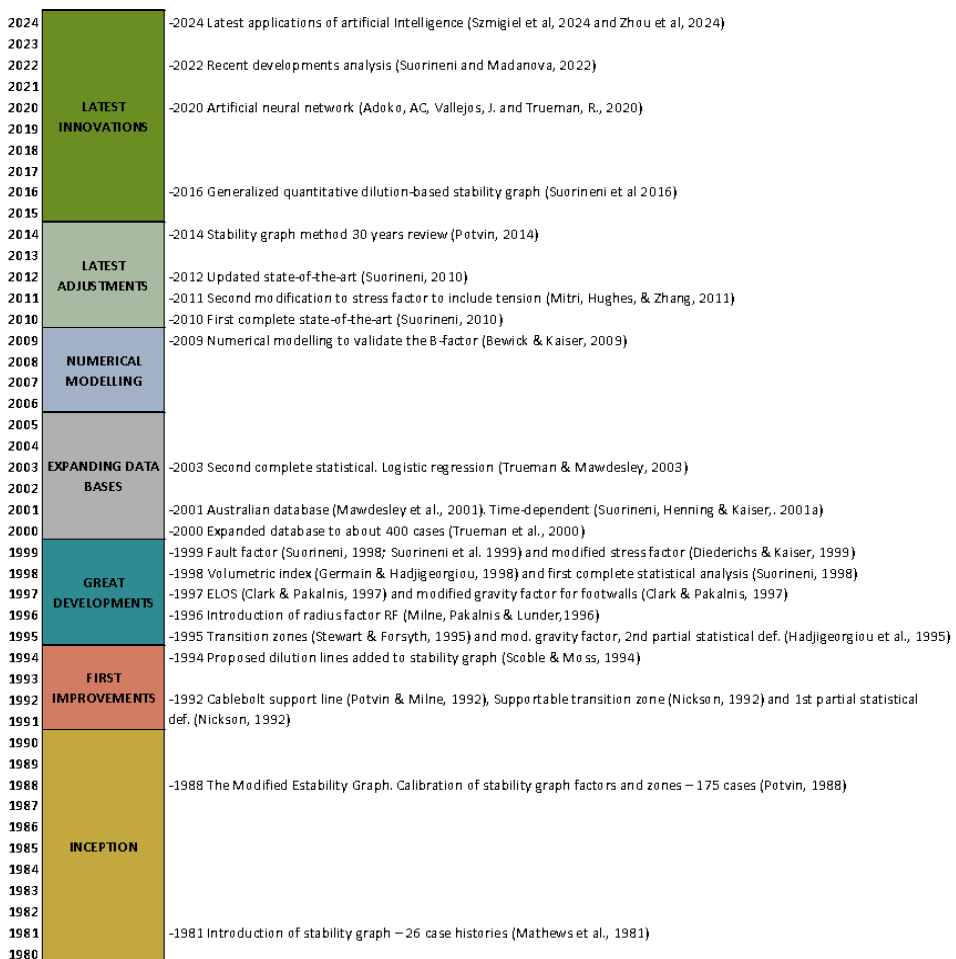


Fig. 2. Stability graph method chronological axis based on [6, 7, 14]

The stability graph method since its inception in 1980 has been studied, improved and modified by a large number of authors (Table 6.2). It has been adapted to different contexts and the most cutting-edge techniques at each period have been applied, i.e. numerical modelling, and artificial intelligence. The historical evolution of the method is illustrated in the following chronological axis (Fig. 6.3) which takes as its starting point the state-of-the-art review conducted by Suorineni in 2012 [10]:

Table 6.2. Stability graph method publications

Publication	Author	Year	Country
Prediction of stable excavation spans for mining at depths below 1000 m in hard rock	Mathews K.E.; Hoek E.; Wyllie D.C.; Stewart S.B.V.	1980	Canada
Empirical Open Stope Design in Canada	Potvin Y.	1988	Canada
Empirical cable bolt support design	Potvin Y.; Milne D.	1992	Canada
Cable support guidelines for underground hard rock mine operations.	Nickson S.D.	1992	Canada
Dilution in underground bulk mining: Implications for production management	Scoble M.J.; Moss A.	1994	Canada
The Mathews method for open stope design	Stewart S.B.V.; Forsyth W.W.	1995	Canada
An update of the stability graph method of open stope design	Hadjigeorgiou J.; Leclaire J.; Potvin Y.	1995	Canada
Surface geometry assessment for open stope design	Milne D.; Pakalnis R.C.; Felderer M.	1996	Canada
Cablebolting in Underground Mines	Hutchinson J.D.; Diederichs M.S.	1996	Canada
On the relationship between stability prediction and observed stope overbreak	Germain P.; Hadjigeorgiou J.; Lesard J.F.	1996	Canada
Rock instability and risk analyses in open stope mine design	Diederichs M.S.; Kaiser P.K.	1996	Canada
Cablebolt optimization in #3 Mine	Tannant D.D.; Diederichs M.S.	1997	Canada
Incorporation of rock mass relaxation and degradation into empirical stope design	Kaiser P.K.; Falmagne V.; Suorineni F.T.; Diederichs M.S.; Tannant, D.D.	1997	Canada
An empirical approach for estimating unplanned dilution from open stope hangingwalls and footwalls	Clark L.M.; Pakalnis R.C.	1997	Canada
Underground design and deformation based on surface geometry	Milne D.	1997	Canada
Minimizing dilution in open stope mining with focus on stope design and narrow vein longhole blasting	Clark L.M.	1998	Canada
Effects of faults and stress on open stope design	Suorineni F.T.	1998	Canada
Influence of stope geometry on mining performance	Germain P.; Hadjigeorgiou J.	1998	Canada

Table 6.2 continued

Fault factor for the stability graph method of open-stope design	Suorineni F.T.; Tannant D.D.; Kaiser P.K.	1999	Canada
The incorporation of stress induced damage factor into Mathew's stability graph	Sprott D.L.; Toppi M.A.; Yi X.P.	1999	Canada
Stability graph design method – A mining operator's guide	Neumann M.F.	1999	Canada
Cablebolt layouts using the modified stability graph	Diederichs M.S.; Hutchinson D.J.; Kaiser P.K.	1999	Canada
Experience in Australia with the application of the Mathews method of open stope design	Trueman R.; Mikula P.; Mawdesley C.; Haries N.	2000	Australia
Incorporation of a fault factor into the stability graph method: Kidd mine case studies	Suorineni F.T.; Tannant D.D.; Kaiser P.K.; Dusseault M.B.	2001	Canada
Likelihood statistic for interpretation of the stability graph for open stope design	Suorineni F.T.; Tannant D.D.; Kaiser P.K.	2001	Canada
The Extended Mathews Stability Graph: Quantifying case history requirements and site specific effects	Stewart P.C.2; Trueman R.	2001	Australia
The stability graph method for open-stope design	Potvin Y.; Hadjigeorgiou J.	2001	Canada
Extending the Mathews Stability Graph for Open-stope Design	Mawdesley C.; Trueman R.; Whiten W.	2001	Australia
Predicting rock mass cavability in block caving mines	Mawdesley C.A.	2002	Australia
Predicting cave initiation and propagation	Trueman R.; Mawdesley C.	2003	Canada
Applying the extended Mathews stability graph: Quantifying case history requirements and site-specific effects	Stewart P.C.; Trueman R.	2003	Australia
A rock mass rating system for evaluating stope stability on the Bushveld Platinum mines	Watson B.P.	2004	South Africa
Influence of stress, undercutting, blasting and time on open stope stability and dilution	Wang J.C.	2004	Canada
Using logistic regression to investigate and improve an empirical design method	Mawdesley C.A.	2004	China
Copper Cliff South Mine (CCSM) stability graph and time evaluation of open stope stability	Whipple R. et al	2009	Canada
Numerical Assessment of Factor B in Mathews' Method for Open Stope Design	Bewick R.P.; Kaiser P.K.	2009	Canada
The stability graph after three decades in use: Experiences and the way forward	Suorineni F.T.	2010	Kazakhstan
New rock stress factor for the stability graph method	Mitri H.S. et al.	2011	Canada
A Critical Review of the Stability Graph Method for Open Stope Design	Suorineni F.T.	2012	Kazakhstan

Table 6.2 continued

Inferred weak rock mass classification for slope design	Ida Forster K.	2013	Canada
Effect of slope construction parameters on ore dilution in narrow vein mining	El Mouhabbis H.Z.	2013	Canada
The Modified Stability Graph Method, More Than 30 Years Later	Potvin Y.	2014	Australia
Empirical design methods in practice	Pakalnis R.	2015	Canada
Análisis tenso-deformacional y diseño de fortificaciones para una explotación de cobre por sublevel stopping. Atacama Kozan (Chile)	Veyrat S.; Galera J.M.	2015	Chile
Development of a generalised dilution-based stability graph for open slope design	Papaioanou A.; Suorineni F.T.	2016	Australia
Stability assessment of shallow limestone caves through an empirical approach: Application of the stability graph method to the Castañar Cave study site	Jorda L. et al	2016	Spain
Three-dimensional effect of stresses in open slope mine design	Vallejos J.A., Delonca A.; Perez E.	2016	Chile
Statistical analysis of the stability number adjustment factors and implications for underground mine design	Vallejos JA., Delonca A., Fuenzalida J.; Burgos L.	2016	Chile
Optimization of slope structural parameters based on Mathews stability graph probability model	Zhang L.; Hu J.H.; Wang X.L.; Zhao L.	2018	China
Stability graph using major geological structures	Vallejos J., Miranda R., Azorin J., Arriagada C., Catalán O., Garrido C., Mondaca M.; Escares P.	2018	Chile
Multi-approach stability analyses of large caverns excavated in low-angled bedded sedimentary rock masses in Singapore	Winn K. et al.	2019	Singapore
Estudio de las distribuciones tensiones y de las resistencias de los rellenos de pasta de la mina subterránea de Aguas Teñidas (Huelva)	Lain Huerta C.	2019	Spain
Optimization calculation of slope structure parameters based on Mathews stabilization graph method	Zhao K.; Wang Q.; Li Q.; Yan Y.J.; Yu X.; Wang J.Q.; Cao S.	2019	China
Stability analysis of underground water-sealed oil storage caverns in China: A case study	Xingdong Z. et al.	2020	China
Empirical and Numerical Finite-Element-Based Model to Improve Narrow Vein Mine Design in Peruvian Mining	Belizario M., Condori R., Pehovaz H., Raymundo C.,2; Perez M.	2020	Perú

Table 6.2 continued

Stability assessment of underground mine stopes subjected to stress relaxation	Adoko AC, Vallejos J.2; Trueman R.	2020	Chile
The Consolidated Mathews Stability Graph for Open Stope Design	Mortazavi A.2; Bakytzhan B.	2021	Kazakhstan
The Qualitative Stability Graph for Open Stope Design – Recent Developments	Suorineni F.T.2; Madenova Y.	2022	USA
Safety analysis of Sormeh underground mine to improve sublevel stoping stability	Hosseini M., Azhari A., Lotfi R.,2; Baghbanan A.	2022	Iran
Design method and application of stope structure parameters in deep metal mines based on an improved stability graph	Zhao X.D.2; Zhou X.	2023	China
Enhancing stability graphs for stope design in deep metal mines using machine learning	Zhou X.; Zhao X.; Qu Q.; Huang Y.	2024	China
Exploring Machine Learning Techniques for Open Stope Stability Prediction: A Comparative Study and Feature Importance Analysis	Szmigiel A.; Apel D.B.; Pu Y.; Pourrahimian Y.; Dehghanpour H.	2024	Canada
Optimization of stope structure parameters by combining Mathews stability chart method with numerical analysis in Halazi iron mine	Cui X.; Yang S.; Zhang N.2; Zhang J.	2024	China

6.5. PENDING LINES OF RESEARCH

Some authors outline the challenges associated when applying the stability graph method. For example, difficulties arise when calculating the hydraulic radius from irregular surfaces [11]. Assessing the stress level in stope corners, where stress concentrations are evident, or applying the method in stopes with and hydraulic radius greater than 12, also present challenges [11].

Other authors, however, have stated that the following issues require further study before they can be properly incorporated into the stability graph method [9]:

- Blasting effects: in the same way the damaged induced by blasting is considered by the D parameter in the Hoek and Brown criterion [3].
- Stand-up time: although an exposure time correction factor has been introduced [14], the concept of stand-up time, introduced by Lauffer in 1958 [23], should be reflected explicitly on the stability graph, similarly it is reflected in the RMR chart.

Future lines of research could consist of the development or refinement of software tools to address the application of the stability graph method, such as the web-based tool StopeSoft recently introduced in 2025 [24].

6.6. PUBLICATION ANALYSIS

In previous sections, the inception and the historical evolution of the stability graph method have been analysed. In this section, other aspects such as geographical distribution or the applicability of the method are also discussed.

Regarding the worldwide distribution of the publications, given that the method was originally developed in Canada, most of the scholarly publications on the subject, as well as the most significant advancements, have emerged from that country. Australia has also contributed to a lesser extent, where open-stope is also an extended underground mining method. Recently, China has also significantly contributed to the state-of-the-art of the stability graph method. It must also be pointed the works developed by Suorineni [9, 10, 15, 19, 25–27] which have been published in several countries. This is illustrated in Figs. 6.3 and 6.4. Figure 6.3 presents a pie chart showing the contribution per continent, while Fig. 6.4 displays a world map indicating the number of publications per country.

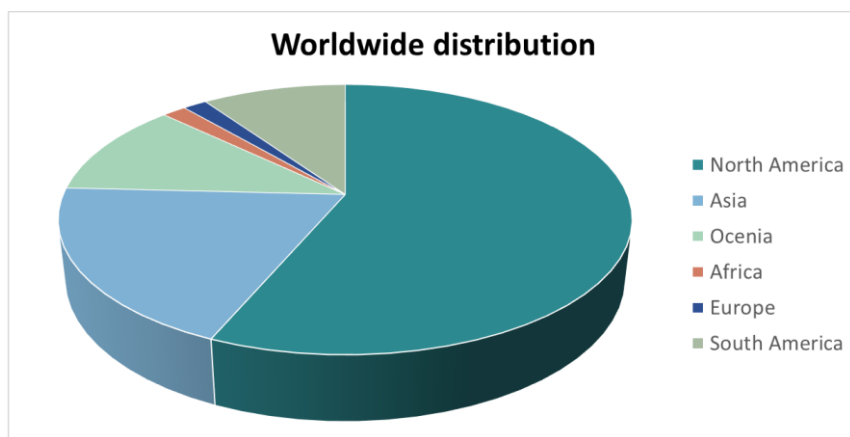


Fig. 6.3. Stability graph method publications per continent

Apart from geographical distribution, it is also important to analyse the applicability of the method, which was originally intended for open-stope mining in hard rock metalliferous orebodies. The method presents limitations when applying in poor rock mass quality, due to the low number of recorded cases under such conditions, or when used in other mining method such as block caving [28] Notable limitations also arise in narrow veins mining, where higher stress relaxation, blasting induced damaged and dilution are expected [9, 29]. The stability graph method is not suitable for high-stress environment involving phenomena such as rock bursting and creeping, nor for entry mining methods [30].

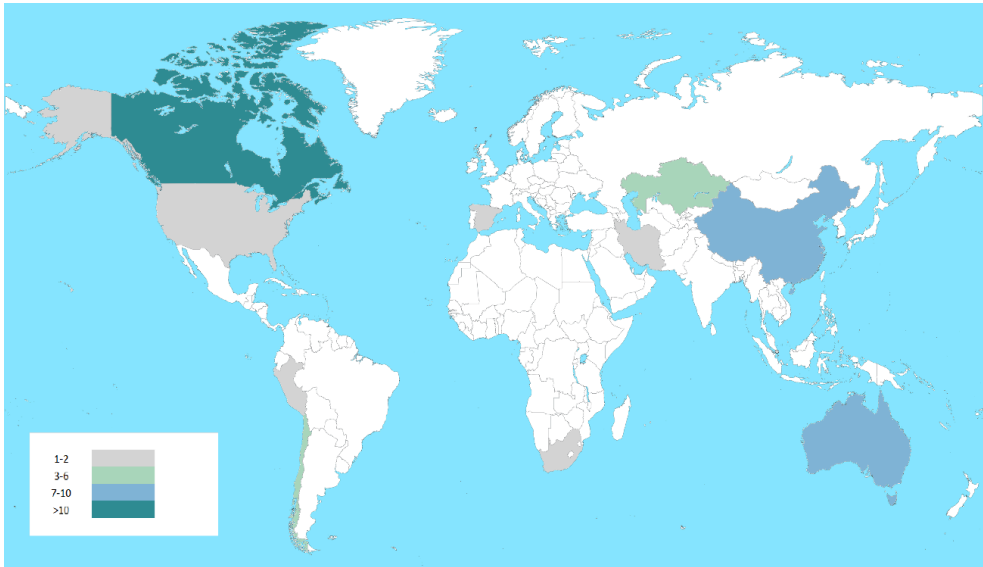


Fig. 6.4. Publications per country. DelMundo.top. (2023).
Blank world map for printing; modified by the author

Besides mining, the method has also been used in different engineering sectors. Despite it was minded for non-entry mining methods, it has been also applied in the design of energy storage underground caverns [31, 32]. Furthermore, it has been applied in geotechnical studies of natural caves [33].

6.7. CONCLUSIONS

The stability graph method has been extensively applied across a large number of countries in underground mining for the design of open stopes. It has proven to be a robust preliminary design tool as it integrates the strengths of classical rock engineering classification systems with specific applicability to underground mining. The method accounts important design aspects such as the stope geometry, the stress environment and the rock mass anisotropy.

Over time, the method has been thoroughly studied, and significant efforts have been made to improve, refine and adapt it to diverse geological and operational environments. These efforts have resulted in numerous publications worldwide, particularly in Canada, Australia and China. In these studies, innovative techniques such as numerical modelling or statistics and machine learning, have been employed for different purposes. Numerical modelling has demonstrated to be a suitable tool for validating or to refining certain parameters or additional factors. However, the relevance of apply-

ing statistical approaches has been questioned, as they may undermine the initial philosophy and hypothesis of the method.

In some publications, future research lines have been identified like blasting induced damage, or the explicit implementation of the stand-up time. Finally, beyond its applicability in the extractive industry, it was also noteworthy that two cases of applicability of the method outside the mining sector were found, underscoring its versatility. Particularly, in these cases the stability graph method was used for civil engineering design of energy storage caverns or for stability analysis in natural caves.

After this state-of-the-art review and publication analysis, future research could focus on compiling records of rock mass data and investigating the applicability of the stability graph method in specific case studies.

REFERENCES

- [1] BARTON N., LIEN R., LUNDE J., *Engineering Classification of Rock Masses for the Design of Tunnel Support*, Rock Mech., 1974, 6, 189–236.
- [2] BIENIAWSKI Z.T., *Engineering Classification of Jointed Rock Masses*, Civ. Eng. S. Afr., 1973, 15, 335–343.
- [3] HOEK E., CARRANZA-TORRES C., CORKUM B., *Hoek–Brown failure criterion – 2002 edition*, Rocscience.
- [4] MATHEWS K.E., HOEK E., WYLLIE D.C., STEWART S.B.V., *Prediction of stable excavation spans for mining at depths below 1000 m in hard rock*, Canada Center for Mineral and Energy Technology. Golder Associates, 1980.
- [5] WHIPPLE R.E.A., *Copper Cliff South Mine (CCSM) stability graph and time evaluation of open stope stability*, Vale Inco Limited, Copper Cliff, Ontario Mansour Group of Companies, Sudbury, Ontario 2009.
- [6] VEYRAT S., GALERA J.M., *Análisis tenso-deformacional y diseño de fortificaciones para una explotación de cobre por sublevel stopping*, Atacama Kozan (Chile). 1er. Congreso Internacional de Diseño de Mina por Métodos Empíricos, Lima, Perú, 2015.
- [7] LAÍN H.C., *Estudio de las distribuciones tensiones y de las resistencias de los rellenos de pasta de la mina subterránea de Aguas Teñidas (Huelva)*, Departamento de Ingeniería Geológica y Minera. Escuela Técnica Superior de Ingenieros de Minas y Energía de Madrid. Universidad Politécnica de Madrid, 2019.
- [8] NICKSON S.D., *Cable support guidelines for underground hard rock mine operations*, University of British Columbia, 1992.
- [9] SUORINENI F.T., *The stability graph after three decades in use: Experiences and the way forward*, Nazarbayev University, 2010.
- [10] SUORINENI F.T., *A Critical Review of the Stability Graph Method for Open Stope Design*, Nazarbayev University, 2012.
- [11] POTVIN Y., *The modified stability graph method more than 30 years later*, In: The modified stability graph method more than 30 years later, Vol. 1, ISRM, Lima, Peru, 2014, p. 10.
- [12] POTVIN Y., *Empirical Open Stope Design in Canada*, Dept. Mining and Mineral Processing, University of British Columbia, 1988.
- [13] CLARK L.M., PAKALNIS R.C., *An empirical approach for estimating unplanned dilution from open stope hangingwalls and footwalls*, Canadian Institute of Mining, Metallurgy and Petroleum, 1997.
- [14] TANNANT D.D., DIEDERICH M.S., *Cablebolt optimization in #3 Mine*, Kidd Mines Division, 1997.

- [15] SUORINENI F.T., *Effects of faults and stress on open stope design*, University of Waterloo, 1998.
- [16] BEWICK R.P., KAISER P.K., *Numerical Assessment of Factor B in Mathews' Method for Open Stope Design*. Proceedings of Third CAN-US Rock Mechanics Symposium, Toronto, Canada, 2009.
- [17] SZMIGIEL A., APEL D.B., PU Y., POURRAHIMIAN Y., DEHGHANPOUR H., *Exploring Machine Learning Techniques for Open Stope Stability Prediction: A Comparative Study and Feature Importance Analysis*, University of Alberta, School of Mining and Petroleum Engineering, Edmonton, Alberta, Canada, 2024.
- [18] ZHOU X. ZHAO X. QU Q. HUANG Y., *Enhancing stability graphs for stope design in deep metal mines using machine learning*, Key Laboratory of Ground Control Management Plan in Deep Metal Mines, National Mine Safety Administration, Northeastern University, 110819, Shenyang, China CSIRO Mineral Resources, Brisbane, QLD, 4069, Australia School of Mechanical and Mining Engineering, The University of Queensland, St Lucia, QLD, 402, Australia, 2024.
- [19] SUORINENI F.T., MADENOVA Y., *The Qualitative Stability Graph for Open Stope Design – Recent Developments*, American Rock Mechanics Association, 2022.
- [20] VALLEJOS J.A. DELONCA A., PEREZ E., *Three-dimensional effect of stresses in open stope mine design*, International Journal of Mining, Reclamation and Environment, 2016.
- [21] VALLEJOS J., DELONCA A., FUENZALIDA J., BURGOS L., *Statistical analysis of the stability number adjustment factors and implications for underground mine design*, Int. J. Rock Mech. Min. Sci., 2016.
- [22] ADOKO AC., VALLEJOS J., TRUEMAN R., *Stability assessment of underground mine stopes subjected to stress relaxation*, Mining Technology, Transactions of the Institutions of Mining and Metallurgy, 2020.
- [23] LAUFFER H., *Gebirgsklassifizierung für den Stollenbau*, Geologie und Bauwesen, 195824 (1), 46–51.
- [24] MADENOVA Y., SUORINENI F.T., XU S., *An automated integrated web-based smart tool for open stope design*, Journal of Sustainable Mining, 2025, Vol. 24, Iss. 1, Article 1.
- [25] SUORINENI F.T., TANNANT D.D., KAISER P.K., *Fault factor for the stability graph method of open-stope design*, Trans. Institut. Min. Metallurg., 1999.
- [26] SUORINENI F.T., TANNANT D.D., KAISER P.K., DUSSEAUULT M.B., *Incorporation of a fault factor into the stability graph method: Kidd mine case studies*, Mineral Res. Eng., 2001. Geomechanics Research Centre, Laurentian University School of Mining and Petroleum Engineering, University of Alberta Department of Earth Sciences, University of Waterloo, 2001.
- [27] SUORINENI F.T., TANNANT D.D., KAISER P.K., *Likelihood statistic for interpretation of the stability graph for open stope design*, Int. J. Rock Mech. Min. Sci., 2001.
- [28] MAWDESLEY C.A., *Predicting rock mass cavability in block caving mines*, Julius Kruttschnitt Mineral Research Centre University of Queensland, 2002.
- [29] CLARK L.M., *Minimizing dilution in open stope mining with focus on stope design and narrow vein longhole blasting*, M.A.Sc. Thesis, University of British Columbia, 1998.
- [30] POTVIN Y., HADJIGEORGIOU J., *The stability graph method for open-stope design*, Underground Mining Methods, 2001.
- [31] WINN K.E.A., *Multi-approach stability analyses of large caverns excavated in low-angled bedded sedimentary rock masses in Singapore*, Nan 2019.
- [32] XINGDONG Z.E.A., *Stability analysis of underground water-sealed oil storage caverns in China: A case study*, Nan 2020.
- [33] JORDÁ L., MARTÍN R., ALONSO A.M., JORDÁ R., ROMERO P.L., *Stability assessment of shallow limestone caves through an empirical approach: Application of the stability graph method to the Castañar Cave study site (Spain)*, Bull. Eng. Geol. Environ., 2016, 75, 1469–1483.
- [34] POTVIN Y., MILNE D., *Empirical cable bolt support design*, International Symposium on Rock Mechanics, 1992.

- [35] SCOBLE M.J., MOSS A., *Dilution in underground bulk mining: Implications for production management*, Geol. Soc. Sp. Publ., 1994.
- [36] STEWART S.B.V., FORSYTH W.W., *The Mathews method for open slope design*, Canadian Institute of Mining, Metallurgy and Petroleum, 1995.
- [37] HADJIGEORGIOU J., LECLAIRE J., POTVIN Y., *An update of the stability graph method of open slope design*, Canadian Institute of Mining, Metallurgy and Petroleum, 1995.
- [38] MILNE D., PAKALNIS R.C., FELDERER M., *Surface geometry assessment for open slope design*, North America Rock Mechanics Symposium, 1996.
- [39] HUTCHINSON J.D., DIEDERICHS M.S., *Cablebolting in Underground Mines*, Bitech Publishers, 1996.
- [40] GERMAIN P., HADJIGEORGIOU J., LESARD J.F., *On the relationship between stability prediction and observed slope overbreak*, North America Rock Mechanics Symposium, 1996.
- [41] DIEDERICHS M.S., KAISER P.K., *Rock instability and risk analyses in open slope mine design*, Can. Geotech. J., 1996.
- [42] KAISER P.K., FALMAGNE V., SUORINENI F.T., DIEDERICHS M.S., TANNANT D.D., *Incorporation of rock mass relaxation and degradation into empirical slope design*, Canadian Institute of Mining, Metallurgy and Petroleum, 1997.
- [43] MILNE D., *Underground design and deformation based on surface geometry*, University of British Columbia, 1997.
- [44] GERMAIN P., HADJIGEORGIOU J., *Influence of slope geometry on mining performance*, Canadian Institute of Mining, Metallurgy and Petroleum, 1998.
- [45] SPROTT D.L., TOPPI M.A., YI X.P., *The incorporation of stress induced damage factor into Mathew's stability graph*, Canadian Institute of Mining, Metallurgy and Petroleum AGM, 1999.
- [46] NEUMANN M.F., *Stability graph design method – A mining operator's guide*, Canadian Institute of Mining, Metallurgy and Petroleum Mine Operators' Conference, 1999.
- [47] DIEDERICHS M.S., HUTCHINSON D.J., KAISER P.K., *Cablebolt layouts using the modified stability graph*, Canadian Institute of Mining, Metallurgy and Petroleum, 1999.
- [48] TRUEMAN R., MIKULA P., MAWDESLEY C., HARRIES N., *Experience in Australia with the application of the Mathews method of open slope design*, Canadian Institute of Mining, Metallurgy and Petroleum, 2000.
- [49] STEWART P.C., TRUEMAN R., *The Extended Mathews Stability Graph: Quantifying case history requirements and site specific effects*, Julius Kruttschnitt Mineral Research Centre University of Queensland, 2001.
- [50] MAWDESLEY C.A., TRUEMAN R., WHITEN W., *Extending the Mathews Stability Graph for Open-slope Design*, Institution of Mining and Metallurgy, Mining Technology, 2001.
- [51] TRUEMAN R., MAWDESLEY C.A., *Predicting cave initiation and propagation*, Canadian Institute of Mining, Metallurgy and Petroleum, 2003.
- [52] STEWART P.C., TRUEMAN R., *Applying the extended Mathews stability graph: Quantifying case history requirements and site-specific effects*, AGCM Conference, 2003.
- [53] WATSON B.P., *A rock mass rating system for evaluating slope stability on the Bushveld Platinum mines*, CSIR Miningtek, Auckland Park. The South African Institute of Mining and Metallurgy, 2004.
- [54] WANG J.C., *Influence of stress, undercutting, blasting and time on open slope stability and dilution*, University of Saskatchewan, 2004.
- [55] MAWDESLEY C.A., *Using logistic regression to investigate and improve an empirical design method*, SINOROCK Symposium, 2004.
- [56] MITRI H.S. et al., *New rock stress factor for the stability graph method*, Department of Mining and Materials Engineering, McGill University Americas Limited, Natural Resources /Oil Sands and Mining, 2011.

- [57] IDA F.K., *Inferred weak rock mass classification for slope design*, University of Saskatchewan, 2013.
- [58] EL MOUHABBIS H.Z., *Effect of slope construction parameters on ore dilution in narrow vein mining*, Department of Mining and Metals and Materials Engineering McGill University, 2013.
- [59] POTVIN Y., *The Modified Stability Graph Method, More Than 30 Years Later*, Australian Centre for Geomechanics, The University of Western Australia, 2014.
- [60] PAKALNIS R., *Empirical design methods in practice*, Pakalnis & Associates University of British Columbia, 2015.
- [61] PAPAIOANOU A., SUORINENI F.T., *Development of a generalised dilution-based stability graph for open slope design*, School of Mining Engineering University of New South Wales, 2016.
- [62] ZHANG L., HU J.H., WANG X.L. ZHAO L., *Optimization of slope structural parameters based on Mathews stability graph probability model*, Advances in Civil Engineering, 2018.
- [63] VALLEJOS J., MIRANDA R., AZORIN J., ARRIAGADA C., CATALÁN O., GARRIDO C., MONDACA M., ESCARES P., *Stability graph using major geological structures*, Universidad de Chile, 2018.
- [64] ZHAO K., WANG Q., LI Q., YAN Y.J., YU X., WANG J.Q., CAO S., *Optimization calculation of slope structure parameters based on Mathews stabilization graph method*, Journal of Vibroengineering, 2019, 21.
- [65] BELIZARIO M., CONDORI R., PEHOVAZ H., RAYMUNDO C., PÉREZ M., *Empirical and Numerical Finite-Element-Based Model to Improve Narrow Vein Mine Design in Peruvian Mining*, Universidad Peruana de Ciencias Aplicadas, 2020.
- [66] MORTAZAVI A., BAKYTZHAN A., *The Consolidated Mathews Stability Graph for Open Slope Design*, Nazarbayev University, 2021.
- [67] HOSSEINI M., AZHARI A. LOTFI R., BAGHBANAN A., *Safety analysis of Sormeh underground mine to improve sublevel stoping stability*, Department of Mining Engineering, Isfahan University of Technology, Isfahan 2022.
- [68] ZHAO X.D., ZHOU X., *Design method and application of slope structure parameters in deep metal mines based on an improved stability graph*, Minerals, 2023, 13.
- [69] CUI X., YANG S., ZHANG N., ZHANG J., *Optimization of slope structure parameters by combining Mathews stability chart method with numerical analysis in Halazi iron mine*, Heliyon 2024, 10.

METODA WYKRESU STABILNOŚCI: AKTUALNY STAN WIEDZY

Na podstawie klasyfikacji masywu skalnego Bartona Q , a specjalnie opracowanej dla metody eksploatacji komorowej (open slope), metoda wykresu stabilności została wprowadzona przez Mathewsa w 1980 roku, a następnie udoskonalona przez Potvina w 1988 roku. W rozdziale tym uwzględniono historyczny rozwój metody aż do dnia dzisiejszego, podkreślając, w jaki sposób najnowsze trendy w poszczególnych okresach wpływały na jej ewolucję. Oprócz analizy historycznej przeprowadzono również przegląd bibliometryczny, klasyfikując opublikowane artykuły według ich rozmieszczenia geograficznego. Niniejszy zwięzły przegląd wskazuje także na nowe sektory zastosowań, wykraczające poza tradycyjne górnictwo komorowe, takie jak projekty magazynowania energii, w których projektuje się wielkoskalowe komory do użytku przemysłowego. Podsumowując, badanie to podkreśla wkład licznych autorów z różnych regionów, którzy pracowali nad udoskonaleniem i rozszerzeniem metody opracowanej pierwotnie w latach 80.

7. IMPLEMENTATION OF OBJECT DETECTION ALGORITHMS IN THE INVENTORY OF TECHNICAL INFRASTRUCTURE, CASE STUDY INSULATORS DETECTION

MATEUSZ CZYRZNAK, JACEK RAPIŃSKI

Department of Geodesy, Faculty of Geoengineering, University of Warmia and Mazury in Olsztyn,
Michała Oczapowskiego street 2, 10-719 Olsztyn, Poland.

Functionality of overhead power lines depends on factors such as conductor material, electrical properties, environmental conditions and insulation. In the case of insulation, the main element ensuring its proper functioning is the insulator. Maintaining them in good condition is essential to ensure proper current flow. Current methods of conducting an inventory of insulators include visual inspections in the field or image analysis. One possible approach to collect images is using cameras mounted on vehicles. This solution enables data acquisition over large areas within a short period of time. However, manual image analysis is considered time-consuming and prone to errors. Object detection algorithms can be employed to automatically identify damaged insulators in images. This method has the potential to significantly reduce the time required for analysis. In this study, a deep learning algorithm was trained for identifying insulators in images of utility poles. These detections can be used in further research to analyze insulators for potential damage. For the object detection algorithm, the YOLO model (You Only Look Once) was chosen, which performs detections in real time, making it highly efficient. For training, 1582 original images of utility poles were used, which were further augmented through rotation and mirroring. Additionally, random images were incorporated into the dataset to reduce the model's tendency for false positive detections. The study demonstrates excellent results in terms of precision, recall, and mAP (mean Average Precision). The achieved *F1*-score exceeds 95%. The performance of this model provides a solid foundation for subsequent further damage analysis of insulators.

Keywords: inventory of technical infrastructure, object detection, insulators, deep learning

7.1. INTRODUCTION

The proper flow of electrical current depends on several factors, including the conductor material, its electrical properties, and environmental conditions, as well as effective insulation. In the case of overhead lines, this insulation is primarily ensured by insulators. Their proper maintenance is crucial to ensure continuity of power supply [1]. Conducting an inventory of insulators through visual inspections is considered very time-consuming. In recent years, modern measurement techniques such as LiDAR

(Light Detection and Ranging) [2] and ground and aerial imaging techniques [3, 4] have been employed for inventory purposes. These methods allow for the collecting data over large areas, reducing both the time and cost of the measurement process [5]. The main problem with gathered data from these devices is their large size. Because of this, analyzing them is very time-consuming. To reduce this time, Artificial Intelligence (AI) algorithms can be used [6]. The main idea is to apply AI algorithms to detect insulators in images. This approach could lead to further research on detecting damaged insulators. In the first step, algorithm for utility pole detection to extract poles from images was developed. The results of this study were published in “Implementation of Object Detection Algorithms in the Inventory of Technical Infrastructure, Case Study of Utility Poles Detection” [7]. In this research, ten YOLOv8 models were trained, with different hyperparameter settings, using 1,736 original ground images of utility poles. After augmentation (through rotation and mirroring) and the addition of randomly selected images, the dataset consisted of 18,849 images. The best-performing model achieved a precision of 98.82%, a recall of 97.29%, and an $F1$ -score of 98.05%. For mAP50 and mAP75, the model achieved scores of 97.92% and 89.93%, respectively. These results confirm the robustness of the proposed approach.

In the context of image analysis, AI techniques have increasingly relied on object detection algorithms [8]. These algorithms belong to a specialized subset of artificial intelligence known as deep learning (DL), which has been widely applied in various pattern recognition and computer vision tasks [9].

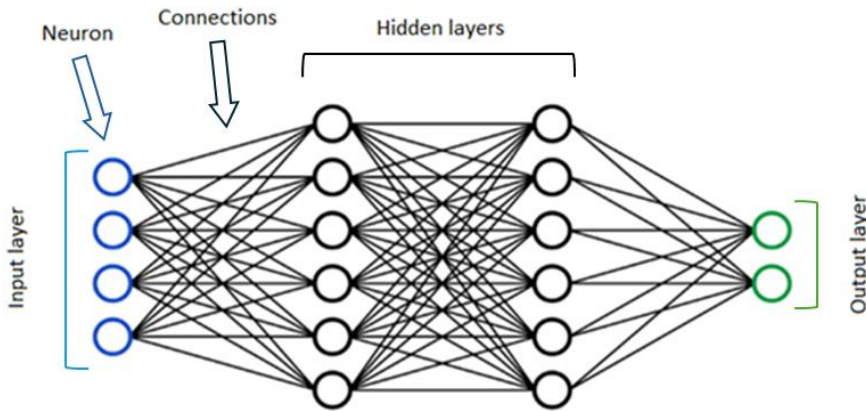


Fig. 7.1. Example structure of Artificial Neural Network (ANN)

The architecture of deep learning algorithms is inspired by the biological neural network. These algorithms use artificial neural networks (ANNs). Similarly to real ones, they are built from interconnected nodes called neurons. This architecture enables AI algorithms to learn how to extract patterns and features from data. Figure 7.1

presents the structure of an ANN, it is composed of layers of interconnected neurons. Each neuron in the input layer is assigned a numerical value from the input data. The values of neurons in the hidden layers and output layer are calculated based on the input values, weights, and biases. The result is then passed through an activation function, which enables the ANN to learn non-linear patterns (Fig. 7.2). The output layer contains the final results of the model. Each neuron in this layer corresponds to one possible answer, and the one with the highest value is selected [10].

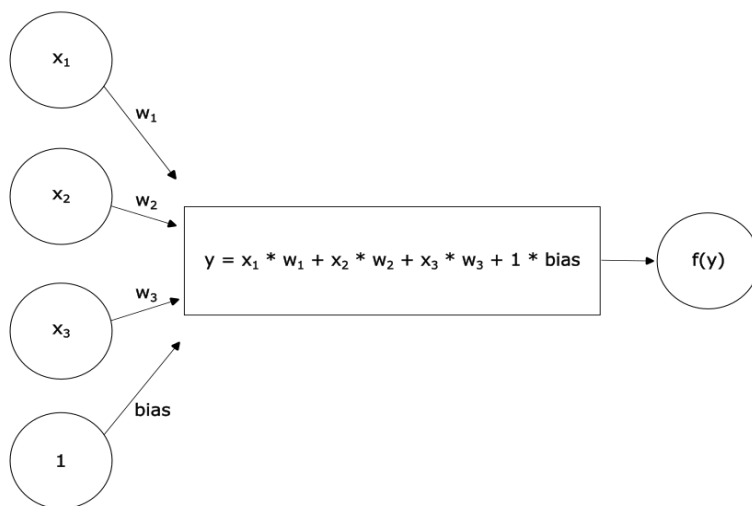


Fig. 7.2. Example of ANN's neuron: x_1, x_2, x_3 – input values, w_1, w_2, w_3 – connection's weight, y – calculated value, $f(y)$ – value of neuron after activation function

Object detection algorithms often use Convolutional Neural Networks (CNNs) [11], which are a more advanced type of ANN (Fig. 7.3). This type of ANN uses layers such

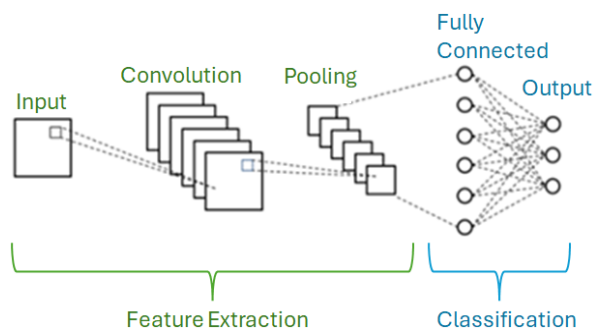


Fig. 7.3. Example of Convolutional Neural Network

as the convolution layer, pooling layer, and fully-connected layer. The convolution layer uses filters that slide over the image and perform calculations. In this process, a feature map is acquired. This map shows the presence of specific features in the input image. The pooling layer is used to downsample the feature maps by reducing their dimensions (width and height). For this task, it also uses filters of a specified size over the feature map. The fully-connected layer is placed at the end of the CNN and is used to conduct classification based on calculations performed by the previous layers. This layer connects each neuron to all neurons in the subsequent layer [12].

7.2. METHODOLOGY

To make the detection process fast and robust, the YOLO (You Only Look Once) model [13] was selected. YOLO performs real-time detections, enabling the processing of large image datasets in a short amount of time. For the purposes of this research, version 8 of the YOLO model was used due to its balanced trade-off between speed and performance [14]. The process of training an object detection algorithm consists of three steps: data collection, hyperparameter optimization, and model evaluation.

7.2.1. DATA COLLECTION

The dataset consists of 1582 images of utility poles extracted using the model for utility pole detection described in [7]. The original images were gathered using three cameras:

- SONY DSC-HX10V (2592×1944);
- Xiaomi Redmi 4X (3210×4160);
- Xiaomi MI 8 Lite (3024×4032).

To augment the dataset, new images were generated through rotation and mirroring. Rotation was applied at three angles: 90° , 180° , and 270° to both the original and mirrored images (Fig. 7.4). The dataset was also enlarged by adding 4961 random images from the Common Objects in Context (COCO) dataset [15] to reduce the model's capacity for false positive detections. These images do not contain any insulators (Fig. 7.5). Based on the insulators' shape and color, three classes were distinguished (Fig. 7.6):

- glass pin, hereinafter referred to as blue mushroom (bm);
- porcelain mushroom, hereinafter referred to as white mushroom (wm);
- porcelain pin, hereinafter referred to as white harmonica (wh).

In the end, the dataset contained 17 617 images. The images were divided into three subsets: training, validation, and test (Table 7.1). All variations of the same image were assigned to the same subset to prevent data leakage and ensure proper generalization.



a) Base image



b) Mirrored image



c) Rotated image

Fig. 7.4. Labeled data



Fig. 7.5. Example images from COCO



a) White harmonica (wh)

b) White mushroom (wm)

c) Blue mushroom (bm)

Fig. 7.6. Types of insulators: a) white harmonica, b) white mushroom, c) blue mushroom

Table 7.1. Distribution of images across subsets

	Train	Val	Test	Total
Images in dataset	13681	1664	2272	17617
Utility poles images	10120	1264	1272	12656
COCO dataset images	3561	400	1000	4961

7.2.2. HYPERPARAMETER OPTIMIZATION

A critical aspect of training a deep learning (DL) models is the selection of optimal hyperparameters [16]. Hyperparameters define how the learning process is structured. In this study, the focus was on optimizing the following hyperparameters: optimization algorithm, learning rate, momentum, weight decay, and image resolution:

- Image resolution: rescales the image to a specified resolution.
- Optimizer: the algorithm used to update the weights and biases of a neural network during training. The primary goal of an optimizer is to minimize the loss function, which quantifies how well the model's predictions match the actual target values [17].
- Learning rate: influences how rapidly the model's weights are updated [18].
- Momentum: a technique used to accelerate the optimization process during training by taking into account the previous updates made to the model parameters [19].
- Weight decay: adds a penalty to the model's weights to prevent overfitting [20].

To estimate the optimal combination of hyperparameter values, a tuning technique was used [21]. Hyperparameter tuning involves training multiple models with different

configurations to identify the most effective combination. Beyond the hyperparameters mentioned above, the following were used with fixed values (Table 7.2):

- Number of epochs: defines the number of iterations. In each iteration, the entire dataset is passed through the model during training [22].
- Cosine learning rate scheduler: adjusts the learning rate by making it follow a cosine curve over the epochs. This helps manage the learning rate for better convergence [23].
- Batch size: defines the number of training samples in one batch [24].

Table 7.2. Fixed values of hyperparameters for tuning

Hyperparameter	Value
Number of epochs	30
Cosine learning rate scheduler	FALSE
Batch size	103/26/10 (depending on used resolution: 640px/1280px/2048px)

The hyperparameters search space is summarized in Table 7.3. In this study, 90 models per optimizer (30 models for each of 3 resolutions) were trained. Then, the 9 best models were selected – one for each combination of optimizer and resolution – and trained further for 300 epochs. Additionally, 3 models were trained, one for each resolution, with automatically adjusted hyperparameters.

Table 7.3. Hyperparameter's search space

Optimizer	Learning rate	Momentum	Weight decay	Image resolution
SGD*	(0.0001, 0.1)	(0.8, 0.98)	(0.00001, 0.001)	640px/1280px/2048px
Adam*	(0.0001, 0.1)	(0.8, 0.98)	(0.0001, 0.001)	640px/1280px/2048px
AdamW*	(0.0001, 0.1)	(0.8, 0.98)	(0.0001, 0.001)	640px/1280px/2048px

* SGD – Stochastic Gradient Descent [25].

* Adam – Adaptive Moment Estimation [26].

* AdamW – Adam with decoupled Weight Decay [27].

7.2.3. MODEL EVALUATION

Evaluation of the final twelve models was conducted using the following metrics: precision, recall, *F1*-score and mean Average Precision (mAP) computed using Intersection over Union (IoU) [28] over 50% (mAP50) and 75% (mAP75).

- Precision (1) – the percentage of correct predictions from all predictions made by model [29].

$$Precision = \frac{T_p}{T_p + F_p}. \quad (1)$$

- Recall (2) – describes percentage of detected objects from all objects [30].

$$Recall = \frac{T_p}{T_p + F_n}. \quad (2)$$

- *F1*-score (3) – estimates model's overall capacity based on precision and recall [31].

$$F1\text{-score} = 2 \cdot \frac{Precision \cdot Recall}{Precision + Recall}. \quad (3)$$

- Mean Average Precision – measures the mean Average Precision (AP) over all classes. AP describes the model's ability to balance between precision and recall across confidence scores and IoU thresholds by calculating the area under the precision-recall curve and comparing the IoU between predicted and ground-truth boxes [32].

$$AP = \int_0^1 Precision(Recall) dRecall. \quad (4)$$

Evaluation of the models trained during the tuning process was performed using the Fitness metric [33]. The Fitness is used to evaluate and select the best model checkpoint during training. It determines which model has the best overall performance based on multiple evaluation metrics. The fitness score is computed as a weighted combination of precision, recall, mAP50, and mAP50–95.

7.3. RESULTS

From all models trained during hyperparameter tuning, the nine best models were selected – one for each optimizer-resolution combination. To this pool, three additional models were added, each trained with automatically selected hyperparameters corresponding to one of the considered resolutions. The selected hyperparameters are presented in Table 7.4.

All twelve best models were then trained for 300 epochs. To accelerate training and mitigate overfitting [34], early stopping was used, terminating training after 50 epochs if no significant improvement was detected [35]. The results of the trained models are summarized in Table 7.5.

An analysis of Table 7.5, shows that all models achieved very high results across all metrics. In terms of precision (Fig. 7.7), recall (Fig. 7.8), and *F1*-score (Fig. 7.9), some

models achieved results approaching 100%. Regarding recall and *F1*-score, the best-performing model was Train11, with scores of 98.10% and 97.90%, respectively. Only in terms of precision was it outperformed by Train5, which achieved a score of 98.70%, surpassing Train11 by 1%. In terms of mAP50 and mAP75, model Train11 also performed best, with scores of 98.80% and 92.52%. Although most models performed similarly in mAP50 (Fig. 7.10), the mAP75 results (Fig. 7.11) showed considerable variation. Only four models achieved a score above 90.00%. The lowest value, 70.23%, was recorded by model Train1. Figure 7.12 illustrates the detection results using model Train11.

Table 7.4. Best model's hyperparameters

Model	Optimizer	Resolution	Learning rate	Momentum	Weight decay	Batch size
Train1	Adam	640	0.00785	0.98000	0.00042	103
Train2	AdamW	640	0.01000	0.94151	0.00050	103
Train3	SGD	640	0.00678	0.98000	0.00055	103
Train4	Auto=SGD	640	0.01000	0.90000	0.00078	100
Train5	Adam	1280	0.00404	0.81367	0.00027	26
Train6	AdamW	1280	0.00924	0.87158	0.00059	26
Train7	SGD	1280	0.00644	0.96679	0.00043	26
Train8	Auto=SGD	1280	0.01000	0.90000	0.00041	26
Train9	Adam	2048	0.00927	0.80000	0.00041	10
Train10	AdamW	2048	0.00473	0.86783	0.00059	10
Train11	SGD	2048	0.00729	0.96826	0.00041	10
Train12	Auto=SGD	2048	0.01000	0.90000	0.00047	10

Table 7.5. Values of evaluation metrics of best models

Model	Optimizer	Resolution	Precision	Recall	<i>F1</i> -score	mAP50	mAP75
Train1	Adam	640	0.963	0.898	0.9294	0.944	0.7023
Train2	AdamW	640	0.948	0.921	0.9343	0.954	0.8696
Train3	SGD	640	0.971	0.923	0.9464	0.958	0.902
Train4	Auto	640	0.963	0.931	0.9467	0.961	0.7368
Train5	Adam	1280	0.987	0.967	0.9769	0.983	0.719
Train6	AdamW	1280	0.98	0.967	0.9735	0.98	0.8868
Train7	SGD	1280	0.982	0.971	0.9765	0.983	0.9111
Train8	Auto	1280	0.983	0.97	0.9765	0.986	0.8736
Train9	Adam	2048	0.974	0.972	0.973	0.987	0.7495
Train10	AdamW	2048	0.983	0.97	0.9765	0.985	0.8733
Train11	SGD	2048	0.977	0.981	0.979	0.988	0.9152
Train12	Auto	2048	0.981	0.976	0.9785	0.985	0.9023

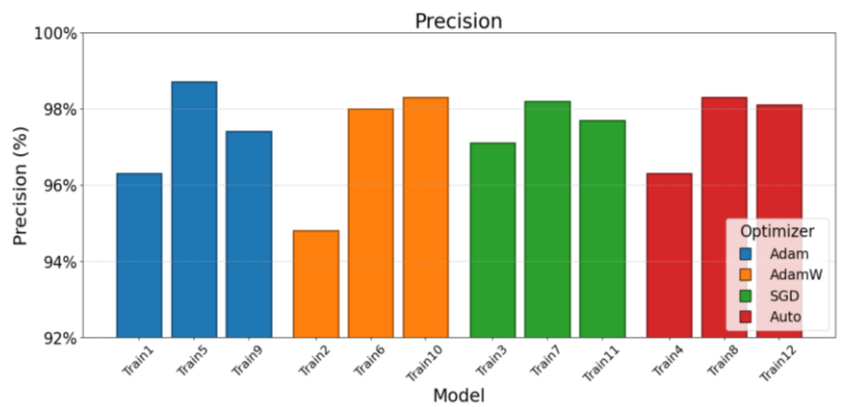


Fig. 7.7. Precision of trained models

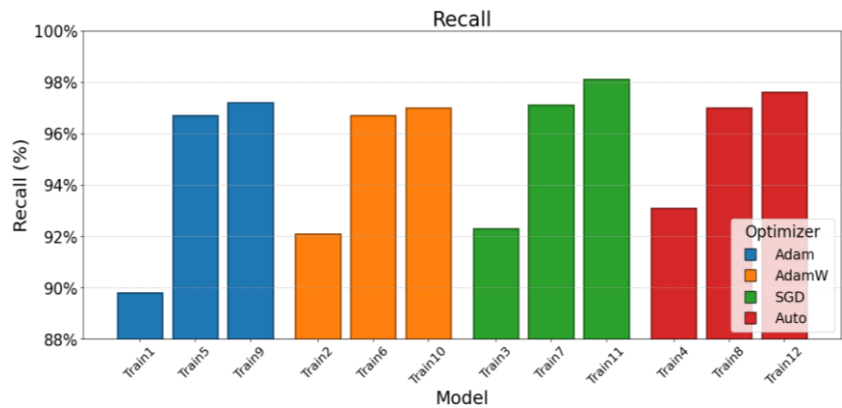


Fig. 7.8. Recall of trained models

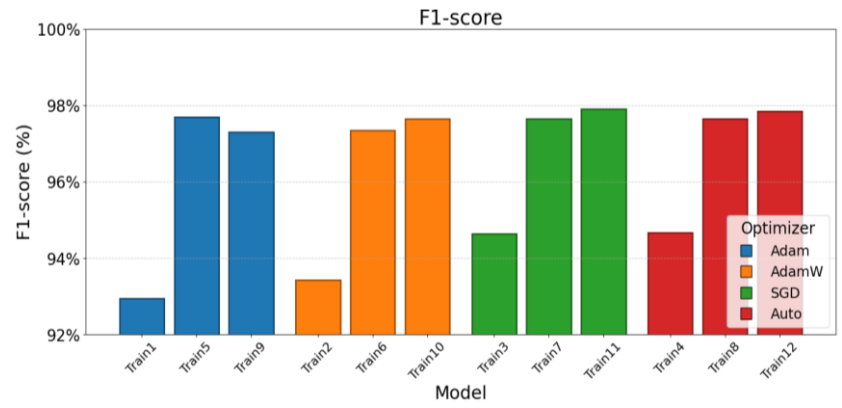


Fig. 7.9. F1-score of trained models

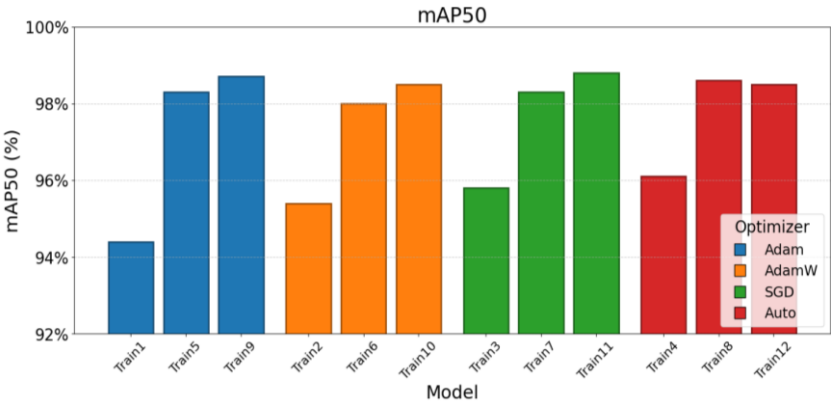


Fig. 7.10. mAP50 of trained models

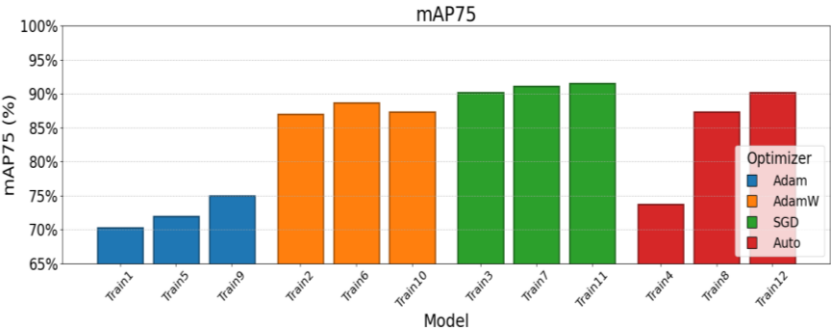
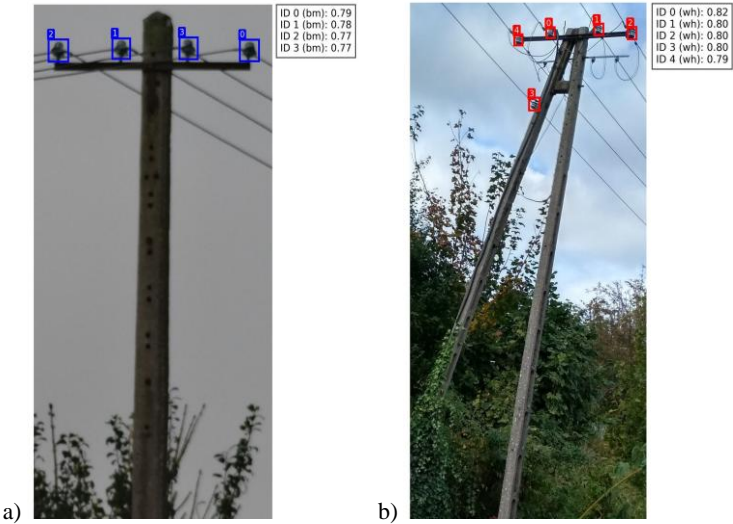


Fig. 7.11. mAP75 of trained models



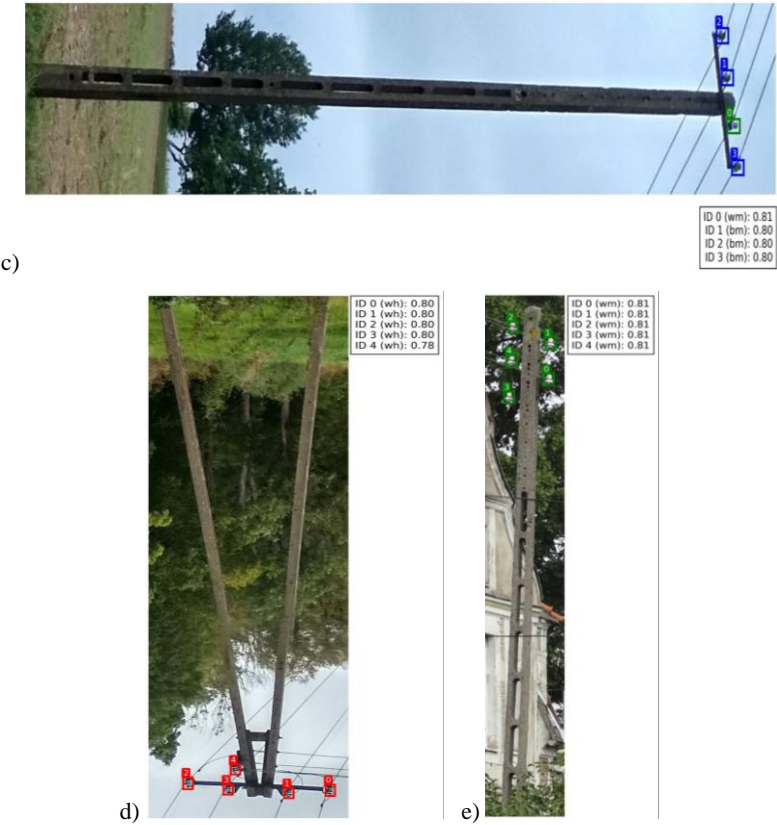


Fig. 7.12. Sample insulators detection results on test dataset: the legend contains information about bounding box id, class of object and confidence score. Subfigures: a), b), e) represent detection of blue mushrooms (bm), white harmonicas (wh) and white mushrooms (wh) on original images. Subfigures c) and d) show detection results on augmented images rotated by 90° and 270°

The trained models were further compared in terms of precision, recall, and *F1*-score for each class. The results are presented in Fig. 7.13, Fig. 7.14, and Fig. 7.15, respectively. Model Train11 again achieved the highest *F1*-score in each class scoring 95.90%, 97.20% and 98.70% for white harmonica, white mushroom and blue mushroom respectively (Table 7.6). These results demonstrate a very high level of performance.

Table 7.6. *F1*-scores across classes (model Train11)

Class	<i>F1</i> -score [%]
White harmonica	95.90
White mushroom	97.20
Blue mushroom	98.70

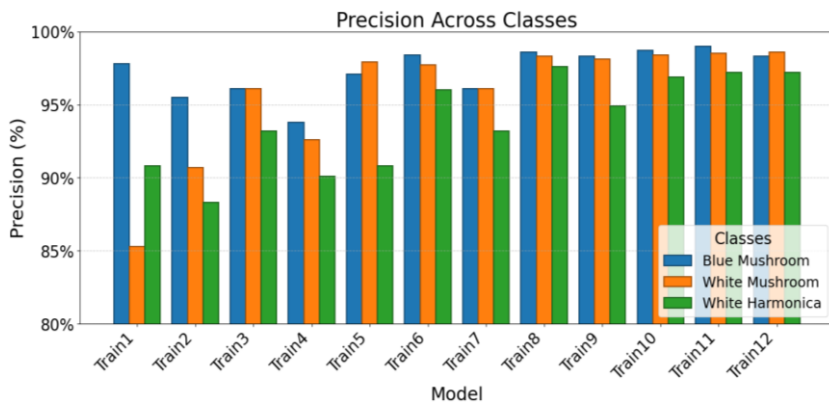


Fig. 7.13. Precision across classes



Fig. 7.14. Recall across classes

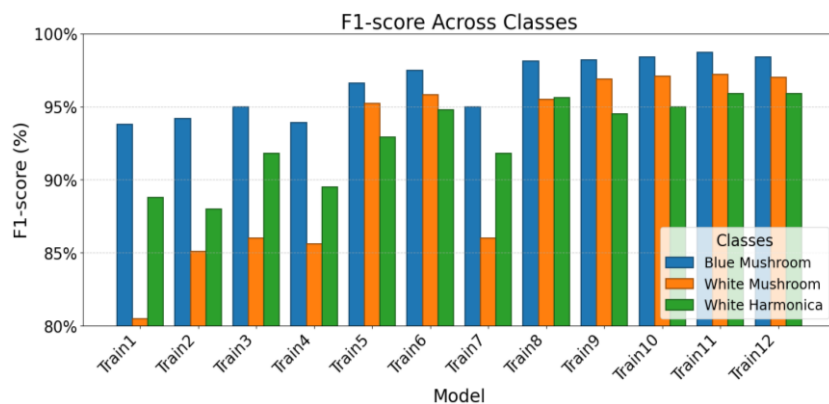


Fig. 7.15. F1-score across classes

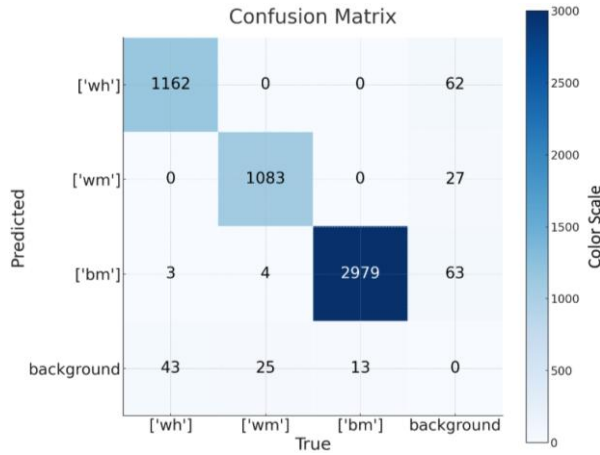


Fig. 7.16. Confusion matrix for model Train11

The analysis of the presented plots reveals that certain trained models (e.g., Train1) exhibit higher misclassification rates for the white mushroom and white harmonica classes compared to the blue mushroom class. This trend may be explained by the higher visual distinctiveness of the blue color, which enhances class separability for the model. Increasing the image resolution hyperparameter reduces the performance disparity between classes. The confusion matrix for model Train11, shown in Fig. 7.16, indicates that the highest number of false-positive detections occurs for the white harmonica and blue mushroom. Among them, the white harmonica class shows the lowest recognition accuracy, representing the most challenging category for the model.

7.4. CONCLUSIONS

Insulators are a key component of utility poles, essential for proper current flow. Conducting an inventory of insulators using traditional methods, such as visual inspection or manual image analysis, is highly time-consuming. In this research, an object detection model for identifying insulators in images was introduced. This approach enables faster detection of insulators, allowing for substantially more efficient inspections.

The best model demonstrates excellent performance in terms of precision, recall, and *F1*-score: 97.70%, 98.10%, and 97.90%, respectively. The model also achieves very good results in terms of mAP, once again outperforming the other trained models. For mAP50, the model achieved a score of 98.80%, and for mAP75, a score of 91.52%. For this study, three classes of insulators were defined based on their color and shape: white harmonica, white mushroom, and blue mushroom. Regarding classification per-

formance, the model achieved *F1*-scores of 95.90%, 97.20%, and 98.70%, respectively, for each class.

The trained model is capable of identifying and extracting insulators from images. At this stage, manual visual inspection remains necessary. In future research, the authors aim to train a model capable of conducting inspections to detect broken or defective insulators. A potential challenge in achieving this goal is the small size of defects, such as cracks on the insulators. This issue could be addressed by employing higher-resolution cameras.

REFERENCES

- [1] ABU-SIADA A., AWAD H., BAJAJ M., GHALY R., GHONEIM S., IBRAHIM A., ZAITSEV I., *Impact of atmospheric conditions on the flash-over voltage of the transmission line insulators using central composite design*, Scientific Reports, 2024, Vol. 14, p. 22395.
- [2] BEHROOZPOUR B., BOSER B.E., SANDORN P.A.M., WU M.C., *Lidar system architectures and circuits*, IEEE Communications Magazine, 2017, Vol. 55, pp. 135–142.
- [3] DOLGIKH L., DOLGIKH O., KALINICHENKO V., PYSMENNYI S., *Choosing a camera for mine surveying of mining enterprise facilities using unmanned aerial vehicles*, Mining of Mineral Deposits, 2020.
- [4] AGÜERA F., CARVAJAL F., PÉREZ M., *Low cost surveying using an unmanned aerial vehicle*, The International Archives of the Photogrammetry, Remote Sensing and Spatial Information Sciences, 2013, Vol. XL–1/W2, pp. 311–315.
- [5] GUAN H., JONATHAN L., SHUANG C., YU Y., *Use of mobile LiDAR in road information inventory: A review*, International Journal of Image and Data Fusion, July 2016, Vol. 7, pp. 219–242.
- [6] ALFIO V. S., COSTANTINO D., PEPE M., SCARINGI D., *Data for 3D reconstruction and point cloud classification using machine learning in cultural heritage environment*, Data in Brief, 2022, Vol. 42, p. 108250.
- [7] CZYRZNAK M., RAPIŃSKI J., *Implementation of object detection algorithms in the inventory of technical infrastructure, case study of utility poles detection*, Civil and Environmental Engineering Reports, 2025, Vol. 35, pp. 177–189.
- [8] AMIT Y., FELZENSZWALB P., GIRSHICK R., *Object detection*, in: *Computer vision: A reference guide*, K. Ikeuchi (Ed.), Springer International Publishing, 2021, pp. 875–883.
- [9] BENGIO Y., HINTON G., LECUN Y., *Deep learning*, Nature, 2015, Vol. 521, pp. 436–444.
- [10] CROSSA J., LÓPEZ A. M., LÓPEZ O. A. M., *Fundamentals of artificial neural networks and deep learning*, In: O.A.M. López, A.M. López, J. Crossa (Eds.), *Multivariate statistical machine learning methods for genomic prediction*, Springer International Publishing, 2022, pp. 379–425.
- [11] KETKAR N., MOOLAYIL J., *Convolutional neural networks*, In: N. Ketkar, J. Moolayil (Eds.), *Deep learning with python: Learn best practices of deep learning models with PyTorch*, Apress, 2021, pp. 197–242.
- [12] NASH R., O'SHEA K., *An introduction to convolutional neural networks*, 2015.
- [13] DIVVALA S., FARHADI A., GIRSHICK R., REDMON J., *You only look once: Unified, real-time object detection*, In: Proceedings of the IEEE conference on computer vision and pattern recognition (CVPR), June 2016.
- [14] NAZIR A., WANI M.A., *You only look once – object detection models: A review*, In: 2023 10th international conference on computing for sustainable global development (INDIACom), 2023, pp. 1088–1095.

- [15] BELONGIE S., BOURDEV L., DOLLÁR P., GIRSHICK R., HAYS J., LIN T., MAIRE M., PERONA P., RAMANAN D., ZITNIC C., *Microsoft COCO: Common objects in context*, In: S. Bernt, T.T.F. David, Pajdla (Eds.), *Computer vision – ECCV 2014*, Springer International Publishing, 2014, pp. 740–755.
- [16] CHO S., KIM J., *Evolutionary optimization of hyperparameters in deep learning models*, In: 2019 IEEE congress on evolutionary computation (CEC), 2019, pp. 831–837.
- [17] SUN R., *Optimization for deep learning: An overview*, Journal of the Operations Research Society of China, 2020, Vol. 8, pp. 249–294.
- [18] BAHRI Y., DYER E., GUR-ARI G., LEWKOWYCZ A., SOHL-DICKSTEIN J., *The large learning rate phase of deep learning: The catapult mechanism*, 2020.
- [19] DAHL G., HINTON G., MARTENS J., SUTSKEVER I., *On the importance of initialization and momentum in deep learning*, In: S. Dasgupta, D. McAllester (Eds.), *Proceedings of the 30th international conference on machine learning*, PMLR, May 2013, pp. 1139–1147.
- [20] HONG B.-W., NAKAMURA K., *Adaptive weight decay for deep neural networks*, IEEE Access, 2019, Vol. 7, pp. 118857–118865.
- [21] AMINI M.H., OHLAND M.W., REZAPOUR S., ZAHEDI L., MOHAMMADI F.G., *Search algorithms for automated hyper-parameter tuning*, 2021.
- [22] ASSAD A., SHAFI S., *Exploring the relationship between learning rate, batch size, and epochs in deep learning: An experimental study*, In: M. Thakur, S. Agnihotri, B.S. Rajpurohit, M. Pant, K. Deep, A.K. Nagar (Eds.), *Soft computing for problem solving*, Springer Nature Singapore, 2023, pp. 201–209.
- [23] KIM C., KIM J., KIM S., KIM S., LEE D., *Automated learning rate scheduler for large-batch training*, 2021.
- [24] CASTELLI M., KANDEL I., *The effect of batch size on the generalizability of the convolutional neural networks on a histopathology dataset*, ICT Express, 2020, Vol. 6, pp. 312–315.
- [25] AMARI S., *Backpropagation and stochastic gradient descent method*, Neurocomputing, 1993, Vol. 5, pp. 185–196.
- [26] NABABAN E. B., SITOMPUL O. S., SINGARIMBUN R. N., *Adaptive moment estimation to minimize square error in backpropagation algorithm*, In: 2019 international conference of computer science and information technology (ICoSNiKOM), 2019, pp. 1–7.
- [27] HUTTER F., LOSHCHILOV I., *Fixing weight decay regularization in adam*, CoRR, 2017, Vol. abs/1711.05101.
- [28] LI S., ZHAO L., *Object detection algorithm based on improved YOLOv3*, Electronics, 2020, Vol. 9.
- [29] CHÁVEZ-URBIOLA E. A., CORDOVA-ESPARZA D.-M., RAMÍREZ-PEDRAZA A., TERVEN J., *A comprehensive survey of loss functions and metrics in deep learning*, Artificial Intelligence Review, Apr. 2025, Vol. 58.
- [30] HELLAS A., LEINONEN J., SARSA S., *Empirical evaluation of deep learning models for knowledge tracing: of hyperparameters and metrics on performance and replicability*, 2022.
- [31] CHICCO D., JURMAN G., *The advantages of the matthews correlation coefficient (MCC) over F1 score and accuracy in binary classification evaluation*, BMC Genomics, 2020, Vol. 21, p. 6.
- [32] FERRARI V., HENDERSON P., *End-to-end training of object class detectors for mean average precision*, 2017.
- [33] AKRAM U., ASHRAF I., GHITH E. S., HUSSAIN W., KIM T., MUSHTAQ M., SHAHROZ M., TLIIJA M., *Ensemble genetic and CNN model-based image classification by enhancing hyperparameter tuning*, Scientific Reports, 2025, Vol. 15, p. 1003.
- [34] LIU X., SALMAN S., *Overfitting mechanism and avoidance in deep neural networks*, 2019.
- [35] BALLLES L., HENNING P., LASSNER C., MAHSERECI M., *Early stopping without a validation set*, 2017.

WYKORZYSTANIE ALGORYTMÓW WYKRYWANIA OBIEKTÓW W INWENTARYZACJI INFRASTRUKTURY TECHNICZNEJ: PRZYKŁAD DETEKCJA IZOLATORÓW

Automatyczna identyfikacja uszkodzonych izolatorów na obrazach może być realizowana przy użyciu algorytmów wykrywania obiektów. Metoda ta pozwala znacząco skrócić czas potrzebny na analizę zdjęć. W niniejszym badaniu wytrenowano algorytm uczenia głębokiego do identyfikacji izolatorów na zdjęciach słupów energetycznych. Wykrycia te mogą być wykorzystane w dalszych badaniach do analizy izolatorów pod kątem potencjalnych uszkodzeń. Do algorytmu wykrywania obiektów wybrano model YOLO (You Only Look Once), który wykonuje detekcje w czasie rzeczywistym, co czyni go bardzo wydajnym. Do treningu wykorzystano 1582 oryginalne obrazy słupów energetycznych, które następnie poddano augmentacji poprzez obrót i lustrzane odbicie. Ponadto do zbioru danych włączono losowe obrazy, aby zmniejszyć tendencję modelu do fałszywych detekcji. Badanie wykazało bardzo dobre wyniki pod względem precyzji, recall oraz mAP (mean Average Precision). Osiągnięty wynik *F1-Score* przekracza 95%. Wydajność tego modelu stanowi solidną podstawę do prowadzenia dalszych analiz uszkodzeń izolatorów.

8. A COMPARATIVE STUDY OF DETERMINISTIC AND STOCHASTIC METHODS FOR GROUNDWATER FLOW MODELLING

AMR MOHARRAM, BALÁZS KOVÁCS

University of Miskolc, Miskolc, Hungary.

Groundwater modelling is one of the most important toolkits for any hydrogeologist as it gives a quantitative framework where many data from different sources are put together to investigate and conceptualise hydrogeologic processes. A wide variety of modelling codes are available which utilise different mathematical methods such as finite difference, finite element or finite volume for deterministic models in addition to applying the principles of probability and statistics to produce stochastic models. Each numerical or statistical method has its own characteristics that makes a code advantageous than others depending on the problem to be investigated. A hypothetical problem is used to compare the results and the workflow between some of the different methods that are applied in the frame of groundwater modelling to study their differences and recommend when they can be applied. MODFLOW, which uses the finite differences method to solve the groundwater flow equation, is the easiest to understand and calculate accurate zone budget, but they cannot be efficiently refined around areas of interest and complex geology is difficult to represent, particularly if there are discontinuous or pinched out layers. MODFLOW-USG, which is specialised for unstructured grid, implement finite volume method. It has efficient refinement since it efficiently refines the grid around areas of interest without ending up with a large number of cells in addition to representing complex geology with discontinuous or pinched out layers. However, it is not easy to use like MODFLOW, Also, MODFLOW-USG does not include observation process within the model, it has to be done outside the model with a different utility programme. Stochastic models have the advantage that they generate multiple realisations of equal probability each with their own uncertainty and risk. However, this means some judgment and experience is needed to choose the best solution available. From the results obtained from the hypothetical models, the best solution observed was the stochastic and Quadtree unstructured grid. Such conclusion was based on the number of cells, the time needed for the model to converge, in addition to root mean square errors.

Keywords: finite-difference, finite-volume stochastic modelling

8.1. BASIC CONCEPTS

8.1.1. IMPORTANCE OF GROUNDWATER MODELLING

To introduce the importance of groundwater modelling, first, hydrologic cycle ought to be shown for a starting point toward the core purpose of this study. Water as

H₂O molecules occur naturally inside, on the surface and in the atmospheric zone of Earth with different proportions and characteristics (Fig. 8.1).

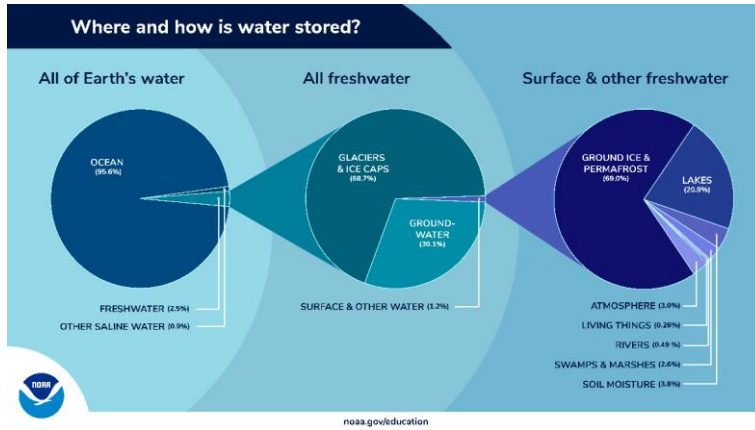


Fig. 8.1. Global water distribution in Earth (Image credit: NOAA Education)

From the above figure, it is shown that the amount of water which can be used for everyday activities is actually limited compared with oceanic water volumes which are not useful to be utilised directly for major needed purposes. As such, it is very important to make use of as much water as possible properly so as not to suffer from lack of water resources in the future. For that end, an understanding of how water molecules behave physically, chemically, how much is gained and how much is lost is very fundamental because, fresh water is not equally distributed globally.

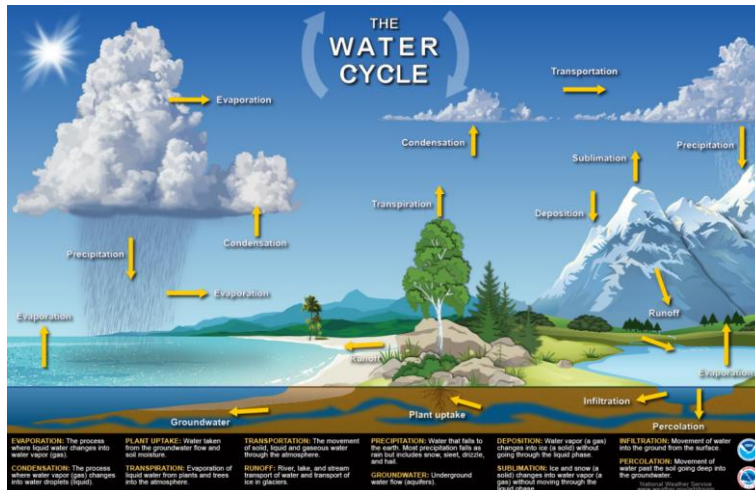


Fig. 8.2. Hydrologic Cycle (Image credit: NOAA Education)

Hydrologic cycle (Fig. 8.2) provides a fundamental framework for studying pathways along which water molecules transport from big water reservoirs such as ocean basins to the atmosphere in addition to how much water is infiltrated to the ground or build up into ice caps on mountains or run off along streams and rivers until ending up back again to ocean basins and the cycle continues.

Indeed, groundwater, as a relatively major resource of freshwater is a national strategic resource especially wherever surface freshwater resources are scarce or lacking.

Groundwater modelling is a field of applied science which purpose is to quantify the subsurface processes that governs groundwater behaviour. After understanding the natural subsurface conditions, hydrogeologists utilise groundwater models to study the effects of human activity such as pumping wells, drains, dewatering for mining or engineering constructions, to make use of the sensitive and limited groundwater resources effectively without causing harm or contamination.

8.1.2. THE CONCEPT OF HEAD

To mathematically represent groundwater, an easily measurable related aspect must be defined. In the literature [1], it has been proved that groundwater level, which is relatively an easily measurable parameter, can mathematically represent groundwater energy. This is a major advantage since energy is governed by laws of physics and can be mathematically studied, in addition since generally, groundwater moves from areas of higher energy (higher water levels; heads) to lower energy areas, groundwater flow directions, areas of recharge and discharge can be delineated if groundwater levels are measured or known.

This can help in calculating water budgets (inflows/outflows) of areas of interest to help decision makers or government managing groundwater effectively and safely.

8.1.3. FUNDAMENTAL GROUNDWATER FLOW EQUATION

Groundwater flow can be mathematically described by the following equation:

$$\frac{\partial}{\partial x} \left(K_x \frac{\partial h}{\partial x} \right) + \frac{\partial}{\partial y} \left(K_y \frac{\partial h}{\partial y} \right) + \frac{\partial}{\partial z} \left(K_z \frac{\partial h}{\partial z} \right) = S_s \frac{\partial h}{\partial t}. \quad (1)$$

The right-hand side of the above equation is related to transient models where change in head with respect to direction is related to time, if it is zero, the model is said to be steady-state where there is no change in heads with respect to time. Solving the partial differential equation to calculate heads in space and time domains is the primary task of groundwater flow models. The solution can be derived analytically or numerically, each of which contains groups of methods and workflows the implementation of which depends primarily on the choice of code and groundwater conditions involved.

8.2. PROBLEM DESCRIPTION

The aim of this study is to compare between different numerical methods, specifically, finite difference, finite volume and stochastic simulation, to assess their practicality, usefulness, advantages and disadvantages, in the context of groundwater modelling flows.

Since this study is a comparative type, 2 hypothetical sites, available from Aquaveo free tutorials, were chosen to cover different modelling conditions and characteristics as criteria for comparison.

8.2.1. SITE1: COASTAL AQUIFER

Figure 8.3 shows a small coastal aquifer in Washington, USA, with three production wells. The no-flow boundary on the upper left corresponds to a parallel-flow boundary, and the no-flow boundary on the left corresponds to a thinning of the aquifer due to a high bedrock elevation. A stream provides a river boundary condition on the lower left, and the remaining boundary is a coastal boundary simulated with a specified head condition.

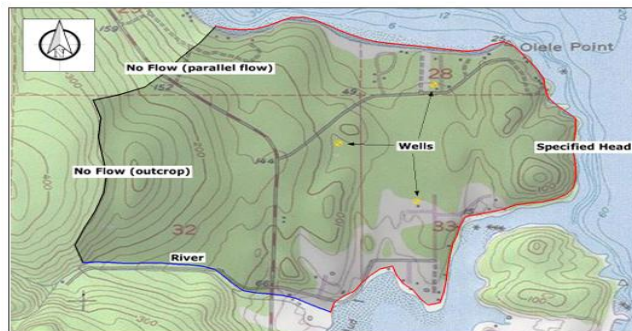


Fig. 8.3. Conceptual model for a Coastal Aquifer, lines explained in text below
(<https://s3.amazonaws.com/gmstutorials-10.8.aquaveo.com/ComplexStratigraphy.zip>)

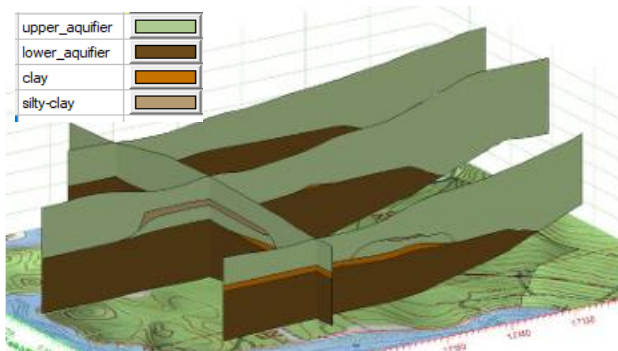


Fig. 8.4. Fence diagram showing the subsurface stratigraphy (credit Aquaveo)

The stratigraphy of the site consists of an upper and lower aquifer with minor semi-confining units (Fig. 8.4).

8.2.2. SITE2: BASIN

A groundwater model for a medium-sized basin is shown in Fig. 8.5. The basin encompasses 72.5 square kilometres. It is in a semi-arid climate, with average annual precipitation of 0.381 m/yr. Most of this precipitation is lost through evapotranspiration. The recharge that reaches the aquifer eventually drains into a small stream at the centre of the basin. This stream drains to the north and eventually empties into a lake with elevation 304.8 meters. Three wells in the basin also extract water from the aquifer. The perimeter of the basin is bounded by low-permeability crystalline rock. There are ten observation wells in the basin. There is also a stream flow gauge at the bottom end of the stream. The model region encompasses fractured and weathered bedrock as well as alluvial material, grading from hydraulically tighter materials in the south to more permeable materials in the north. Furthermore, the materials around the stream tend to be coarser, cleaner, and thus more permeable. The topmost region of the model near the lake has a high level of phreatophytic plant life.

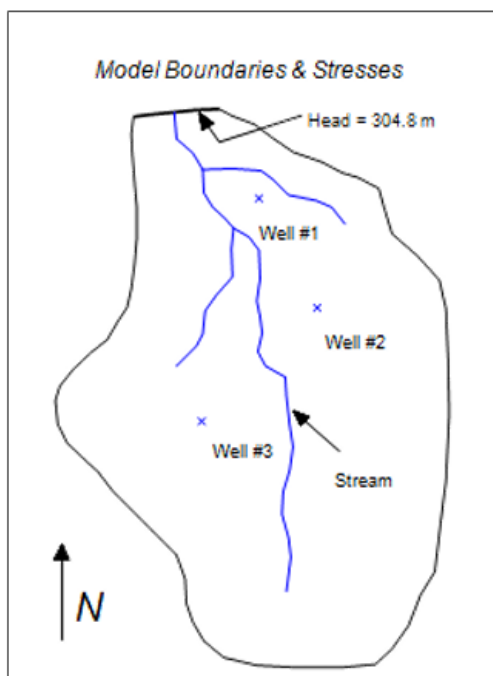


Fig. 8.5. Hypothetical basin conceptual model
(<https://s3.amazonaws.com/gmstutorials-10.8.aquaveo.com/calib.zip>)

8.3. MATERIALS AND METHODS

In the present study, a three-dimensional finite difference (FD), finite volume (FV) and stochastic models were used to simulate groundwater flow. MODFLOW-2000 and MODFLOW-USG were selected for FD and FV, respectively. PEST, T-PROGS, and Monte Carlo methods were utilised for stochastic and inverse modelling in addition to calibration.

8.4. RESULTS AND DISCUSSION

8.4.1. FINITE-DIFFERENCE

In finite-difference [3], the space domain is discretised into structured cell grid, the centre of each cell defines a node that represent the average head within the cell. The partial differential equation is mathematically transformed to a difference equation that includes matrices which are solved numerically to give a calculated head at each node.

The FD method is simple relatively to other numerical methods and gives accurate budget calculations since each cell is uniformly defined and regularly spaced with its inputs/outputs are very clear. However, due to its structured trait, refinements of the grid are not only focused on areas of interest but have to be incrementally changed outward to avoid numerical errors. This means a higher amount of cells are produced more than necessary which slows down the model convergence. Also, since the cell shape is uniform and structured, finite-difference method are rarely used when stratigraphy is complex or discontinuous, that is it cannot easily or directly handle geometries like pinch-outs or lenses (Fig. 8.6).

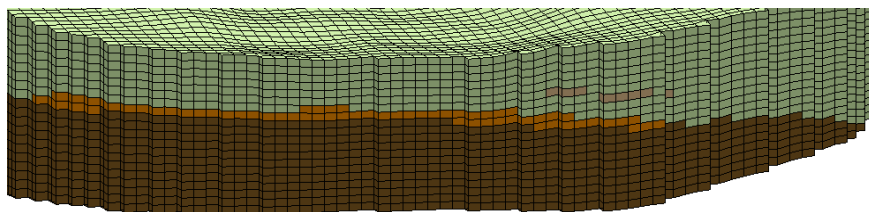


Fig. 8.6. Stratigraphy of coastal aquifer represented by FD 90×70 grid, compare with Fig. 8.4

Since the site2: Basin conceptual model had relatively simpler geometry, the FD results were more representative and accurate. The model was calibrated manually, with PEST and by using pilot points. PEST has a restriction that the number of parameters to be calibrated has to be less than the number of observation points. The best results were obtained when the model was calibrated using pilot points (Fig. 8.7).

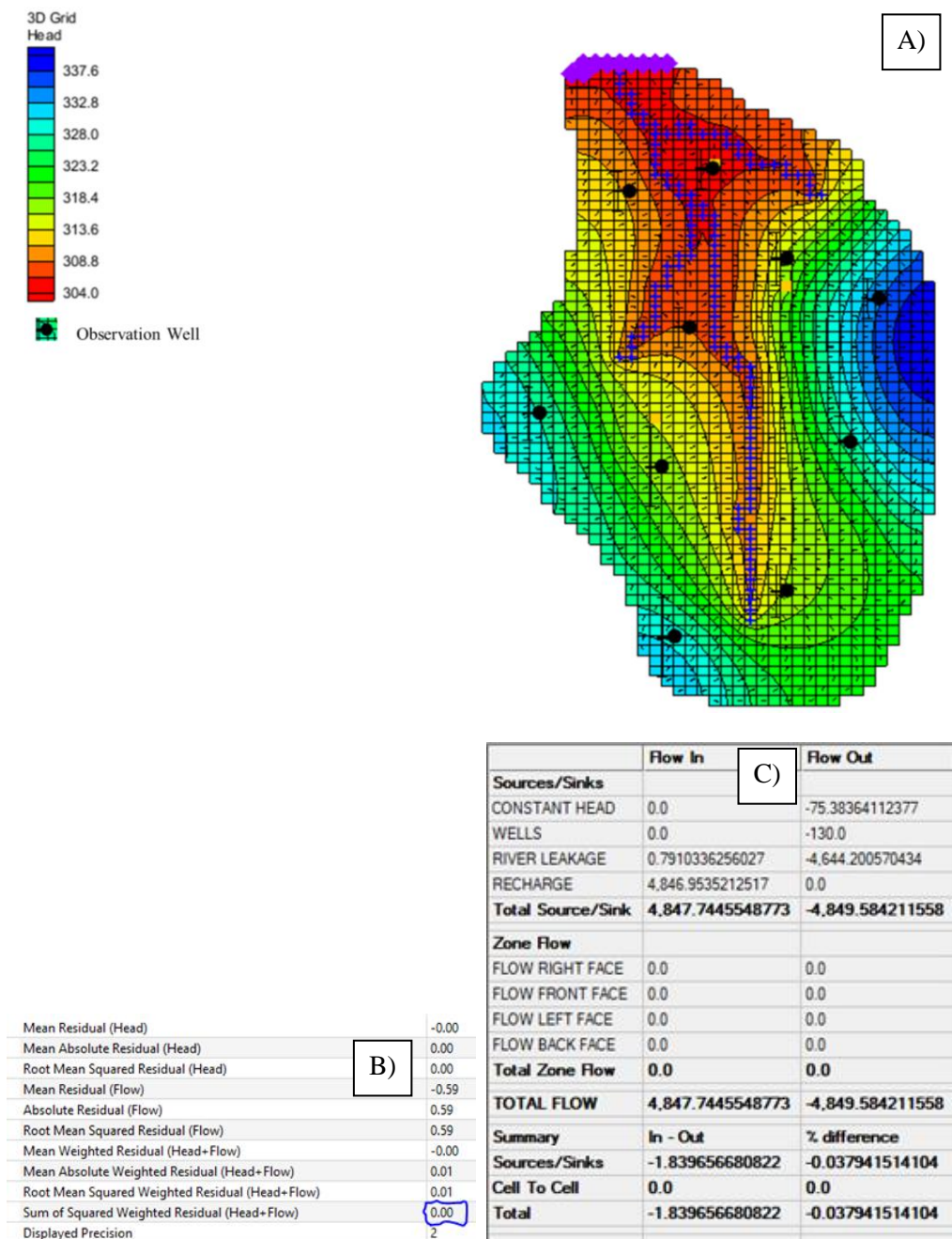


Fig. 8.7. FD model for the Basin site calibrated with pilot points:

A) Head Contours, B) Squared residuals C) Flow budgets

8.4.2. FINITE-VOLUME

The FV method [2] is advantageous to FD since it offers similar budget calculation accuracy with the ease of handling complexity of stratigraphic layers (Fig. 8.8). That is, it has the flexibility to handle such geometries which are very hard to simulate with standard FD.

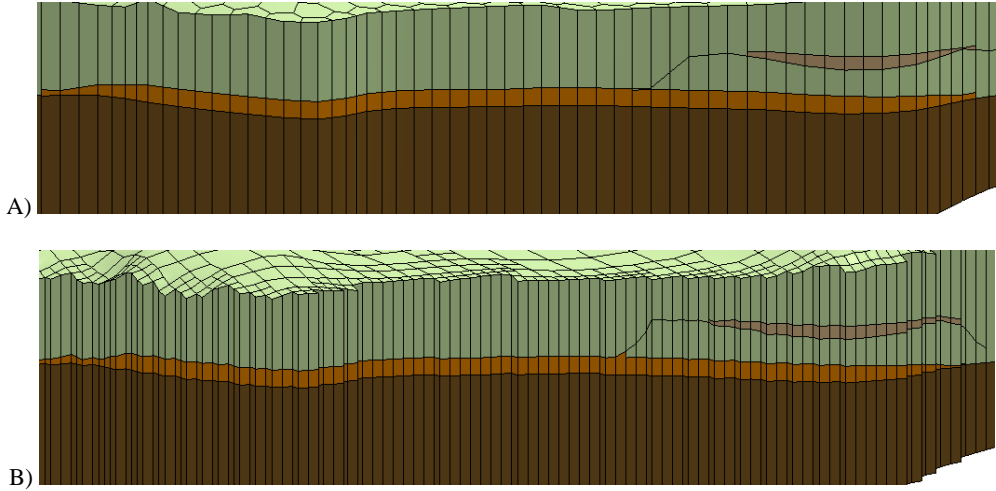


Fig. 8.8. FV grids representing the coastal aquifer example: A) Voronoi, B) Quadtree. Both are very similar to the Fence diagram shown in figure 4 but Voronoi has smoother edges and lesser amount of cells hence less amount of time until model converges

Moreover, the spatial discretisation can be locally refined around only selected areas of interest rather than being extended along the whole model as in the case of FD. Unstructured grids can be Quadtree/Octree or Voronoi or others, each of which has its own pros and cons. Quadtree is very similar with FD with respect to budget calculations, yet Voronoi has an advantage in handling discontinuous and irregular geometries. FV models were calibrated, with PEST, parallel PEST with SVD assist and pilot points with pilot points producing the best results (Fig. 8.9).

8.4.3. STOCHASTIC SIMULATION

Until now, the model simulations given do not include any information regarding uncertainty or risk because they were deterministic solutions, that is the most probable (single) solution based on input values. In contrast to deterministic simulations, stochastic simulations include uncertainty [4].

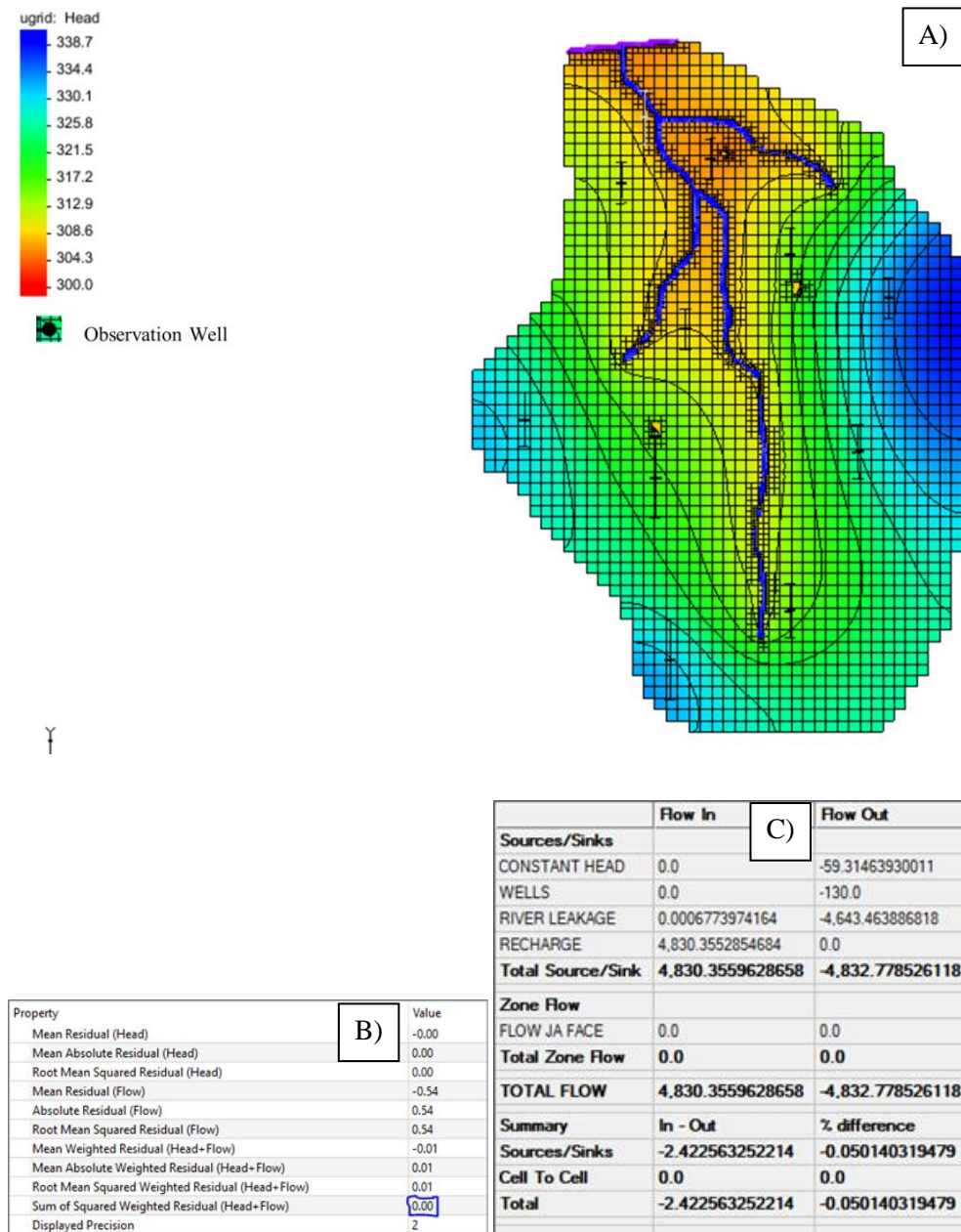


Fig. 8.9. FV Quadtree model for the Basin site calibrated with pilot points:
A) Head Contours, B) Squared residuals C) Flow budgets

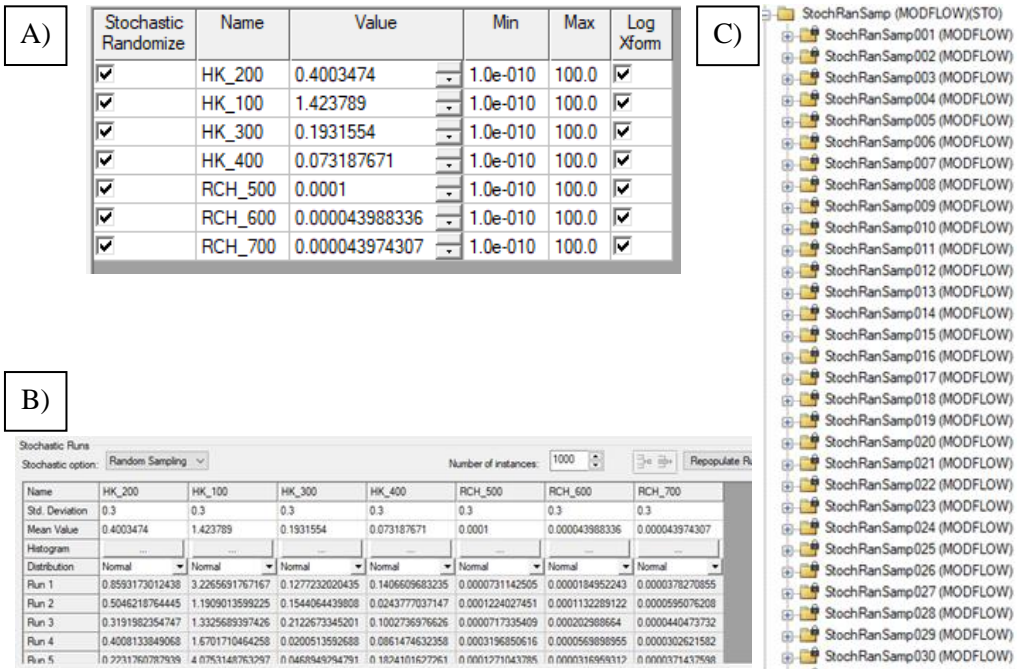


Fig. 8.10. A) Selected parameters for randomisation,
 B) Each combination of values of randomised parameters defines a model run,
 C) List of model realisations each of which has equal probability

Here, selected parameters (Fig. 8.10A) are randomised around a mean value in a probability density function (PDF), from which random values are sampled, and each combination of values of parameters give rise to a realisation (Fig. 8.10B) thus producing multiple model realisations of equal probability (Fig. 8.10C). If there are for example as in this case, 1000 model realisation and after setting a threshold for water budget or squared residuals, that is to see how many realisations from the 1000 runs have met the criteria. Stochastic modelling has a big advantage as it gives with the results something about uncertainty or risk, which is not encountered with deterministic approaches. For calibration, stochastic inverse modelling which functions like PEST, read the output heads and compare it with given observation data like observation wells and flow to estimate the best values for hydraulic conductivities and recharge parameters to produce multiple calibrated realisations each of which is equally probable. Another advantage is that, aquifer heterogeneity can be introduced in the model with T-PROGS (Fig. 8.11B) in addition to having the option to run a capture zone analysis (Fig. 8.13) which is very important when applied for a contamination risk study of well head protection.

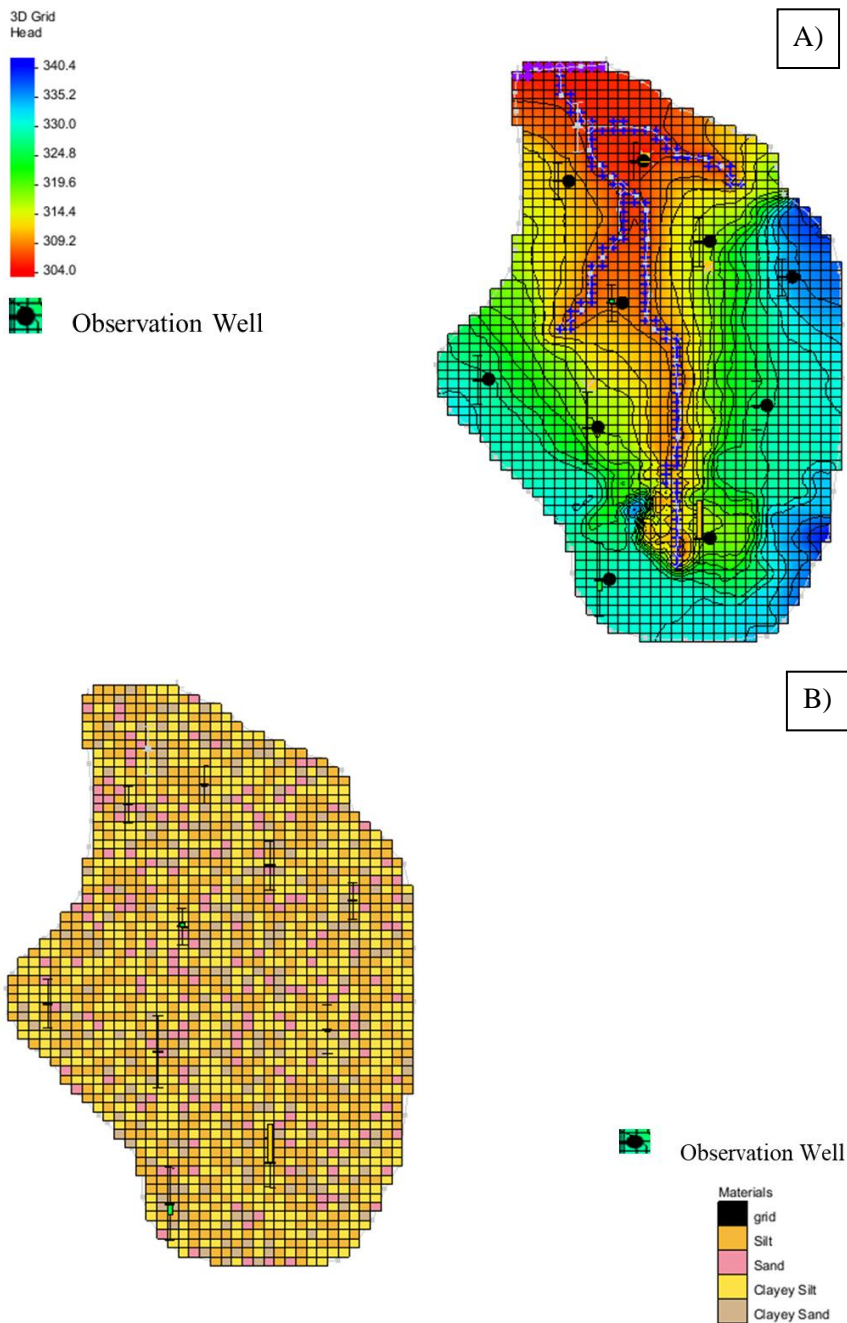


Fig. 11. Calibrated inverse stochastic model for the Basin site:
 A) Head Contours, B) Facies Heterogeneity introduced with T-PROGS

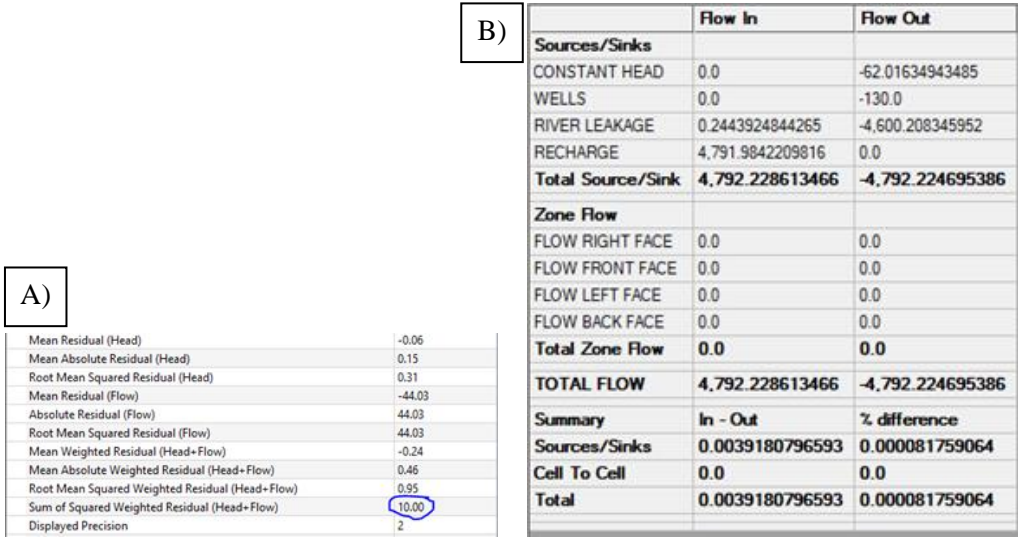


Fig. 8.12. Calibrated inverse stochastic model for the Basin site: A) Squared residuals, B) Flow budgets

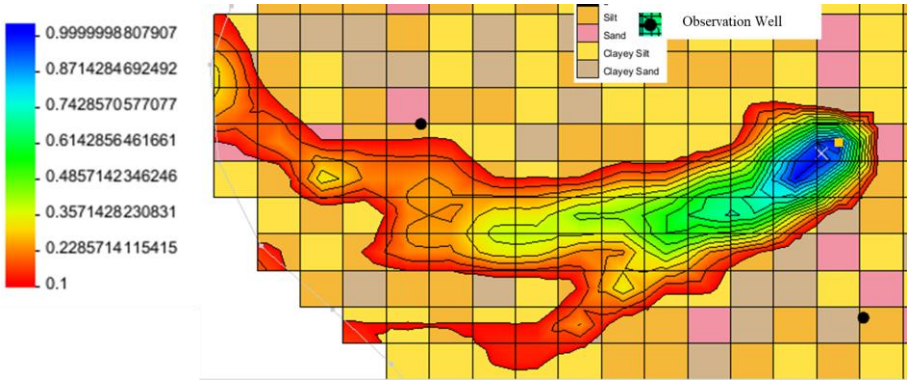


Fig. 8.13. Capture zone analysis for Well-3 (small yellow dot at the edge of the blue zone), the squared cells are colour coded with lithofacies the same as those in Fig. 8.11B, the black dots are observation wells, the coloured contours are probability of capture, with red characterising least probability of capture and blue symbolises most probability of capture, this was based on all the inverse stochastic realisations

8.5. SUMMARY AND CONCLUSIONS

It has been shown that while FD is the easiest numerical method for modelling and probably has the most accurate calculations, but its use is very limited when heterogeneity is involved. FV with its flexible grid geometries to handle all complex situations

but still doesn't give any information regarding uncertainty of risk. Stochastic modelling has the advantage of giving information about uncertainty and producing more than one solution but, an experience and judgment is needed to get a solution which is consistent with the hydrogeology of the area in question.

REFERENCES

- [1] FREEZE R.A., CHERRY J.A., *Groundwater*, Prentice Hall, 1979, 1–604.
- [2] PANDAY S., LANGEVIN C.D., NISWONGER R.G., IBARAKI M., HUGHES J.D., *MODFLOW-USG Versions 1: An Unstructured Grid Version of MODFLOW for Simulating Groundwater Flow and Tightly Coupled Processes Using a Control Volume Finite-difference Formulation*, U.S. Geological Survey Techniques and Methods, 2013, Vol. 6, No. A45, 1–66.
- [3] REMSON I., HORNBERGER G.M., MOLZ F.J., *Numerical Methods in Subsurface Hydrology*, Wiley-Interscience, John Wiley & Sons, Inc., New York 1971, 1–389.
- [4] ZHOU H., GOMEZ-HERNANDEZ J.J., LIANGPING L., *Inverse Methods in Hydrogeology: Evolution and Recent Trends*, Advances in Water Resources, 2014, Vol. 63, 22–37.

PORÓWNIANIE METOD DETERMINISTYCZNYCH I STOCHASTYCZNYCH W MODELOWANIU PRZEPŁYWU WÓD PODZIEMNYCH

Modelowanie wód podziemnych jest jednym z najważniejszych narzędzi pracy każdego hydrogeologa, ponieważ stanowi ilościowe ramy, w których dane pochodzące z różnych źródeł są łączone w celu badania i konceptualizacji procesów hydrogeologicznych. Istnieje szeroka gama dostępnych kodów modelujących, wykorzystujących różne metody matematyczne, takie jak metoda różnic skończonych, metoda elementów skończonych czy metoda objętości skończonych w modelach deterministycznych, a także zasady rachunku prawdopodobieństwa i statystyki w modelach stochastycznych. Każda metoda numeryczna lub statystyczna ma swoje charakterystyczne cechy, które sprawiają, że dany kod może być bardziej korzystny od innych, w zależności od rodzaju analizowanego problemu. W badaniu porównano wyniki oraz przebieg pracy między wybranymi metodami stosowanymi w modelowaniu przepływu wód podziemnych, wykorzystując hipotetyczny problem w celu pokazania różnic między nimi i wskazania sytuacji, w których ich zastosowanie jest najbardziej odpowiednie. MODFLOW, wykorzystujący metodę różnic skończonych do rozwiązania równania przepływu wód podziemnych, jest najłatwiejszy do zrozumienia i umożliwia dokładne obliczenie bilansu strefowego. Jednak nie pozwala on na efektywne zagęszczenie siatki obliczeniowej w obszarach szczególnego zainteresowania, a także ma ograniczone możliwości odwzorowania złożonej budowy geologicznej, zwłaszcza w przypadku warstw nieciągłych lub klinowatych. MODFLOW-USG, który wykorzystuje siatkę nieustrukturyzowaną i implementuje metodę objętości skończonych, umożliwia bardziej efektywne zagęszczanie siatki wokół obszarów zainteresowania bez generowania nadmiernej liczby komórek oraz pozwala na lepsze odwzorowanie złożonej budowy geologicznej z warstwami nieciągłymi lub zanikającymi. Jednocześnie jest on trudniejszy w użyciu niż klasyczny MODFLOW, a ponadto nie zawiera procesu obserwacyjnego w samym modelu, należy go przeprowadzić osobno przy użyciu dodatkowego programu pomocniczego. Modele stochastyczne mają tę zaletę, że generują wiele realizacji o jednakowym prawdopodobieństwie, z których każda ma swoje własne niepewności i ryzyko. Wymaga to jednak doświadczenia i subiektywnej oceny, aby wybrać najlepsze możliwe rozwiązanie. Na podstawie wyników uzyskanych z modeli hipotetycznych stwierdzono, że najlepszym rozwiązaniem jest zastosowanie modelu stochastycznego oraz siatki nieustrukturyzowanej typu Quadtree. Wniosek ten oparto na analizie liczby komórek, czasu potrzebnego na zbieżność modelu oraz błędów średniokwadratowych (RMSE).

9. MINERAL PROPERTY APPRAISAL WITH REFERENCE TO LOCAL SPATIAL DEVELOPMENT PLAN LIMITATIONS

MICHAŁ DUDEK¹, ANNA NOWEL-ŚMIGAJ²

¹ Wrocław University of Science and Technology, Faculty of Geoengineering, Mining and Geology, Department of Geodesy and Geoinformatics, Wybrzeże S. Wyspiańskiego 27, 50-370 Wrocław, Poland.

² Wrocław University of Environmental and Life Sciences, Faculty of Spatial Management and Landscape Architecture, Institute of Spatial Management, Norwida 25, 50-375 Wrocław, Poland.

Local Spatial Development Plans (LSDPs) can severely impact property rights and economic viability. This paper analyzes an overly restrictive LSDP using a case study of a 7.94-hectare mineral property in Krzczonów, Poland, containing a 786 000-tonne sand deposit. While the local plan designates the area for mineral extraction, it imposes an arbitrary annual production limit of 10 000 tonnes. This restriction is economically prohibitive, as the operational break-even point is estimated at 35 000–40 000 tonnes per year. Furthermore, the cap is significantly more stringent than national simplified concession laws, which would permit at least 34 000 tonnes. Consequently, the mandated low production rate makes the venture unprofitable, as revenue fails to cover fixed costs like property tax and land-use conversion fees. This renders the property's designated economic function void and creates a valuation impasse: the income approach is inapplicable due to negative cash flow, and the comparable sales approach is invalidated by the unique legal constraint. The study concludes that such a restrictive provision constitutes a misuse of planning authority, effectively nullifying the property's value and undermining the balance between public interest and private property rights.

Keywords: mineral property, valuation, local spatial development plan, POLVAL

9.1. INTRODUCTION

9.1.1. LSDP AS A TOOL FOR SPATIAL REGULATION – ECONOMIC CONSEQUENCES

Urban planning regulations significantly impact economic growth, regional competitiveness, and the functioning of market mechanisms. Well-designed Local Spatial Development Plans (LSDPs) can enhance attractiveness for investors by ensuring legal predictability and regulatory stability. Conversely, plans that are excessively restrictive or vague may elevate investment costs and constrain real estate availability, thereby driving up market prices [1]. As outlined in [2], when a local plan is adopted or

amended, and the current use or designated purpose of a property becomes unattainable or significantly restricted, the property owner may claim compensation from the municipality for actual damages incurred, or request the purchase of the property or its part. Compensation claims are not applicable if the restriction arises not solely from the municipality's decisions but also from factors such as hydrological, geological, geomorphological, or natural conditions, like flood occurrences and associated restrictions such as a construction ban. The municipality may also fulfil compensation claims by offering the property owner a substitute property. Furthermore, if the adoption or amendment of a local plan leads to a decrease in the property's value and the owner or perpetual lessee sells the property without exercising the rights, they can seek compensation from the municipality equivalent to the decrease in value. This compensation amount is calculated from the sale date, and the decrease is the difference between the property's value considering the land's intended use post-plan adoption or amendment and its value based on the previous land use plan or the property's actual use before the plan's adoption. Claims related to the sale of devalued real estate must be reported within five years from the enactment date of the local plan or its amendment. Selling real estate that has decreased in value or utility can be particularly challenging if buyer interest is lacking. To prevent losing compensation opportunities related to value loss, transactions are sometimes conducted between related parties. Legally, such transactions are permissible and effectively interrupt the five-year timeframe. The legislator likely did not intend for owners to engage in fictitious transactions, but documenting actual damages is challenging, and waiting for a court expert (expert witness) to indicate the value difference, which may then be contested, is often easier. The restrictiveness of the plan, also expressed through intensity limits, the minimum share of biologically active area, or the prohibition of certain functions, raises the question of the fiscal measurability of such actions. Piotrowska [3] shows that with a restrictive building intensity index (≤ 0.4) the predicted decrease in property tax revenues translates into a reduction in land value by an average of 15% – an effect visible within the first five years of the plan's adoption. Czekiel-Świtalska [4] on the other hand, shows that extending the forecast horizon to 10 years overestimates the expected revenue from the planning fee by approximately 23%, which artificially softens the image of the costs of restrictive provisions. On a national scale, Śleszyński et al. [5] estimate that the lack of coupling of the forecast with value capture tools generates a municipal budget deficit equal to 0.4% of GDP annually. Meanwhile, the investment fee model described by Botticini and Auzins [6] allows the recovery of approximately 30% of lost revenues while stabilizing transactional land prices.

In the research [7], an examination of the misuse of municipal planning authority was conducted. Various judgments reflected the stance that the wording of the Spatial Planning and Development Act clearly demonstrates that public interest does not take precedence over individual interest. The legal frameworks outlined in the Act are founded on the principle of balancing the national interest, the interest of the municipality,

and the interest of the individual. This implies a duty to meticulously balance individual rights (citizens' interests) and the public interest, especially crucial when these interests conflict. Additionally noteworthy is the Provincial Administrative Court in Łódź's ruling on November 30, 2005 (II SA/Łd 528/05), which discussed the concept of circumventing the law within the context of municipal planning authority. The court determined that when municipal authorities introduce specific prohibitions in local plans to achieve a legal effect (such as stopping the use of environmentally harmful technology in production) similar to that resulting from an administrative decision by the relevant body, it constitutes a circumvention of laws specifically regulating environmental impacts and breaches Article 6 of the Municipal Self-Government Act. This article stipulates that all local public affairs not allocated to other entities by law fall within the municipality's operations. The court's reasoning is akin to the concept of procedural abuse, more commonly recognized in French law [8]. Procedural abuse is identified when an authority opts for one of the applicable procedures over another, despite not fulfilling its conditions, because the chosen procedure offers certain advantages to the authority.

9.2. CASE STUDY

9.2.1. CASE STUDY AREA (LAND PLOT) AND PROVISIONS OF LAND AND BUILDING REGISTER

According to the geographical regionalization by J. Kondracki, the area lies within the larger regional unit of the Sudetes and the Sudeten Foreland (Przedgórze Sudeckie), specifically in its marginal part, bordering the Silesian Lowland (Nizina Śląska) to the northeast. Breaking it down into smaller units (mesoregions), the deposit is situated on the Świdnica Plain (Równina Świdnicka). To the northeast, the Świdnica Plain is bordered by the Kielcyn Hills (Wzgórza Kielczyńskie), which are a microregion of the neighboring Ślęża Massif (Masyw Ślęży). Within the Świdnica Plain, dome-shaped elevations stand out – the Krzczonów Hills (Krzczonowskie Wzgórza) and, on its northern edge, the Imbramowice Hills (Wzgórza Imbramowickie). The Świdnica Plain is bordered to the west by the Strzegom Hills (Wzgórza Strzegomskie), to the northeast by the Środa Upland (Wysoczyzna Średzka), and further south by the Kąty Plain (Równina Kącka). The Bystrzyca river valley cuts across the Świdnica Plain. The predominant elevations on the Świdnica Plain are between 200–230 meters above sea level. The deposit area itself is a dome-shaped hill with elevations ranging from 245–254 meters above sea level. The terrain slopes distinctly to the north, west, and partially to the south, while gently transitioning eastward into slightly lower ground. Transportation conditions for raw material are favorable. A paved dirt road runs 800 meters to the north, connecting to the asphalt road between Świdnica and Łagiewniki, or from the south to the road between Świdnica

and Dzierżoniów. These roads provide easy access in all directions. The “Krzczonów” deposit is located in the southernmost part of the village of Krzczonów, administratively belonging to the municipality of Świdnica, approximately 7 km to the northwest. Geographically, it is situated on a dome-shaped hill (245–254 m elevation) on the Świdnica Plain, which is part of the Sudeten Foreland. The sands from this deposit are suitable in their natural state for road and construction embankments and, after screening, for use in mortars and concrete. The aggregate is intended for the local market around Dzierżoniów, Świdnica, and Wałbrzych, with potential for use in small residential projects and larger investments within the Wałbrzych Special Economic Zone, as well as the new Dzierżoniów–Świdnica road planned to run about 300 meters from the site. Favorable transport conditions provide easy access for raw material distribution.



Fig. 9.1. Case study area (green area arrow pointed),
source: www.polska.e-mapa.net

Table 9.1. Case study area (land plot)
according to Land and Building Register

Location	Soil class	Area [ha]
Krzczonów	RIIIa	0.2200
	RIIIb	2.7600
	RIVa	2.6800
	RIVb	0.8800
	RV	1.1800
	K	0.0847
	dr	0.1400
Total area [ha]		7.9447

9.2.2. DESIGNATION IN LOCAL SPATIAL DEVELOPMENT PLAN

In accordance with the provisions of the local plan, as well as a certificate issued by the head (wójt) of the Świdnica municipality, pursuant to resolution No. IV/27/98 of the Świdnica Municipal Council dated December 17, 1998, regarding the adoption of the local spatial development plan for the “Krzczonów” mining area, case study area in the is designated in part as areas for the surface extraction of natural aggregates, marked on the plan’s drawing with the symbol 18.2.1PE, and in part as the surface of the mining area, marked on the plan’s drawing with the symbol 18.2.2RP. As detailed designation, it is stated that maximum annual production from deposit cannot exceed 10 000 tonnes.

9.2.3. CALCULATION OF MINERAL PROPERTY MARKET VALUE

For the purpose of this research, the market value of case study mineral property was calculated with assumptions that there is no limitation according to mining production in local spatial development plan [9, 10]. Sand unit price in the time of analysis for 2011 year was 9 zł/t. Annual production rate calculated from previous 3 years based on 22 mine sites was 100 thousand tonnes of sand (considering small to medium scale mining sites). Real estate tax 0.73 zł/m², Operating fee 0.51 zł/t, Liquidation fund 0.051 zł/t. Cost of required services include annual cost of mining supervision, geology and surveying and health and safety supervision. Basic mining equipment includes digger and loader. Cost of exclusion from agricultural production was calculated separately according to [11]. Available resources in deposit are 786 thousand tonnes.

Table 9.22. Mineral property market value calculation

	Years of analysis							
	1	2	3	4	5	6	7	8
Production, thousand tonnes	100	100	100	100	100	100	100	86
Income, thousand zł	900	900	900	900	900	900	900	774
Real estate TAX	58	58	58	58	58	58	58	58
Operating fee	51	51	51	51	51	51	51	44
Liquidation fund	5	5	5	5	5	5	5	4
Cost of excl. from agricult. prod.	287	103	103	103	103	103	103	103
Cost of equipment operators	15	15	15	15	15	15	15	15
Cost of required services	30	30	30	30	30	30	30	30
Cost of basic mining equipment	479							-60
Cost of basic mining equipment	897							-112
Cost of diesel	133	133	133	133	133	133	133	133
Residual Value, thousand zł								181

Table 9.2 continued

Discount rate	10%							
Discount factor	0.91	0.83	0.75	0.68	0.62	0.56	0.51	0.47
Net Operating Income, thousand zł	-1055	505	505	505	505	505	505	418
NOI x Discount factor, thousand zł	-959	417	379	345	314	285	259	195
Market Value, thousand zł	1236							

9.3. RESULTS AND DISCUSION

As observed in table 2 market value without local spatial development plan limitation for production rate is 1236 thousand zł. For discount rate 15% estimated market value would be 882 thousand zł.

The limitation of the extraction rate to 10 thousand tonnes in the local plan is all the more peculiar given that even under the simplified concession procedure (a concession from the *County Mayor*), it is possible to extract the amount up to 20 000 m³ annually, provided the area of the documented deposit not covered by mining ownership does not exceed 2 hectares [12].

Due to the specific density (approx. 1.7 t/m³), the aforementioned 20 000 m³ can be converted to at least 34 thousand tonnes – three times more than the amount allowed by the local spatial development plan, which supposedly enables the mining development of the property. Considering only the property tax and the fees associated with the exclusion of land from agricultural production, the total sum will be so large that limiting extraction to 10 thousand tonnes will result in revenue being unable to cover even a portion of the costs (basically loss). Only by achieving an output of 35–40 thousand tonnes per year will it be possible to exceed the break-even point. Taking into account that available resources in deposit are 786 thousand tonnes, their extraction at rate 10 thousand tonnes per year would result in 78 years of mining activity. The total available amount of sand might be as well extracted in 2 years (or even 1) considering medium scale mine sites.

From the standpoint of real property valuation, it is widely recognized that the designated function of a property as outlined in the local spatial development plan can significantly impact its value. This is due to the fact that such plans, along with other relevant regulations, determine the allowable uses of the property. Since local spatial development plans are considered acts of local law, they require strict compliance. Even if a specific provision within a local plan is deemed inadequate, it can only be disregarded following its official revocation through the appropriate legal process. Until formally repealed, the provision remains legally enforceable.

Because economic approach seems not applicable with local spatial development plan limitation comparable sales approach should be used. It is very questionable if such property with legal limitations can be compared to operating mines. In authors opinion this local spatial development plan limitations is equivalent to situation where mineral

deposit has agricultural designation in local spatial development plan, deposit exists but at the time of valuation it cannot be extracted.

REFERENCES

- [1] PETERSON G.E., *Unlocking land values to finance urban infrastructure*, Vol. 7, World Bank Publications, 2009.
- [2] Ustawa z dnia 27 marca 2003 r. o planowaniu i zagospodarowaniu przestrzennym, Dz.U.2024.0.1130, t.j.
- [3] PIOTROWSKA L., *Okres prognozowania skutków finansowych uchwalenia miejscowego planu zagospodarowania przestrzennego*, Przestrzeń, Ekonomia, Społeczeństwo, 2017, pp. 263–280.
- [4] CZEKIEL-ŚWITALSKA E., *Prognoza skutków finansowych uchwalenia miejscowego planu zagospodarowania przestrzennego a budżet gminy*, Przestrzeń i Forma, 2013, pp. 51–62.
- [5] ŚLESZYŃSKI P., NOWAK M., SUDRA P., ZAŁĘCZNA M., BLASZKE M., *Economic consequences of adopting local spatial development plans for the spatial management system: The case of Poland*, Land, 2021, 10, 112.
- [6] BOTTICINI F., AUZINS A., LACOERE P., LEWIS O., TIBONI M., *Land Take and Value Capture: Towards More Efficient Land Use*, Sustainability, 2022, 14, <https://doi.org/10.3390/su14020778>
- [7] PARCHOMIUK J., *Abuse of the Municipality's Planning Authority*, Samorząd Terytorialny, 2014, pp. 22–37.
- [8] AUBY J.M., *The Abuse of Power in French Administrative Law*, The American Journal of Comparative Law, 1970, 18, 549–564.
- [9] Ustawa z dnia 21 sierpnia 1997 r. o gospodarce nieruchomościami, Dz.U.2024.0.1145, t.j.
- [10] SAŁUGA P. (Ed.), *The Polish Code for the Valuation of Mineral Assets (POLVAL)*, 2021 Edition, Kraków 2021.
- [11] Ustawa z dnia 3 lutego 1995 r. o ochronie gruntów rolnych i leśnych, Dz.U.2024.0.82, t.j.
- [12] Ustawa z dnia 9 czerwca 2011 r. – *Prawo geologiczne i górnicze*, Dz.U.2023.0.633, t.j.

WYCENA NIERUCHOMOŚCI ZE ZŁOŻAMI KOPALIN W NAWIĄZANIU DO OGRANICZEŃ WYNIKAJĄCYCH Z ZAPISÓW MIEJSCOWEGO PLANU ZAGOSPODAROWANIA PRZESTRZENNEGO

Miejscowe Plany Zagospodarowania Przestrzennego (MPZP) mogą znacząco wpływać na prawo własności i rentowność przedsięwzięcia surowcowego. Niniejszy artykuł analizuje nadmiernie restrykcyjne zapisy MPZP na podstawie studium przypadku nieruchomości o powierzchni 7,94 ha w Krzczonowie w Polsce, stanowiącej nieruchomość ze złożem piasku o zasobach 786 000 ton. Chociaż plan miejscowy przeznacza ten obszar pod eksploatację kopalin, narzuca arbitralny roczny limit wydobycia wynoszący 10 000 ton. Ograniczenie to jest ekonomicznie nieuzasadnione, ponieważ operacyjny próg rentowności szacuje się na 35 000–40 000 ton rocznie. Co więcej, limit ten jest znacznie bardziej rygorystyczny niż krajowe uproszczone przepisy koncesyjne, które pozwoliłyby na wydobycie co najmniej 34 000 ton. W rezultacie narzucony niski poziom wydobycia czyni przedsięwzięcie nierentownym, ponieważ przychody nie są w stanie pokryć kosztów stałych, takich jak podatek od nieruchomości i opłaty za wyłączenie gruntu z produkcji rolnej. Ograniczenie poziomu wydobycia w miejscowym planie stwarza impas w wycenie, gdyż podejście dochodowe jest niemożliwe do zastosowania z powodu ujemnych przepływów pieniężnych, a stosowanie podejścia porównawczego jest utrudnione z powodu unikalnego ograniczenia prawnego. W konkluzji stwierdzono, że tak restrykcyjny zapis może stanowić nadużycie władztwa planistycznego, skutecznie ograniczając wartość nieruchomości i podważając równowagę między interesem publicznym a prawem własności prywatnej.

10. ANALYSIS OF THE RECONSTRUCTION OF AN ACCIDENT FROM A COURT CASE TO IMPROVE OCCUPATIONAL SAFETY

KINGA MARTUSZEWSKA¹, DAWID SZURGACZ²

¹ District Bar Association in Katowice, Lawyer's office, ul. Jankowicka 23/25, 44-200 Rybnik.

² Faculty of Geoengineering, Mining and Geology, Wrocław University of Science and Technology,
Na Grobli 15, 50-421 Wrocław, Poland.

The publication is an initial assessment of the participants' behavior made by a court expert based on the reconstruction of the event. The reconstruction of the accident for the purposes of court proceedings was carried out based on the evidence from the court case file. Audio-video technology was used for this purpose. Based on this, the causes and effects of the accident were determined. The aim of the publication is to assess the usefulness of reconstruction in terms of the possibilities of improving work safety. In this respect, a fatal accident that occurred in one of the industrial plants was assessed. The expert's reconstruction answered the court's questions. The established cause was the lack of proper communication among the team of employees. The accident reconstruction carried out for the purposes of the court case may be used in the future as training material for improving work safety.

Keywords: fatal accident, participants' behavior, accident at work, reconstruction of the event, forensic expert opinion

10.1. INTRODUCTION

In every industry, accidents occur mainly as a result of non-compliance with applicable laws. Such an example could be the mining industry extracting raw materials using underground or open-pit methods [1, 2, 5]. Most events do not result from natural hazards at the workplace but from a lack of sufficient compliance with occupational health and safety rules [3, 4].

The mining industry is a very dynamically developing industry in terms of the amount of scientific research carried out [8, 9] and implemented innovations [10, 11]. The implementation of new solutions is intended to improve occupational safety. This is in line with the policy of sustainable development, which is to combine all innovations related to improving working conditions in industrial plants. Relevant literature on re-

search and innovations in the mining industry provides significant information [13, 19]. The authors of this publication, based on a review of literature and problems arising from court cases seeking compensation for an accident at work [6, 12], undertook an attempt to evaluate the usefulness of accident reconstruction by a court expert in order to introduce this element as one of the training tools for improving occupational safety [7, 14, 17, 18].

10.2. MATERIALS AND METHODS

The expert's research material is the evidence collected in the course of a case pending before the District Court in Gliwice 1st Civil Division in case file reference number I C 795/23. The court hearing the case based on Article 278 § 1 of the Code of Civil Procedure admitted evidence from the opinion of a court expert in the field of mining and geology to determine the causes of the event, and in particular to assess the behavior of the participants of the event in terms of possible contribution of the injured party to the consequences of the event [15, 16]. The expert, having the files of the case, was obliged to familiarize himself with the procedural position of the parties to the proceedings, i.e., the plaintiff, being the wife of the deceased employee, and the defendant insurance company, as well as the evidentiary proceedings conducted so far in the form of hearing witnesses of the event. The positions of the parties were diametrically opposed. The plaintiff sought payment of compensation in connection with the death of the employee in the course of his professional duties, whereas the insurance company requested dismissal of the claim. Thus, it was necessary to first determine the course of the event itself and subsequently determine the cause of its creation.

It was difficult to establish the detailed course of events on the basis of the evidence, as there were no direct witnesses to the accident. Moreover, witnesses testifying in the case described the course of the event in an imprecise manner, providing no basis for reconstructing the accident. Furthermore, the limited recording area of the hall's surveillance camera and the low-quality image hindered a faithful reconstruction of the accident. The material collected in the case should be considered selective and chaotic, unable to provide the court with a clear explanation of how the accident occurred, how the participants behaved, and ultimately, the underlying causes of the incident, which resulted in the tragic death of one of the participants.

The analysis included the post-accident documentation, protocols of witness interviews, results of technical tests and monitoring records. The reconstruction of the event in the form of audio-video visualization played a key role. Comparative analysis methods were used: the findings were compared with applicable health and safety regulations and scientific literature. Methodological limitations were also considered, including the lack of reliable recordings and the lack of direct witnesses to the event. Different types of reconstruction are included: visual (step-by-step reconstruction),

simulation (digital models of mechanisms) and analytical (time schemes). Each of them provides different information and can be used in the education of employees of the plant.



Fig. 10.1. View of a railway wagon type WAP/Fs

The expert should be primarily obliged to reconstruct the chronology of events, which he made on the basis of witness statements, additional information obtained by the post-accident team, surveillance footage, and inspection of the accident site itself. It was also necessary to verify the preparedness of the accident participants, particularly their technical readiness to perform such work, as well as their current training and medical examinations. According to the expert's opinion, the employees performing the repairs had up-to-date preventive medical examinations, health and safety training, were familiar with occupational risk assessments and instructions, and had many years of professional experience in repairing Fals WAP/Fs-type freight wagons (Fig. 10.1).

It is impossible not to mention that the deceased employee had over 42 years of experience in the repair of rolling stock, and the accident occurred during the repair of the FALS WAP/Fs-type wagon. Next, the expert's role was to determine the mechanism of operation and efficiency of the device itself, because the accident occurred while opening the flaps, which moved down and to the left, in an elliptical motion. Additionally, it was necessary to determine the location of each employee, their distance from each other, their position relative to the device itself, the division of roles for each employee during the repair work, and the communication between them during the work (Fig. 10.2).

Based on the above, it was established that the incident occurred during work on the FALS WAP/Fs-type wagon. Two experienced employees were performing tasks related to the flap mechanism. The team had the required examinations and training. The operating mechanism of the machine was in proper working condition, as con-

firmed by post-accident testing. On the basis of the above, it was established that the employees started checking the wagon flaps. The deceased employee, acting as coordinator, was located in the danger zone. The same employee gave the order to close the flaps to his co-worker. The employee's order was carried out immediately without checking the position of his co-worker. This was followed by crushing, resulting in the death of the employee.

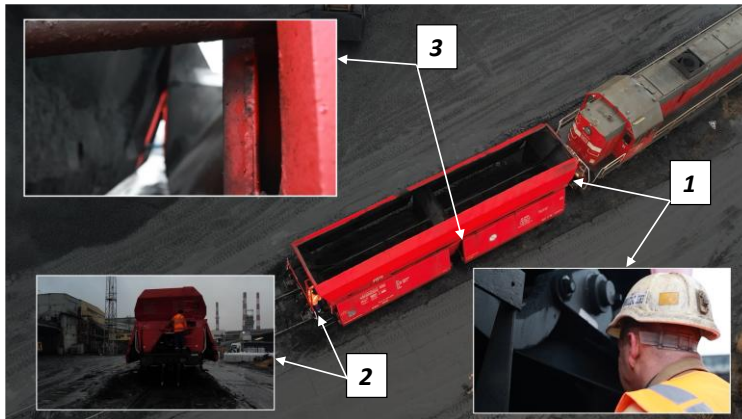


Fig. 10.2. Reconstruction from a film image: 1 – the place where the victim was standing, 2 – the place where the co-worker activated the mechanism for opening and closing the flaps, 3 – opening the side flaps

10.3. RESULTS

The essence of the opinion was to provide answers to the questions posed in the evidentiary thesis. To answer the court's questions, the expert used the knowledge gained from analysis of the case files to perform a reconstruction of the event in the form of a video recording. The purpose of the accident reconstruction was to reproduce the sequence of events that occurred. The objective was to **determine exactly what happened, in what order, who did what or failed to do something, and** what exactly led to the accident. The person competent to perform such a reconstruction is an individual possessing specialized technical knowledge, that is, a court-appointed expert witness qualified in fields such as engineering, occupational safety, mechanics, or industrial safety. The purpose of the reconstruction is **to understand how and why the accident occurred, and whether it could have been avoided** if the regulations, procedures, or caution had been observed. The author of this opinion is a court expert entered on the list of experts at the District Court in Gliwice. Interestingly, none of the experts listed in that registry indicated that the field of their activity is to prepare a reconstruction of an

accident event. The only reconstructions of events that are carried out as part of expert opinions are reconstructions of road accidents; there are 27 experts in this field on the aforementioned list. Taking into account the comparable importance of accidents at work in which employees are injured, compared to road accidents, there is undoubtedly a need to develop this area of expertise by creating reconstructions of specific accident events.

In the present case, the reconstruction accurately re-created the workstation that was simultaneously the site of the accident. The expert ensured that the same model of machine was used as the one on which the repair work was carried out. The operation of the flaps was indicated, their direction and movement were demonstrated, and the workstations of each employee were determined. The reconstruction of the accident made it possible to exclude external factors resulting from the organization of the workplace itself or the technical characteristics of the equipment (Fig. 10.3). Based on the analysis of the file supported by the expert's own verification, it was established that the machine was fully operational and that the employees had received appropriate training and experience in its use, including repair work. The exclusion of technical aspects as the cause of the fatal accident suggested to the expert that further investigation was necessary. The expert concluded that the cause of the incident was errors in communication between employees. Despite experience and training, employees did not apply the "stop and check" principle. The lack of a confirmation procedure was negatively assessed and model behavior was indicated, which should include ensuring that the area of operation and another co-worker in that area are located in a safe zone, as well as mandatory repetition and confirmation of the communication.



Fig. 10.3. Operation of the wagon flaps along with the participants' workplace:

1 – the place where the victim was standing,

2 – location where the wagon flap is activated by a colleague

10.4. DISCUSSION

The reconstruction of the accident at work, with particular emphasis on the specificity of mining plants, is fully justified in the present case. Conducting such an opinion based on the evidence collected in the case files allowed for the objective, technical and substantive verification of the course of the accident event, and will also enable the court to better understand the mechanisms that led to its occurrence. What is often clear to a specialist in a particular field is not necessarily, and often is not, understandable to the participants in the proceedings or other recipients. Undoubtedly, mining plants are a specific work environment, in which there are various threats on a daily basis, related both to the nature of the work performed, as well as to the equipment used, geological conditions or the specificity of the technologies used. The circumstances of accidents in such an environment are often complex and their analysis requires specialist knowledge and the ability to assess them from a technical and engineering perspective. In the present case, it is important not only to determine **whether an accident has occurred**, but above all – **what were its causes**, whether there was **a cause and effect relationship between the actions (or omissions) of specific persons and the consequences of the accident**, and **whether it was possible to avoid the event** with due diligence and compliance with applicable safety procedures.

An accident reconstruction expert will be able to reconstruct the possible course of an event based on an analysis of the collected evidence (e.g., post-accident documentation, witness statements, monitoring records, health and safety records, technical diagrams, as well as documentation of machinery and equipment used in the mine). This reconstruction will make it possible to determine the sequence of events, what technical or organizational factors may have contributed to the accident, and whether it could have been avoided. However, this should not be confused with conducting a procedural experiment, which is also one of the possible evidentiary measures. A procedural experiment is an institution included in the Code of Criminal Procedure, Art. 211, which states that: “In order to verify the circumstances of significant importance to the case, an experiment may be carried out or a reproduction of the course of events or parts thereof by means of a procedural experiment” [20]. In civil procedure, such a means of evidence has not been explicitly specified. However, given that there is no closed catalog of means of evidence in civil proceedings, it is possible to conduct a procedural experiment by the court conducting the case *ex officio* or at the request of either party. A procedural experiment is an attempt to deliberately cause, under staged conditions, the event that is the subject of court proceedings. This is to examine the possibility of the event occurring on the basis of the collected case files or to examine the possibility of their perception under certain conditions. Reconstruction, on the other hand, is intended to check whether the event could have had a certain course, and therefore must be carried out at the scene of the event. As a rule, a more extensive and more difficult task is to recreate the course of events. It is logical that for the result of such a proce-

dural experiment to be reliable, the conditions and circumstances of its execution must be as close as possible to those that existed at the time of the accident. A process experiment should be distinguished from an expert experiment. The fundamental difference between the two is that, unlike a procedural experiment, which is not conducted by a court but by an expert, it has been pointed out that “the main characteristic distinguishing a procedural experiment from an expert experiment is that a procedural experiment is a procedural act, in a *strict sense*, while an expert experiment is a component of an expert’s opinion. An expert experiment is carried out by experts, while a procedural experiment is carried out by procedural authorities” [20]. The expert is not able to oblige a party or witnesses to take part in such activities. The effects of the conducted reconstruction must always be the result of expert research, their own activities, observations and works. In addition, reconstruction can also serve as **a tool to verify the consistency and credibility of the testimonies of witnesses and participants in the event**, allowing the court to draw appropriate conclusions as to the responsibility of individual persons or institutions. Moreover, it can indicate whether there have been any deficiencies in compliance with health and safety regulations, technical supervision, work organization or training of employees in the workplace. This is all the more important in the case in question, where the testimony of witnesses did not give an unambiguous answer about the course of the event.

The preventive aspect is also important: a comprehensive analysis of the accident, based on the expert’s specialist knowledge, can help identify systemic irregularities in the functioning of the mine that may pose a potential threat to other employees. Therefore, such an opinion may also have a preventive value and contribute to improving occupational safety in the future. In this particular case, the reconstruction made it possible for the expert to formulate a positive model of behavior (which would have prevented the accident) in contrast to the negative model that occurred. The expert identified a specific systemic (human) error, namely a lack of communication and inappropriate coordination, as the likely main cause of the accident. It was impossible to rule out a communication error involving misunderstanding, lack of precision, or overinterpretation of the command given. Since the lack of communication was the cause of the accident, and other safety aspects (mechanism efficiency, experience, training, workplace order) were fulfilled, the reconstruction of the event using audio-video technology is a potentially valuable training tool. Visualization and step-by-step reconstruction of what exactly happened (negative behavior) and what should happen (positive behavior) allows for effective emphasis on life-saving principles, even in the case of work performed by a highly experienced team. The usefulness of the reconstruction is therefore the possibility of using its results to create dedicated training materials that focus not only on technical instructions, but above all on safe communication procedures, especially when issuing safety-critical commands. Given the above, Fig. 4 below shows a diagram of preparation that the expert should take into account in order to reconstruct the accident.

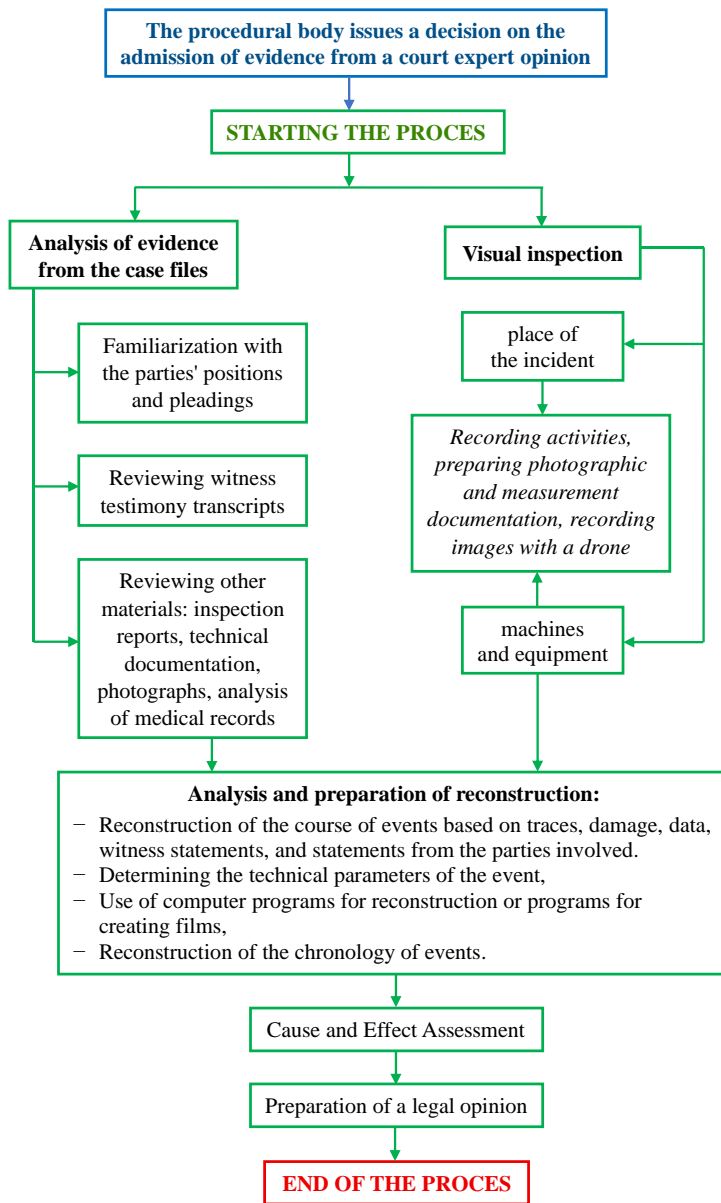


Fig. 10.4. Schematic diagram of the preparation of an expert opinion, including accident reconstruction

It is also worth noting the economic dimension in the preparation of a reconstruction, where every accident is not only a human tragedy, but also costs for the company and the state. Prevention through education is therefore an investment, not just a legal requirement.

10.5. CONCLUSIONS

Apart from the role of evidence, the expert's opinion may become a starting point for developing training and organizational procedures aimed at implementing model behaviors and preventive actions in workplaces. It would be desirable for accident reconstructions to be implemented in occupational health and safety training programs. This approach can become an innovative standard in occupational health and safety management. However, based on an analysis of the lists of court experts, there are currently no experts specializing in conducting accident reconstruction at work. In the field of event reconstruction, the only experts who can be found are those who perform road accident reconstruction. However, taking into account the benefits of accident reconstruction at work, there is also a need to develop occupational health and safety.

REFERENCES

- [1] ADACH-PAWELUS K., PAWELUS D., *Influence of remnant size on the geomechanical situation and safety in the mining field based on numerical modeling*, Mining Science, 2025, Vol. 32, 47–63.
- [2] APANOWICZ B., MILCZAREK W., KOWALSKI A., *Advanced InSAR-SBAS method for determining the extent of mining-induced deformations*, Geocarto International, 2025, 40 (1).
- [3] BAJDA M., HARDYGÓRA M., *Analysis of Reasons for Reduced Strength of Multiply Conveyor Belt Splices*, Energies, 2021, 14, 1512.
- [4] BEZYK Y., SZURGACZ D., STRĄPOĆ D., MISZ-KENNAN M., FABIAŃSKA M.J., SZRAM E., KRUSZEWSKI Ł., ZIMNOCH M., NĘCKI J., SÓWKA I., KOWALSKI T., CARIAN VAN DER VEEN, RÖCKMANN T., GÓRKA M., *Understanding coalbed gas distribution from longwall mining: Geochemical and isotopic approach*, International Journal of Coal Geology, 2025, Vol. 309, 104859.
- [5] BŁASZKÓW A., RATAJCZAK T., SZYSZKA D., *Flotation of hydrophobic minerals in Hallimond tube*, Mining Science, 2024, Vol. 31, 219–227.
- [6] DLOUHA D., POKORNY J., PODKUL M., BRUMAROBÁ B., SZURGACZ D., TOMASKOVA M., VLCEK V., ZHIRONKIN S., *Calculation technique CSN for smoke layer interface assessment during fires in industry*, Journal of Loss Prevention in the Process Industries, 2025, Vol. 94, 105564.
- [7] KAMRAN-PISHHRSARI A., MONIRI-MORAD A., SATTARVAND J., *Applications of 3d reconstruction in virtual reality-based teleoperation: A review in the mining industry*, Technologies, 2024, 12 (3), 40.
- [8] MORAVIČ M., MARASOVÁ D., KAŠŠAY P., OZDOBA M., LOPOY F., BORTNOWSKI P., *Experimental Verification of a Compressor Drive Simulation Model to Minimize Dangerous Vibrations*, Applied Sciences, 2024, 14, 10164.
- [9] RZESZOWSKA A., JURDZIAK L., BŁAŻEJ R., LEWANDOWICZ P., *Analysis of Uncertainty in Conveyor Belt Condition Assessment Using Time-Based Indicators*, Applied Sciences, 2025, 15, 7939.
- [10] SMENTEK A., KACZMAREK A., EKSERT P., BLACHOWSKI J., *Monitoring surface water dynamics in mining areas using remote sensing indices: a review and cross-case analysis*, Water, 2025, 17 (19), 1–35.
- [11] SIEJKA M.W., KASZA D., WAJS J., *Methodology of spatial data acquisition and development of high-definition map for autonomous vehicles – case study from Wrocław, Poland*, Civil and Environmental Engineering Reports, 2024, Vol. 34, No. 1, pp. 87–103.

- [12] STRZAŁKOWSKI P., WOŹNIAK J., GÓRNIAK-ZIMROZ J., DELIJEWSKA B., BEŚ P., SOLATYCKA D., JANISZEWSKA M., *Identification and systematics of safety hazards in surface rock mining*, Science Reports, 2025, 15, 30492.
- [13] SUCHORAB-MATUSZEWSKA N., KAWALEC W., KRÓL R., *Study of Long-Distance Belt Conveying for Underground Copper Mines*, Energies, 2025, 18, 4872.
- [14] TETZLAFF E., EGER T., PEGORARO A., DORMAN S., PAKALNIS, V., *Analysis of recommendations from mining incident investigative reports: a 50-year review*, Safety, 2020, 6 (1), 3.
- [15] USTAWA KODEKS POSTĘPOWANIA CYWILNEGO z dnia 17.11.1964 r., Dz.U. 1964 Nr 43, poz. 296.
- [16] USTAWA KODEKS POSTĘPOWANIA KARNEGO z dnia 6.06.1997 r., Dz.U. 1997 Nr 89, poz. 555.
- [17] VAN TONDER C.L., GROENEWALD J.P., *Of mining accidents and sense-making: traversing well-trodden ground*, Journal of Global Business and Technology, 2011, 7 (1), 57.
- [18] WEBBER-YOUNGMAN R.C., VAN WYK E.A., *Incident reconstruction simulations-potential impact on the prevention of future mine incidents*, Journal of the Southern African Institute of Mining and Metallurgy, 2013, 113 (6), 519–528.
- [19] WRÓBLEWSKI A., BANASIEWICZ A., KROT P., TRYBAŁA P., ZIMROZ R., ZINCHENKO A., *A New Method of Airflow Velocity Measurement by UAV Flight Parameters Analysis for Underground Mine Ventilation*, Sensors, 2025, 25, 5300.
- [20] WYROK SĄDU NAJWYŻSZEGO z dnia 3.10.2006 r., sygn. akt IV KK 209/06.

ANALIZA WYKONANEJ REKONSTRUKCJI WYPADKU ZE SPRAWY SĄDOWEJ DLA POPRAWY BEZPIECZEŃSTWA PRACY

Publikacja stanowi wstępną ocenę zachowań uczestników, której dokonał biegły sądowy na podstawie przeprowadzonej rekonstrukcji zdarzenia. Odtworzenie na potrzeby postępowania sądowego zaistniałego wypadku było przeprowadzone na podstawie materiału dowodowego z akt sprawy sądowej. W tym zakresie została wykorzystana technika audio-video. W oparciu o to zostały ustalone przyczyny i skutki zdarzenia wypadkowego. Celem publikacji jest ocena przydatności rekonstrukcji pod względem możliwości poprawy bezpieczeństwa pracy. W tym zakresie oceniono wypadek śmiertelny, który miał miejsce w jednym z zakładów przemysłowych. Wykonana rekonstrukcja biegłego odpowiedziała na pytania sądu. Ustaloną przyczyną był brak odpowiedniej komunikacji w zespole pracowników. Wykonana rekonstrukcja wypadku na potrzeby sprawy sądowej może w przyszłości zostać wykorzystana jako materiał szkoleniowy w zakresie poprawy bezpieczeństwa pracy.

11. ASSESSMENT FRAMEWORK FOR ARTISANAL AND SMALL-SCALE MINING: CASE STUDY OF PODMOKY, CZECH REPUBLIC

DAVID STEJSKAL

Vysoká Škola Báňská – Technická Univerzita Ostrava,
17. Listopadu 2172/15, 708 000 Ostrava-Poruba.

Artisanal and Small-Scale Mining (ASM) is a standard method of mineral resource extraction worldwide. However, in the Czech Republic it has not yet been legally adopted, as this form of mining is not regulated by legislation. Potential stakeholders currently lack tools to comprehensively assess the feasibility of ASM at selected sites. In the Czech context, the issue of ASM has received little attention so far. The aim of this paper is therefore to present an initial proposal of a framework for ASM evaluation in the form of the Micro-Mining Readiness Index (MMRI). The proposed methodology comprehensively evaluates the legislative, economic, environmental, and social aspects of micro-mining. The paper also identifies the strengths and weaknesses of ASM. The methodology is applied to the case study of the Podmoky locality.

Keywords: micro-mining (ASM), assessment framework (MMRI), Podmoky

11.1. INTRODUCTION

Artisanal and Small-Scale Mining (ASM) is an integral part of the mining sector. However, precise and up-to-date global data on the scale of ASM are not available, since this activity is conducted informally or illegally in most countries, which prevents systematic statistical monitoring.

According to estimates, more than 40 million people are directly dependent on ASM, and up to 150 million people indirectly rely on it [26, 27]. A frequently cited study by Hilson [12] states that ASM accounts for approximately 15–20% of global mineral production. Although this figure comes from an early 2000s publication, it can, in line with World Bank [27] and Verbrugge and Geenen [26], still be understood as an indicative benchmark, especially as no recent global quantification has been published.

Artisanal and Small-Scale Mining (ASM) is commonly defined as low-tech, labor-intensive mineral extraction carried out by individuals, families, or small groups with limited use of mechanization [13]. The World Bank [27] emphasizes that ASM opera-

tions are generally characterized by low levels of capitalization, small production volumes, and employment of a relatively small workforce. According to the OECD [22], although exact definitions vary across countries and commodities, the main features include manual or semi-mechanized techniques, informal organizational structures, and limited adherence to industrial safety and environmental standards.

Since ASM is a sector that is difficult to measure, the international discourse increasingly emphasizes its formalization. The goal of formalization is to improve working conditions, reduce environmental impacts, and ensure greater benefits for local communities [14, 22].

For contrast, one can mention Brazil, where the state recognizes small-scale mining (ASM) as a distinct category. A special license, *Permissão de Lavra Garimpeira* (PLG), allows individuals or cooperatives to legally extract so-called *garimpo minerals* – primarily gold. In some regions, such as the state of Pará, simplified environmental licenses have been introduced to facilitate the transition of miners from the informal to the legal sphere [8]. Nevertheless, a significant portion of production remains informal, which brings serious environmental and social challenges [18].

While ASM represents a common form of organized mining activity in many regions worldwide – particularly in Sub-Saharan Africa, Latin America, and parts of Asia, where it provides livelihoods for more than 40 million people and indirectly supports more than 100 million [13, 26, 27] – the situation in the Czech Republic is different. Even though the Czech legal framework, based on Act No. 44/1988 Coll. on the Protection and Utilization of Mineral Resources (the Mining Act), does not explicitly exclude ASM, it also does not provide any specific provisions for this form of mining.

Section 5a of the mentioned Act states: “*Legal and natural persons who, within their business activities and in compliance with the conditions set by legal regulations, carry out the exploration, prospecting, or extraction of exclusive deposits or other mining activities, shall be considered organizations under this Act*” (Act No. 44/1988 Coll.).

An exclusive deposit refers to deposits of designated (reserved) minerals explicitly listed in §3 of the Mining Act. These include, for example, radioactive minerals, magnesite, oil, natural gas, rock salt, minerals for industrial metal production, granite, mica, and kaolin. Other minerals are classified as non-reserved and are considered part of the land.

Czech mining law does not differentiate between so-called large-scale and small-scale mining. At present, mineral extraction in the Czech Republic is carried out predominantly by corporations. An exception is the Granát Turnov Cooperative, which has successfully mined and processed Czech garnets for decades [8]. This model demonstrates that even smaller-scale mining activities can be legally and economically viable in the Czech context.

The author argues that the current situation calls for verifying ASM as an alternative that could provide an opportunity for those interested in engaging legally in mining

activities, not only of non-reserved minerals. One of the localities where ASM could potentially be applied is Podmoky (Havlíčkův Brod district; see Fig. 11.1). At this site, in the alluvial deposits of the Brslenka stream, rutile, minor amounts of gold, and other minerals occur.

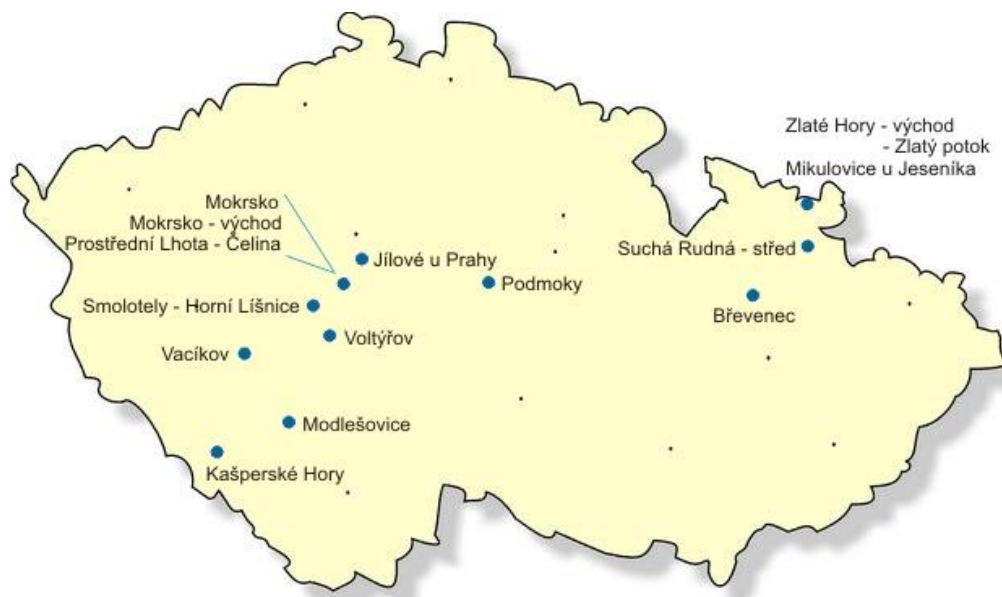


Fig. 11.1. Gold localities in the Czech Republic, including the Podmoky deposit in comparison to other historical and contemporary gold occurrences.

Source: http://geologie.vsb.cz/loziska/loziska/loziska_cr.html

Given the legislative framework governing mining activities in the Czech Republic, it is clear that ASM can hardly operate under current conditions in the case of reserved minerals. In particular, small-scale gold mining operates on the borderline of legality. If ASM is to be developed in the Czech Republic, it will be necessary to address not only the legal aspects of such mining, but also a number of other related areas. This creates the need for a systematic tool that would make it possible to assess whether a specific site has potential for the controlled and supervised development of ASM.

The outcome of ongoing research in this field is the proposed methodological framework of the Micro-Mining Readiness Index (MMRI), which integrates legislative, economic, environmental, and social criteria in order to comprehensively evaluate the readiness of a given deposit for small-scale mining.

The objective of this paper is to present the MMRI framework and demonstrate its application on the model locality of Podmoky.

11.2. MICRO-MINING READLINESS INDEX (MMRI)

The section introduces the concept of MMRI, its theoretical foundations, and the methodology for applying the framework to the selected locality.

11.2.1. MMRI: CONCEPT AND INSPIRATION

Micro-Mining Readiness Index (MMRI) is designed as a multi-criteria assessment framework for evaluating the readiness of a deposit and its surrounding environment for a small-scale mining project (ASM – Artisanal and Small-Scale Mining). The index is based on similar principles to project readiness indices commonly applied in the mining industry, i.e., it evaluates to what extent the key prerequisites for successful project implementation are met [24]. In recent years, a number of tools for assessing project readiness have emerged in the mining sector to support managerial decision-making on whether to proceed with further investment [1]. Thus, MMRI is not a purely subjective construct – comparable frameworks have been developed, such as the Project Definition Rating Index (PDRI) and other readiness checklists for large investment projects [1, 24]. However, no universally accepted standard exists to date; there is still no globally adopted readiness index for mining projects [24]. MMRI seeks to fill this gap in the specific domain of small-scale mining.

In contrast to a conventional feasibility study, which focuses primarily on geological and economic aspects of a project, MMRI gives equal weight to legislative and social dimensions. The inclusion of these criteria reflects the fact that the success of small-scale mining projects depends not only on the quality of the deposit but also on the favorability of the regulatory environment and the support of local communities.

The framework draws inspiration from sustainability assessment methodologies and project readiness evaluation tools published, for example, by the Southern African Institute of Mining and Metallurgy (SAIMM). Nevertheless, MMRI represents the first framework explicitly tailored to the conditions of small-scale mining in the Czech context.

11.2.2. MAIN ASSESSMENT CATEGORIES

The MMRI is divided into four key dimensions (pillars), which together cover all essential factors affecting the readiness of a deposit for small-scale mining. This can be expressed as follows:

$$MMRI = \frac{S_{leg} + S_{eko} + S_{env} + S_{soc}}{4},$$

where:

S_{leg} – Legislative readiness (0–5),

S_{eco} – Economic viability (0–5),

S_{env} – Environmental feasibility (0–5),

S_{soc} – Social acceptance (0–5).

In the following section, we will examine the content of each of these four categories in more detail.

Legislative readiness

This pillar evaluates the regulatory environment and the legal framework for ASM – in particular the accessibility of permits, the administrative burden, and possible spatial restrictions. At Podmoky, the current legislation does not recognize small-scale mining, meaning that even a minor project would have to undergo the same permitting procedure as a large-scale mine. In contrast, some jurisdictions have introduced regulations that ease the entry of small-scale mines. For example, in the Canadian province of Newfoundland & Labrador, small-scale mines are exempted from certain legal requirements, which significantly accelerates project start-up [21]. A low score in this category therefore represents a major obstacle to project implementation.

Economic viability

This pillar assesses the economic potential of the deposit and the market conditions affecting the profitability of small-scale mining. It considers the estimated quantity and quality of the ore (e.g., gold content or other valuable minerals), current market prices of the target commodities, mining and processing costs at a small scale, and the availability of capital to finance the project. An important factor is whether there is a viable market for the output of small-scale mining – for example, the ability to sell gold or by-products (rutile, garnet, etc.) on domestic or specialized markets. This category broadly corresponds to the classic feasibility analysis of a mining project but adapted to small-scale operations: it reflects that artisanal miners may have limited resources and must achieve profitability quickly at modest production volumes.

Environmental and technical feasibility

This pillar evaluates the potential environmental impacts of mining and the practicality of proposed technical solutions. It considers the possibility of environmentally friendly methods (e.g., mercury-free gravity panning), the difficulty of land reclamation, and impacts on water and ecosystems. The deposit's location is also important (e.g., whether it lies within a protected area), as well as practical aspects such as accessibility, infrastructure, and processing facilities. In the case of Podmoky, the risks are relatively low – the deposit is shallow and easily accessible, which represents a favorable factor within the MMRI framework.

Social and institutional acceptance

This pillar assesses the attitudes of local communities, municipalities, and institutions toward the project (“social license to operate”). It evaluates whether mining is perceived as an opportunity for the region (e.g., jobs, development, tourism) or as a threat (e.g., conflicts, public opposition). It also considers the level of support from universities, research institutions, or government authorities, as well as the availability of local human resources. In the case of Podmoky, a rather neutral stance from the municipality can be expected; achieving a higher score would depend on active community involvement and institutional support.

For each category, a set of specific indicators was defined and evaluated on a 0–5 scale. A score of 0 represents completely unfavorable conditions / unpreparedness, while a score of 5 indicates optimal, fully favorable conditions for an ASM project. This five-point scale (0–5) provides sufficient granularity to distinguish different levels of readiness.

Each indicator has predefined criteria for the individual levels. For example, in the legislative category, the indicator “*Existence of a special license for small-scale mining*” receives 0 points if such an option is entirely absent from the law (as is the case in the Czech Republic), and 5 points if the legislation explicitly provides for and applies a dedicated ASM license. Similarly, indicators such as the duration of the permitting process (0 = extremely long, 5 = short) or the administrative burden (0 = very complex, 5 = minimal bureaucracy) are scored accordingly. In each category, several such partial values are averaged to obtain the final score.

Since the author considers all four pillars (legislative, economic, environmental, and social) equally important and interdependent from the perspective of sustainable development, each dimension was assigned the same weight. This approach ensures that no pillar is overlooked a priori – a small-scale mining project must perform adequately across all dimensions simultaneously in order to be realistically viable.

11.2.3. EVALUATION PROCEDURE

The methodology follows four basic steps:

1. Site description – providing the fundamental geological and contextual information.
2. Formation of the expert team – assembling an interdisciplinary panel of specialists for each pillar.
3. Assignment of scales and weights to indicators – scoring based on predefined criteria.
4. Interpretation of results – visualisation using a spider chart and calculation of the overall score.

11.2.4. INTERPRETATION OF RESULTS

It is important to emphasize that MMRI is a conceptual framework rather than a finalized methodology. It represents the first step towards a systematic assessment of small-scale mining projects in the Czech Republic. We are aware of its main limitations:




- the assessment depends on the availability and quality of data,
- results may vary depending on the composition of the expert group,
- the scales need further testing for different commodities (gold, rutile, etc.).

The outcomes of MMRI can be clearly displayed using a spider chart, where each axis represents one category and its length corresponds to the achieved score. Although such a visualization helps to reveal the strengths and weaknesses of a project, it does not in itself lead to a clear conclusion about whether the selected site is suitable for ASM. To facilitate interpretation, we therefore propose scaling the final MMRI value (converted into percentages) into three categories, represented by red, yellow, and green, similar to a traffic-light system (see Table 1).

In the field of mining sector assessment, composite indices are often interpreted through qualitative bands. For example, the global Resource Governance Index (RGI) evaluates the governance of mineral resources in individual countries on a scale from 0–100. The results are clearly divided into categories ranging from “failing” to “good” governance – specifically, scores above 75 are considered good, 60–74 satisfactory, 45–59 weak, 30–44 poor, and below 30 failing [19].

Table 1. MMRI Ranges and Recommended Interpretation.

Source: author's own processing

MMRI range (%)	Category	Color	Characteristics	Recommended action
0–40%	unsuitable	 red	The ASM project is not suitable for implementation. Negative factors prevail (legislation, economics, environment).	STOP – do not proceed unless fundamental conditions change (e.g., legislation)
40–65%	conditionally suitable	 yellow	The project shows potential but also weaknesses; feasibility is uncertain. Additional verification is necessary	CAUTION – conduct detailed surveys (geology, economics), involve the community
65–100%	suitable/feasible	 green	The ASM project is realistically feasible – legislation, economics, environment, and social conditions are favorable.	PROCEED – prepare the project for implementation and initiate pilot mining.

A similar principle of scaling is used for MMRI: certain percentage intervals are translated into qualitative labels such as “unsuitable / conditionally suitable / suitable”. The aim, as with RGI, is to give readers a clear understanding of whether a specific result is excellent, average, or insufficient (see Table 1).

The threshold values (40% and 65%) are based on expert judgment and analogies with established practices. The ranges are not perfectly symmetrical but correspond to the intuition that projects with an MMRI score below 40% exhibit fundamental barriers to implementation. Scores between 40–65% fall into a so-called “grey zone,” where feasibility is uncertain and requires caution and further analysis. Above 65%, positive indicators prevail, and the project can be considered feasible with a reasonable degree of confidence. This categorization serves as a quick orientation tool, similar to a traffic-light system – immediately signaling whether a project should be stopped, further investigated, or advanced [11].

11.3. APPLICATION OF MMRI TO THE PODMOKY LOCALITY

For the purpose of verifying the proposed methodology, the Micro-Mining Readiness Index (MMRI) was applied to the Podmoky locality. The Podmoky site is situated in the Kutná Hora District, on the border between the Central Bohemian and Vysočina regions, within the catchment area of the Brslenka (Čáslavka) stream. Geologically, it represents a placer-type deposit of heavy minerals, composed mainly of gold and rutile concentrate, accompanied by ilmenite and cassiterite. Historical records confirm that the area was known for gold panning as early as the Middle Ages, while intensive prospecting took place again in the 1980s as part of research by the former Czech Geological Survey [23, 25]. At present, Podmoky is designated as a Protected Deposit Area (CHLÚ), which underlines its importance for the raw material policy of the state [6]. A specific feature of Podmoky is the presence of spoil heaps from earlier exploration, which still contain residual gold in the form of fine grains and flakes, together with heavy minerals, and thus represent a suitable testing block for the proposed pilot application of the ASM framework. Previous geological studies have documented the presence of gold with an average content of approximately 2 g/t [22, 24] and significant rutile concentrations reaching up to ~40 kg/t [22]. This polymetallic character, combined with the shallow and easily accessible nature of the deposit, creates favorable conditions for potential controlled extraction [6].

In cases where multiple indicators were defined for one category, the arithmetic mean of the partial values was calculated (see Table 2).

Table 2. MMRI assessment for the Podmoky site. Source: author's own processing

Category	Score (0–5)	Characteristics
Legislative readiness	1	No special license for ASM, complex and time-consuming permitting process
Economic viability	3	Gold content approx. 2 g/t and rutile up to 40 kg/t; economically interesting but small in volume
Environmental feasibility	4	Shallow, easily accessible deposit, outside protected areas, low risk of impacts
Social acceptance	3	Interest from amateur gold panners, possible involvement of universities, municipality without major objections

The total MMRI for Podmoky thus reached the value:

$$MMRI = \frac{1 + 3 + 4 + 3}{4} = 2,75.$$

This result corresponds to approximately 55 % of the maximum possible readiness. The graphical representation (Fig. 11.2) shows a radar chart, where it is evident that the weakest area is legislation, while the economic, environmental, and social conditions appear relatively favorable.

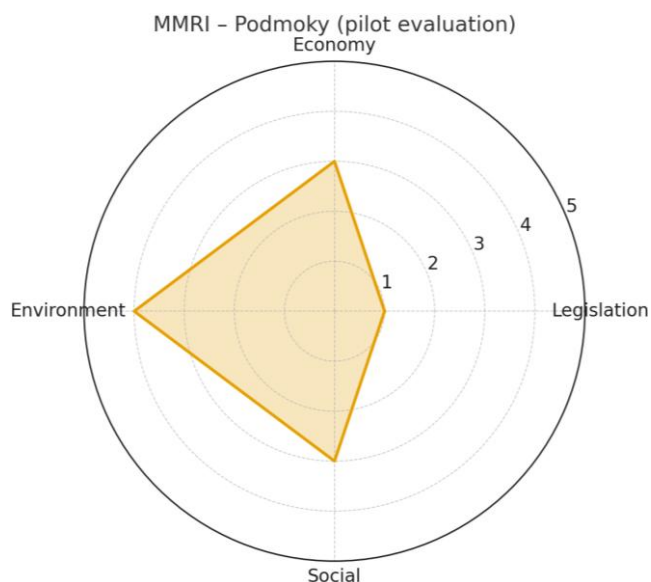


Fig. 11.2. Graphical evaluation of the Podmoky site

When evaluated using the traffic-light system introduced in Chapter 2, the Podmoky site falls into the yellow category. This means that feasibility is potentially achievable but conditional upon further steps. In practice, this would imply a recommendation to continue with additional exploration (e.g., verifying the actual reserves of gold/rutile through more detailed geological surveys, conducting an economic assessment of small-scale mining, and especially addressing legislative obstacles, for instance by initiating discussions on the introduction of an ASM license). Once further information becomes available, it will be appropriate to reassess the site using the MMRI framework.

11.4. DISCUSSION

The results of applying the Micro-Mining Readiness Index (MMRI) methodology to the Podmoky site showed that, from a geological perspective, the potential is real, but the main obstacles lie in the legislative framework and institutional readiness. This finding is consistent with international experience, which emphasizes that legal and institutional environments largely determine the success or failure of ASM [13, 26].

In many developing countries, ASM is *de facto* tolerated, even if conducted informally. The challenge there lies more in regulation and integration into the official economy. Efforts in Africa and Latin America therefore focus on formalization of ASM through licensing, the establishment of cooperatives, or the provision of technical support to miners [3, 27].

In contrast, ASM does not exist in the Czech Republic because it is not legally recognized and is not practiced in a formal way. Czech mining legislation makes no distinction between large- and small-scale mining and requires complex permitting processes designed primarily for industrial-scale operations. This situation prevents the development of small, community-oriented mining projects, even in cases where sites show potential for local or educational use.

A particularly relevant example for the Czech context is the cooperative model. In countries such as Tanzania and Mozambique, the organization of small-scale miners into cooperatives has been shown to improve their bargaining position, facilitate access to finance and technology, and enable better oversight of environmental impacts [26, 27]. In the Czech Republic, a comparable tradition exists in the form of the Granát Turnov Cooperative, which has long operated in the gemstone sector. This model demonstrates that even in the Czech context, smaller-scale mining can be viable if organized within cooperatives or companies with strong regional ties.

Another important aspect is the issue of economic viability. While ASM worldwide often represents a crucial source of livelihood, in the Czech Republic it could take more of a supplementary or community-oriented role. This does not mean, however, that it is

insignificant – even small-scale production of gold or rutile could find applications in domestic industry or jewelry. In combination with educational and tourism activities, the ASM model could generate synergistic effects contributing to regional development [13, 27].

Overall, international experience points to two lessons: (i) the risks of unregulated ASM, which should serve as a warning in the Czech context, and (ii) the opportunities of formalized ASM, which could inspire pilot projects in the Czech Republic. The Podmoky site could thus become the first case of a European-style ASM model, based on regulation, community involvement, and cooperation with expert institutions.

It should be acknowledged that in some other indices, weights are assigned differently depending on importance. For example, the Fraser Institute's ranking of mining jurisdictions combines geological potential and political factors with a 60:40 ratio in favor of geology [9], since investors consider a strong geological base more decisive than bureaucratic hurdles. Similarly, studies on Project Readiness show that certain factors (e.g., reserve verification) have a far greater impact on project success than others (e.g., resolving site drainage) [1, 24]. Should future applications of MMRI reveal that specific categories correlate more strongly with project success or failure, it may be appropriate to introduce differentiated weights reflecting this reality.

It should also be noted that the size of the expert group represents a limitation of this study. The assessment was conducted by the author and two consultants with backgrounds in geology and mining economics, which enabled basic triangulation and reduced subjectivity, but a broader panel would be desirable for more robust results. Recruiting a sufficient number of experts willing and able to engage in detail is not straightforward, especially given the specific nature of the topic and the limited tradition of ASM in the Czech context. In the future, it would therefore be advisable to test the MMRI methodology within a larger expert workshop, possibly involving regulators and local community representatives, to better verify the consistency of results.

Engaging a greater number of evaluators reduces the risk of subjective bias and ensures that the final scores more accurately reflect a consensus view. A similar multi-assessor approach is common internationally: some frameworks function as self-assessment tools for project teams, while others require review by an independent expert or commission [4]. For example, the Project Definition Rating Index (PDRI) is completed by an interdisciplinary team of project managers and engineers to cover all aspects of project readiness [1, 24].

In practice, MMRI could therefore be applied either directly by a mining company as an internal tool for assessing project potential, or externally – e.g., by a mining authority or advisory board of experts – to evaluate whether a given project meets the minimum conditions to justify further consideration. There are also international examples where regulators define specific check-list criteria that a small mining project must meet in order to qualify for simplified permitting. As mentioned earlier, some Canadian pro-

vinces define “small-scale mines” through clear thresholds (e.g., production volume, investment costs) and, if a project remains under these thresholds, it proceeds through a fast-track permitting process [21]. Such a decision is effectively made by an administrative authority through a standardized evaluation – analogously, MMRI could serve as a standardized form for assessing the readiness of a deposit prior to granting a special ASM license.

11.5. CONCLUSION

The application of the MMRI to the Podmoky deposit indicates that this locality has potential for pilot testing of micro-mining in the Czech Republic. Despite its relatively small size, the site demonstrates conditions that make it suitable for controlled extraction and further evaluation.

Podmoky could therefore serve as a pioneering pilot case, contributing to the wider European debate on the role of artisanal and small-scale mining (ASM). It illustrates that micro-mining does not necessarily imply uncontrolled or environmentally risky activity, but rather a regulated, monitored, and community-oriented model.

The successful implementation of such a pilot project could broaden the spectrum of domestic resource utilization, support regional development, and strengthen the Czech Republic’s position in the European discussion on sustainable mineral supply. This study presents a proposal of the MMRI concept, which will be further elaborated. In particular, the methodology for evaluating and interpreting the results will be refined in future research.

REFERENCES

- [1] ANDERSEN J., FLYVBJERG B., GARBUIO M., LOVALLO D., *The quest to establish a project readiness assessment*, Journal of the Southern African Institute of Mining and Metallurgy, 2016, 122 (9), 497–510.
- [2] BANERJEE C., ADENLE A.A., VIRK P., *Feasibility study of vertical farming in developing countries: A case for investment in the EBRD region*, CAB Reviews, 2017, 12 (14), 1–14, <https://doi.org/10.1079/PAVSNNR201712014>
- [3] BUXTON A., *Responding to the challenge of artisanal and small-scale mining: How can knowledge networks help?*, International Institute for Environment and Development (IIED), 2013, <https://pubs.iied.org/16532IIED>
- [4] Copper Mark, *Responsible Raw Materials Assurance (RRA) – Criteria Guide v3.0*, 2023, https://coppermark.org/wp-content/uploads/2023/10/RRA-v3.0-Criteria-Guide_2023.pdf
- [5] Český Báňský Úřad (ČBÚ), *Databáze chráněných ložiskových území (CHLÚ)*, 2023, <https://mapy.geology.cz/chlu>
- [6] Česká Geologická Služba, *Registr chráněných ložiskových území – Podmoky (Geofond)*, 2024, <https://www.geofond.cz>

- [7] CLIMATE POLICY INITIATIVE, *Global Landscape of Climate Finance 2023*. Available at: <https://www.climatepolicyinitiative.org/wp-content/uploads/2023/11/Global-Landscape-of-Climate-Finance-2023.pdf> [Accessed 18.11.2025].
- [8] Družstvo Granát, d.u.v., *Oficiální webová prezentace*, 2023, <https://www.granat.eu>
- [9] European Commission, *National minerals policy indicators*, Raw Materials Information System (RMIS), 2018, https://rmis.jrc.ec.europa.eu/uploads/scoreboard2018/indicators/13._National_minerals_policy.pdf
- [10] European Commission, *Critical Raw Materials Act – List of Critical and Strategic Raw Materials*, Brussels, 2023, https://single-market-economy.ec.europa.eu/sectors/raw-materials/areas-specific-interest/critical-raw-materials_en
- [11] Fareham Borough Council, *Core Strategy: Issues and Options Sustainability Appraisal*, Fareham: Fareham Borough Council, 2009, <https://www.fareham.gov.uk>
- [12] Fareham Borough Council, *Infrastructure Planning and Viability Study*, Fareham: Local Development Framework, 2011, <https://www.fareham.gov.uk>
- [13] HILSON G., *Small-scale mining and its socio-economic impact in developing countries*, Natural Resources Forum, 26 (1), 3–13, 2002, <https://doi.org/10.1111/0165-0203.00065>
- [14] HILSON G., McQUILKEN J., *Four decades of support for artisanal and small-scale mining in sub-Saharan Africa: A critical review*, The Extractive Industries and Society, 1 (1), 104–118, 2014, <https://doi.org/10.1016/j.exis.2014.01.002>
- [15] HILSON G., POTTER C., *Structural adjustment and subsistence industry: Artisanal gold mining in Ghana*, Development and Change, 2005, 36 (1), 103–131, <https://doi.org/10.1111/j.0012-155X.2005.00404.x>
- [16] Horní Zákon, 1988, *Zákon č. 44/1988 Sb., o ochraně a využití nerostného bohatství (horní zákon), ve znění pozdějších předpisů*. <https://www.zakonyprolidi.cz/cs/1988-44>
- [17] IGF (Intergovernmental Forum on Mining, Minerals, Metals and Sustainable Development), *Global ASM Policy Database – Formalization of Artisanal and Small-Scale Mining*, International Institute for Sustainable Development, 2017, <https://igfmining.org>
- [18] MORÁVEK P. et al., *Ložiska zlata v Československu*, Academia, 1989.
- [19] Natural Resource Governance Institute, *2017 Resource Governance Index*, NRGI, New York 2017, <https://resourcegovernance.org/analysis-tools/publications/2017-resource-governance-index>
- [20] NOVÁK J., *Český granát a jeho ložiska*, Národní museum, 2010.
- [21] Novamera, Inc., *Permitting for small-scale mining in Newfoundland & Labrador, Canada*, 2023, <https://novamerainc.com/permitting-for-small-scale-mining/>
- [22] OECD, *OECD due diligence guidance for responsible supply chains of minerals from conflict-affected and high-risk areas*, OECD Publishing, 2016, <https://doi.org/10.1787/9789264252479-en>
- [23] PAULIŠ P. et al., *Výsledky geologického průzkumu rozsypových ložisek zlata na Čáslavsku*, Český geologický ústav, 1985.
- [24] POTGIETER H., *Definition Rating Indexes in mining projects*, Journal of the Southern African Institute of Mining and Metallurgy, 2016, 122 (7), 377–386, <https://www.saimm.co.za/Journal/v122n07p377.pdf>
- [25] SEJKORA J., PAULIŠ P., *Mineralogické poměry zlatonosných náplavů na Čáslavsku*, Acta Musei Nationalis Pragae, Series B, Historia Naturalis, 2012, 68 (1–2), 45–56.
- [26] VERBRUGGE B., GEENEN S., *Global gold production touching ground: Expansion, informalization, and technological innovation*. 2020, London: Palgrave Macmillan.
- [27] World Bank, & Pact, *2019 State of the Artisanal and Small-Scale Mining Sector*, Washington, DC, World Bank, 2019, <https://www.delvedatabase.org/resources/2019-state-of-the-artisanal-and-small-scale-mining-sector>

RAMY OCENY GÓRNICICTWA RZEMIEŚLNICZEGO I MAŁOSKALOWEGO:
STUDIUM PRZYPADKU PODMOKY, REPUBLIKA CZESKA

Zastosowanie metody MMRI do oceny złoża Podmoky pokazuje, że mimo mniejszych rozmiarów wykazuje ono realny potencjał dla rozwoju mikrogórnictwa, dzięki obecności zarówno złota, jak i znaczących koncentracji rutyłu. Ten polimineralny charakter, w połączeniu z płytkim zaleganiem i łatwą dostępnością złoża, stwarza korzystne warunki dla kontrolowanej eksploatacji.

Podmoky mogłyby zatem stać się pionierskim projektem pilotażowym dla Republiki Czeskiej i wnieść wkład w szerszą europejską debatę na temat roli ASM. Może ono pokazać, że mikrogórnictwo nie musi oznaczać działalności niekontrolowanej i ryzykownej środowiskowo, lecz raczej model regulowany, monitorowany i korzystny dla społeczności. Sukces takiego projektu pilotażowego poszerzyłby spektrum wykorzystania krajowych zasobów, wsparł rozwój regionalny i wzmocnił pozycję Republiki Czeskiej w europejskiej dyskusji na temat zrównoważonego zaopatrzenia w surowce mineralne.

Przedstawiono propozycję metody MMRI, która będzie dalej rozwijana. W szczególności zostanie dopracowana metodologia oceny i interpretacji wyników.

12. GREEN HYDROGEN: A KEY DRIVER OF SUSTAINABLE ENERGY SYSTEMS IN EUROPE

MAROŠ BEGÁNI

Technical University of Košice, Faculty of Mining, Ecology, Process Control and Geotechnologies
– Institute of Earth Resources, Letná 1/9 042 00 Košice-Sever, Slovak Republic.

Green hydrogen, produced from renewable energy sources through water electrolysis, represents a crucial element in the transition toward sustainable and low-carbon energy systems. As the European Union accelerates its decarbonisation goals under the European Green Deal, Fit for 55 package and REPowerEU plan, hydrogen has emerged as both a clean energy carrier and a strategic vector for achieving climate neutrality by 2050. This paper provides a theoretical overview of green hydrogen technologies, exploring their environmental benefits, integration into energy systems, and the main challenges for large-scale deployment in Europe. The analysis focuses on policy frameworks, technological readiness, infrastructure requirements, and sustainability impacts. The study concludes that the hydrogen economy – if based on renewable sources – has the potential to reduce greenhouse gas emissions, enhance energy independence, and foster cross-sectoral innovation across European industries.

Keywords: green hydrogen, sustainability, renewable energy, European Green Deal, energy transition

12.1. INTRODUCTION

The transition toward sustainable and decarbonised energy systems is one of the greatest challenges of the twenty-first century. The European Union has committed to achieving climate neutrality by 2050 through ambitious initiatives such as the *European Green Deal*, the *Fit for 55* legislative package, and the *REPowerEU* strategy [1]. These frameworks emphasise renewable energy expansion, electrification, and diversification of energy carriers to reduce dependence on fossil fuels and imported natural gas. Within this context, hydrogen – particularly green hydrogen produced from renewable electricity – has become a cornerstone of Europe’s long-term energy vision. Its versatility allows application across power generation, mobility, heating, and industrial processes [2]. Green hydrogen is not only a technological innovation but also a strategic element in achieving environmental, economic, and geopolitical stability. Its potential to decarbonise “hard-to-abate” sectors such as steel, cement, and chemical production makes it a key enabler of the low-carbon economy [3]. Furthermore, hydrogen development

directly supports the United Nations Sustainable Development Goals (SDG 7 and 13), focusing on affordable clean energy and climate action [4]. Recent studies underline that large-scale hydrogen deployment could contribute significantly to reducing global CO₂ emissions by up to 10% by 2050, provided that production is based on renewable sources [5]. In this context, the European Commission has positioned hydrogen as one of the main pillars of the new industrial strategy, aiming to enhance resilience and competitiveness within the green transition [11]. The aim of this paper is to explore the role of green hydrogen as a driver of sustainable energy systems in Europe. The study is based on a theoretical approach employing **comparison, analysis, and synthesis** of secondary sources, policy frameworks, and academic research. Through this analytical overview, the paper seeks to identify the current challenges and opportunities of integrating green hydrogen within the European energy transition.

12.2. METHODS OF THEORETICAL ANALYSIS

This paper is based on a **theoretical and analytical approach**, employing qualitative research methods focused on secondary data interpretation. The methodological framework combines **comparison, analysis, and synthesis** of existing scientific literature, strategic documents of the European Union, and international policy reports related to hydrogen technologies and sustainable energy. The **comparative method** was used to examine and contrast the development of green hydrogen strategies among European countries and international frameworks. **Analysis** focused on identifying the main factors influencing hydrogen deployment, such as technological readiness, environmental implications, and economic viability. Subsequently, **synthesis** was applied to integrate findings into a coherent perspective, highlighting the interconnections between policy, technology, and sustainability. This methodological structure provides a comprehensive overview of the current state of green hydrogen research while allowing a critical evaluation of its role in achieving energy transition objectives. The approach reflects the interdisciplinary nature of the topic, bridging environmental, technological, and economic aspects within the European context.

12.3. EUROPEAN ENVIRONMENTAL AND ENERGY FRAMEWORKS

Several European countries are already demonstrating significant progress in implementing hydrogen technologies across various sectors, supported by national hydrogen strategies aligned with EU objectives. **Germany** represents a frontrunner in the hydrogen transition. Its *National Hydrogen Strategy* (2020) sets clear targets for developing large-scale electrolysis capacities, with a focus on industrial decarbonisation and transport. The country has invested heavily in research and infrastructure, including

the construction of hydrogen refuelling stations and integration of renewable hydrogen in steel and chemical industries [7]. **France** is another major player, aiming to achieve carbon neutrality through strong public investment and industrial cooperation. Its *France Hydrogène* initiative promotes the use of hydrogen in mobility and regional energy systems. France also supports domestic electrolyser production and hydrogen trains, which are already operating in regions such as Occitanie and Bourgogne-Franche-Comté [8]. **The Netherlands** has adopted a pragmatic approach, focusing on international cooperation and infrastructure. As part of the *North Sea Hydrogen Corridor*, the country develops port-based hydrogen hubs in Rotterdam and Groningen, connecting offshore wind energy with hydrogen storage and transport networks [9]. **Spain** combines high renewable potential with ambitious hydrogen development goals. The *Hydrogen Roadmap Spain 2030* emphasises the integration of solar-powered electrolysers, with several pilot projects for hydrogen buses and industrial use in Andalusia and Aragón [10].

In contrast, **Central and Eastern European countries**, including **Slovakia**, remain in the early stages of hydrogen adoption. National frameworks are still being developed, and large-scale infrastructure is limited. However, several demonstration projects – such as hydrogen-powered buses in Bratislava – indicate the first steps toward practical implementation and future alignment with EU strategies [11]. This cross-country comparison reveals that while Western European nations are already deploying hydrogen at an industrial scale, many Central European countries are still focusing on establishing legislative and technical foundations. The experience of Germany, France, the Netherlands, and Spain provides valuable insights for shaping hydrogen policy and investment strategies across the European Union.

12.4. THE CONCEPT OF GREEN HYDROGEN

Hydrogen is the lightest and most abundant element in the universe, yet on Earth it rarely exists in its pure molecular form. It must be extracted from compounds such as water or hydrocarbons through energy-intensive processes [3]. The colour classification – grey, blue, turquoise, and green – denotes the method of production and associated carbon footprint [4]. Green hydrogen is produced via electrolysis of water, using electricity from renewable sources like solar, wind, or hydropower. The process emits only oxygen as a by-product, making it virtually carbon-free. However, the efficiency of electrolysis remains a limitation, typically 65–75% depending on the technology used [5]. Despite higher costs compared with fossil-based hydrogen, rapid decreases in renewable electricity prices and advances in electrolyser technologies are expected to close this gap in the near future.

Electrolyser technologies: There are three main types of electrolysers currently used for green hydrogen production:

- Alkaline electrolyzers (AEL): the most mature technology, operating at low costs and moderate efficiency (60–70 %).
- Proton exchange membrane (PEM) electrolyzers: offering higher efficiency (70–80%) and faster response, suitable for coupling with intermittent renewables.
- Solid oxide electrolyzers (SOEC): still in development, operating at high temperatures with efficiency up to 85%, suitable for industrial-scale hydrogen generation [12].

Each of these technologies contributes differently to the sustainability of hydrogen systems, depending on available resources and intended applications.

12.5. EUROPEAN ENVIRONMENTAL AND ENERGY FRAMEWORKS

Europe has positioned itself as a global leader in the hydrogen transition. The *EU Hydrogen Strategy* (2020) established a roadmap for scaling up renewable hydrogen production, with a target of installing 40 GW of electrolyzers by 2030 [6]. Member states including Germany, the Netherlands, Spain, and Poland have adopted national hydrogen roadmaps to align with this vision. Hydrogen is integrated into the *European Green Deal* as a critical enabler for achieving climate neutrality, complementing other renewable technologies. The *Fit for 55* package introduces incentives for low-carbon fuels, while the *REPowerEU* plan – adopted after the 2022 energy crisis – aims to accelerate hydrogen deployment and diversify energy imports. The environmental impact of green hydrogen extends beyond emission reduction: it contributes to improved air quality, reduced dependency on fossil fuels, and promotion of circular-economy principles [7].

European projects and initiatives: Several **large-scale European projects** are advancing the hydrogen ecosystem. The *Important Projects of Common European Interest (IPCEI Hydrogen)* initiative supports industrial deployment through joint state aid and innovation funding [13]. *Hydrogen Valleys* across regions like Northern Netherlands, North Rhine-Westphalia, and the Danube area integrate hydrogen production, distribution, and consumption in local energy networks. Other projects, such as the *North Sea Hydrogen Corridor*, aim to connect offshore wind energy with hydrogen hubs across Belgium, Germany, and Denmark. These efforts demonstrate Europe’s leadership in coordinating cross-border projects that align industrial strategy with environmental responsibility.

12.6. THE ROLE OF GREEN HYDROGEN IN SUSTAINABILITY

Green hydrogen acts as a missing link between renewable energy generation and end-use applications. It enables long-term storage of renewable electricity and facilitates decarbonisation in sectors that are difficult to electrify directly, such as heavy in-

dustry, aviation, and maritime transport [8]. The integration of hydrogen into existing energy systems supports energy flexibility and resilience. Excess renewable electricity can be converted into hydrogen (power-to-gas) and later used in fuel cells to regenerate power (gas-to-power). This bidirectional process strengthens energy security, particularly in regions with variable renewable generation [9]. **Environmental and socioeconomic impacts:** The environmental benefits of green hydrogen include a substantial reduction in greenhouse gas emissions, air pollutants, and noise compared to conventional fuels [14]. In transport, hydrogen-powered buses and trains offer zero-emission alternatives for regional mobility. From a socioeconomic perspective, the development of hydrogen infrastructure creates thousands of skilled jobs, especially in engineering, manufacturing, and maintenance. The *Clean Hydrogen Partnership* estimates that by 2030, up to one million new jobs could be generated across Europe. The simplified process of renewable hydrogen production, storage, and utilisation is illustrated in Fig. 12.1.

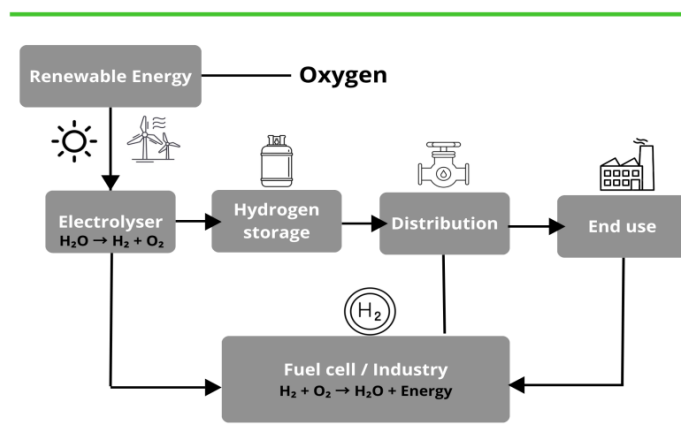


Fig. 12.1. The green hydrogen cycle. Source: Own elaboration

12.7. CHALLENGES AND FUTURE PERSPECTIVES

Despite significant progress, several challenges hinder large-scale deployment of green hydrogen. These include high production costs, lack of infrastructure, limited availability of renewable electricity, and safety concerns related to hydrogen storage and transport [10]. Furthermore, policy harmonisation among EU member states remains incomplete. Cross-border certification of renewable hydrogen, market integration, and investment mechanisms will be crucial for ensuring competitiveness. Continued support for research and innovation – particularly in electrolyser efficiency, materials, and

storage technologies – will determine the pace of progress. In the long term, coupling hydrogen with digitalisation, artificial intelligence, and smart grid systems could create a fully integrated low-carbon economy, aligning with the objectives of the European Green Deal.

Economic and technical barriers. The cost of producing green hydrogen (LCOH) remains in the range of 4–6 EUR/kg, compared to 1.5–2.5 EUR/kg for grey hydrogen [15]. Achieving cost parity requires continued decline in renewable electricity prices and mass production of electrolyzers. Moreover, hydrogen storage technologies – such as metal hydrides, liquid organic carriers, or underground salt caverns – need further research to ensure safety and scalability.

Education and public acceptance: Another key challenge lies in public perception and education. Many citizens still associate hydrogen with high risks due to historical incidents. Increasing awareness, promoting education, and transparent communication will be essential to foster social acceptance and accelerate adoption. In the long term, coupling hydrogen with digitalisation, artificial intelligence, and smart grid systems could create a fully integrated low-carbon economy, aligning with the objectives of the European Green Deal.

12.8. CONCLUSIONS

Green hydrogen stands at the forefront of Europe's sustainable energy transformation. As an emission-free energy carrier, it provides environmental benefits, enhances energy independence, and promotes technological innovation. While economic and infrastructural barriers persist, coordinated policy efforts and technological progress are steadily transforming the hydrogen vision into reality. In a broader perspective, green hydrogen serves as a foundation for deep decarbonisation across multiple sectors of the European economy. Its integration into power grids, industry, and transport supports long-term resilience and energy security. By enabling flexible use of renewable electricity, hydrogen helps stabilise systems increasingly based on variable renewable sources. The next decade will be crucial for scaling up production and infrastructure. Achieving the EU's 2030 targets – 40 GW of electrolyzers and 10 million tonnes of renewable hydrogen – will require strong cooperation between governments, industry, and research institutions. Green hydrogen not only supports climate goals but also stimulates innovation, education, and job creation, strengthening Europe's role as a global leader in clean technologies. Ultimately, the hydrogen economy represents more than a technological shift – it embodies a transition toward circular, self-sufficient, and sustainable energy systems. If guided strategically, green hydrogen can become a cornerstone of a prosperous Europe where economic progress aligns with environmental responsibility.

ACKNOWLEDGEMENTS

The paper was supported by VEGA 1/0328/25, Strategy for the effective and sustainable use of Earth Resources within the Slovak Republic, with an emphasis on the Raw Materials Policy of the EU& by the Horizon 2020 project, no. 101180341 Interregional EU innovation Hubs for the circularity and green supply of Raw Materials to achieve the resilience of the main underdeveloped regions specialised on the critical industrial value chain

REFERENCES

- [1] MAKHA A.O.M., MEHMOOD M., *Green hydrogen energy production: Current status and potential*, Clean Energy, 2024, 8, 1–7.
- [2] FERNÁNDEZ-ARIAS P., ANTÓN-SANCHO Á., LAMPROPOULOS G., VERGARA D., *On Green Hydrogen Generation Technologies: A Bibliometric Review*, Appl. Sci., 2024, 14, 2524.
- [3] WEI S., SACCHI R., TUKKER A., SUH S., STEUBING B., *Future environmental impacts of global hydrogen production*, Energy Environ. Sci., 2024, 17, 2157–2172.
- [4] MAESTRE V.M., ORTIZ A., ORTIZ I., *Challenges and prospects of renewable hydrogen-based strategies for full decarbonization of stationary power applications*, Renew. Sustain. Energy Rev., 2021, 152, 111628.
- [5] JOHNSON K., VEENSTRA M.J., GOTTHOLD D., SIMMONS K., ALVINE K., HOBEIN B., HOUSTON D., NEWHOUSE N., YEGGY B., VAIPAN A., *Advancements and Opportunities for On-Board 700 Bar Compressed Hydrogen Tanks in the Progression Towards the Commercialization of Fuel Cell Vehicles*, SAE Int. J. Altern. Powertrains, 2017, 6, 201–218.
- [6] DURKIN K., KHANAFER A., LISEAU P., STJERNSTRÖM-ERIKSSON A., SVAHN A., TOBIASSON L., ANDRADE T.S., EHNBERG J., *Hydrogen-Powered Vehicles: Comparing the Powertrain Efficiency and Sustainability of Fuel Cell versus Internal Combustion Engine Cars*, Energies, 2024, 17, 1085.
- [7] KAKOULAKI G., KOUGIAS I., TAYLOR N., DOLCI F., MOYA J., JÄGER-WALDAU A., *Green hydrogen in Europe – A regional assessment: Substituting existing production with electrolysis powered by renewables*, Energy Convers. Manag., 2021, 228, 113649.
- [8] SINGLA M., GUPTA J., BERYOZKINA S., SAFARALIEV M., SINGH M., *The Colorful Economics of Hydrogen: Assessing the Costs and Viability of Different Hydrogen Production Methods – A Review*, Int. J. Hydrogen Energy, 2024, 61, 664–677.
- [9] ZHANG H., XIONG P., YANG S., YU J., *Renewable energy utilization, green finance and agricultural land expansion in China*, Resour. Policy, 2023, 80, 103163.
- [10] HYDROGEN COUNCIL. HYDROGEN FOR NET-ZERO: A Critical Cost-Competitive Energy Vector, 2021. Available online: <https://hydrogencouncil.com/wp-content/uploads/2021/11/Hydrogen-for-Net-Zero.pdf> [Accessed on 17 January 2024].
- [11] IRENA, *Green Hydrogen: A Guide to Policy Making*, 2020. Available online: https://www.irena.org/-/media/Files/IRENA/Agency/Publication/2020/Nov/IRENA_Green_hydrogen_policy_2020.pdf [Accessed on 17 January 2024].
- [12] AJANOVIC A., SAYER M., HAAS R., *The Economics and the Environmental Benignity of Different Colors of Hydrogen*, Int. J. Hydrogen Energy, 2022, 47, 24136–24154.
- [13] RAUB A.A.M., BAHRU R., NASHRUDDIN S.N.A.M., YUNAS J., *Advances of nanostructured metal oxide as photoanode in photoelectrochemical (PEC) water splitting application*, Heliyon, 2024, 10, e39079.
- [14] ABD-ELRAHMAN N.K., AL-HARBI N., AL-HADEETHI Y., ALRUQI A.B., MOHAMMED H., UMAR A., AKBAR S., *Influence of Nanomaterials and Other Factors on Biohydrogen Production Rates in Microbial Electrolysis Cells – A Review*, Molecules, 2022, 27, 8594.

- [15] CHEN J., LI Q., WANG L., FAN C., LIU H., *Advances in Whole-Cell Photobiological Hydrogen Production*, Adv. Nanobiomed. Res., 2021, 1, 2000051.

ZIELONY WODÓR: KLUCZOWY CZYNNIK ROZWOJU ZRÓWNOWAŻONYCH SYSTEMÓW ENERGETYCZNYCH W EUROPIE

Zielony wodór, wytwarzany z odnawialnych źródeł energii poprzez elektrolizę wody, stanowi kluczowy element transformacji energetycznej w kierunku zrównoważonego rozwoju. W niniejszym rozdziale przedstawiono teoretyczny przegląd technologii zielonego wodoru w kontekście polityki europejskiej, w tym Europejskiego Zielonego Ładu, pakietu Fit for 55 i planu REPowerEU. Omówiono korzyści środowiskowe, wyzwania technologiczne oraz znaczenie wodoru dla osiągnięcia neutralności klimatycznej do 2050 roku. Zielony wodór może przyczynić się do redukcji emisji gazów cieplarnianych, poprawy bezpieczeństwa energetycznego oraz wspierania innowacji w sektorach przemysłowych Europy.

13. LEGAL ANALYSIS OF POLISH COURT CASE LAW ON THE PHENOMENON OF A REACTIVE DEPRESSIVE ON THE EXAMPLE OF MINING EMPLOYEE

KINGA MARTUSZEWSKA

District Bar Association in Katowice, Lawyer's Office, ul. Jankowicka 23/25, 44-200 Rybnik.

The publication presents an analysis of Polish case law concerning the classification of a reactive depressive episode as an injury within the meaning of the Act on Social Insurance for accidents at work and occupational diseases. The case of a mining plant employee was used to discuss the problem of interpreting the concepts of "external cause" and "characteristics of suddenness" of an event in the context of mental disorders caused by stress and interpersonal conflicts in the workplace. The article presents the course of court proceedings, including the decisions of the courts of both instances and the position of the Supreme Court, which confirmed the possibility of recognizing a psychological trauma as an accident at work. The analysis of court decisions indicates that stress and conflict situations can be a real, external cause of a harmful event if they lead to permanent or sudden deterioration of the employee's health. The study is complemented by a survey conducted among mine employees, which confirmed that interpersonal conflicts and a tense working atmosphere are an important source of stress, reducing work efficiency and safety. The conclusions point to the need to treat mental health as an integral part of occupational safety and health and to implement preventive measures, such as mediation and psychological support, to prevent mental injuries and accidents at work.

Keywords: accident at work, stress, interpersonal conflicts, psychological trauma

13.1. INTRODUCTION

When thinking about an "accident at work" in a mining company, the image of a seriously injured miner comes to mind. For many years, accidents at work were associated exclusively with physical injuries. A typical example is when an employee suffers a limb fracture, burns, or other sudden bodily injury in connection with the work performed.

However, the modern work environment, especially in jobs with high levels of risk and stress, increasingly reveals phenomena that elude this classic image. The realities of the working environment increasingly show that mental burdens can be just as severe and the effects on the employee's health just as serious. The analysis of case-law

indicates that stress and its consequences can be considered as an external cause of an accident at work, and the injury can take the form of a psychological trauma [2]. The literature [3–6] on the diagnosis of occupational stress among coal mine workers shows that the most important social factor in the work environment causing occupational stress is a conflict situation. Social factors in the work environment that cause occupational stress include:

- a) the need to choose between following a supervisor's orders and losing respect for colleagues – from 22% to 40% of positive responses of respondents;
- b) having to follow orders without being convinced of their validity – from 57% to over 82% positive responses of respondents;
- c) conflict between employees and administration – from 40% to over 60% of positive responses of respondents;
- d) conflict with supervisors, co-workers or subordinates – from 42% to more than 60% of positive responses of respondents.

13.2. DESCRIPTION OF AN ACCIDENT AT WORK

In the analyzed case, the event took place in the Polish Mining Group, where the employee provided work as a physical employee in the Lampownia branch (storage room and maintenance of personal mining lamps) in a three-shift system. While cleaning the hall, the employee was verbally attacked by another employee who directed threats and offensive language at him. As a result of the violent argument, the employee suffered severe somatic symptoms such as nasal hemorrhage, palpitations, body tremors, increased blood pressure, and feelings of severe anxiety. The paramedic called to the scene decided to refer the employee to the hospital. This resulted in hospitalization for more than 7 days and the diagnosis of a reactive depressive episode, which was a consequence of severe stress in the workplace. The medical records of the injured employee show that the condition in which the employee found himself was a condition directly threatening his life due to the impact of the stress reaction with other concomitant diseases. It is important to point out that the tense atmosphere in the working environment had been ongoing for a long time. Clear divisions had formed among the staff, with a group emerging that treated other colleagues inappropriately. For a long time, the injured employee felt intimidated and had the impression of being mobbed by other employees, and the superiors did not react despite reports addressed to them. The growing stress and anxiety in the workplace culminated on the day of the accident with threats and profanity directed at the employee, which directly caused the psychological trauma he suffered. The employee had never previously received psychiatric treatment and did not seek the help of a psychologist. Despite the incident, the mine did not initiate any post-accident proceedings to determine the circumstances of the incident, considering the employee's health status as a mere illness.

The injured employee disagreed with this position and initiated proceedings to establish the event as an occupational accident. The case proceeded through two court instances and ultimately reached the Supreme Court. In the first instance, the district court hearing the case dismissed the injured employee's claim and subsequently dismissed the claim. That court found that the event did not have the character of suddenness but was part of a wider conflict at the workplace. It was also pointed out that there was no classic injury understood as physical injury, which, in the court's opinion, ruled out the possibility of recognizing the event as an accident at work. The injured employee disagreed with this decision and filed an appeal. The district court, as an appeal court, did not share the position of the district court and changed the judgment by recognizing in its entirety the claim of the injured employee. The appeal court found that the sudden quarrel was a sufficient external factor and the result was real psychological injury. The ruling emphasized that the injury does not have to be limited to personal injury – mental disorders also meet the statutory criterion, provided they are a direct consequence of the event. The mining company, disagreeing with this ruling, lodged an extraordinary appeal, known as cassation, with the Supreme Court. The employer, justifying the above, pointed to the need to interpret Article 3 of the Act of October 30, 2002 on social insurance for accidents at work and occupational diseases [1], which, in its opinion, raises serious doubts and causes discrepancies in court decisions regarding the interpretation of the concept of suddenness and determining when this characteristic occurs, which is one of the conditions for recognizing an event as an accident at work in the context of determining whether an event (resulting in an injury) has the characteristic of suddenness when it occurs within a period not longer than one working day, or whether a sudden event constituting the cause of the accident may be a sequence of events over a longer period of time, one of which was one element of a sequence of events, and which only as a whole led to the manifestation of the injury in the form of a reactive depressive episode in the plaintiff. The employer also expressed doubts as to whether it could be said that the injury was a sudden event when a series of events related to a tense and stressful work situation led to the injury, which only as a whole led to the injury being revealed or whether it was sufficient to establish the presence of a sudden event that one of the events in that series was a contributing cause of the injury. However, the Supreme Court refused to accept the complaint for examination, considering it to be manifestly unfounded. As a result, the judgment recognizing the events described earlier as an accident at work was upheld.

13.3. STRESS AND MENTAL ILLNESS, AS A POTENTIAL EXTERNAL CAUSE OF AN ACCIDENT AT WORK RESULTING INJURY

The main problem in the described factual situation concerned the interpretation of two key elements of the definition of an accident at work, i.e., the external cause and

the occurrence of damage. According to Article 3 of the Act of October 30, 2002 [1], on social insurance in respect of accidents at work and occupational diseases, an accident at work is considered to be a sudden event caused by an external cause causing injury or death, which occurred in connection with work:

- 1) during or in connection with the performance by the employee of normal activities or instructions of superiors;
- 2) during or in connection with the performance of activities by the employee for the employer, even without instruction;
- 3) while the employee remains at the disposal of the employer on the way between the employer's registered address and the place of performance of the obligation arising from the employment relationship.

According to Article 2 of the above-mentioned Act, injury is damage to the tissues of the body or organs of a person as a result of an external factor.

While it was obvious that the harmful event occurred during the course of work and at the workplace and that it could not be predicted that such a situation would occur, doubts arose on the grounds that stress in the form of a long-standing inappropriate working atmosphere resulting in a dispute could be considered an external cause, and the occurrence of a reactive depressive episode could be treated as an injury within the meaning of the Accident Act.

In the circumstances of this case, the injured employee did not suffer any injury understood as damage to human tissue or organs as a result of the incident. The court-appointed expert confirmed a "reactive depressive episode", a form of depressive disorder commonly referred to as depression. A depressive episode most often develops in response to a difficult life situation, and its symptoms – such as deep sadness, loss of energy and interest, apathy – persist for at least two weeks, significantly affecting daily functioning [15]. A stressful situation most often involves a series of events, with the stress spread over time. This created another interpretative problem of whether an argument on a particular day in itself could have caused such an injury or whether the long-lasting stressful atmosphere at the workplace was the ultimate cause for the occurrence of a mental illness. This is crucial for assessing the cause of the accident and whether it should be considered sudden within the meaning of the Act. Despite the doubts of the district court, the regional court unequivocally stated that the occurrence of a reactive depressive episode constituting an injury referred to in Article 3 of the Act of October 30, 2002 [1], on social insurance for accidents at work and occupational diseases can be considered as a disease entity. The employee, both before the accident and before the occurrence of an inappropriate atmosphere in the workplace, did not receive psychiatric treatment, did not use any pharmacotherapy and did not use psychological therapy. The psychological changes only occurred as a result of the work environment and the verbal assault by another employee. In his opinion, the court expert clearly indicated that the disease did not occur as a result of the argument itself, but as a result of the occurrence of

two causative factors, i.e., a generally tense situation in the workplace and a harmful event immediately preceding the reaction of the organism in the employee. However, if it were not for the situation of that particular day and the aggressive behavior of the co-worker despite the persistent negative atmosphere in the workplace, such disease consequences might not have occurred; hence, it should be known that the aggressive behavior of the employee was a direct stressor constituting the external cause of the accident at work. According to the Supreme Court judgment of 10/28/2014, case no. II UK 23/14 [10] “when classifying a specific circumstance as an external cause of an event constituting an accident at work, it is important that it constitutes the causative cause of the event, but it does not have to be the sole cause.” In the judgment of January 6, 2000, case no. II UKN 282/99 [11], the Supreme Court held that when a specific circumstance is classified as an external cause, it is important that it constitutes the causal cause of the event, but it does not have to be the sole cause. In the present case, the causative cause of the event at issue was a specific quarrel which resulted in the nervous breakdown in the employee, a nosebleed and other symptoms that led to a reactive depressive episode. The resolution of the seven judges of the Supreme Court of February 11, 1963, case no. III PO 15/62 [12] stated that the causative cause of the event can be any external factor (i.e., not resulting from internal human characteristics) capable of causing harmful effects under existing conditions. In this sense, the external cause of the event may not only be a work tool, machine, or natural forces, but also the behavior and actions of the injured person or other co-workers. The injured employee’s work was not stressful, but the sudden outbreak of aggression by one of the co-workers led to psychological trauma, which allows the event from that day to be considered an accident at work in accordance with the Accident Act. Supreme Court case law has held that excessive exertion (stress) should be assessed taking into account the employee’s individual characteristics (current health status, functional capacity) and the circumstances in which the work is performed. It is therefore permissible that even the daily activities performed under normal conditions by a worker with reduced performance, either as a result of illness or age-related changes in the body, may, depending on the circumstances, be considered to have been undertaken with excessive effort for that worker. However, there must be a special (extraordinary) circumstance in the course of work in order for the injury to be considered as an external cause. “Work itself” cannot constitute an external cause within the meaning of the definition of an accident at work, but it can only be defined as an exceptional situation connected with this work, which becomes a cooperating external cause (judgment of the Supreme Court of March 28, 2001, II UKN 283/00) [13]. The mere fact of being upset due to the employee being transferred to another job that does not meet his or her wishes cannot be considered an external cause (judgment of the Supreme Court, case no. III PRN 12/77) [14]. In addition to a thorough analysis of the facts and an assessment of the event, it is also important to determine the scope of

normal activities and the circumstances in which the work is performed. According to the Supreme Court's rulings, a different level of stress and other circumstances justify stress as an external cause in the case of an ordinary employee, and this will be assessed differently in the case of a person holding a managerial position.

13.4. SURVEY

In order to verify the presented problem, a survey was carried out on a group of 40 men who were manual employees of the coal mine of Polish Mining Group, who were asked 17 questions (Table 13.1), covering the issues of interpersonal conflicts, as a stressor that could potentially affect the quality of work performed, employee motivation, and above all as a potential cause of an accident at work and the reactions of superiors as well as alternative methods of solving problems.

Table 13.1. Employee survey

Question	Yes	No	I don't know
Are there any conflicts between employees at your workplace?			
Does a conflict situation at work cause you stress?			
Does conflict at work have a negative impact on the performance of your duties?			
Have you noticed a decrease in concentration or productivity as a result of a workplace conflict?			
Has a conflict with another employee ever influenced your professional decisions, such as avoiding cooperation, resigning from tasks?			
Have you experienced a psychological tension that made it difficult to perform your duty after a conflict at work?			
Did the psychological tension at work associated with the work conflict persist over a longer period of time?			
Do conflicts in your team affect the quality of your work?			
Do you think that interpersonal conflicts in workplaces can pose a real threat to occupational safety or lead to accidents at work?			
Do you have conflict resolution procedures in your workplace (e.g., mediation, conversations with your supervisor)?			
Does your supervisor respond to tensions and conflicts in the team?			
Have you ever felt a victim of mobbing or verbal aggression at work?			
Is stress at work underestimated by management?			
Has anyone in your facility suffered a mental or physical injury as a result of stress or conflict?			
Do you have training in stress management or interpersonal relationships at your workplace?			

Table 13.2 continued

In a stressful situation at work, do you have the opportunity to get support (e.g., psychologist, health and safety department, supervisor)?			
Do you think that improving communication and mediation could reduce the number of conflicts and stressful situations at work?			

The answers to these questions are as follows:

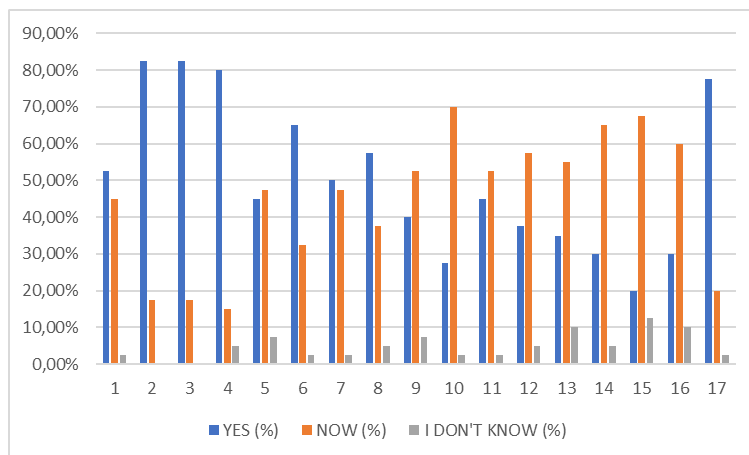


Fig. 13.1. Percentage representation of respondents' answers

Based on the analysis of the surveys provided, it can be pointed out that the vast majority of respondents confirm that there are conflicts between employees in their workplace. In addition, the overwhelming majority of respondents believe that the conflict situation causes them stress (Fig. 13.2). The vast majority (33 out of 40, or 82.5%) of respondents confirm that conflicts between employees occur in their workplace. Almost all respondents (37 out of 40, or 92.5%) indicated that the conflict situation caused them stress. These situations have a negative impact on the efficiency and quality of work because they make it difficult to perform duties. A large proportion of respondents (32 out of 40, or 80%) experience psychological tension that makes it difficult to perform duties after a conflict at work. Three-quarters of the respondents (30 out of 40, or 75%) noticed a decrease in concentration or work efficiency as a result of the conflict.

Conflicts negatively affect the performance of employee duties (31 out of 40) and lead to deterioration in the quality of work performed (27 out of 40). Moreover, 26 out of 40 respondents indicated that the conflict affected professional decisions (e.g., avoiding cooperation, resigning from tasks). The dominant majority (34 out of 40, or 85%) felt that the psychological tension associated with the work conflict persisted over a long period of time. This result suggests that conflicts are not resolved quickly and

effectively. 17 out of 40 (42.5%) respondents admitted that mental or physical injury was caused by stress or conflict in their work environment, corresponding to the fact that 21 of 40 respondents (52.5%) believe that interpersonal conflicts can pose a real threat to occupational safety or lead to accidents at work.

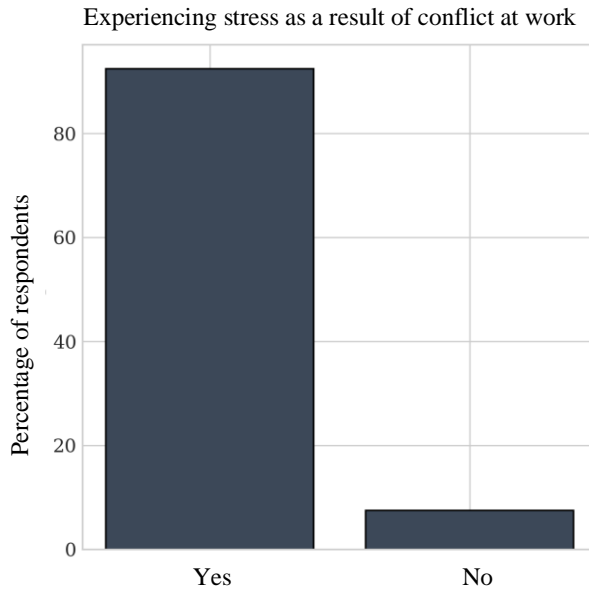


Fig. 13.2. Experiencing stress in the workplace as a result of interpersonal conflict

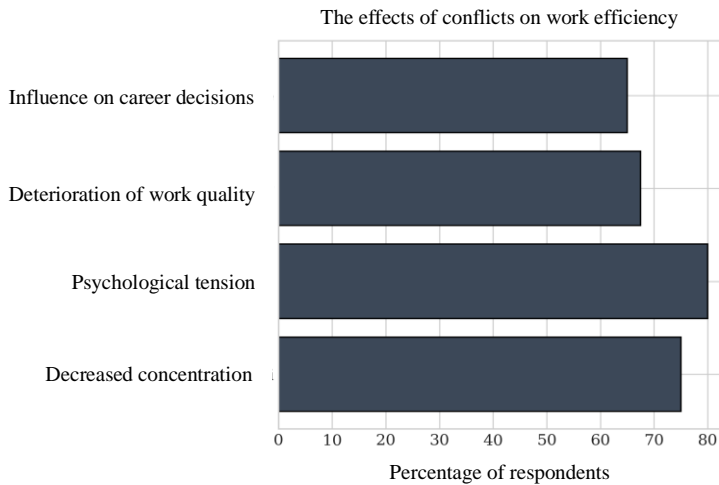


Fig. 13.3. The effects of conflicts on work efficiency

The survey results indicate an inconsistent and often insufficient response from management, as well as problems with the availability of formal support. Opinions on the reactions of supervisors are divided: Half (20 out of 40) believe that the supervisor responds to tensions and conflicts in the team, but 17 out of 40 (42.5%) say that the supervisor does not respond. 23 out of 40 (57.5%) respondents have the opportunity to receive support in a stressful situation (e.g., psychologist, health and safety department, supervisor). However, 13 out of 40 (32.5%) say that this is not possible. The analysis of the surveys does not indicate that seniority (from 3 to 27 years) has any effect on feelings related to long-term stress. Employees see a specific way to improve the situation. A vast majority (33 out of 40, or 82.5%) believe that improving communication and mediation could reduce the number of conflicts and stressful situations at work.

13.5. CONCLUSIONS

In conclusion, the survey reveals that interpersonal conflicts are a common and significant problem in the organization, having a significant, long-term and negative impact on the effectiveness of work and well-being of employees. Support systems and management responses are seen as insufficient or inconsistent. This is consistent with the case law set presented above, which allows long-term stress in the work environment resulting from interpersonal conflicts as an external cause of an accident at work and a possible psychological injury. A prerequisite for the development of appropriate preventive measures is the correct diagnosis of the causes of an accident at work. In practice, this means that employers should implement anti-mobbing procedures and psychological support programs, and post-accident commissions must take into account not only material events, but also psychological events. It is important to respond early to conflict situations in the work environment, introduce mediation as one of the tools for amicable settlement of conflict situations in the workplace and strive for an amicable settlement of cases.

REFERENCES

- [1] Act of October 30, 2002 on social insurance for accidents at work and occupational diseases for accidents at work, Journal of Laws of 2002 No. 199, item 1673.
- [2] HIBNER M., *Kultura bezpieczeństwa wśród pracowników kopalni*, Zeszyty Naukowe Państwowej Wyższej Szkoły Zawodowej im. Witelona w Legnicy, 2021, Vol. 40 (3), 103–112.
- [3] JACHIMOWICZ M., APANOWICZ B., MILCZAREK W., *Odpowiedzialność karna pracodawcy w razie wystąpienia wypadku przy pracy*, Studia z zakresu nauk prawnoustrojowych, Tom XIII, Miscellanea, 2023, 57–79.
- [4] KRZYŚKÓW B., ORDYS Sz., PAWŁOWSKA Z., PĘCIŁŁO-PACEK M., *Badanie wypadków przy pracy*, Centralny Instytut Ochrony Pracy – Państwowy Instytut Badawczy, Warszawa 2015.

- [5] MORCINEK-SŁOTA A., PIECHA M., *Stres zawodowy u górników – badania ankietowe pracowników kopalni węgla kamiennego*, Przegląd Górniczy, 2016, Vol. 12, 79–83.
- [6] MORCINEK-SŁOTA M., *Stres zawodowy wśród górników z uwzględnieniem stażu pracy oraz zajmowanego stanowiska*, Przegląd Górniczy, 2018, Vol. 9, 41–45.
- [7] Judgment of The District Court in Jastrzębie-Zdrój of April 29, 2021, case no. IV P 216/17.
- [8] Judgment of The District Court in Rybnik of September 27, 2021, case no. IV Pa 49/21.
- [9] Judgment of The Supreme Court of September 8, 2022, case no. I PSK 38/22.
- [10] Judgment of The Supreme Court of 10/28/2014, case no. II UK 23/14.
- [11] Judgment of The Supreme Court of 01/06/2000, case no. II UKN 282/99.
- [12] Resolution of the composition of seven Judges of The Supreme Court of 02/11/1963, case no. III PO 15/62.
- [13] Judgment of The Supreme Court of 03/28/2001, case no. II UKN 283/00.
- [14] Wyrok Sądu Najwyższego z dnia 21.06.1977 r., sygn. akt III PRN 12/77.
- [15] MOLEK-WINIARSKA D., *Źródła stresu zawodowego wśród pracowników sektora wydobywczego*, Management Sciences, 2015, Vol. 2 (23), 74–92.

ANALIZA PRAWNA POLSKIEGO ORZECZNICTWA SĄDOWEGO
W ZAKRESIE ZJAWISKA REAKTYWNEGO EPIZODU DEPRESYJNEGO
NA PRZYKŁADZIE PRACOWNIKA ZAKŁADU GÓRNICZEGO

W publikacji przedstawiono analizę polskiego orzecznictwa dotyczącego kwalifikacji reaktywnego epizodu depresyjnego jako urazu w rozumieniu ustawy o ubezpieczeniu społecznym z tytułu wypadków przy pracy i chorób zawodowych. Na przykładzie sprawy pracownika zakładu górniczego omówiono problem interpretacji pojęcia „przyczyny zewnętrznej” oraz „cechy nagłości” zdarzenia w kontekście wystąpienia zaburzeń psychicznych spowodowanych stresem i konfliktami interpersonalnymi w środowisku pracy. W niniejszym rozdziale zaprezentowano przebieg postępowania sądowego, w tym rozstrzygnięcia sądów obu instancji, oraz stanowisko Sądu Najwyższego, który potwierdził możliwość uznania urazu psychicznego za wypadek przy pracy. Analiza orzeczeń sądowych wskazuje, że stres oraz sytuacje konfliktowe mogą stanowić realną, zewnętrzną przyczynę zdarzenia szkodowego, jeśli prowadzą do trwałego lub nagłego pogorszenia zdrowia pracownika. Uzupełnieniem opracowania jest badanie ankietowe przeprowadzone wśród pracowników kopalni, na podstawie którego potwierdzono, że konflikty interpersonalne i napięta atmosfera pracy są istotnym źródłem stresu, obniżającego efektywność i bezpieczeństwo pracy. Wnioski wskazują na potrzebę traktowania zdrowia psychicznego jako integralnego elementu bezpieczeństwa i higieny pracy oraz wdrażania działań profilaktycznych, takich jak mediacje i wsparcie psychologiczne w celu zapobiegania urazom psychicznym i wypadkom przy pracy.



WUST Publishing House prints
can be obtained via mailorder:
zamawianie.ksiazek@pwr.edu.pl
www.ksiegarnia.pwr.edu.pl

978-83-8134-007-6

DOI: 10.37190/Interdisciplinary_topics

